UAB
Universitat Autònoma de Barcelona

Contribution of neuroinflamation to the pathology of the Ndufs4 KO mouse model of Leigh syndrome

Kevin Aguilar Ludwig

PhD THESIS NEUROSCIENCE 2023

INc Institut de Neurociències

UAB Universitat Autònoma de Barcelona

BCFI

GOBIERNO DE ESPAÑA MINISTERIO DE CIENCIA E INNOVACIÓN

European Union
European Regional Development Fund

Contribution of neuroinflammation to the pathology of the *Ndufs4 KO* mouse model of Leigh syndrome

A major role of microglial cells

Kevin Aguilar Ludwig

Instituto de Neurociencias

Departamento de Biología Celular, Fisiología e Inmunología
Unitat de Fisiologia Animal
Facultat de Biociències

THESIS SUPERVISORS

JUAN HIDALGO PAREJA | **ELISENDA SANZ IGLESIAS**

Instituto de Neurociencias

Departamento de Biología Celular, Fisiología e Inmunología

Memoria de tesis presentada por

Kevin Aguilar Ludwig

para optar al grado de Doctor en Neurociencias
por la Universidad Autónoma de Barcelona.

Este trabajo ha sido realizado bajo la dirección

del Doctor

Juan Hidalgo Pareja

catedrático de universidad
del Departamento de Biología Celular, Fisiología e Inmunología
de la Universidad Autónoma de Barcelona

y la Doctora

Elisenda Sanz Iglesias

Investigadora Santiago Ramón y Cajal
del Departamento de Biología Celular, Fisiología e Inmunología
de la Universidad Autónoma de Barcelona.

Aprender es creer en algo y describirlo, dar una lección,
mirar de arriba abajo al ignorante, recibir información
nueva, dejar de creer, dar una lección al respecto,
mostrarse vehemente, equivocarse de nuevo,
dar otra lección, perder la vehemencia, sorprenderse,
dar una lección pequeña, optar por esperar,
ser más prudente, reservarse la lección de la prudencia,
formarse, dudar, ser paciente, empezar una lección
sobre la paciencia y cortarla a tiempo, dejar, por fin,
de dar lecciones

Rodrigo Cortés, *Los años extraordinarios*

Toda sed de comprender cualquier motivo;
el sinsentido,
ha dejado a hombres de ciencia
sin salir de sus porqués

Love of Lesbian, *Bajo el volcán*

A los Sebastianes de mi vida, y por supuesto,
a mi padre, y a Gemma

The following funding agencies supported this study:

Agència de Gestio d'Ajuts Universitaris i de Recerca
2017SGR-323 and 2017SGR-104

Consejo Europeo de Investigación
ERC2014-StG-638106

Fondo Europeo de Desarrollo Regional and Ministerio de Ciencia, Innovación y Universidades
RTI2018-101105-B-I00 and RTI2018-101838-J-I00

Fondo Europeo de Desarrollo Regional and Ministerio de Ciencia e Innovación
PID2020-114977RB-I00 and PID2021-126602OB-I00

Fundació "la Caixa"
ID 100010434

Secretaría de Estado de Investigación, Desarrollo e Innovación
SAF2014-57981P and SAF2017-88108-R

And the following fellowships:

Ministerio de Educación, Cultura y Deporte
FPU17/02065

European Molecular Biology Organization
EMBO Scientific Exchange Grant 9416

This research has been mainly performed at the Universitat Autònoma de Barcelona. Still, some of the analyses were performed at the Biomedicum Helsinki of the University of Helsinki in Dr. Anu Suomalainen Wartiovaara`s laboratory as a result of my three months short stay (April-June 2022). In addition, part of the results derived from this thesis project have already been published and are available at: https://doi.org/10.1002/glia.24234.

Index

Abstract

Leigh syndrome (LS) is a mitochondrial disease with an estimated prevalence of 1/40.000 live births and is typically accompanied by a progressive neurodegenerative disorder. As is commonly seen in other central nervous system (CNS) neurodegenerative diseases, patients with LS present abundant neuroinflammatory hallmarks accompanying neurodegeneration. Mice lacking systemically the subunit NDUFS4 of the complex I of the electron respiratory chain, known as *Ndufs4* knockout (KO) mice, develop fatal progressive encephalopathy resembling LS and die approximately at the postnatal day 55. As the disease progresses, neurodegeneration increases being the main responsible for the neurological symptoms. As in LS, prominent neuroinflammation is observed in affected brain areas. Surprisingly, despite the magnitude of this neuroinflammation, the roles of either the neuroimmune pathways or their main cellular components have barely been addressed in *Ndufs4 KO* mice. We hypothesized that neuroinflammation is by itself a harmful process in this mouse model of LS and not just a consequence of neurodegeneration.

Firstly, we studied the contributions of microglia, the specialized immune cell of the CNS, to the *Ndufs4 KO* mouse pathology. We used a pharmacological approach consisting of the chronic administration of a colony stimulation factor 1 receptor (CSFR1) antagonist, PLX3397, which has the capability of depleting mouse microglia from the CNS parenchyma. We found that microglia contribute to the progression of the pathology since their partial depletion extended survival, delayed the onset of the disease, and alleviated brain pathology.

Secondly, we tried to find putative mediators responsible for the microglial detrimental actions in *Ndufs4 KO* mice. To do so, we studied the role of an important neuroinflammatory mediator, the cytokine interleukin-6 (IL-6), which is known to have strong detrimental effects during chronic neuroinflammation. In this case, we generated a Double KO mouse line with a combined complete deficiency of IL-6 and NDUFS4 and appropriate controls. In short, knocking out *Il6* had minor effects on the development of the *Ndufs4 KO* mice pathology.

Finally, once we proved that decreasing the neuroimmune response by depleting microglial cells had beneficial effects in *Ndufs4 KO* mice, we wanted to assess the opposite paradigm and test whether a chronic induction of a neuroinflammatory state in the CNS of *Ndufs4 KO* mice would be detrimental or not. For that purpose, we took advantage of

the GFAP-IL6 mouse, which overexpresses IL-6 only in astrocytes and produces chronic microglia and astrocyte reactivity, by generating a mouse line with CNS IL-6 overexpression and whole-body NDUFS4 deficiency. IL-6 overexpression in the CNS aggravated the phenotype of female mice to some extent but did not affect the phenotype of male mice. Interestingly, an abnormal neuroinflammatory response to IL-6 overexpression was observed in *Ndufs4 KO* mice compared to controls, which may have potential implications for understanding LS.

Taken together, our results demonstrate that neuroinflammation, especially the microglial response, is a pathogenic driving mechanism of the *Ndufs4 KO* mice encephalopathy that should be considered as a target for future therapies in patients with LS.

Resumen

El síndrome de Leigh (SL) es una enfermedad mitocondrial con una prevalencia estimada de un caso por cada 40.000 nacimientos. Típicamente, el SL se acompaña de un proceso neurodegenerativo agudo y progresivo. Tal y como se observa en otras enfermedades neurodegenerativas del sistema nervioso central (SNC), pacientes con SL presentan abundantes sellos distintivos de un proceso neuroinflamatorio acompañando a la neurodegeneración. Los ratones que carecen de forma sistémica de la subunidad NDUFS4 del complejo I de la cadena transportadora de electrones, conocidos como ratones *Ndufs4* knockout (KO), desarrollan una encefalopatía de características similares a la que se observa en pacientes con SL y que acaba provocando su muerte cuando apenas tienen 55 días de vida. A medida que progresa la enfermedad, la neurodegeneración aumenta, siendo ésta la principal responsable de los síntomas neurológicos. Como en pacientes con SL, se observa una prominente neuroinflamación en las regiones cerebrales afectadas. Sorprendentemente, a pesar de la magnitud de la neuroinflamación asociada a las lesiones cerebrales, el papel que juegan las vías neuroinmunitarias junto con sus componentes celulares más importantes no se ha estudiado de manera detallada en los ratones *Ndufs4 KO*. Hipotetizamos que la neuroinflamación es un proceso perjudicial *per se* en el modelo murino de SL, y no únicamente un mero subproducto de la neurodegeneración.

En primer lugar, estudiamos las contribuciones de la microglía, la célula especializada del sistema inmune en el SNC, en el desarrollo de la patología del ratón *Ndufs4 KO*. Usamos una aproximación farmacológica que consistió en la administración de un antagonista del receptor 1 del factor estimulador de colonias (CSF1R), conocido como PLX3397, que nos permitó eliminar la microglía del parénquima del SNC. Nuestros resultados indican que la microglía contribuye a la progresión de la enfermedad, dado que su depleción parcial extendió la supervivencia, retrasó la aparición de la enfermedad y mejoró la patología cerebral.

En segundo lugar, intentamos hallar posibles mediadores responsables de las acciones perjudiciales de la microglía. Para ello, estudiamos el papel de un mediador neuroinflamarorio muy importante, la interleuquina-6 (IL-6), conocida por jugar papeles perjudiciales en el contexto de una neuroinflamación crónica. En este caso, generamos una línea murina Doble KO que presentaba una deficiencia completa de IL-6 y NDUFS4 junto con sus respectivos controles. Brevemente, eliminar la producción de IL-6 tuvo un impacto menor en el desarrollo de la patología de los ratones *Ndufs4 KO*.

Finalmente, una vez demostrado que disminuir la respuesta neuroinmunitaria a través de la depleción de las células microgliales tiene efectos beneficiosos en los ratones *Ndufs4 KO,* quisimos examinar el paradigma opuesto y estudiar si la inducción de un estado neuroinflamatorio crónico en el SNC de los ratones *Ndufs4 KO* sería perjudicial o no. Con este objetivo en mente, nos beneficiamos del modelo de ratón GFAP-IL6, que sobreexpresa la IL-6 exclusivamente en astrocitos produciendo una reactividad microglial y astrocítica crónica. Generamos una línea murina doble transgénica con sobreexpresión de IL-6 en el SNC y deficiencia completa de NDUFS4 junto con sus controles. Observamos que la sobreexpresión de esta interleuquina agravaba significativamente el fenotipo de las hembras *Ndufs4 KO* pero no así el de los machos. Es importante mencionar que los ratones *Ndufs4 KO* con sobreexpresión de IL-6 mostraron una respuesta neuroinflamatoria anómala en comparación con los ratones control, lo que podría tener implicaciones en la comprensión del SL.

En conjunto, nuestros resultados demuestran que la neuroinflamación, especialmente la respuesta microglial, es un mecanismo patogénico que contribuye al desarrollo de la encefalopatía de los ratones *Ndufs4 KO*, y que, por tanto, debe ser considerado como diana para futuras terapias en pacientes con SL.

Relevant abbreviations

ADAM: A Disintegrin and Metalloprotease
ADP: Adenosine diphosphate
ATP: Adenosine triphosphate
a.u.: Arbitrary units
BBB: Blood-brain barrier
BS: Brainstem
CI/II/III/IV/V: Respiratory chain complex number
CAMs: CNS-associated macrophages
CD3: Cluster of differentiation 3
CNS: Central nervous system
Control: Ctrl
CSF: Cerebrospinal fluid
CSF1: Colony stimulation factor 1
CSF1R: Colony stimulation factor receptor 1
DAM: Disease-associated microglia
DAMP: Danger-associated molecular patter
DAP12: DNAX-activation protein 12
DEG: Differentially expressed genes
DNA: Deoxyribonucleic acid
ETC: Electron transport chain
FADH2: Reduced form of flavin adenine dinucleotide
GFAP: Glial fibrillary acidic protein
GO: Gene ontology
Gp130: Glycoprotein 130
IBA-1: Ionized calcium-binding adaptor protein-1
IFN: interferon
IL-1β: Interleukin-1β
IL-10: Interleukin-10
IL-6: Interleukin-6
IL-6R: Interleukin-6 receptor
IMM: Inner mitochondrial membrane
ISH: *In situ* hybridization
IP: intraperitoneal
JAK: Janus kinase
KO: Knockout
L-LS: Leigh-like syndrome
LS: Leigh syndrome
LPS: Lipopolysaccharide
mIL-6R: Membrane-bound IL-6 receptor
mtDNA: Mitochondrial DNA
mRNA: Messenger ribonucleic acid
mTOR: Mammalian target of rapamycin
NADH: Reduced form of nicotinamide adenine dinucleotide
nDNA: Nuclear DNA
NDUFS4: NADH dehydrogenase (ubiquinone) Fe-sulfur protein 4
NeuN: Neuronal nuclear protein
OB: Olfactory bulb
OF: Open field test
OMM: Outer mitochondrial membrane
OXPHOS: Oxidative phosphorylation
p: p-value
padj: p-adjusted value
PAMP: Pathogen-associated molecular pattern
PMD: Primary mitochondrial disease
PI3K: Phosphoinositide 3-kinase
PKC: Protein kinase C
PLX3397: Pexidartinib, CSF1R inhibitor
POLG: DNA polymerase gamma
PRR: Pattern recognition receptor
RNA: Ribonucleic acid
RNAseq: RNA sequencing
ROS: Reactive oxigen species
rRNA: Ribosomal RNA
RT: Room temperature
sIL-6R: Soluble form of the IL-6 receptor
SMD: Secondary mitochondrial disease
TCA: Tricarboxylic acid cycle
TLR: Toll-like receptor
TMEM119: Transmembrane protein 119
TNF-α: Tumor necrosis factor α
TREM2: Triggering receptor expressed on myeloid cells 2
tRNA: Transfer RNA
Veh: Vehicle solution
VN: Vestibular nuclei
ψΔm: Mitochondrial electrochemical gradient

1

Introduction

1.1 Mitochondria: origin, main features, and functions

Mitochondria were first described in 1857 by Rudolf von Kölliker, but it was not until 1898 that Carl Brenda gave them their current name from the Greek words *mitos* (thread) and *chondros* (granule) (Ernster and Schatz, 1981; Cogliati et al., 2016). One century after Von Kölliker described this organelle for the first time, in 1967, Lynn Margulis (then Lynn Sagan) formulated her endosymbiotic theory to explain the origin of a set of eukaryote organelles (Sagan, 1967). Margulis`s postulate became one of the most crucial turning points in the history of biology. She hypothesized that millions of years ago, at the dawning of evolution, in an increasing oxidizing atmosphere, some eukaryote organelles, including mitochondria, evolved from endosymbiotic bacteria: "*an aerobic prokaryotic microbe (i.e., the protomitochondrion) was ingested into the cytoplasm of a heterotrophic anaerobe. This endosymbiosis became obligate and resulted in the evolution of the first aerobic amitotic amoeboid organisms*" which evolved in complexity to give rise to the actual eukaryote organisms (Sagan, 1967). Regarding its initial controversy, the theory has been confirmed over the years (Lane and Martin, 2010; Roger et al., 2017).

Mitochondria are tubular-shaped organelles with two different membranes: the outer mitochondria membrane (OMM) and the inner mitochondrial membrane (IMM). The IMM contains specialized structures, called cristae, that adapt their shape and function depending on physiological conditions (Cogliati et al., 2016). These membranes define two different spaces: the intermembrane space and the mitochondrial matrix (**Figure 1**). The latter contains both circular plasmid-like DNA molecules composed of a light and a heavy strand (Roger et al., 2017) and the enzymes necessary to support mitochondrial metabolic biochemical reactions (i.e., tricarboxylic acid cycle, fatty acid oxidation, heme biosynthesis) (Smoly et al., 1970). The mitochondrial genome has been reduced during evolution and progressively transferred to the nuclear genome in a process that probably started when protomitochondria were no longer capable of replicating outside the host cell (Roger et al., 2017). Currently, human mtDNA is a double-stranded DNA molecule with a genetic code with unique features that encodes for 13 peptide subunits of oxidative phosphorylation (OXPHOS) and 24 RNAs (2 rRNAs and 22 tRNA) required for mitochondrial protein synthesis (Taanman, 1999).

During evolution, far from being just an advantageous adaptation to the increasingly oxidized environment, mitochondria turned into integral parts

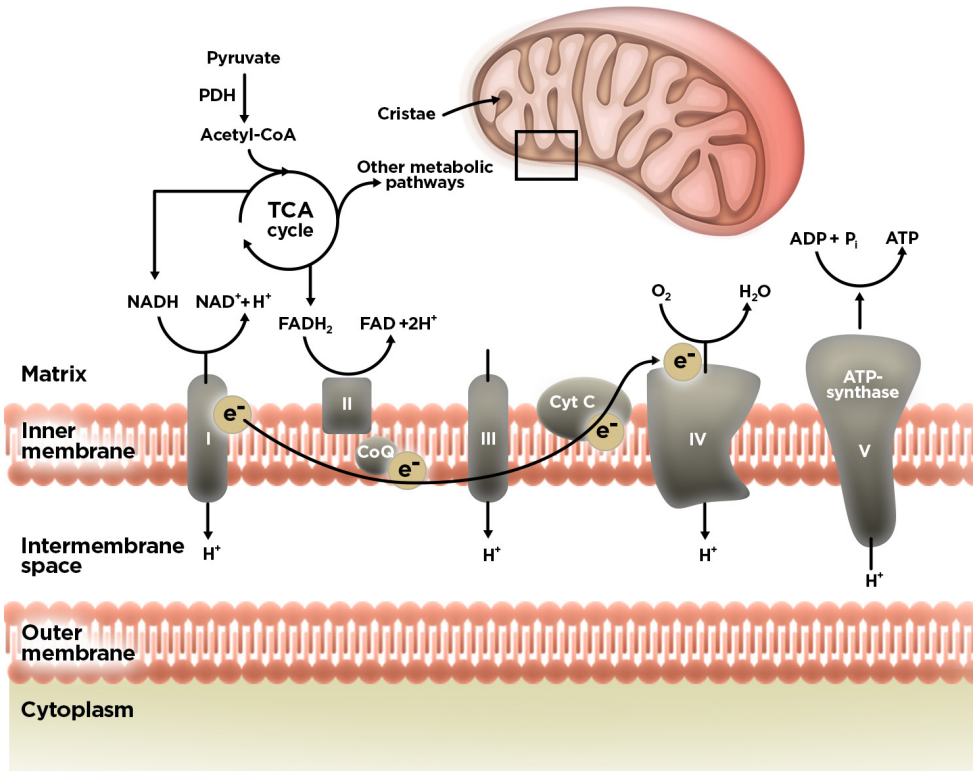

Figure 1. Schematic representation of OXPHOS and the different mitochondrial compartments.

Co-factors NADH and $FADH_2$ are generated in the TCA cycle and serve as electron donors for the ETC. Electrons are sequentially transferred through the different ETC complexes allowing the generation of the electrochemical gradient necessary to generate ATP. Arrows indicate the direction of the reaction. I-V indicate the number of the ETC complex. CoQ: ubiquinone; Cyc C: cytochrome C; e^-: electrons; H^+: protons; PDH: pyruvate dehydrogenase. *Adapted from Vercellino and Sazanov 2021 and Schubert and Vilarinho 202.*

of cellular physiology. This organelle has functions in energy generation and metabolism (Ernster and Schatz, 1981), cell death (Bock and Tait, 2020), autophagy (Okamoto and Kondo-Okamoto, 2012), calcium signaling (Bravo-Sagua et al., 2017), innate and adaptative immunity (West and Shadel, 2017), endocrine communication (Chung et al., 2017), oxidative stress (Murphy, 2009), aging (Sun et al., 2016), as well as being a sensor in a wide range of pathological conditions (i.e., nutrient starvation, proteotoxic stress, hypoxia) (Quirós et al., 2016; Mottis et al., 2019). Since more than 1200 proteins are present in mitochondria, only 13 are encoded by mtDNA (Roger et al., 2017), tight crosstalk between the nucleus and mitochondria regarding transcription, translation, and protein import into the mitochondria must occur. This process is generally known as mitonuclear communication (Quirós et al., 2016) and we can differentiate between anterograde and

retrograde. On the one hand, anterograde communication refers to nucleus to mitochondria control, which can increase or decrease mitochondrial activity and promote mitobiogenesis. On the other hand, retrograde communication refers to mitochondria-to-nucleus regulation that enables cellular homeostasis and cellular adaptations to stressors (Quirós et al., 2016; Mottis et al., 2019).

1.2 Oxidative phosphorylation

1.2.1 Electron transport chain and energy production

The mitochondrial OXPHOS is the primary source of energy for eukaryotic cells providing over 90% of the energetic requirements. OXPHOS is a metabolic pathway in which the energy coming from the oxidation of nutrients is used by the electron transport chain (ETC) to generate an electrochemical gradient ($\psi\Delta m$) that allows the production of adenosine triphosphate (ATP) (Mitchell, 1961) (**Figure 1**). The ETC consists of four complexes: complex I (NADH: ubiquinone oxidoreductase), complex II (succinate dehydrogenase), complex III (cytochrome bc_1 oxidoreductase), and complex IV (cytochrome *c* oxidase). In addition, the ETC also requires two mobile electron carriers: ubiquinone (CoQ) and cytochrome *c* (cyt c). Complex I and II oxidize the cofactors NADH (reduced nicotinamide adenine dinucleotide) and $FADH_2$ (reduced flavin adenine dinucleotide), respectively, mainly produced in the tricarboxylic acid cycle (TCA) and source electrons to reduce CoQ. Then, Complex III accepts electrons from ubiquinone and reduces cyt c which donates them to Complex IV for the final reduction of molecular oxygen (O_2) into water (H_2O). For a correct redox process, complexes contain oxide-reduction cofactors in form of iron-sulfur clusters (Fe-S clusters) and heme groups. During the electron transport, Complexes I, III, and IV also pump H^+ protons from the mitochondrial matrix into the intermembrane space, which creates an $\psi\Delta m$ (mitochondrial electrochemical gradient). The generated proton gradient is then used by the ATP synthase to transform ADP and inorganic phosphate into ATP (Chance and Williams, 1956; Mitchell, 1961; Enríquez, 2016; Vercellino and Sazanov, 2021).

1.2.2 Supramolecular organization of ETC complexes

Structural organization has always been fundamental to explain the functions of single and complexes of proteins, as well as the consequences of their dysfunction. Two classical models of the supramolecular organization of ETC components have been proposed since the discovery of this process: the solid model and the fluid model, together with a recently proposed one named plasticity-model. The solid-model proposes the

formation of a functional entity between complexes (oxysome) that helps electron transfer and ATP synthesis (Chance et al., 1963), whereas, in the fluid-model, complexes and electron carriers diffuse freely in the IMM (Hackenbrock, 1977). After Schägger and Pfeiffer described for the first time large supramolecular structures formed by a combination of different ETC complexes, called supercomplexes, in both yeast and mammalian mitochondria (Schägger and Pfeiffer, 2000), a third model, that reconciles the solid and the fluid model, has been proposed. The so-called plasticity-model states that both individual complexes and supercomplexes co-exist (Acín-Pérez et al., 2008). Nowadays, the initial skepticism regarding the existence of supercomplexes has disappeared, respiratory supercomplexes are real physical entities. Five different mammalian supercomplexes have been clearly described and crystalized: $CICIII_2CIV$, $CICIII_2$, $CI_2CIII_2CIV_2$, $CIII_2CIV_2$, and $CICIICIII_2CIV_2$ (Javadov et al., 2004; Enríquez, 2016; Vercellino and Sazanov, 2021; Mühleip et al., 2022). Several physiological roles of SCs have been proposed and described, which include: to regulate OXPHOS flux and adapt it to metabolic demands, to increase the stability of individual complexes and to decrease both reactive oxygen species production (ROS) and protein aggregation (Javadov et al., 2004; Enríquez, 2016; Vercellino and Sazanov, 2021). Moreover, this intricate organization explains why defects in individual complexes affect the function of the others, having potential implications in mitochondrial diseases (Mimaki et al., 2012; Mukherjee and Ghosh, 2020).

1.3 Mitochondrial diseases

Mitochondrial diseases (MDs) are rare genetic disorders caused by mutations in genes essential for proper mitochondrial function (**Figure 2**). Since the first mutations were described (Holt et al., 1988; Wallace et al., 1988), more than 350 causal mutations in nDNA or mtDNA have been identified. Mutations comprise X-linked, autosomal, or mitochondrial/maternal types of transmission (Ng et al., 2021). This enormous plethora of mutations give rise to a wide range of heterogeneous diseases that vary in disease onset, prognosis, tissue susceptibility, and treatment (Gorman et al., 2016). Several general classifications have been used to categorize patients suffering from these diseases considering either the etiology, the disease onset, or the clinical features (**Table 1**). In terms of etiology, we can subdivide MDs between primary and secondary mitochondrial diseases (PMD and SMD, respectively) (Niyazov et al., 2016). PMDs are caused by germline mutations in nDNA or mtDNA genes directly involved in either OXPHOS function or production that impact its optimal performance,

Figure 2. Summary of processes involved in mitochondrial function associated with human mitochondrial diseases

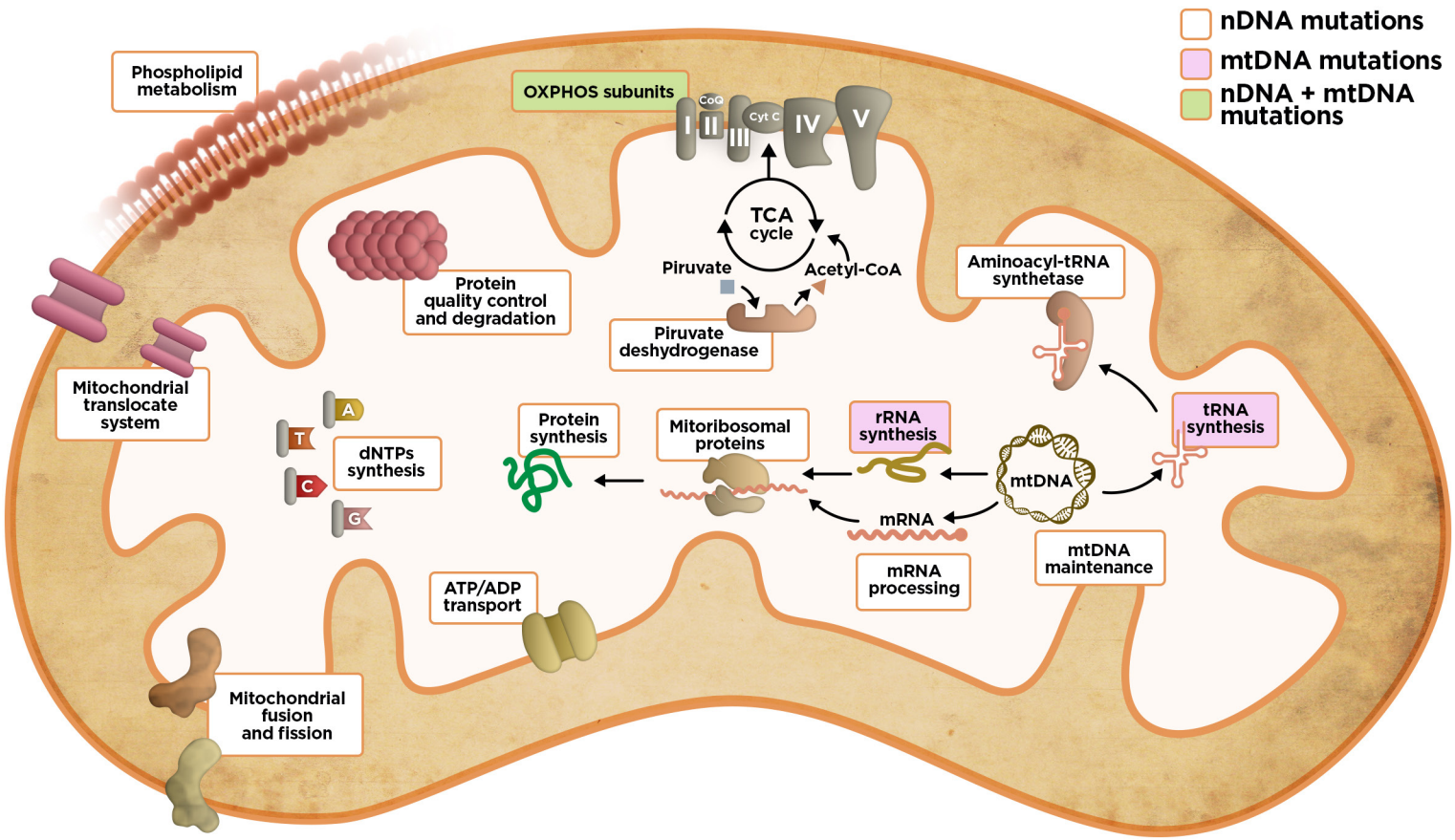

nDNA and mtDNA mutations in genes involved in a variety of mitochondrial processes can lead to mitochondrial diseases. Not only direct mutations in OXPHOS subunits are behind these diseases, but also mutations involved in mtDNA maintenance, mitochondrial protein synthesis, mitochondrial fission/fusion, and other metabolic processes. dNTPs: deoxynucleotide triphosphates; mRNA: messenger ribonucleic acid; rRNA: ribosomal RNA; tRNA: transfer RNA. *Adapted from Gorman et al 2016.*

Table 1. Main syndromes in primary and secondary mitochondrial diseases: etiology and main phenotypic features.

Adapted from Gorman et al 2016 and Niyazov et al 2016.

Primary mitochondrial diseases		
Disease	**Genetic etiology**	**Clinical features**
Childhood-onset		
Leigh syndrome (LS)	>75 mutations in nDNA and mtDNA	Neurodevelopmental regression, hypotonia, dystonia, hypopnea, dysphagia, epilepsy, failure to thrive, encephalopathy, basal ganglia and brainstem lesions
Alpers-Huttenlocher (AHS)	DNA polymerase gamma (POLG) -related mutations	Intractable epilepsy, psychomotor regression and liver disease
Ataxia neuropathy syndrome (ANS) or mitochondrial recessive ataxia syndrome (MIRAS)	POLG-related mutations	Sensory and cerebellar ataxia
Pearson syndrome	Single, large-scale mtDNA deletion or rearrangements of mtDNA	Anemia, pancreatic dysfunction, pancytopenia and renal tubulopathy
Congenital lactic acidosis (CLA)	nDNA, *de novo* or inherited mtDNA point mutations	Progressive neuromuscular weakness and accumulation of lactate in the blood
Myoclonic epilepsy myopathy sensory ataxia (MEMSA)	POLG-related mutations	Epilepsy, seizures, dysarthria, dementia, spasticity and myopathy
Adult-onset		
Leber hereditary optic neuropathy (LHON)	Mutations in mtDNA	Subacute painless bilateral visual loss
Mitochondrial myopathy, encephalopathy, lactic acidosis and stroke-like episodes (MELAS)	Mutations in mtDNA	Stroke-like episodes, deafness, cardiomyopathy, cerebellar ataxia, seizures, encephalopathy, lactic acidosis and mitochondrial myopathy
Mitochondrial neurogastroinstestinal encephalopathy (MNGIE)	mtDNA deletions and depletions due to mutations in TYMP gene encoding thymidine phosphorylase	Gastrointestinal dysmotility, muscle weakness and atrophy, neuropathy and retinopathy

Kearns-Sayre syndrome	Single, large-scale mtDNA deletion	Pigmentary retinopathy, cerebellar ataxia, myopathy, cardiac conduction abnormalities, diabetes and dementia.
Myoclonic epilepsy with ragged red fibers (MERRF)	Mutations in mtDNA	Progressive myoclonic epilepsy, ataxia and weakness
Neurogenic muscle weakness, ataxia and retinitis pigmentosa (NARP)	Mutations in mtDNA	Sensorimotor neuropathy, ataxia and pigmentary retinopathy, seizures, learning disability, dementia, proximal neurogenic muscle weakness
Secondary mitochondrial diseases		
Disease	**Etiology**	**Clinical features**
Friedreich's ataxia	Mutations in *FXN* (frataxin gene)	Ataxia, muscle weakness, cardiomyopathy
Wilson's diseases	Mutations in *ATP7B* (copper-transporting ATPase 2 gene)	Hepatic disease due to copper deposition, ataxia, tremor, depression
Spinal muscular atrophy	Mutations in *SMN1* (survival motorneuron 1 gene)	Hypotonia and muscle weakness due to loss of motoneurons
Drug-induced mitotoxicity	Propofol, statins, doxoribucin, risperidone, acetaminophen	Most affected organs are usually the liver, heart, and skeletal muscle

whereas SMDs involve germline mutations in genes not directly involved in OXPHOS function or production that secondarily produce a mitochondrial malfunction. In addition, SMDs can also be caused by external factors that alter mitochondrial functioning. PMD and SMD classification can sometimes be blurred due to overlapping patient's signs and symptoms, but the distinction is important since they usually require different therapeutic approaches to reduce morbidity and mortality when a non-mitochondrial etiology is behind the primary disease as ocurrs in SMDs (Niyazov et al., 2016). Furthermore, PMDs can also be classified according to childhood or adult-onset and divided into different syndromes/conditions depending on clinical features (Ylikallio and Suomalainen, 2012; Gorman et al., 2016; Ng et al., 2021). The most detailed studies suggest that the prevalence in children below 16 years of age is 5-15 cases per 100.000 individuals and ≈ 23/100.000 for adults. The latter includes both individuals with MD and those at risk of developing any form of MD (Gorman et al., 2015).

The huge number of different disease etiologies of PMDs, which involve different defects in mitochondrial biology that finally impact OXPHOS (**Figure 2**), explains the high degree of heterogeneity and the difficulty to establish effective treatments (Ylikallio and Suomalainen, 2012; Gorman et al., 2016). Not only different mutations can result in different clinical features, but also the same mutation, especially relevant in the case of mtDNA-related mutations with different levels of heteroplasmy (White et al., 1999), might lead to different disease penetrance and severity. The central nervous system (CNS) and muscles are the most affected tissues since they have elevated energy requirements that rely on correct OXPHOS function, but PMDs can encompass dysfunction of any organ or tissue (**Figure 3**) (Ylikallio and Suomalainen, 2012; Gorman et al., 2016). Pathophysiological mechanisms vary depending on the specific mutations, showing organ, tissue and even cell-type specificity. The complexity that characterizes PMDs turns almost into an entelechy to find a single treatment for PMDs with similar clinical features and reinforces the idea of the need to investigate the pathological mechanisms defined by specific mutations (Ylikallio and Suomalainen, 2012; Gorman et al., 2016; Russell et al., 2020).

1.3.1 Leigh syndrome

1.3.1.1 History, definition and clinical features

Leigh syndrome (LS) (OMIM 25600), also referred to as subacute necrotizing encephalopathy, is a primary mitochondrial disease that was first described in 1951 by the neuropathologist Dr. Denis Archibald Leigh. Back then, he reported the case of a 7-months-old boy that developed normally until 6 weeks before the hospital admission date, when clinical signs began. The patient progressively worsened until his death 4 days after admission. Symptoms included: lethargy, sweating, optic atrophy with non-reactive pupils, and spastic limbs. The neuropathological evaluation revealed necrotic symmetrical focal lesions from thalamus to pons, the inferior olive, and the posterior columns of the spinal cord accompanied by vascular and astroglial proliferation (Leigh, 1951). Since this first report, the knowledge of this condition has increased substantially regarding clinical features, diagnosis, genetic etiology, pathophysiology mechanisms, and patient`s management, but despite these advances no effective treatments are currently available (Schubert and Vilarinho, 2020).

LS has an estimated prevalence of 1 case per 40.000 individuals (Rahman et al., 1996). Some founder effects have been described in Ashkenazi Jews (Assouline et al., 2012), Feroe Islanders (1:1700) (Ostergaard et al., 2007),

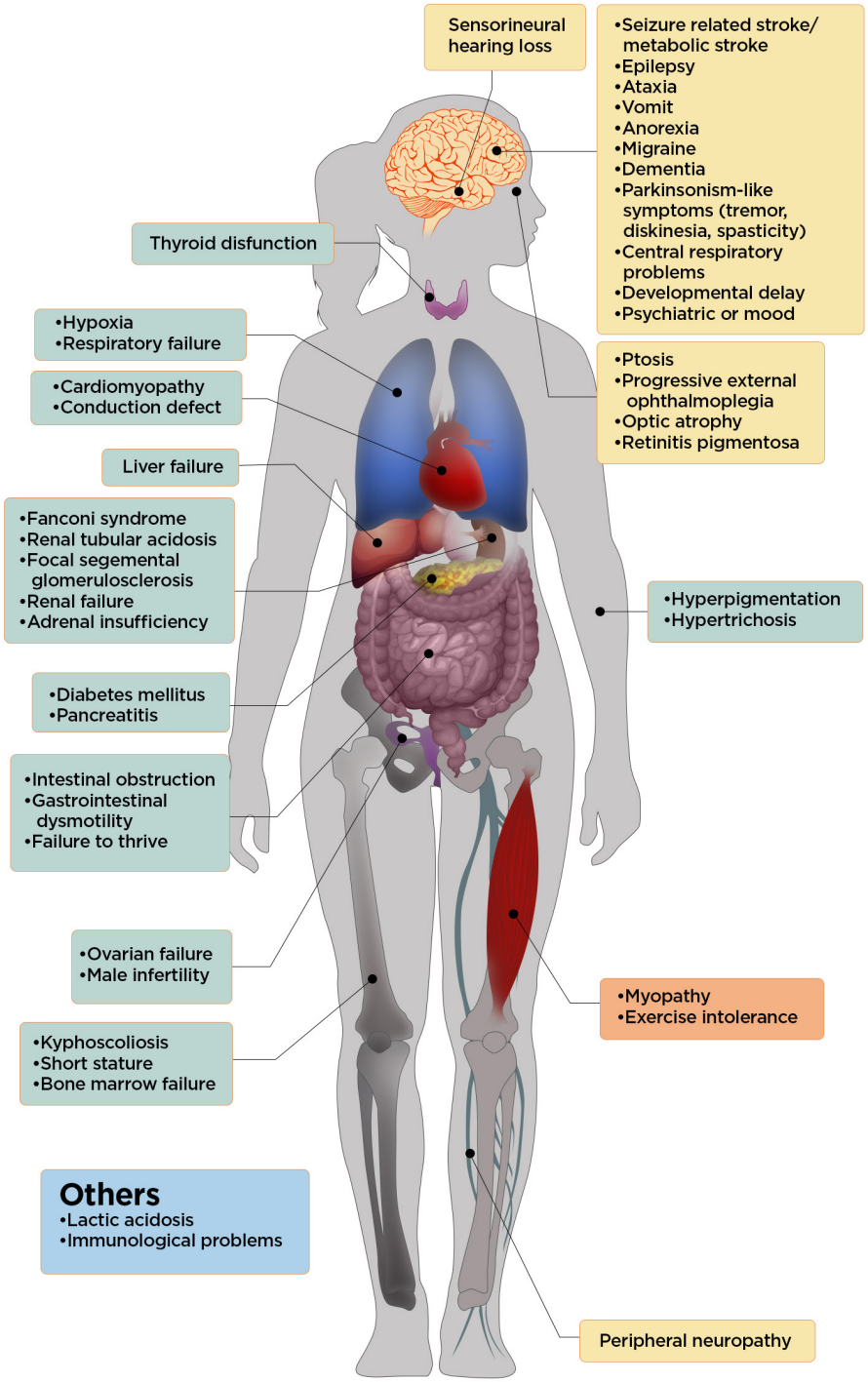

Figure 3. Clinical signs that can be found in patients with a mitochondrial disease.

While any type of organ or tissue can be affected (green), most mitochondrial diseases mainly manifest neurological (yellow) and/or muscular symptoms (orange).
Adapted from Gorman et al 2016.

and the Canadian region of Saguenay-Lac-Saint-Jean (1:2000) (Morin et al., 1993). Like all the major syndromes defined as PMDs, LS is a relatively heterogeneous disease. Usually disease onset starts at 2 years of age after an initial period of normal development followed by a physiological challenge (i.e., infection, surgery) and has a fatal prognosis with a mean survival of 2 years after the first symptoms (Sofou et al., 2014). Most patients mainly present a neurological clinical picture that includes: neurodevelopmental delay, epilepsy, respiratory abnormalities, ataxia, hypotonia, motor polyneuropathy, optical atrophy, and lactic acidosis in cerebrospinal fluid (CSF) (Sofou et al., 2014; Schubert and Vilarinho, 2020). T2-weight neuroimaging reveals symmetrical hyperintense images in brainstem and/or basal ganglia, but lesions can also be found in cerebellum, spinal cord, white matter, and thalamus. Histologically, lesions are characterized by necrotic tissue damage, vacuolation, demyelination, gliosis, and vascular proliferation. Despite being mainly neurologic, *classical* LS can also affect almost any organ or tissue. This typical neuropathological presentation led to the proposal, in 1996, of the following stringent criteria for LS diagnosis (Rahman et al., 1996), subsequently revised in 2016 (Lake et al., 2016):

1. Clinical features compatible with brainstem and/or basal ganglia dysfunction.
2. rogressive neurodegenerative disease with motor and intellectual development delay.
3. Severe deficits in the activity of OXPHOS or pyruvate dehydrogenase complex, mutations in genes related to mitochondrial energetic machinery, and elevated lactate in CSF or blood serum.

Adult manifestations of LS are rare and more heterogeneous compared to those of infantile-onset (McKelvie et al., 2012). The pathology onset ranges from the early stages of adulthood until the elderly, and, in some cases, can be accompanied by a lethal fast progressive disease (within weeks/months) (McKelvie et al., 2012; Sofou et al., 2014). The clinical picture may include psychiatric disorders, intellectual decline, ataxic behaviors, memory loss, headache, and multiple sclerosis-like phenotype.

When both pediatric and adult patients just partially fulfill the aforementioned criteria and present non-neurological symptoms (cardiac, gastro-intestinal, hepatologic, or hematological) a diagnosis of Leigh-like syndrome (L-LS) can be considered, particularly in patients with an atypical neurodegenerative process or unaffected lactate levels (Rahman et al., 1996; Sofou et al., 2014; Lake et al., 2016).

1.3.1.2 Etiology

Leigh syndrome is caused by genetic mutations in genes related to essential mitochondrial functions, being the most common those that produce errors of metabolism due to OXPHOS dysfunction. The first links of LS to mitochondrial energy metabolism were reported during the '60s and '70s. In the course of these two decades, a lack of pyruvate carboxylase activity and deficiencies in pyruvate decarboxylase, pyruvate dehydrogenase complex, and cytochrome c were described in patients with LS, but it was not until 1991 when the first genetic mutation, in the lysine transfer RNA mitochondrial gene, was identified (Hammans et al., 1991). To date, more than 75 genes have been related to the appearance of any form of LS (**Table 2**) and each of those genes can present different types of mutations (Lake et al., 2016). Mutations in nDNA genes represent 80% of LS cases, whereas mtDNA mutations represent 20%. In addition, the most frequent causes of LS are mutations in complex I, accounting for 34% of the total cases. The vast number of genetic etiologies explains the clinical heterogeneity of LS similarly to the one found in other PMDs (Rahman et al., 1996).

1.3.1.3 Available treatments for Leigh syndrome

No effective treatments are currently available for patients with Leigh syndrome. The main clinical management of patients is based on symptomatic therapy (a medical therapy of a disease that only affects its symptoms and not the underlying cause), so therapeutic strategies are mainly focused on ameliorating symptoms in order to improve the patient's quality of life (Baertling et al., 2014; Gerards et al., 2016). In any case, the aforementioned genetic and clinical heterogeneity must always be considered when treating patients, because depending on the specific genetic etiology of the diseases, not all treatments are valid.

Usually, the treatment consists of the administration of a combination of dietary supplements (coenzyme Q10, L-carnitine, α-lipoic acid, creatine-monohydrate, biotin, pyruvate, thiamine, and riboflavin) and dietary interventions (ketogenic diet or reduction of dietary valine). The main rationale for the use of these strategies is explained by their antioxidant properties, their function as OXPHOS cofactors, or their ability to restore some metabolites imbalance. Some of the effects of these interventions include: increasing the electron flux in the ETC, the ATP synthesis, or the β-oxidation of fatty acids as well as reducing the lactic acidosis or the accumulation of mitochondrial metabolite intermediates (Baertling et al., 2014; Gerards et al., 2016; Lee et al., 2020; Schubert and Vilarinho, 2020).

Table 2. nDNA and mtDNA mutations affecting mitochondrial biology that are described to cause Leigh or Leigh-like syndrome in humans.

NDUFS4 is highlighted in bold due to its importance for this thesis.

Adapted from Schubert and Vilarinho 2020.

	Affectation	Mutated gene/s
Mutations in nDNA	Complex I subunit/assembly factor	*NDUFA1, NDUFA2, NDUFA9, NDUFA10, NDUFA12, NDUFS1, NDUFS2, NDUFS3, NDUFB8,* ***NDUFS4****, NDUFS7, NDUFS8, NDUFV1, NDUFV2, NDUFAF2, NDUFAF4, NDUFAF5, NDUFAF6, C17ORF89, FOXRED1, NUBPL*
	Compl ex II subunit/assembly factor	*SDHA, SDHAF1*
	Complex III subunit/assembly factor	*UQCRQ, BCS1L, TTC19*
	Complex IV subunit/assembly factor	*NDUFA4, COX8A, SURF1, COX10, COX15, SCO2, PET100*
	Pyruvate Dehydrogenase Complex deficiency	*PDHA1, PDHX, PDHB, DLAT, DLD*
	Biotinidase deficiency	*BTD*
	Thiamine deficiency	*TPK1, SLC19A3*
	Lipoic acid deficiency	*LIPT1, LIAS, BOLA3*
	Amino acid	*HIBCH, ECHS1*
	Coenzyme Q10 deficiency	*PDSS2, COQ9*
	Mitochondrial DNA maintenance	*FBXL4, POLG, POLG2, SUCLA2, SUCLG1, TWNK, SLC25A4, MPV17*
	Mitochondrial translation	*GTPBP3, TRMU, EARS2, FARS2, IARS2, GFM1, GFM2, LRPPRC, TACO1, MTFMT, C12Orf65, MRPS34, MRPS39 (PTCD3), NARS2, TSFM*
	Mitochondrial dynamics dysfunction	*SLC25A46, DNM1L, MFN2, RRM2B*
	Mitochondrial material import/export	*SLC25A19*
	Membrane phosphocomponents	*SERAC1*
	Sulfur dioxygenase	*ETHE1*
	AAA oligomeric +/– ATPase	*CLPB, SPG7*
	RNA import	*PNPT1*
	RNA-specific adenosine deaminase	*ADAR, RNASEH1*
	Nuclear translocation system	*RANBP2*
	Nuclear pore complex	*NUP62*
	Manganese transportation	*SLC39A8*
Mutations in mtDNA	Complex I subunit	*ND1, ND2, ND4, ND4L, ND5, ND6*
	Complex III subunit	*CO-III*
	Complex V subunit	*ATP6*
	tRNA	*MT-TK, MT-TL, MT-TV, MT-TW*

1.3.1.4 Current clinical trials

Thanks to the development of valuable preclinical models during the past years, the understanding of the Leigh syndrome pathology has increased. Unfortunately, this knowledge has not been yet reflected in new treatments for patients. Moreover, just a few clinical trials in patients with Leigh syndrome are currently ongoing according to the U.S. National Institutes of Health (NIH) data base (https://www.clinicaltrials.gov).

1. Using vatiquinone (EPI-743), a drug based on vitamin E that has been shown to improve the function of cells with defective mitochondria (phase 3, NCT05218655).
2. Using sonlicromanol (KH176), a drug that acts as a ROS modulator (phase 2, NCT04846036).

1.4 NDUFS4, a complex I subunit

Complex I, first named as NADH:ubiquinone oxidoreductase, is the first component of the ETC. It regenerates the NAD^+ pool oxidizing NADH to sustain the TCA and fatty-acid oxidation. As a result, it supplies ubiquinol for the rest of the ETC by reducing ubiquinone with the donor electrons and using the energy of the redox reactions to pump four protons across the membrane, essential to generate the $\psi\Delta m$ (Agip et al., 2019; Vercellino and Sazanov, 2021). Mammalian complex I contains 45 subunits: 14 homologs subunits found from bacteria to humans and 31 accessory subunits accumulated in the course of evolution (**Figure 4**). NDUFS4 (NADH dehydrogenase ubiquinone iron-sulfur protein 4) is a small (18 kD) accessory subunit of the complex I (**Figure 4**), and mutations in the nuclear gene encoding NDUFS4 have been described to produce LS (**Table 2**) (Fassone and Rahman, 2012; Kahlhöfer et al., 2021).

Several pieces of evidence suggest that NDUFS4 has functions in the stabilization and assembly of complex I. Blue native PAGE (polyacrylamide gel electrophoresis) studies in skin fibroblast of patients with NDUFS4 mutations revealed abnormal assembly profiles with complete loss of fully assembled CI, and only a sub-assembled CI of 830 kD, apparently catalytically inactive, was detected (Assouline et al., 2012). Moreover, both fibroblasts from patients and tissues from mice have reduced levels of CI structural subunits but do not present a reduction of other complexes subunits (CII-CV) (Assouline et al., 2012; Calvaruso et al., 2012). Importantly, despite these shortcomings, partial complex I activity could still be measured. This phenomenon could be explained by the formation of supercomplexes (Calvaruso et al., 2012).

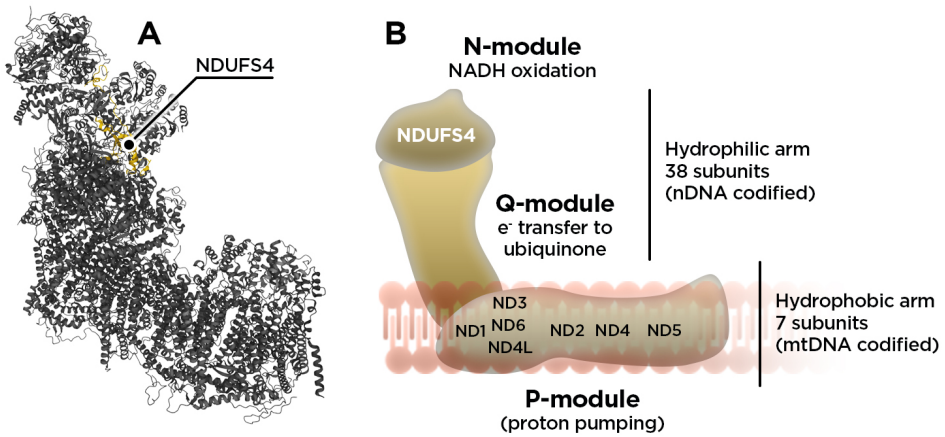

Figure 4. Mammalian complex I structure and NDUFS4 location. (A,B).

In mammals, complex I has an L-shape structure with one hydrophobic arm (containing 7 subunits encoded by mtDNA) and one hydrophilic arm (with 38 subunits, of which 37 are unique, encoded by nDNA). Moreover, it can be subdivided into three different modules based on their functions: The P-module that pumps protons across the IMM, the Q-module responsible for transferring electrons to ubiquinone, and the N-module that oxidizes NADH. NDUFS4 subunit belongs to the N-module. **(A)** Mammalian complex I structure (*Ovis aeris*) taken from Protein Data Bank (6ZKC). **(B)** *Adapted from Agip et. al 2019.* NDUFS4: NADH:Ubiquinone oxidoreductase subunit S4; ND1-6: NADH:Ubiquinone oxidoreductase core subunits.

In *Ndufs4 KO* mice tissues, CIII partially stabilizes CI in supercomplexes ($CI+CIII_2$) in the absence of NDUFS4 and provides partial CI activity, whereas other supercomplexes are absent ($CI+CIII_2+CIV_{1-4}$)(Calvaruso et al., 2012). Noteworthy, an important factor to consider when studying ETC components is the potential introduction of preparation artifacts that can hinder the study of the *in vivo* situation. Compromised CI stability due to the absence of NDUFS4 could explain the null CI activity found in some reports. To overcome this limitation, studies in yeast, which have a more stable CI, found that deletion of the NDUFS4 ortholog in yeast (NUYM) disturbed the iron-sulfur cluster of the electron input domain decreasing CI activity (Kahlhöfer et al., 2017). Taken together, the experimental data clearly suggest that NDUFS4 is necessary for correct CI function by playing a role in the stabilization and assembly of the fully functional mature complex.

1.4.1 *Ndufs4 KO* mouse as a model of Leigh syndrome

Mice lacking NDUFS4 were generated in 2008 in Dr. Richard Palmiter's laboratory by excision of the exon 2 of the *Ndufs4* gene (Kruse et al., 2008). In mice, exon 2 encodes for a part of the mitochondrial targeting sequence and the 17 first amino acids of the mature protein. The excision of exon 2 produces a frameshift that impedes the formation of the NDUFS4 mature protein (Kruse et al., 2008). As expected, *Ndufs4 KO* mice have reduced CI

activities in all tissues analyzed when compared to wildtype (WT) mice: 44% in the heart, 29% in muscle, 25% in the kidney, 19% in the liver, 17% in the pancreas, 26% in whole-brain, and 9% in the lung (Calvaruso et al., 2012).

Of note, other whole-body NDUFS4 deficient mice have been generated in the past years using different strategies. Essentially, total knockouts were phenotypically similar to *Ndufs4 KO* mice, but not always identical (Ingraham et al., 2009; Leong et al., 2012; Wang et al., 2017; Emmerzaal et al., 2020). Since the original *Ndufs4 KO* mouse is the one extensively used and the object of this thesis, most of the attention will be paid to this particular NDUFS4 deficient model.

1.4.1.1 CNS affectation, the deadly phenotype

The *Ndufs4 KO* mouse recapitulates most of the aspects of human LS brain pathology (**Table 3**) and has been broadly accepted as a relevant mouse model of LS (van de Wal et al., 2022). *Ndufs4 KO* mice develop a progressive encephalopathy with neuronal loss and strong neuroinflammation beginning at postnatal day P30 that finally produces the death of the animal at around P55 (Kruse et al., 2008; Quintana et al., 2010). The disease progression in *Ndufs4 KO* mice can be subdivided into three different stages in which clinical signs increase in severity: early stage (P0–P29), mid stage (P30–41), and late stage (over P41) (Quintana et al., 2010).

Table 3. Clinical signs present in patients with LS and *Ndufs4 KO* mice.
Adapted from Bolea et al 2019.

Clinical signs	Patients with LS	*Ndufs4 KO* mice
Decreased lifespan	Yes	Yes
Ataxia, motor alterations	Yes	Yes
Problems to thrive	Yes	Yes
Growth retardation	Yes	Yes
Respiratory abnormalities	Yes	Yes
Seizures	Yes	Yes
Hypotonia	Yes	Yes
Brainstem lesions	Yes	Yes, abundant
Basal ganglia lesions	Yes	Yes, moderate
Olfactory bulb lesions	Not described	Yes, abundant
Vestibular nuclei	Yes/dorsal brainstem	Yes, abundant

During the course of the disease, *Ndufs4 KO* mice manifest growth retardation, decreased body weight, ataxia, paw paralysis, seizures, and respiratory abnormalities (Kruse et al., 2008; Quintana et al., 2010, 2012b; Johnson et al., 2013). Moreover, *Ndufs4 KO* mice are hypersensitive to volatile anesthetics and propofol but resistant to ketamine (Quintana et al.,

2012a). The main symptoms have been shown to have a neurological origin since Cre-driven *Ndufs4* deletion in neurons and glia (Nes-KO) essentially demonstrated the same phenotype as systemic *Ndufs4 KO* mice (Quintana et al., 2010). *Ndufs4 KO* mice present marked regional neurodegeneration with the vestibular nuclei (VN), olfactory bulb (OB), brainstem (BS), basal ganglia, and cerebellum (Quintana et al., 2010; Johnson et al., 2013) being the most affected regions; which in many cases is consistent with observations in human patients with LS (**Table 3**) (Arii and Tanabe, 2000; Lake et al., 2016). *Ndufs4 KO* mice also present neurodegeneration in the retina, where abundant retinal ganglion cell loss has been described (Yu et al., 2015).

We currently know that defined neuronal populations contribute differently to drive the phenotype of *Ndufs4 KO* mice. Thus, loss of NDUFS4 in glutamatergic neurons is responsible for VN, BS, and cerebellar pathology, leading to ataxia, motor alterations, and respiratory abnormalities as well as being responsible for the sensitivity to volatile anesthetics, whereas its loss in GABAergic neurons is responsible for OB and basal ganglia lesions, and the appearance of the seizures (Zimin et al., 2016; Bolea et al., 2019). *Ndufs4* loss in striatal medium spiny neurons produced a slight progressive motor impairment with no apparent neuronal loss (Chen et al., 2017). In contrast, cholinergic or dopaminergic neuron-specific *Ndufs4 KO* mice did not show a phenotype compared to WT mice (Choi et al., 2017; Bolea et al., 2019). This selective susceptibility to neurodegeneration could be partially explained by especially low CI activities, (when compared to WT) in lesion-prone areas (14% in OB, 25% in BS, and 28% in cerebellum) with respect to non-neurodegenerative areas (62% in the anterior cortex)(Terburgh et al., 2021a), but these pieces of evidence must be taken with caution since CI activities were measured in late stage animals, where lesion prone areas have a high number of reactive glial cells (microglia and astrocytes) that are not present in non-lesioned areas, potentially explaining these differences. In any case, the selective neuronal susceptibility to NDUFS4 deficiency remains somewhat a mystery.

Since neuroinflammation, mainly microgliosis and astrogliosis, has been established as a hallmark of the disease in regions where neurodegeneration occurs in *Ndufs4 KO* mice (Quintana et al., 2010), it is surprising that it has never been studied *per se* as a contributor to the disease. This is remarkable because neuroinflammation and neuroimmune responses are: (i) widely known contributors to the pathology in neurodegenerative diseases (Colonna and Butovsky, 2017); (ii) the main gene ontology processes upregulated in *Ndufs4 KO* brains (Balsa et al., 2020; Perry et al., 2021); and (iii) have

been shown to be reduced by all interventions that ameliorate *Ndufs4 KO* phenotype (Johnson et al., 2013; Martin-Perez et al., 2020; Perry et al., 2021) (**Table 4**).

1.4.1.2 Effects of NDUFS4 deficiency in peripheral tissues

Growth is severely compromised due to OXPHOS deficient function in *Ndufs4 KO* mice, as a consequence, they have dramatical reduced body weight and size. Moreover, *Ndufs4 KO* mice develop alopecia starting at ≈P16 with a peak around P20-24 followed by a complete regrowth of hair after this period. Alopecia is mainly explained by systemic inflammation with extensive recruitment of monocytes and macrophages into the skin. *Ndufs4 KO* mice also present increased inflammatory markers in the liver, bone marrow, spleen, and serum. This process is in part mediated by TLR2/4 signaling which leads to a systemic increase in macrophage numbers towards a pro-inflammatory state at early ages (Jin et al., 2014). In addition, global NDUFS4 deficiency decreased bone resorption and increased bone mass (Jin et al., 2014). *Ndufs4 KO* mice also have a slight cardiac pathology. They present hypertrophic cardiomyopathy with an increased heart-to-body weight ratio and also aberrant and increased number of cardiomyocytes (Reynaud-Dulaurier et al., 2020). Importantly, some patients with mutations in NDUFS4 also develop cardiomyopathy (Ortigoza-Escobar et al., 2016). Interestingly, *Ndufs4* conditional KO in the heart did not produce any evident cardiac pathology at one year of age (Karamanlidis et al., 2013; Zhang et al., 2018) highlighting the complexity and pathological interplay between different tissues in the whole-body knockout. However, despite no evident pathology in basal conditions, heart-specific *Ndufs4 KO* mice developed accelerated heart failure after pressure overload or repeated pregnancy (Karamanlidis et al., 2013). Regarding skeletal muscle, decreased CI activity was found in isolated mitochondria (Calvaruso et al., 2012) as well as whole-tissue metabolite imbalance (Terburgh et al., 2021b), and some histological abnormalities (Kruse et al., 2008).

1.4.2 Main pathological contributors described in *Ndufs4 KO* mice: focus on oxygen and mTOR

During the past decade, increasing knowledge has been gained regarding the pathological mechanism operating in *Ndufs4 KO* mice. Usually, this knowledge has been obtained by using different interventions or treatments that target specific biological processes and evaluating their impact on the *Ndufs4 KO* phenotype (**Table 4**). Some of the interventions can exert multiple effects that could potentially explain the benefits.

Table 4. Most remarkable interventions in *Ndufs4 KO* mice summarizing both the benefit and target of the intervention.

Intervention	Benefit of the inervention	Intervention target/ effect	Refs.
Ketogenic diet	**None**	Carbohydrate/ Lipid metabolism	Bornstein et al., 2022
OPA1 overexpression	↑	Mitochondrial dynamics	Civiletto et al., 2015
Rapamycin	↑↑↑	mTORC1 inhibition	Johnson et al., 2013
Hypoxia	↑↑↑	Reduced O_2	Jain et al., 2016, 2019; Ferrari et al., 2017
Phlebotomy	↑↑↑	Reduced O_2	Jain et al., 2019
AAV gene therapy	↑↑↑	Gene replacement	Reynaud-Dulaurier et al., 2020; Corrà et al., 2022
Doxycycline	↑↑	Mitochondria protein synthesis inhibition, inhibition of microglia reactive state	Perry et al., 2021
Fenofibrate	↑	Lipid metabolism	Schirris et al., 2021
AD4	↑	Antioxidant	Liu et al., 2015
PLX3397*	↑↑/↑↑↑ **depending on dose**	Inhibitor of CSF1R (also of c-Kit), microglia/leukocyte depletion	Aguilar et al., 2022; Stokes et al., 2022
IPI-549	↑↑	PI3K-γ catalytic subunit inhibitor	Stokes et al., 2022
GO6983, GF109203X, and ruboxistaurin	↑↑	Inhibition of PKC	Martin-Perez et al., 2020
GPD1 overexpression	↑↑	Increases Glycerol-3-phosphate biosynthesis, regeneration of cytosolic NAD^+	Liu et al., 2021

The number of arrows indicates the extent of the benefits derived from the intervention in terms of survival and motor phenotype. ↑: low-mild improvement; ↑↑: considerable improvement; ↑↑↑: extensive improvement. **AD4**: N-acetylcysteine amide; **c-KIT**: KIT proto-oncogene receptor tyrosine kinase; **CSF1R**: colony stimulation factor receptor 1; **GPD1**: Glycerol-3-Phosphate Dehydrogenase 1; **mTORC1**: mammalian target of rapamycin complex 1; **OPA1**: optic atrophy gene 1; **PI3K-γ**: Phosphoinositide 3-kinase isoform γ; **PKC**: protein kinase C; **PLX3397**: pexidartinib.

*** Described in this thesis project.**

Thus, for some of the treatments we still do not have a clear understanding of the precise mechanisms beyond their beneficial effects. This is the case when targeting oxygen availability and the mammalian target of rapamycin (mTOR), two of the interventions that extended survival and ameliorated *Ndufs4 KO* pathology the most (Johnson et al., 2013; Jain et al., 2016; Ferrari et al., 2017).

1.4.2.1 Oxygen

Molecular oxygen (O_2) is the last electron acceptor of the ETC that together with hydrogen finally forms water (Mitchell, 1961). Indeed, 90% of the breath oxygen is used as an ETC substrate (Rich, 2003). In physiological conditions, around 0,2% to 2% of electrons that go through the ETC do not finally reduce O_2, but instead, produce superoxide radicals (O_2^-). Superoxide is a reactive oxygen species (ROS) and the main precursor of other ROS. In the cell, both CI and CIII are the main source of ROS (Murphy, 2009). Despite ROS have important roles in cell signaling and homeostasis, they are highly toxic molecules that can lead to oxidative damage in membranes, DNA, RNA, or proteins. To avoid these undesired consequences, cells have a complex antioxidant network that limits ROS concentration, but when the production of ROS exceeds the buffering capacity of cells, oxidative stress ensues, and consequences can be fatal (Murphy, 2009; Schieber and Chandel, 2014).

In normoxic conditions (21% O_2), *Ndufs4 KO* mice oxygen consumption is impaired, which in turn, produces increased brain oxygen levels. Strikingly, exposing *Ndufs4 KO* mice to a hypoxic environment (11% O_2) normalized brain oxygen levels, extended the median survival until P270, and dramatically prevented neuropathology, whereas exposure to hyperoxia (55% O_2) produced the death of mice within days (Jain et al., 2016; Ferrari et al., 2017). Furthermore, other interventions that reduce brain oxygen levels, such as phlebotomy-induced anemia or exposure to carbon monoxide, are also effective in preventing *Ndufs4 KO* neuropathology (Jain et al., 2019). Whether the hypoxic response program is necessary for pathology rescue during hypoxic conditions is yet unknown (Jain et al., 2019). Indeed, chronic activation of the canonical hypoxic response (vHL-PHD-HIF) was insufficient to rescue *Ndufs4 KO* disease.

Despite O_2 toxicity seems to be dramatically responsible of the *Ndufs4 KO* pathology, the precise mechanism/s by which these elevated oxygen levels are harmful remain mostly unknown. Since previous research has shown that the formation of superoxide radical in isolated mitochondria is highly dependent on the levels of oxygen (Stepanova et al., 2019), it has

been speculated that the increased brain oxygen levels of *Ndufs4 KO* mice might increase oxidative stress (Jain et al., 2019). Indeed, one study found increased generation of superoxide radical in the cerebellums of *Ndufs4 KO* mice by using a two-photon fluorescence probe (Lyu et al., 2022). In addition, elevated ROS levels have also been found in less complex models of NDUFS4 deficiency. NDUFS4-deficient primary mouse fibroblasts and NDUFS4-homolog (*ldp-5*) depleted *Caenorhabditis elegans* showed increased levels of ROS (Valsecchi et al., 2013; Maglioni et al., 2022). Moreover, ROS accumulation has been described to be pathogenic in several *Drosophila melanogaster* mitochondrial mutants, where a ROS-activated route in neurons prior to neuronal loss onset causes lipid droplet (LD) formation and peroxidation in glial cells favoring neurodegeneration (Liu et al., 2015). A similar pathway of LD accumulation was also observed in microglia and astrocytes of *Ndufs4 KO* mice in all disease stages suggesting an evolutionarily conserved phenomenon (Liu et al., 2015).

Importantly, increased levels of ROS can affect processes that are tightly regulated by redox signaling like inflammation. A slight elevation of ROS levels is necessary for a proper inflammatory response (both innate and adaptative). Yet, when very high, they can induce hyperactivation of the inflammatory responses (D'Autréaux and Toledano, 2007; Mittal et al., 2014; Schieber and Chandel, 2014). This is not only applicable to peripheral tissues, but also to the CNS. ROS are important regulators and, in some cases, inducers of microglial activation (Rojo et al., 2014), which is the main immune cell type of the brain. In addition, ROS have been widely involved in the pathogenicity of neurodegenerative diseases like Alzheimer's disease or Parkinson's disease (di Filippo et al., 2010; Rojo et al., 2014). Unfortunately, treating *Ndufs4 KO* with antioxidant agents such as N-acetylcysteine amide (AD4) had very low beneficial effects (Liu et al., 2015). Moreover, there are not studies trying to genetically boost the antioxidant response, for instance, by overexpressing antioxidant enzymes. Only one research described that overexpression of metallothionein 1, a protein that protects from oxidative stress consequences, in *Ndufs4 KO* mice did not modify their phenotype (Miller et al., 2020). More research is required to comprehend how the observed neurodegeneration and neuroinflammatory response are caused by these increased oxygen levels and potentially by imbalanced ROS levels.

1.4.2.2 mTOR

mTOR is an evolutionarily conserved serine/threonine protein kinase mainly known for being a master metabolic hub of the cell. At the metabolic level, mTOR acts as a nutritional signaling system having pleiotropic effects

by controlling cell growth, proliferation, and survival via the mTORC1 and mTORC2 complexes. It stimulates anabolic processes such as protein synthesis (translation of mRNA, ribosome biogenesis, etc.) and lipid synthesis while inhibiting catabolic processes such as autophagy (Laplante and Sabatini, 2009). Similarly, mTOR has been linked to mitochondrial metabolic activity and biogenesis (Schieke et al., 2006; Cunningham et al., 2007). Then, the mTOR pathway integrates signals from growth factors, oxygen levels, amino acids, ATP, and ADP to regulate all these processes and adjust them to the metabolic requirements of a particular context (Laplante and Sabatini, 2009). mTOR has been shown to be hyperactivated in several models of MDs including the *Ndufs4 KO* (Johnson et al., 2013; Ising et al., 2015; Khan et al., 2017). Indeed, treating *Ndufs4 KO* mice with rapamycin, a mTORC1 inhibitor, extended median lifespan (≈ P120), and delayed both the onset of symptoms and the development of brain lesions (Johnson et al., 2013). However, the mechanism of the rapamycin rescue remains largely unknown.

Rapamycin has well-documented immune-modulatory properties (Powell et al., 2012), so to test if the improvement was due to its immunosuppressive consequences (mainly abolishing neuroinflammation), Johnson et al., treated *Ndufs4 KO* mice with FK-506 (tacrolimus), an immunosuppressive medication that binds to the same target as rapamycin, FKBP12, but inhibits calcineurin signaling rather than mTOR (Tamura et al., 1994). FK-506 did not influence pathology initiation or progression, showing that the off-target disruption of calcineurin by FKBP12 binding is not likely to account for rapamycin's effects (Johnson et al., 2013). Moreover, they did not find any direct recovery of mitochondrial function upon treatment. They finally proposed, based on metabolomics data, that rapamycin promotes a metabolic shift away from glycolysis and toward amino and fatty acid catabolism, reducing the accumulation of toxic glycolytic intermediates. In another study, rapamycin was found to inhibit signaling through both mTOR complexes, to restore some mitochondrial protein levels, and to reduce the abundance and activity of multiple protein kinase C (PKC) isoforms (Martin-Perez et al., 2020). When *Ndufs4 KO* mice were treated with pan-PKC or PKC-β inhibitors, an extended survival and reduced skin and brain inflammation was observed. Specifically, PKC inhibitors downregulated the NF-κB inflammatory response in the brain. So, the authors propose that rapamycin's effects on PKC and the downstream inflammatory attenuation is, at least to some extent, mediating its beneficial effects (Martin-Perez et al., 2020). Other authors have postulated that the benefits of mTOR inhibition are due to the disturbance of phosphoinositide 3-kinase (PI3K) signaling,

an upstream regulator of mTORC1. By administrating specific inhibitors of different PI3K isoforms, they showed that the inhibition of the PI3K-γ, which is mainly expressed in leukocytes, produced comparable effects to those of rapamycin (Stokes et al., 2022). Despite probable (Dibble and Cantley, 2015), the connections between mTOR inhibition and PI3K signaling or between PI3Kγ inhibition and mTOR signaling are not directly proven in the *Ndufs4 KO* brain context (Stokes et al., 2022). It might be also possible that PI3K inhibition has other effects rather than mTOR signaling modulation that could potentially explain the benefits of the therapy in *Ndufs4 KO* mice.

1.5 Neuroinflammation and neuroimmune responses in brain disorders

The neuroimmune system can be defined as the system responsible for the protection of the nervous system in front of a perturbation of any kind (i.e., injury, infection, or neuronal dysfunction due to genetic mutations) in order to restore homeostasis. Generally, in response to any potential threat, a plethora of innate immune sensors engage a complex biological machinery that involves the activation of different cellular responses and the secretion of different immune mediators to allow cell-to-cell communication (Takeuchi and Akira, 2010; Kigerl et al., 2014; Colonna and Butovsky, 2017; Vainchtein and Molofsky, 2020). This immune-like process is known as neuroinflammation. Importantly, the neuroinflammatory response is not always beneficial, it has been described to be harmful in a variety of situations like aging, cancer, autoimmune diseases, or situation in which the neuroinflammation cannot be switched off because the cause of the response cannot be eliminated (e.g., dysregulation of cellular processes governing the response) or because the perturbation is intrinsically linked to the system (e.g., genetic mutations causing neuronal death). Both situations are particularly relevant in the context of neurodegenerative diseases in which neuroinflammation could end up being noxious. Importantly, neuroimmune components do not only play key roles in neuroinflammation, as occurs with the peripheral immune system in peripheral tissues, they have important roles that are essential for the correct function of the CNS under physiological conditions. Examples of those functions are, among multiple others, the correct development of the CNS, regulation of neuronal activity, trophic support to neurons, or the maintenance of the blood-brain barrier (BBB) (Colonna and Butovsky, 2017; Liddelow and Barres, 2017; Li and Barres, 2018; Han et al., 2021b). The main orchestrators of neuroinflammation are microglia and astrocytes (Vainchtein and Molofsky, 2020).

1.5.1 Main cellular players in neuroinflammation

1.5.1.1 Microglia

Just like the discovery that neurons are the basis for brain function, microglia characterization also had a Spanish father. Pío del Río-Hortega, a Spanish researcher born in a small village of Valladolid, first described microglial cells in 1919 in his collection of four magnificent papers *El "tercer elemento" de los centros nerviosos*. (Río-Hortega, 1919a, 1919b, 1919c, 1919d). More than just describing the presence of these cells in the brain, he also described some of their main features: microglia are highly plastic cells that can migrate, proliferate and phagocyte, especially during pathological conditions when they undergo morphological changes. Moreover, Río-Hortega also hypothesized that microglia are of mesodermal origin (Río-Hortega, 1919c), something that could not be clearly proved until 2010 (Ginhoux et al., 2010).

Microglial are the resident macrophages of the CNS (Li and Barres, 2018). They account for around 10% of the total number of adult CNS cells and present heterogeneous densities and morphologies across different CNS regions (**Figure 5 A**) (Lawson et al., 1990). It was believed for years that microglia had a similar origin as the mononuclear phagocytic system (Ransohoff and Perry, 2009) but *in vivo* linear tracing in mice showed that microglia arise solely from c-KIT^{+}CD45^{-} primitive erythromyeloid progenitors in the yolk sack, in a process dependent on CSF1R, PU.1, and IRF8, that start to invade the developing brain around embrionary day 8.5 (E8.5)(Ginhoux et al., 2010; Kierdorf et al., 2013a). In humans, this process occurs around 4.5 to 5.5 gestational weeks (Andjelkovic et al., 1998). The differentiation of microglia to finally become mature homeostatic cells is a long process that requires multiple steps and the influence of other CNS resident cells which are essential for microglia to acquire and maintain their homeostatic signature (Baxter et al., 2021; Borst et al., 2021; Prinz et al., 2021). Microglial functions go far beyond immunity; they have been described to participate in key processes during CNS development and function. Some of these functions include: (i) supporting neurogenesis, oligodendrogenesis, vasculogenesis, and myelination, (ii) ensuring correct BBB function and its adaptation to physiological needs, (iii) monitoring and pruning synapses, or (iv) regulating neuronal connectivity and activity. For all these functions to correctly occur, microglia do not only rely on their ontogeny; bidirectional communications with the rest of the cells that integrate the CNS are essential (Lenz and Nelson, 2018; Sierra et al., 2019; Borst et al., 2021; Prinz et al., 2021).

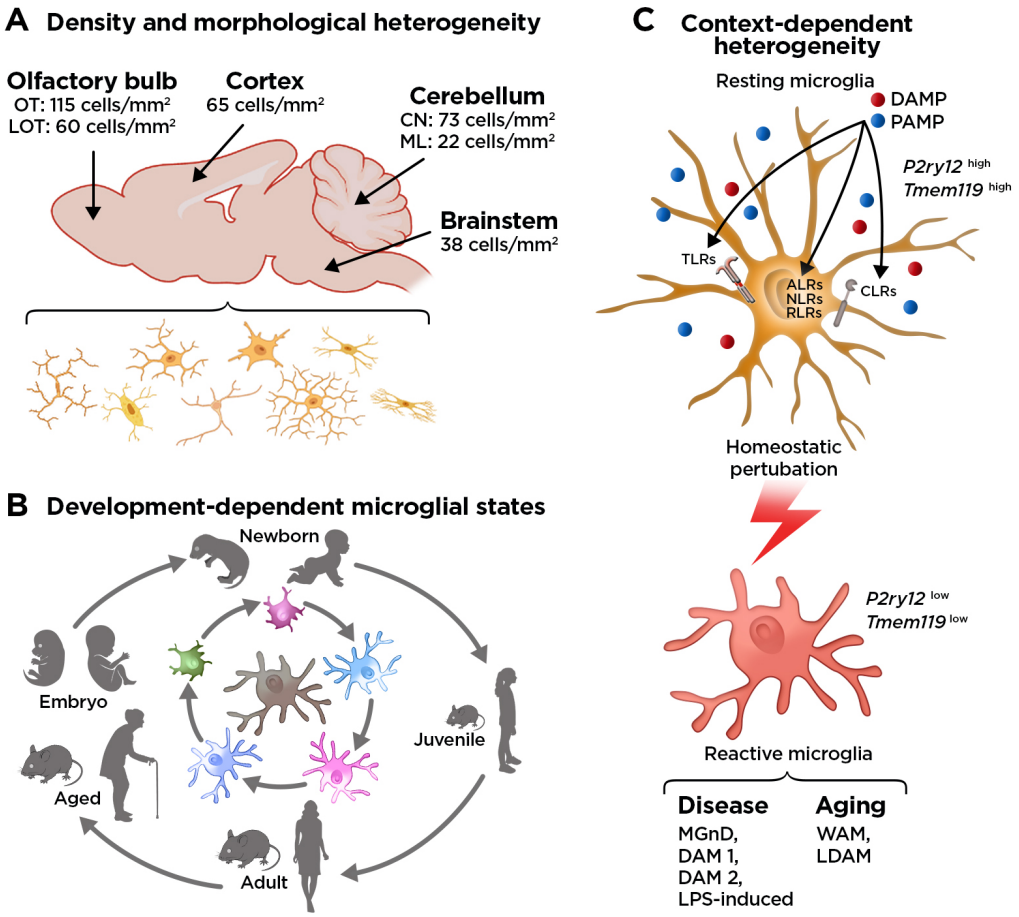

Figure 5. Different levels of microglial heterogeneity in mice.

(A) Microglia present density and morphological heterogeneity across different brain regions. Density and morphology vary substantially even within the different parts of a particular brain region (e.g., olfactory bulb or cerebellum). Microglial cell densities were taken from Lawson et al 1990. **(B)** Different microglial states (at least at the transcriptomic level) arise at different developmental and age time points. **(C)** Resting microglia have a high expression of homeostatic microglial genes such as *P2ry12* and *Tmem119* that decreases dramatically once microglia become reactive. Microglial cells are able to sense a wide range of homeostatic perturbations trough pattern recognition receptors. These receptors can recognize a plethora of PAMP and DAMP molecules that allow microglia to become reactive. The specific characteristics of a given homeostatic disruption generate different microglial subsets, some of which have been mainly characterized based on their transcriptomic signature. ALR: AIM2-like receptor; CLR: C-type lectin receptor; CN: cerebellar nuclei; DAM: disease-associated microglia; LDAM: lipid-droplet-accumulating microglia; LOT: lateral olfactory tract; LPS: lipopolysaccharide; MGnD: neurodegenerative microglia; ML: molecular layer of the cerebellum; NLR: Nod-like receptor; OT: olfactory tubercle; *P2yr12*: purinergic receptor P2Y12 gene; RLR: RIG-like receptor; TLR: Toll-like receptor; *Tmem119*: transmembrane protein 119 gene; WAM: white matter-associated microglia. **(B)** *Adapted from Prinz et al 2021.*

In resting conditions, adult microglia are highly ramified and motile cells distributed in nonoverlapping territories within the CNS parenchyma and characterized by high expression of *Tmem119, P2ry12, P2ry13, Hexb, Csf1r,* and *Cx3cr1* genes (Li et al., 2019). Indeed, *ex vivo* manipulation of microglial cells drastically changes their morphology and transcriptomic profile, which are rapidly re-acquired when cells are exposed again to a CNS environment (Bennett et al., 2018). In these steady-state conditions, microglia are long-lived cells that show self-renewal properties, without input from other peripheral myeloid cells, by coupling proliferation and apoptosis rates to maintain a homogenous density through lifetime (Ajami et al., 2007; Kierdorf et al., 2013b; Askew et al., 2017; Huang et al., 2018).

Despite having crucial non-immune functions, microglial cells have been mostly known for their central involvement in the CNS immune response (**Figure 5 C**). Microglia are, by far, the most important and representative immune resident cells in the CNS (Li and Barres, 2018). They belong to the innate immune system, and like other innate immune-related cells in the periphery, they express a variety of pattern recognition receptors (PRRs) which are responsible for sensing potential pathogens and tissue disruptions (Takeuchi and Akira, 2010; Kigerl et al., 2014). The main families of PRRs include Toll-like receptors (TLRs), Nod-like receptors (NLRs), RIG-like receptors (RLRs), C-type lectin receptors (CLRs), and AIM2-like receptors (ALRs) (Medzhitov et al., 1997; Yamasaki et al., 2008; Rathinam et al., 2010; Szabo et al., 2012; di Virgilio, 2013). PRRs ligands can be divided between those released from pathogens, called pathogen-associated molecular patterns (PAMPs), or those from endogenous origin, called danger-associated molecular patterns (DAMPs). The binding of these molecules to PRRs induce signaling cascades that finally stimulate immunity and host defense (Takeuchi and Akira, 2010; Kigerl et al., 2014). Moreover, microglial cells have a complex expression array of chemokine, cytokine, scavenger, and neurotransmitter receptors (Pocock and Kettenmann, 2007; Colonna and Butovsky, 2017). Therefore, it is not surprising that microglial cells are involved in virtually any disruption of CNS homeostasis. Under threatening conditions (infection, injury, disease), microglia sense the danger and rapidly adapt, shifting their morphology and both transcriptomic and metabolic profiles in order to induce and modulate a broad spectrum of cellular processes to cope with the insult.

As mentioned above, morphological changes of microglia are known since their description (Río-Hortega 1919b, 1919d). Once microglia sense a damage or a pathogen cue, they lose their so-called *resting* ramified morphology

and become reactive (**see Box 1**), changing their shape towards an ameboid-like. Historically, microglial morphology has been divided into 3 different types: ramified (homeostatic condition), hypertrophied/bushy (reactive cells with enlarged cell bodies and reduced number of cellular processes), and ameboid/rounded (reactive cells with huge phagocytic activity). Despite being useful, the morphology of microglial cells upon stimulation is rather a continuum than fixed states. High-resolution microscopy together with in-depth software analysis have allowed characterizing microglial morphological changes using specific morphometrical parameters (e.g., circularity, number of processes, etc.; Leyh et al., 2021).

Box 1. Nomenclature recommendations for microglial biology.

Through the literature, nomenclature associated with aspects of microglial biology can sometimes be confusing and even outdated. Hereby, following recent recommendations, homeostatic microglia refers to cells that are under physiological conditions and are actively undertaking a vast number of functions that are not associated with any homeostatic perturbation, whereas reactive microglia refers to cells that are actively reacting to a particular stimulus or condition (Paolicelli et al., 2022).

Functional states of microglia have often been categorized using the *in vitro* macrophage paradigm as either pro-inflammatory/neurotoxic (M1) or anti-inflammatory/protective (M2). This M1/M2 categorization, despite being helpful *in vitro*, is inadequate to describe the *in vivo* situation (Ransohoff, 2016; Colonna and Butovsky, 2017). In fact, state-of-the-art techniques developed in the past few years have determined that microglial responses are highly heterogeneous (**Figure 5 C**). The emergence of powerful single-cell techniques such as single-cell RNA sequencing (scRNA-seq), single-nuclei RNA sequencing (snRNA-seq), and cytometry by time-of-flight mass spectrometry (CyTOF) have allowed to describe different microglial transcriptomic profiles during development, homeostasis, aging, and disease that rarely display a bias towards M1/M2 states (Masuda et al., 2020; Prinz et al., 2021). Indeed, only adult homeostatic microglial cells are relatively homogeneous across the entire CNS, showing a transcriptional continuum with no clearly defined clusters (Hammond et al., 2019; Li et al., 2019; Masuda et al., 2019). During development, aging, and disease microglial cells present a huge transcriptomic heterogeneity with numerous cellular subsets associated with a specific context (**Figure 5 B, C**). The precise functional impact of each of these microglial states and whether they are beneficial or detrimental in disease conditions is one of the biggest questions in the field (Masuda et al., 2020; Prinz et al., 2021).

In the context of pathology and disease, the resolution of the microglial response is generally crucial for recovery. In those scenarios in which the microglial response cannot be ended due to microglial overactivation, loss of function of key microglial regulatory process, or changes in microglial communication with neighboring cells, microglia can be detrimental and exacerbate pathology. As mentioned above, microglia can adopt different states depending on the context, so it is possible that different microglial states might be happening simultaneously and that their balance, nature, and abundance are what determine the overall impact (Colonna and Butovsky, 2017; Li and Barres, 2018; Sousa et al., 2018; Green et al., 2020; Vainchtein and Molofsky, 2020; Baxter et al., 2021; Borst et al., 2021; Prinz et al., 2021; Safaiyan et al., 2021). In the past few years, genetic and pharmacological methods for depleting microglial cells have been developed. Despite some limitations, these new approaches have allowed the study of the overall impact of microglial cells in a wide range of pathologies (Green et al., 2020). Moreover, microglia can be direct inducers of disease. In their utmost forms, monogenic mutations that affect microglia function have been reported to produce severe brain disorders, currently known as microgliopathies (Rademakers et al., 2011; Goldmann et al., 2015; Oosterhof et al., 2019; Schwabenland et al., 2019). In addition, a huge number of rare coding variants of microglial-associated genes increase the risk of suffering several neurodegenerative diseases such as Alzheimer's disease or multiple sclerosis (de Jager et al., 2009; Sims et al., 2017).

Altogether, microglial cells have been proven to exert important physiological functions in homeostatic conditions as well as protective effects in the context of pathology, but dysregulation of microglial biology can contribute to the development and progression of diseases. Microglial states are enormously complex, with increasing evidence indicating that different states coexist, which are highly multivariate, depending on factors such as age, sex, brain region, or context (i.e., the nature of the homeostatic perturbation). Context-dependent studies are then required to elucidate the specific contributions of microglia to disease, especially in pathologies with marked active neuroimmune processes.

1.5.1.2 Astrocytes

Astrocytes are star-shaped cells distributed throughout the entire CNS in nonoverlapping domains but connected by gap junctions through their processes (Sofroniew and Vinters, 2010). They derive from the neuroepithelium. Specifically, astrocytes arise from the radial glia adjacent to the ventricular zone during early brain development (Rowitch and

Kriegstein, 2010). They account for around 50% of cells in the human CNS and have critical trophic, structural, and metabolic roles in CNS development and physiology. The most crucial functions include control of synapses development, maturation, and function, metabolic support of neurons, being an integral part of BBB function or being key in the neuroinflammatory response in partnership with microglia and other CNS cells (Allen and Eroglu, 2017; Linnerbauer et al., 2020; Han et al., 2021b).

During the late 19th and early 20th centuries, several morphological subsets of astrocytes were described to be present in homeostatic conditions, which include fibrous white matter astrocytes, protoplasmic gray matter associated astrocytes, and specialized astrocyte subtypes like Bergmann or Müller glia (Kölliker, 1889; Andriezen, 1893; Kettenmann and Verkhratsky, 2008). The morphological classification has been extended to nine different subtypes in recent years (Matyash and Kettenmann, 2010). Importantly, all the astrocyte classes are found in both human and rodent brains, albeit human astrocytes are bigger and more branched (Matyash and Kettenmann, 2010; Oberheim et al., 2012). Moreover, it is now clear that astrocytic morphology is influenced by both local cytoarchitecture and region-specific functional demands. For instance, the formation of extensive astrocyte branching appears to be caused by neuron-astrocyte interactions rather than just being a cell-autonomous property (Stogsdill et al., 2017). Furthermore, astrocytes also present a huge degree of transcriptional heterogeneity across brain regions, developmental stages, aging, and disease (Boisvert et al., 2018; Batiuk et al., 2020; Bayraktar et al., 2020; Hasel et al., 2021; Sadick et al., 2022), and similar to microglia, these different transcriptional subsets have not yet been efficiently paired to functional manifestations.

In pathological scenarios, astrocytes have the ability to elicit profound and robust responses to insults. This process in response to pathology is what has been named reactive astrogliosis, (**see Box 2**) which involves the production of reactive astrocytes, which engage morphological, molecular, and functional changes in response to many types of pathological condition. This response is possible thanks to a vast sensing machinery that enables astrocytes to respond to a wide range of molecules from different sources, including pathogens, serum-derived proteins, and signals from any cell type of the CNS or circulating immune cells, that finally trigger the conversion of astrocytes to a reactive state (Liddelow and Barres, 2017; Escartin et al., 2019, 2021; Sofroniew, 2020). Once thought to be an irreversible and unidirectional process, recently, an elegant study found that reactive astrocytes isolated from an injured spinal cord reverted to a naïve-like state

when transplanted into an uninjured spinal cord, whereas they formed astrocytic scars when transplanted into an injured spinal cord, indicating that environmental cues are the main contributors to the plasticity of reactive astrocytes (Hara et al., 2017). Reactive astrocytes are able to secrete cytokines, chemokines, complement components, growth factors, extracellular matrix components, and metabolites that interact with other CNS cells in order to coordinate a response (Liddelow and Barres, 2017; Sofroniew, 2020; Escartin et al., 2021).

As being mainly influenced by context-specific non-cell autonomous signals, increasing evidence indicates that different subtypes of reactive astrocytes arise as a result of the particular context-dependent molecular signaling created by a certain brain tissue disruption (Itoh et al., 2018; Diaz-Castro et al., 2019; Habib et al., 2020; Wheeler et al., 2020; Hasel et al., 2021; Sadick et al., 2022). These astrocyte subtypes may exert different functions, with subpopulations having even opposite effects, that all together mark the outcome of the astrocyte reactivity (Escartin et al., 2021).

Box 2. Nomenclature recommendations for reactive astrocytes.

Astrocytosis, astrogliosis, reactive gliosis, astrocyte activation, astrocyte reactivity, astrocyte re-activation, and astrocyte reaction are all the terms used to describe astrocyte phenotypes in brain pathology (Escartin et al., 2021). Recently, a consensus statement authored by over 80 astrocyte experts proposed the use of the terms ***reactive astrogliosis*** and ***astrocyte reactivity*** to refer to astrocyte responses to pathology. The term ***diseased astrocytes*** is proposed for disorders that directly impact astrocytic cells, such as inherited pathogenic astrocytic gene variations or diseases-risk polymorphisms associated with some neurodegenerative diseases (e.g., mutations in *GFAP* in Alexander diseases or *APOE* in Alzheimer`s diseases, respectively). Finally, the term ***astrocyte activation*** ought to be used for physiological conditions and not used for pathological contexts (Escartin et al., 2021).

It is important to emphasize that astrocyte reactivity is highly conserved across mammalian species and that it emerged as a normal physiological response to protect, preserve and maintain CNS tissue homeostasis (Sofroniew, 2020). It has crucial protective functions in CNS injury (Faulkner et al., 2004), stroke (Liu et al., 2014), infection (Drögemüller et al., 2008), and neurodegenerative diseases (Chen et al., 2009; Kraft et al., 2013; Wang et al., 2013; Katsouri et al., 2020). As a counterpoint, loss or gain of functions in reactive astrocytes as a result of context-specific signaling can also lead to detrimental or maladaptive effects. It has been argued that chronic exposure to reactivity-trigger signals can drive excessive inflammation that promotes neurodegeneration (Brambilla et al., 2009; Argaw et al., 2012; Kim et al., 2014; Ceyzériat et al., 2018; Wheeler et al., 2020).

When studying a particular pathology, it is also important to consider that cell-autonomous astrocyte dysfunctions may also occur. These diseased astrocytes (**Box 2**) can initiate or contribute to neurodegeneration even before the appearance of reactive astrogliosis. Moreover, in some pathologies, disease-induced astrocyte dysfunction can blur, exaggerate or alter normal astrocyte reactivity and worsen the outcome of the disease. Therefore, it is crucial to distinguish between normal astrocyte reactivity, either beneficial or detrimental, from those effects produced by diseased astrocytes in order to generate disease-specific therapies (Sofroniew, 2020; Escartin et al., 2021).

1.5.1.3 Microglia and astrocyte communication

At first sight, microglia and astrocyte have little in common apart from their CNS location; they share neither developmental origin, structural properties nor surveillance functions, but their tight bidirectional coordination (**Figure 6**) is extremely important in both physiological and pathological conditions (Liddelow et al., 2020; Vainchtein and Molofsky, 2020).

In physiological conditions, recent studies have shed light on the mechanism of such interactions. For example, astrocytic CSF1, IL-34, TGF-β, and cholesterol act as trophic support molecules required for proper microglia specification and function both *in vivo* and *in vitro* (Bohlen et al., 2017; Baxter et al., 2021). A cytokine-mediated communication is also necessary for correct synaptic pruning; near a redundant synapse, astrocytes release interleukin-33 (IL-33), which attracts microglia to the region for synapse engulfment (Vainchtein et al., 2018). Astrocyte-microglia coordination is also found in neuronal corpse removal in which astrocytes engulf small dendritic apoptotic bodies, whereas microglia is responsible for soma and apical dendrites engulfment (Damisah et al., 2020).

While our knowledge of this coordination in physiology is still very limited, much more is known about the nature and the consequences of microglia-astrocyte communication in sickness. Upon a lipopolysaccharide (LPS) challenge, usually used to resemble a bacterial infection, some astrocytic-secreted factors stimulate microglia immune response (Kano et al., 2019). In addition, microglial release of C1q, IL-1β, and TNF-α promotes a neurotoxic astrocyte reactive phenotype that induces neuronal and oligodendrocyte death in LPS-induced neuroinflammation and CNS injury (Liddelow et al., 2017; Guttenplan et al., 2021). In case of brain viral infection, IFN-I signaling in both neurons and astrocytes is required for proper microglial activation in the OB to avoid further viral spreading (Chhatbar et al., 2018). In mice experimental autoimmune encephalomyelitis (EAE), a mouse

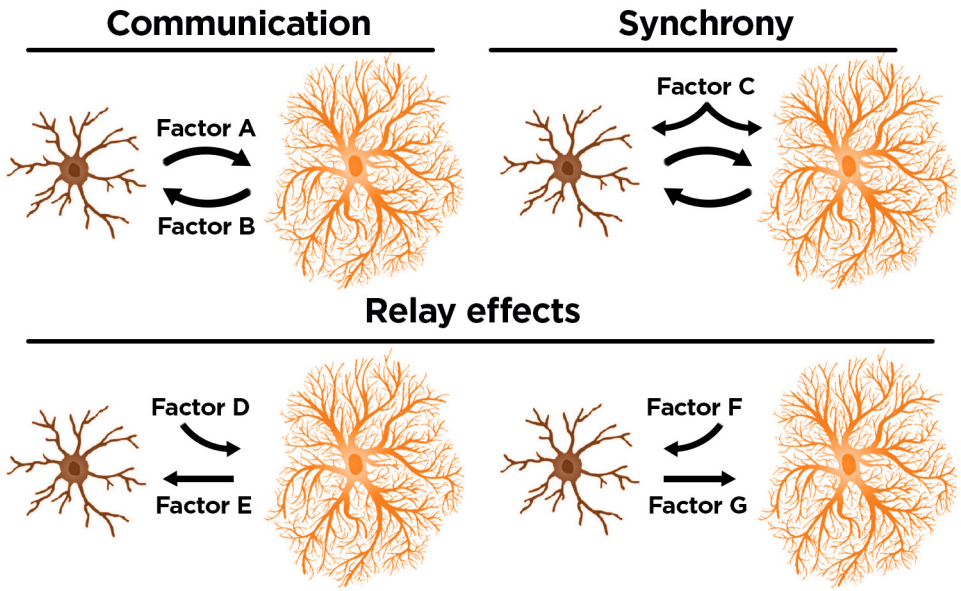

Figure 6. Mechanisms of microglia-astrocyte coordination.

Communication: bidirectional signaling between microglia (brown) and astrocytes (orange) can be established to guide a particular process in which different factors (A and B) from each cell can modulate the response of the other, regardless of whether the particular response is individual or shared between cells. For example, some authors have hypothesized that brain microglial repopulation after microglial depletion could be tightly controlled by such a communication. **Synchrony:** particular ligands targeting both cells (factor C) can adjust the response to allow cells to concertedly respond. For instance, both microglia and astrocyte possess purinergic receptors that facilitate local purine sensing in both cells to elicit a common response. **Relay effects:** Specific ligands target one cell type (factors D and F) that indirectly alters the other (factors E and G). For example, LPS-stimulated microglia produce a specific neurotoxic subtype of reactive astrocytes through the secretion of C1q, IL-1β, and TNF-α; or that astrocytic secretion of IL-3 enhances microglial clearance capacity and motility in a mouse model of Alzheimer's diseases. *Adapted from Vainchtein and Molofsky 2020.*

model of multiple sclerosis, astrocyte and microglia cell-to-cell contacts via membrane-bound proteins boost inflammation and enhance pathology (Clark et al., 2021).

Collectively, what these studies demostrate, among multiple others (Rothhammer et al., 2018; McAlpine et al., 2021), is that crosstalk between microglia and astrocytes is essential for (i) physiological functioning, (ii) responding to pathology, and (iii) explaining detrimental effects of these cells in brain infection, injury or diseases.

1.5.1.4 Other cells involved in CNS inflammation

In steady-state conditions, microglia are generally the only immune cells present in the CNS parenchyma, but an important repertoire of other immune cells can be found at the CNS borders. Between the most relevant

subpopulations, we can find the CNS-associated macrophages (CAMs) which include perivascular macrophages (PVMs), meningeal macrophages (MMs), and choroid plexus macrophages (CPMs) (Li and Barres, 2018). In mice, both microglia and MMs share a common prenatal progenitor, whereas PVMs originate from perinatal meningeal macrophages after birth. CPMs are also established from myeloid perinatal progenitors and in contrast to the other subpopulations, are the only ones being constantly replenished by circulating monocytes (Goldmann et al., 2016; Masuda et al., 2022). In addition, other important myeloid cells in the CNS borders are peripheral monocytes, which are directly derived from the bone marrow. Under physiological conditions, the presence of other myeloid cells apart from microglia in the brain parenchyma is rare, but not during disease conditions. For example, peripheral monocytes are an important source of infiltrating cells that contribute to inflammation during EAE (Mildner et al., 2009), viral infection (Cusick et al., 2013), acute demyelination (Plemel et al., 2020), stroke (Ritzel et al., 2015), epilepsy (Varvel et al., 2016), peripheral organ inflammation (D'Mello et al., 2009), or BBB integrity disruption (Mildner et al., 2007), among others. Despite recent important advances (e.g., scRNAseq, microglial-specific Cre driver mouse lines), the study of the specific contributions of every particular myeloid subpopulation is still very challenging due to overlapping markers and functions, especially during injury and disease. Thus, the creation of tools to distinguish and selectively manipulate microglia, CAMs, and infiltrating monocytes is a constant and vast field of research (Bennett et al., 2016; Li and Barres, 2018; Dumas et al., 2021; Prinz et al., 2021). Other immune cell populations present in CNS borders include lymphocytes (B and T-cells), basophils, neutrophils, mast cells, and dendritic cells. Similarly to monocytes, during BBB impairment and CNS disease these cells can infiltrate into the brain parenchyma and contribute to the outcome of a given perturbation. In summary, the repertoire of immune cells that may participate in CNS inflammation is large and complex. Specific cellular functions rely on the particular context in which every cell type, establishes intricate connections with neighboring cells that coordinately guide the overall response (Prinz and Priller, 2017).

1.6 How do mitochondria and mitochondrial defects induce inflammation?

As organelles with a bacterial origin, mitochondria possess a repertoire of molecules that can be recognized by PRRs. Especially, mtDNA and mtRNAs are analogous to those of bacterial origin and are fully able to elicit both

antiviral-like and bacterial-like innate immune responses (West et al., 2015; Dhir et al., 2018). In a context of mitochondrial stress, damage, or dysfunction, mtDNA and mtRNAs can escape the mitochondrial matrix, be released to the cytoplasm, and engage an inflammatory response via inflammasome, TLR9, mitochondrial antiviral signaling proteins (MAVS), and/or cGAS-STING pathways (Zhong et al., 2019; Gong et al., 2020; Luna-Sánchez et al., 2021). Noteworthy, these signaling networks allow explaining why throughout many severe disabling diseases, mitochondrial malfunction, neurodegeneration, and persistent inflammation occur together. Therefore, it has been speculated that the mitochondria-innate immune cross-talk contributes to the pathobiology of PMDs (Luna-Sánchez et al., 2021). Indeed, in polymerase gamma (POLG) mutator mice, a mouse model of mtDNA instability that mirrors some clinical features of patients with POLG-related PMD and aging (Trifunovic et al., 2004), one study found that aged mice present a chronic cGAS-STING–dependent interferon type-I (IFN-I) signaling in heart, liver, kidney, and expansion of the myeloid cell population. Moreover, these mice showed a hyperresponsive pro-inflammatory phenotype upon an LPS challenge also triggered by a cGAS-STING–IFN-I signaling (Lei et al., 2021). In addition, mtDNA promotes inflammation and muscle atrophy in mouse models of mitochondrial-related myopathies (Rodríguez-Nuevo et al., 2018; Irazoki et al., 2023). These findings strongly suggest considering direct immune-guided pathological consequences in PMDs. Importantly, bulk RNA sequencing (RNAseq) of brains of both whole-body and brain-specific *Ndufs4* knockout mice revealed that innate immune responses, including antiviral-related IFN signaling pathways, are the most enriched (McElroy et al., 2020; Perry et al., 2021), suggesting the potential implication of the immune response in this mouse model. Importantly, based on the aforementioned evidence, neurons and astrocytes are required for proper microglial response to viral infection in the OB (Chhatbar et al., 2018) (one of the most remarkable neurodegenerative areas in *Ndufs4 KO* mice). But how these IFN-I signaling pathways are triggered in *Ndufs4 KO* mice remain largely unexplored.

1.7 Neuroinflammation in mitochondrial defective mouse models

Several mouse models of mitochondrial dysfunction have been developed so far in an attempt to study the pathological consequences of such abnormal function (Iommarini et al., 2015; Torraco et al., 2015). Different strategies have been used to model PMDs, which include: whole-body knockouts,

tissue or cell-type specific knockout mice, or by introducing mutations in specific genes by gene targeting. Unsurprisingly, and similar to what occurs in patients suffering from PMDs, the particular phenotypic manifestations of mice (age of onset, severity, tissue affected, etc.) depend on the precise gene disrupted, and can vary substantially even when genes have relatively similar mitochondrial functions. The pathological specificity related to a particular gene affectation makes it very challenging to translate and generalize pathological mechanisms and therapeutical approaches to other gene disruptions even when they do not differ much in terms of the phenotype they cause, highlighting once again the importance of considering the genetic etiology behind the disease (Ylikallio and Suomalainen, 2012; Gorman et al., 2016; Suomalainen and Battersby, 2018).

A number of these mouse models have allowed the study of brain pathology, but most of the studies have been purely descriptive, and specific knowledge of pathogenic mechanisms is still lacking. Moreover, in most cases, just like in the *Ndusf4 KO* mouse model, a "neuron-centric" view of neurodegeneration has prevailed because mitochondrial malfunction is assumed to play a direct role in cell-autonomous neuronal death due to the large dependency of neurons on OXPHOS ATP production. Thus, little attention has been paid to test or discuss the potential impact that the inflammation associated to neurodegeneration could have *per se* in the progression of the pathology (Rose et al., 2017; McAvoy and Kawamata, 2019). So, in general, neuroinflammation and its main cellular players have been widely overlooked despite most mitochondrial dysfunctions that affect the brain in mice (**Table 5**), but also in humans, showed the presence of neuroinflammatory hallmarks. Only a few studies have focused on the direct role of astrocyte mitochondrial dysfunction (Ignatenko et al., 2018, 2020; Fiebig et al., 2019; Murru et al., 2019), but it was not until very recently that two studies, which include ours, directly tested the role of microglia (Aguilar et al., 2022; Stokes et al., 2022).

Reports using astrocytic mitochondrial dysfunction models have shown that, in some cases, not solely neuronal mitochondrial abnormalities are responsible for a particular disease. Despite direct OXPHOS dysfunction does not seem to produce any pathological phenotype (COX 10 and NDUFS4 deficiencies) (Supplie et al., 2017; Ramadasan-Nair et al., 2019), other mitochondrial perturbations in astrocytes produced a severe disease in which neurodegeneration and neuroinflammation are highly present (Ignatenko et al., 2018; Murru et al., 2019). Similar to what occurs with whole-body or neuronal-specific knockouts, concrete mechanisms by which particular mitochondrial malfunctions in astrocytes lead to disease (e.g.,

loss of astrocytic trophic support to neurons, reactive astrocytes generating an exacerbated inflammatory environment detrimental to neurons, etc.) are unknown. Moreover, even when the dysfunctions do not produce any overt phenotype, non-cell autonomous effects on neuronal survival can not be discarded in the context of injury or disease, as observed in the astrocytic-specific conditional *Tfam KO* mice, possibly due to malfunctional astrocyte reactivity (Fiebig et al., 2019). Therefore, untangling cell-type specific contributions (both cell autonomous and non-cell autonomous) will be key for the complete understanding of mitochondrial diseases.

Table 5. Relevant mouse models of mitochondrial dysfunction with brain affectation: mitochondrial affected process, phenotype of the mouse, and described neuroinflammatory hallmarks.

Model	Direct mitochondrial affectation	Phenotype	Neuro-inflammatory hallmarks	Refs.
Astrocyte-specific *Twinkle* KO	Mitochondrial DNA replication	Progressive diseases between 3-8 months of age with motor impairment and spongiotic encephalopathy	Astrogliosis and microgliosis	Ignatenko et al., 2018
Neuron-specific *Twinkle* KO	Mitochondrial DNA replication	Sudden death at 8 months due to rapid neuropathology appearance after a healthy period	Astrogliosis and microgliosis	Ignatenko et al., 2018
Astrocyte-specific *Afg3l1* and *Afg3l2* double KO	m-AAA protease complex; quality control and regulatory functions	Ataxia, reduced body weight, death of Bergmann glia (BG), Purkinje cell (PC) abnormalities	Reactive astrogliosis and inflammatory signature	Murru et al., 2019
***Twinkle* point mutations (IOSCA model)**	Mitochondrial DNA replication	Seizures, loss of PC, hippocampal pyramidal neurons abnormalities	Not assessed	Nikkanen et al., 2016
***Wars2* mutant**	Aminoacylation of mitochondrial tRNA	Sensorineural hearing loss	Not assessed	Agnew et al., 2018
Total neuronal, PC, and forebrain *Dars*-specific KOs	Aminoacylation of mitochondrial tRNA	Motor impairment, extensive neuronal death in KO region/cell type	Astrogliosis and microgliosis in PC KO, microgliosis in neuronal and forebrain KOs (astrogliosis not assessed). Immune pathway activation in total neuronal KO	Nemeth et al., 2020; Rumyantseva et al., 2022

***Parl* whole body KO and neuron-specific**	Mitochondrial protease	Generalized necrotizing encephalomyelopathy	Extensive astrogliosis and microgliosis	Spinazzi et al., 2019
***HtrA2* KO**	Mitochondrial serine protease	Neuronal loss in striatum, parkinsonian-like phenotype, death by P30.	Not assessed	Martins et al., 2004
***p32* brain-specific KO**	RNA and protein chaperone in mitochondrial translation	Leukoencephalopathy with undifferentiated oligodendrocyte and axon degeneration	Astrogliosis but not microgliosis	Yagi et al., 2017
Neuronal-specific *Ndufs3* KO	Complex I subunit	Motor impairment, neuronal loss in hippocampus	GFAP increased measured in cortex and hippocampus. Slight tendency to IBA-1 increase in hippocampus. Both measured by WB	Peralta et al., 2020
Neuronal-specific *Ndufa5* KO	Complex I subunit	Mild chronic encephalopathy with motor impairment	No astrogliosis. Microgliosis not assessed	Peralta et al., 2014
Neuronal-specific *Risp* KO	Complex III subunit	Encephalopathy with lesions in the piriform cortex	Astrogliosis. Microgliosis not assessed	Diaz et al., 2012
Neuronal-specific *Cox10* KO	Complex IV subunit	Encephalopathy with lesions in piriform cortex, striatum, hippocampus, and cortex	Astrogliosis. Microgliosis not assessed	Diaz et al., 2012
Astrocyte-specific *Cox10* KO	Complex IV subunit	No evidence of pathological phenotype	None	Supplie et al., 2017
Neuronal-specific *Tfam* KO	mtDNA maintenance	Late-onset cortico-hippocampal neurodegeneration	Astrogliosis. Microgliosis not assessed	Sörensen et al., 2001
Astrocyte-specific *Tfam* KO	mtDNA maintenance	Increased neuronal death upon photothrombotic lesion	Astrogliosis in cortex under physiological conditions	Fiebig et al., 2019
Astrocyte-specific *Ndufs4* KO	Complex I subunit	Abnormal response to anesthesia	Not assessed	Ramadasan-Nair et al., 2019)
Neuronal-specific *Drp1* KO	Mitochondrial fission	Induction of integrated stress response. No neuronal loss found	None	Restelli et al., 2018
Low *Aifm1* expressing mice	Apoptosis regulation	Cerebellar neuronal loss	Astrogliosis and microgliosis. Incresed pro-inflammatory cytokine levels	Fernández-de la Torre et al., 2020
***Slc25a46* KO**	Mitochondrial fusion-fission dynamics	Optic atrophy, cerebellar neuronal loss, ataxia	Astrogliosis and microgliosis in the cerebellum	Li et al., 2017

Table 5. Abbreviations.
Afg3l1/2: AFG3-like AAA ATPase 1/2 genes; ***Aifm1***: apoptosis-inducing factor mitochondria associated 1 gene; **BG**: Bergmann glia; ***Cox10***: cytochrome C oxidase assembly factor heme A:Farnesyltransferase COX10 gene; ***Dars2***: aspartyl-tRNA synthetase 2 gene; ***Drp1***: dynamin-related protein 1 gene; ***HrtA2***: high-temperature requirement protein A2 gene; **IOSCA**: infantile-onset spinocerebellar ataxia; ***Ndufa5***: NADH-ubiquinone oxidoreductase 1 alpha subcomplex subunit 5 gene; ***Ndufs3***: NADH-ubiquinone oxidoreductase iron-sulfur protein 3 gene; ***Ndufs4***: NADH dehydrogenase (ubiquinone) Fe-sulfur protein 4 gene; ***Parl***: presenilins-associated rhomboid-like protein gene; **PC**: Purkinje cell; ***Risp***: rieske iron-sulfur protein gene; ***Slc25a46***: solute carrier family 25 member 46 gene; ***Tfam***: nuclear mitochondrial transcription factor A gene; ***Wars2***: tryptophanyl-tRNA synthetase 2 gene; **WB**: western blot.

1.8 Interleukin-6

Cytokines are small secreted and soluble proteins that can have either autocrine, paracrine, or endocrine functions. Cytokines are potent biological factors that were first discovered by their ability to control and modulate the immune system. Soon after, they were shown to exert important functions in other systems, including the CNS in both physiological and pathological conditions. Within this group of factors, the interleukin-6 (IL-6) has been proven to have relevant roles in a variety of CNS pathologies (Ozaki and Leonard, 2002; Spooren et al., 2011; Erta et al., 2012).

IL-6 is a four-helix bundle cytokine and it is considered the founding member of the neuropoietin family (Murakami et al., 2019). In 1985, it was described as a B-cell differentiation factor (BSF-2) that promoted B-cell maturation into antibody-producing cells (Hirano et al., 1985). Finally renamed as IL-6, it has important functions in the acute phase response, the transition of innate to adaptative immunity, angiogenesis, and bone mass regulation, as well as acting as a growth factor for hematopoietic progenitor cells (Heinrich et al., 1990; Hurst et al., 2001; de Benedetti et al., 2006; Gopinathan et al., 2015). In the CNS, IL-6 is produced by microglia, astrocytes, neurons, endothelial cells, and oligodendrocytes (**Figure 7**) (Spooren et al., 2011) and primarily involved in neuroinflammation. The first pieces of evidence were obtained using GFAP-IL6 (Campbell et al., 1993) and NSE-IL6 transgenic mice (di Santo et al., 1996), which have targeted IL-6 overexpression in astrocytes and neurons, respectively. In these mice, chronic overexpression of IL-6 induces profound reactive phenotypes in both astrocytes and microglia and increases the brain inflammatory milieu, even leading to cerebellar neuronal loss and motor alterations in GFAP-IL6 mice (Campbell et al.,

1993; di Santo et al., 1996). Moreover, IL-6 is highly induced in acute (e.g., traumatic brain injury, facial nerve axotomy) and chronic brain disorders, such as Alzheimer's disease, Parkinson's disease, and multiple sclerosis (Erta et al., 2012).

IL-6 effects are highly dependent on context (nature and intensity of the insult). This complexity of IL-6 actions has made it difficult to decipher the specific roles of this cytokine in the neuroinflammation associated with different neuropathologies. Nowadays, but not exempt from certain reductionism, IL-6 is believed to be beneficial in acute CNS injury acting as a neurotrophic factor, reducing excitotoxicity, and stimulating recovery after brain ischemia, whereas in chronic neuroinflammation, like in neurodegenerative disorders, it seems to have detrimental effects (Spooren et al., 2011; Erta et al., 2012).

During the course of this thesis project, two different research groups reported increased expression of *Il6* mRNA (Balsa et al., 2020) or IL-6 signaling pathways (McElroy et al., 2020) in brains with NDUFS4 deficiency.

1.8.1 Interleukin-6 signaling

Part of the complexity of IL-6 in neurodegenerative processes can be explained by its types of signaling (**Figure 7**). Hitherto, three different types of signaling have been described; all of which involve the interaction of IL-6, the IL-6 receptor, and the gp130 protein (Jones and Jenkins, 2018).

The first one to be described was the classic signaling, in which IL-6 binds to the class I cytokine receptor, the membrane-bound IL-6 receptor (mIL-6R) (Yamasaki et al., 1988). For signal transduction, this binding alone is not sufficient to elicit an intracellular signaling cascade. It requires oligomerization of the IL-6/mIL-6R complex with the membrane-bound gp130 (Müllberg et al., 1993). The gp130 receptor is constitutively associated with tyrosine kinase enzymes of the Janus kinase family (JAK1, JAK2, and TYK2) (Lütticken et al., 1994; Stahl et al., 1994, 1995). The gp130 homodimerization leads to the activation of JAK proteins which cross-phosphorylate between them and phosphorylate gp130 tyrosine residues favoring the recruitment of signal transductors. This process may lead to the activation of two different intracellular transduction pathways: phosphorylation and activation of STAT1/3 proteins that homo or heterodimerize and are translocated to the nucleus or the binding of SHP2 that activates the PI3K pathway, which produces activation of AKT leading to the stimulation of NF-kB and the Ras pathways (Heinrich et al., 2003). This type of signaling can only occur in cells that express the mIL-6R and gp130.

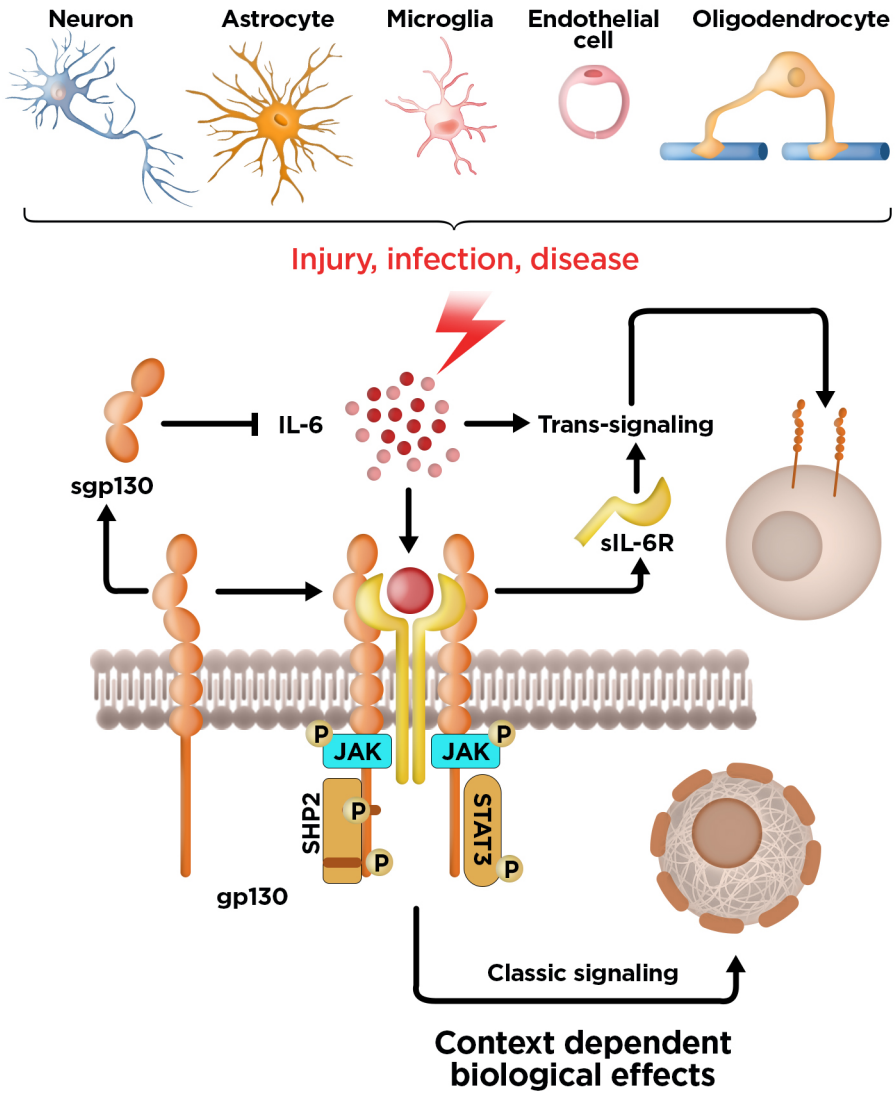

Figure 7. Summary of IL-6 complexity in the CNS.

IL-6 can be produced by all resident CNS cells. Upon an insult, IL-6 is produced in different amounts depending on the cellular source. In the brain, IL-6 mainly signals trough two different types of signaling: the classic signaling and the trans-signaling. Classic signaling can only take place in cells that express the membrane-bound IL-6 receptor, whereas trans-signaling can occur in all cells that express gp130. The latter can be inhibited by the production of a soluble form of the gp130 (sgp130). This complex signaling machinery may explain the enormous complexity of IL-6 biological actions during injury, infection, and disease. *Adapted from Erta et al 2012.*

The second type of IL-6 signaling described was the trans-signaling (Müllberg et al., 1993), in which IL-6 binds extracellularly to the soluble form of the IL-6 receptor (sIL-6R) previously generated by the proteolytic actions of ADAM10/17 proteases upon the membrane receptor (mIL-6R) in

mice and humans, or also by alternative mRNA splicing only in humans (Schumacher et al., 2015). Then, the IL-6/sIL-6R complex can interact with gp130 proteins located in the plasma membrane that produce the activation of the intracellular transduction cascade. Since the gp130 is ubiquitously expressed, this ternary complex can induce responses in cells that do not express the mIL-6R, explaining the pleiotropic actions of IL-6 (Murakami et al., 2019). Moreover, trans-signaling can be inhibited by the soluble form of gp130 (spg130), generated by alternative splicing, that binds to the IL-6/sIL-6R complex preventing its interaction with membrane gp130 (Jostock et al., 2001). It is especially worth highlighting that trans-signaling has a major role in the pathogenic actions of IL-6 in the brain, whereas classic signaling has been proposed to guide mainly regenerative and anti-inflammatory actions (Rose-John, 2012; Campbell et al., 2014; Chucair-Elliott et al., 2014; Rothaug et al., 2016).

Finally, a third type of signaling mechanism has been recently proposed for dendritic cells in the context of multiple sclerosis: the cluster signaling. This type of signaling is key for the development of EAE in mice since systemic *Il6 KO* mice are resistant to EAE induction (Samoilova et al., 1998; Giralt et al., 2013; Heink et al., 2017). Briefly, dendritic cells present an IL-6/IL-6R complex to a gp130-expressing T cell, which in combination with a T-cell receptor (TCR) signal elicits a JAK/STAT signaling in the T lymphocyte allowing the pathogenic Th17 differentiation of T cells (Heink et al., 2017).

2

Hypothesis and objectives

Ndufs4 KO mice, a well-established mouse model of Leigh syndrome, present a lethal, fastly-progressing encephalopathy with abundant neurodegeneration and neuroinflammation. We hypothesize that the neuroinflammation associated with this progressive brain pathology contributes to the disease, rather than being just a consequence of the neurodegeneration.

To this aim, the main objectives of this thesis were the following:

1. To study the contribution of microglia, the main immune cells of the brain, to the neuropathology in *Ndufs4 KO* mice by pharmacologically depleting them using a CSF1R antagonist.

2. To study the role of IL-6, one of the main neuro-inflammatory cytokines, analyzing the effects of its whole-body deficiency in *Ndufs4 KO* mice.

3. To study the effects of chronic neuroinflammation in *Ndufs4 KO* by transgenic IL-6 overexpression in astrocytes.

3

Material, methods, and experimental design

3.1 Mice

All mice used in this study were fed *ad libitum* and housed in a 12-hour light-dark cycle under specific pathogen-free conditions at constant temperature (22 ± 2°C) in the Servei d'Estabulari of the Universitat Autònoma de Barcelona. All experiments were performed as per the approval of the Ethics Committee on Animal Experiments of the Universitat Autònoma de Barcelona (Ref. 3971 and 4155).

3.2 Mice generation

The parental mouse strains used in this study were *Ndufs4*$^{+/-}$ (MGI:5614092) (Kruse et al., 2008), *Il6*$^{-/-}$ mice (MGI:6468229) previously generated in our laboratory (Sanchis et al., 2020a), and GFAP-IL6 mice (MGI:7327600) (Campbell et al., 1993). All mouse lines were backcrossed with a C57BL/6 background for at least ten generations. Both male and female mice were used in the present study.

For the experiment with PLX3397, male and female *Ndufs4*$^{+/-}$ mice were bred with each other to obtain control (Ctrl; *Ndufs4*$^{+/+}$, *Ndufs4*$^{+/-}$) and *Ndufs4 KO* mice (*Ndufs4*$^{-/-}$). Using this crossing strategy, animals were born in frequencies similar to the expected mendelian ratios (**Figure 8 A**). Three rounds of breeding were required to generate double-deficient mice lacking IL-6 and NDUFS4 (**Figure 8 B**). (i) Firstly, constitutive IL-6 deficient mice (*Il6*$^{-/-}$/*Ndufs4*$^{+/+}$) were crossed with heterozygous *Ndufs4* (*Il6*$^{+/+}$/*Ndufs4*$^{+/-}$) mice. (ii) *Il6*$^{+/-}$/*Ndufs4*$^{+/-}$ offspring were crossed with *Il6*$^{-/-}$ mice. (iii) Finally, the resulting *Il6*$^{-/-}$/*Ndufs4*$^{+/-}$ and *Il6*$^{+/-}$/*Ndufs4*$^{+/-}$ mice were bred to obtain the four genotypes included in the current study: control (*Il6*$^{+/-}$/*Ndufs4*$^{+/-}$), *Il6 KO* (*Il6*$^{-/-}$/*Ndufs4*$^{+/-}$), *Ndufs4 KO* (*Il6*$^{+/-}$/*Ndufs4*$^{-/-}$), and Double KO (*Il6*$^{-/-}$/*Ndufs4*$^{-/-}$). Since *Ndufs4 KO* mice (*Ndufs4*$^{-/-}$) cannot be used for breeding, to maximize the efficiency of mice generation and reduce the number of animals, in the final crossing, we decided to cross *Il6*$^{+/-}$/*Ndufs4*$^{+/-}$ and *Il6*$^{-/-}$/*Ndufs4*$^{+/-}$ instead of crossing two *Il6*$^{+/-}$/*Ndufs4*$^{+/-}$ mice. This strategy increases the expected mendelian ratio of Double-KO mice generation from 6,25% to 12,5% (**Figure 8 B**), but it also makes it impossible to obtain *Il6*$^{+/+}$ mice; thus heterozygous mice were used as controls for IL-6 deficiency. To be consistent, heterozygous mice for the NDUFS4 deficiency (*Ndufs4*$^{+/-}$) were chosen for the control groups. It should be mentioned that both *Il6*$^{+/-}$ and *Ndufs4*$^{+/-}$ mice are almost indistinguishable from their wildtype counterparts (*Il6*$^{+/+}$ and *Ndufs4*$^{+/+}$) in basal conditions (Kruse et al., 2008; van de Wal et al., 2022). Regarding the astrocytic-targeted IL-6 overexpression (**Figure 8 C**), (i) firstly, *GFAP-IL6* mice were crossed with *Ndufs4*$^{+/-}$ mice. (ii) From the

resulting offspring, *Ndufs4*$^{+/-}$ and *GFAP-IL6/Ndufs4*$^{+/-}$ mice were crossed, producing six different genotypes; four of them were considered for this study: control (*Ndufs4*$^{+/-}$), GFAP-IL6 (*GFAP-IL6/Ndufs4*$^{+/-}$), *Ndufs4 KO* (*Ndufs4*$^{-/-}$), and GFAP-IL6/*Ndufs4 KO* (*GFAP-IL6/Ndufs4*$^{-/-}$). In this case, IL-6 overexpression was conserved in hemizygosis since mice harbouring two copies of the transgene have a severe motor disorder at early ages (Campbell et al., 1993). In addition, to be consistent with the IL-6 deficient mouse line, heterozygous mice for the NDUFS4 deficiency (*Ndufs4*$^{+/-}$) were again chosen as controls. In both IL-6 lines (deficiency and overexpression) *Ndufs4 KO* mice were not born following mendelian ratios, with frequencies of 17.41% and 17.9% for the IL-6 deficiency line and IL-6 overexpression line, respectively, compared to the 25% expected (**Figure 8 B, C**). Genotyping was carried out at P21 (just after weaning), which potentially may explain the observed non-mendelian ratios for *Ndufs4*$^{-/-}$ births, since we did not detect an increased death frequency of *Ndufs4*$^{-/-}$ mice between P0-P20, this suggests that some intrauterine death could be happening in the different *Ndufs4 KO* mice.

3.3 Genotyping

All mice were genotyped by PCR (**Tables 6, 7, and 8**) using DNA extracted from 2 to 5 mm of the tail. For DNA extraction, the tails were boiled in 100 µL of 50 mM NaOH solution for 7 min. Primers and oligonucleotides were purchased from Sigma-Aldrich. DNA polymerase and buffers were obtained from Thermoscientific (DreamTaq™ Green DNA polymerase, EP0713). DNA was amplified using a Prime Thermal Cycler (Techne, Staffordshire, United Kingdom). PCR products were run in 2% agarose gels at 110 V for 35 minutes. After running, gels were incubated in SYBR Safe stain (S33102, Invitrogen) for DNA staining following the manufacturer's instructions.

Figure 8. Breeding strategy for the generation of the mice used in this project. **(A)** Breedings for the PLX3397 experiment. *Experimental groups:* control (includes *Ndufs4*$^{+/+}$ and *Ndufs4*$^{+/-}$ *mice)* and *Ndufs4 KO* mice. **(B)** Breedings required to study the effects of IL-6 deficiency in *Ndufs4 KO* mice. *Experimental groups:* control, *Ndufs4 KO*, *Il6 KO*, and Double KO mice. **(C)** Breedings required to study the effects of CNS IL-6 overexpression in *Ndufs4 KO* mice. *Experimental groups:* control, *Ndufs4 KO*, GFAP-IL6, GFAP-IL6/*Ndufs4 KO* mice. **(A-C)** For *Il6* and *Ndufs4*, "+" and "–"symbols indicate the wildtype and the deficient gene variant, respectively. Percentages indicate birth rations: in italics for the expected mendelian ratio and bold for the observed ratio.

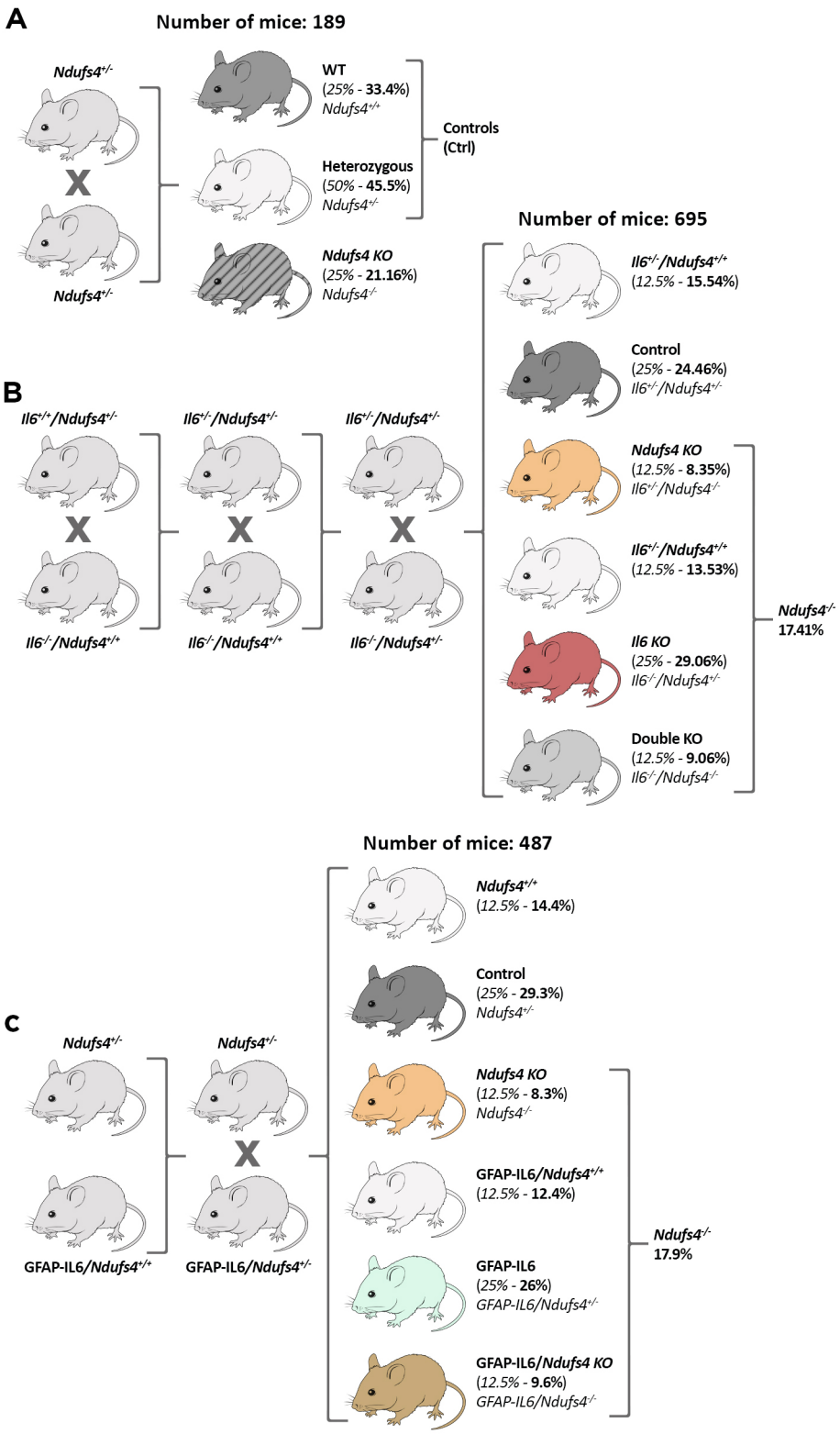
A
Number of mice: 189
Ndufs4+/-
X
Ndufs4+/-
WT
(25% - 33.4%)
Ndufs4+/+
Heterozygous
(50% - 45.5%)
Ndufs4+/-
Controls
(Ctrl)
Ndufs4 KO
(25% - 21.16%)
Ndufs4-/-
B
Il6+/+/Ndufs4+/-
X
Il6-/-/Ndufs4+/+
Il6+/-/Ndufs4+/-
X
Il6-/-/Ndufs4+/+
Il6+/-/Ndufs4+/-
X
Il6-/-/Ndufs4+/-
Number of mice: 695
Il6+/-/Ndufs4+/+
(12.5% - 15.54%)
Control
(25% - 24.46%)
Il6+/-/Ndufs4+/-
Ndufs4 KO
(12.5% - 8.35%)
Il6+/-/Ndufs4-/-
Il6+/-/Ndufs4+/+
(12.5% - 13.53%)
Il6 KO
(25% - 29.06%)
Il6-/-/Ndufs4+/-
Double KO
(12.5% - 9.06%)
Il6-/-/Ndufs4-/-
Ndufs4-/-
17.41%
C
Ndufs4+/-
X
GFAP-IL6/Ndufs4+/+
Ndufs4+/-
GFAP-IL6/Ndufs4+/-
Number of mice: 487
Ndufs4+/+
(12.5% - 14.4%)
Control
(25% - 29.3%)
Ndufs4+/-
Ndufs4 KO
(12.5% - 8.3%)
Ndufs4-/-
GFAP-IL6/Ndufs4+/+
(12.5% - 12.4%)
GFAP-IL6
(25% - 26%)
GFAP-IL6/Ndufs4+/-
GFAP-IL6/Ndufs4 KO
(12.5% - 9.6%)
GFAP-IL6/Ndufs4-/-
Ndufs4-/-
17.9%

Table 6. PCR to determine the gene variant of *Ndufs4*.
WT variant shows a band at 150 bp, whereas KO variant shows a 300 bp band.

	Volume (µl)	Final concentration
Buffer 10x	1.5	1x (2 mM)
dNTPs	0.45	300 µM each
Primer 1 5'-AGCCTGTTCTCATACCTCGG-3'	0.3	0.2 µM
Primer 2 5'- GGTGCATACTTATACTACTAGTAG-3'	0.3	0.2 µM
Primer 3 5'- GTCCTCTATGAGGGTACAGAG-3'	0.3	0.2 µM
Taq polymerase	0.08	26.7 mU/µL
H2O	12.07	
Final volume	15	
Sample	1	

	Temperature (°C)	Time (s)	Cycles (n)
Inicial denaturation	95	180	1
Denaturation	95	10	34
Hybridation	53	30	
Elongation	65	30	
Final elongation	72	300	1

Table 7. PCR to determine the gene variant of *Il6*.
WT variant shows a band at 300 bp, whereas KO variant shows a 150 bp band.

	Volume (µl)	Final concentration
Buffer 10x	1.5	1x (2 mM)
dNTPs	0.45	300 µM each
Primer *Rev1* 5'- GAGACTGTGAGAGAGGAGTGTG-3'	0.23	0.15 µM
Primer *Rev2* 5'- CATCTTATCTGGGCTGACCCTAG-3'	0.23	0.15 µM
Primer *Rev3* 5'- TCTCTGCTGGGATCTAGGGCC-3'	0.3	0.2 µM
Taq polymerase	0.08	26.7 mU/µL
H2O	12.21	
Final volume	15	
Sample	1	

	Temperature (°C)	Time (s)	Cycles (n)
Inicial denaturation	95	180	1
Denaturation	95	30	34
Hybridation	56		
Elongation	72		
Final elongation	72	300	1

Table 8. PCR to determine the GFAP-IL6 transgene.

Positive samples for the transgene will show a band at 196 bp. A control PCR was used as a positive control for the PCR reaction using primers for the *Mt1* gene. Control band should appear in all samples at 178 bp.

	Volume (µl)	Final concentration
Buffer 10x	1.5	1x (2 mM)
dNTPs	0.15	0.5 µM each
Primer GFAP-IL6 F 5'- GATCCAGACATGATAAGATA-3'	0.45	0.2 µM
Primer GFAP-IL6 R 5'- CCGAAAAAACTCGGAATGG-3'	0.3	0.2 µM
Primer *Mt1* F 5'- TCACCAGATCTCGGAATGG-3'	0.23	0.15 µM
Primer *Mt1* R 5'- AAGAACCGGAATGAATCGC-3'	0.23	0.15 µM
Taq polymerase	0.08	26.7 mU/µL
H2O	11.76	
Final volume	15	
Sample	1	

	Temperature (°C)	Time (s)	Cycles (n)
Inicial denaturation	95	180	1
Denaturation	95	30	33
Hybridation	53		
Elongation	72		
Final elongation	72	300	1

3.4 Disease staging and phenotype

Disease stages of NDUFS4-deficient mice have been previously described in detail (Quintana et al., 2010). In brief, disease progression in *Ndufs4 KO* mice can be subdivided into three stages: early stage (P0–P29), mid stage (P30–40), and late stage (<P40) in which clinical signs increase in severity (Kruse et al., 2008; Quintana et al., 2010). Early stage *Ndufs4 KO* mice (<P30) have decreased body weight and length, alopecia, breathing abnormalities, and decreased total ambulation when compared with control mice. During this period, mice are able to grow and gain some weight and do not present visible signs of discomfort. Within the mid stage window (P30–40), *Ndufs4 KO* mice start to lose weight around P35 and become slightly ataxic. Clasping, body twisting, and epilepsy generally appear around P36–40, and motor coordination progressively worsens. Symptoms progress rapidly and around P40 *Ndufs4 KO* mice enter the late stage phase

in which mice present severe ataxia, spontaneous rotation behavior, paw paralysis, severe respiration deficits, sudden weight drop, and ultimately, they die around P55.

3.5 Experimental designs

Several major experiments were conducted in the course of this thesis project. For clarification, the different experimental designs are summarized in **Figures 9** and **10**.

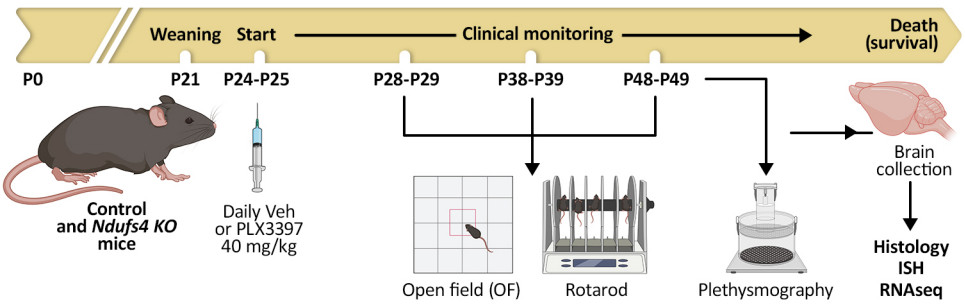

Figure 9. Experimental design of the PLX3397 experiment.

Control and *Ndufs4 KO* mice were weaned at P21. Beginning at P24-P25 mice were injected intraperitoneally 6 days a week with vehicle solution or 40 mg/kg of PLX3397. Mice went through two different tests (open field and accelerating rotarod) at 3 different ages which correspond with the early, mid, and late stages of the disease. Moreover, the respiration pattern was also assessed by plethysmography at P47–P48. Furthermore, mice were weighed every day and monitored for disease progression. Brains were collected at P48–P49 for different purposes which include histology, ISH, and RNAseq.

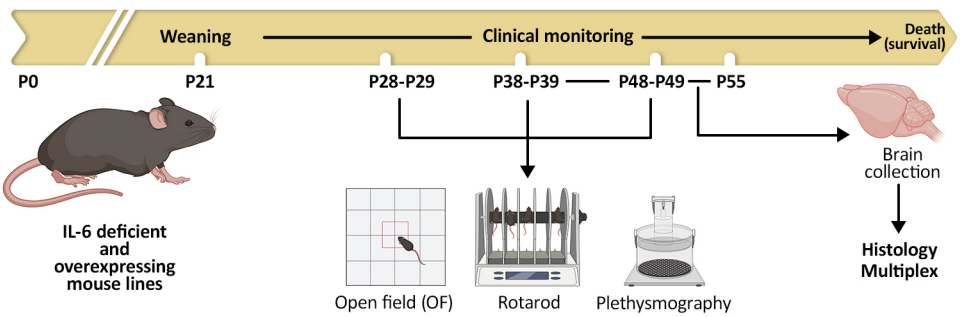

Figure 10. Experimental design of the IL-6 deficient and IL-6 overexpressing experiments.

Mice from the different genotypes were weaned at P21. Mice went through open field, rotarod, and plethysmography tests at every disease stage. Mice were weighed and monitored for disease progression every other day. At P38–P39 and P49–P55 mice were euthanized and the brain was collected for histology and multiplex analyses.

3.6 Microglial depletion with the colony-stimulating factor 1 receptor (CSF1R) inhibitor, PLX3397

A dose-response study was performed to set the appropriate PLX3397 dose. For that purpose, 50 days-old WT mice were intraperitoneally (IP) injected 6 days a week for two weeks with vehicle solution (Veh) or 4, 8, 16, or 40 mg/kg of PLX3397 (MedChem, HY-16749). The daily injected volume was 0,1 ml for every 10 g of weight. PLX3397 was dissolved in a solution of 20% DMSO, 40% PEG-300, 5% Tween-80, and 35% saline (v/v). The 40 mg/kg dose was finally selected. So, control and *Ndufs4 KO* mice were injected with Veh or 40 mg/kg of PLX3397 IP 6 days a week beginning on postnatal days P24–P25 (**Figure 9**). To minimize litter effects, mice from the same litter and with equal genotype were assigned different treatments.

3.7 Clinical evaluation

In the course of this project, mice were weighed and examined daily or every other day for clinical signs (ataxia, and gait/postural alterations). Paw clasping behavior and body twisting were examined by suspending the animals by the tail for 20 seconds and measured as the presence or absence of the behavior; the day of onset was recorded. Food pellets and hydrogel were placed on the cage floor when *Ndufs4 KO* mice start to present paw paralysis. Finally, mice were humanely euthanized after a 20% loss of maximum body weight, after veterinary recommendation, or when they were found moribund.

3.8 Behavioral tests

Mice were tested at the early, mid, and late stages at postnatal days P27–29, P38–39, and P48–49, respectively. All mice were tested after 30 minutes of habituation in the testing room. It should be mentioned that due to the extremely narrow temporal window, some of the animals included in the experiments could not perform all tests at all ages. Nevertheless, this situation was avoided as far as possible.

3.8.1 Rotarod

The rotarod test was used to monitor motor coordination. The task consisted of placing the animals on a rotating bar that accelerated from 4 rpm to 40 rpm in 300 s (Harvard Apparatus, Holliston, MA, USA). The latency time to fall from the rod to the ground was measured. At the early disease stage, mice underwent two consecutive training trials the day before the first rotarod test. A training trial was considered successful when mice did not

fall before starting the task and did not jump during the execution of it. The following day, the test was performed thrice with a minimum lapse of 10 min between trials, and the mean of the trials was calculated.

3.8.2 Open field (OF)

The mice were placed in one of the corners of a methacrylate white box (56 [W], 36.5 [D], 31 [H] cm) and allowed to explore the apparatus freely for 10 minutes. The measured parameters include the total ambulation distance (horizontal activity) and the number of rearings (vertical activity; the number of times the mouse stood on its rear limbs). The activity of the mice was recorded through videography. The total distance traveled was analyzed using EthoVision XT tracking software (Noldus Information Technology bv., Wageningen, the Netherlands), whereas rearings were visually counted by the experimenter. Rotation behavior was assessed only in the late stage open field test and measured as the presence or absence of the behavior.

3.8.3 Whole-body plethysmography

Unrestrained whole-body plethysmography was used to assess the ventilatory function. The detailed protocol has been described previously (Prada-Dacasa et al., 2020). Briefly, the mice were allowed to acclimatize to the plethysmograph chamber (EMMS, ref. PLY310) for 45 min, followed by 15 min of the experimental period. The chamber was cleaned between the different mice. Tidal volume (volume of air moved into or out of the lungs during a normal breath) normalized per body weight ($\mu L \cdot g^{-1}$) and respiratory frequency (breaths$\cdot$ min^{-1}) are reported in this study.

3.9 Tissue preparation for immunostaining

All mice used in the study were euthanized by decapitation. Mice ages were at P47–P48 for the PLX3397 experiments; at P38–39 and P48–P55 for mid and late stages, respectively, in the IL-6 deficiency and overexpression experiments (now referred to as IL-6 experiments). All brains dissected for histology were fixed in 4% paraformaldehyde (PFA) solution at 4°C for 24 h and then transferred to cryoprotective 30% sucrose in PBS (Phosphate-buffered saline) (0.01 M pH 7.4) solution for 48 h at 4°C.

In PLX3397 and IL-6 experiments, the entire brain was preserved for immunostaining. Before freezing, olfactory bulbs (OB) were separated from the rest of the brain by cutting coronally the prefrontal cortex. OBs were embedded in OCT medium and frozen in dry ice, whereas the remaining brain was frozen by immersion in isobutane at -30°C. All brains used for immunostaining were kept at -80°C until sectioning.

3.10 Cryosectioning and immunostaining

In PLX3397 and IL-6 experiments, 20 µm coronal sections of the brain were obtained using a Leica CM3050 S cryostat (Leica Biosystems GmbH, Wetzlar, Germany). Brains were sectioned from bregma 0.62 mm to -2.46 mm, and from bregma -5.34 mm to -6.64 mm following Franklin and Paxinos mouse brain atlas (Paxinos & Franklin, 2013). The sections were preserved in an anti-freezing solution (50% PBS 0.01M, 30% ethylene, and 20% glycerol) at -20°C until staining. OBs were also cut at 20 µm, but directly mounted on Superfrost slides (Thermo Fisher Scientific), dried at room temperature (RT) (20–26°C), and stored at -80°C until staining.

Antibodies used for immunostaining are summarized in **Table 9**. IBA-1 (ionized calcium-binding adaptor protein-1) and TMEM119 (transmembrane protein 119) were used to stain for microglia, and GFAP (glial fibrillary acidic protein), NeuN (neuronal nuclear protein), CD3 (cluster of differentiation 3), and podocalyxin were used to stain for astrocytes, neurons, T-lymphocytes, and blood vessels, respectively. Immunostaining negative controls, consisting of samples incubated only with secondary antibodies, were included (not shown).

Table 9. List of the different antibodies used for the immunostainings.

Antibody	Conjugated	Manufacturer	Catalogue #	Host	Dilution
Anti-IBA1	-	Wako	019-19741	Rabbit	1/1000
Anti-TMEM119	-	Abcam	ab209064	Rabbit	1/1000
Anti-GFAP	-	Dako	Z0334	Rabbit	1/1000
Anti-NeuN	-	Millipore	ABN91	Chicken	1/500
Anti-Podocalyxin	-	R&D Systems	MAB1556	Rat	1/100
Anti-CD3	-	Dako	A0452	Rabbit	1/100
Anti-Rabbit	Alexa Fluor 568	ThermoFisher	A11011	Goat	1/600
Anti-Chicken	Alexa Fluor 488	ThermoFisher	A11039	Goat	1/600
Anti-Rabbit	Biotin	Vector	BA-1000	Goat	1/200
Anti-Mouse	Alexa Fluor 488	ThermoFisher	A-11001	Goat	1/500

In the PLX3397 and IL-6 experiments, duplicate sections of free-floating brain slices or mounted OBs were selected within the following brain coordinates: cortex and hippocampus (between bregma -1.94 mm and -2.30 mm), VN and cerebellum (between bregma -5.88 mm and -6.12 mm), and OB (between bregma 4.28 mm and 3.20 mm). For immunostaining, sections

were washed once in PBS and then blocked in 1% BSA and 0.2% Triton X-100 in PBS solution for 1 h at RT. Slides were then incubated overnight at 4°C with the chosen primary antibody diluted in blocking solution. The following day, sections were left for 1 h at RT, washed three times with PBS (10 min each), and incubated with the specific secondary antibody diluted in blocking solution 1 h at RT carefully protected from light. Finally, sections were washed again three times with PBS (10 min each), and free-floating brain slices were mounted on Superfrost slides (Thermo Fisher Scientific). The slides were then dried and mounted with DAPI Fluoromount (Southern Biotech).

For immunohistochemical analysis of $CD3^+$ cells, brain sections were first mounted on slides, incubated with citrate buffer (10 mM sodium citrate, 0.05% Tween, pH 6) for 20 min at 96°C for antigen retrieval, and incubated with endogenous peroxidase blocking solution (70% methanol and 3% hydrogen peroxide) for 15 min. Slices were then blocked as described previously, incubated overnight at 4°C with the primary antibody diluted in blocking solution. The next day, sections were washed three times with PBS (10 min each) and incubated for 1 h at RT with the secondary antibody again diluted in blocking solution. Afterwards, section were again washed three times with PBS (10 min each) and incubated for 1h at RT with horseradish peroxidase-coupled streptavidin (1:600, Vector SA-5004). The immunoreactivity was visualized using 0.5 mg/ml 3,3-diaminobenzidine and 0.033% hydrogen peroxide for 10 min at RT. Finally, the slides were dehydrated and covered with DPX mounting medium. In this case, as the presence of $CD3^+$ cells in the brain parenchyma in basal conditions is extremely rare (Prinz and Priller, 2017), a positive control (GFAP-IL6 mouse brain) described to have $CD3^+$ cell infiltrates was included and used to verify successful CD3 detection (Quintana et al., 2009; Giralt et al., 2013).

3.11 *In situ* hybridization using RNAscope

In situ hybridization (ISH) using *RNAscope Multiplex Fluorescent kit* (Advanced Cell Diagnostics) was used to detect *Gad2* (GABAergic neurons) and *Slc17a6 (*glutamatergic neurons) transcripts. Briefly, 48–49-day old mice were euthanized, and their brains were immediately embedded in OCT medium and frozen with dry ice. Fourteen-micrometer brain cryosections containing the VN region were obtained, directly mounted on slides, and kept at -80°C until use. First, sections (between bregma -5.88 mm and -6.00 mm) were fixed in cold PBS containing 4% PFA for 30 min at RT. Following two quick washes in PBS, the brain slices were dehydrated in 50% (5 min),

70% (5 min), and 2 × 100% (5 min each) ethanol solutions and treated with protease IV solution at RT for 30 min. Protease was washed away with two PBS washes (2 min each). Target and negative control probes were applied directly to the sections and incubated at 40°C for 2 h in a HybEZ oven (Advanced Cell Diagnostics, Inc., Newark, CA, USA). Next, the slides were incubated with preamplifier (AMP1, 40°C for 30 min) and amplifier reagents (AMP2, 40°C for 15 min; AMP3, 40°C for 30 min). The slides were then incubated with fluorescent labels (AMP4- Alt C). Finally, the brain sections were mounted using DAPI Fluoromount.

3.12 Microscopy and image quantification

Immunofluorescence and immunohistochemistry images of brains from the PLX3397 and IL-6 experiments were captured using a Nikon Eclipse 90i microscope coupled to a Nikon Digital Camera DXM1200F using the ACT-1 v2.70 capture software (Nikon, Tokyo, Japan) for GFAP, IBA-1, TMEM119, and CD3 stainings. Cornus Ammonis 1 (CA1) and VN were photographed at 20X magnification, while images of the cortex, whole hippocampus, OB, and cerebellum slices were taken at 10X magnification. Images were captured under specific detector sensitivity conditions for each area; exposure and gain settings were optimized for each staining and maintained constant during entire the acquisition. The samples were quantified using ImageJ software (FIJI version 1.51). For GFAP, IBA-1, and TMEM119 immunofluorescence quantification, fluorescence intensity was measured and normalized by area. Intensity is reported in arbitrary units (a.u.) since the output values from the ImageJ software do not have a specific measurement unit. The total number of IBA-1$^+$ or CD3$^+$ cells were manually counted and relativized by area. Microglial morphological phenotypes were visually discriminated. Podocalyxin images were captured using a Zeiss LSM800 confocal microscope (Carl Zeiss AG, Oberkochen, Germany) at 20X magnification using a Plan-Apochromat 20x/0.8 objective. *In situ* hybridization images were captured using a Zeiss LSM700 confocal microscope (Carl Zeiss AG, Oberkochen, Germany) at 20X magnification using a Plan-Apochromat 20x/0.8 objective. Maximal intensity projections of Z-stacks were created using ImageJ software. Positive *Gad2* and *Slc17a6* neurons were counted and relativized by area.

3.13 RNA extraction and sequencing

For RNA sequencing experiments, brain samples were obtained from 48–49 days old control and *Ndufs4 KO* mice treated with Veh or PLX3397. Hippocampi were manually dissected, whereas VNs were dissected

using a 1 mm coronal brain matrix. A 2 mm coronal brain slice was obtained from the VN region, and the cerebellum and the brainstem were removed. Hippocampi and VNs were flash-frozen in liquid nitrogen and kept at -80°C until RNA extraction; later they were homogenized in Precellys lysing tubes (ref. P000918-LYSK0-A) containing 1 ml of TRIzol (Invitrogen™, ref. 15596018) using a Precellys 24 tissue homogenizer (Bertin Instruments, Montigny-le-Bretonneux, France) (3x5000 rpm, 7s per cycle). The homogenate was incubated for 5 min at RT and transferred to a clean 1.5 ml Eppendorf tube. Then, 200 µl of chloroform was added to each tube, vigorously shaken, incubated for 3 min, and centrifuged (12000 g, 15 min, 4°C). After centrifugation, the upper aqueous phase containing the RNA was carefully removed and placed in a clean Eppendorf tube. 1.5 volumes of 100% ethanol for molecular biology were added to every tube for each volume of the collected RNA-containing aqueous phase. Afterward, RNA was purified using the RNeasy Mini Kit (Qiagen, ref. 74106) according to the manufacturer's instructions. RNase-free DNase set (Qiagen, ref. 79254) was used during the RNA purification protocol for genomic DNA digestion. RNA purity (260/230 and 260/280 ratios) and concentration were measured using a DS-11 FX+ Spectrophotometer/Fluorometer (DeNovix Inc., Wilmington, DE, USA). For accurately assessing RNA concentration, Qubit™ RNA High Sensitivity assay was used (Thermo Fisher Scientific, ref. Q32852) following the manufacturer's instructions. Before sequencing, RNA integrity was measured in the Agilent 4200 TapeStation (Agilent Technologies, Santa Clara, CA, USA) using the High Sensitivity RNA ScreenTape (ref. 5067-5579). Only RNAs samples with RIN (RNA integrity number) values ≥ 8 were used. Libraries were constructed and samples sequenced, trimmed, and aligned to the reference genome by the Biomedicum Functional Genomics Unit at the Helsinki Institute of Life Science at the University of Helsinki. Sequencing was performed with NextSeq High Output 75 cycle flow cell on the NextSeq 500 (Illumina Inc., San Diego, CA, USA). Raw BCL read files were converted to FASTQ format using bcl2fastq, trimmed with Trimmomatic (Bolger et al., 2014), and aligned to mouse GRCm39 reference genome using STAR (Dobin et al., 2013).

3.14 Multiplex

Mice were euthanized by decapitation at P38 for mid stage and between P47–P55 for late stage. Brain areas were dissected, flash-frozen in liquid nitrogen, and kept at -80°C until further use. Multiplex analysis for brain tissue was previously optimized and validated in our laboratory (Sanchis et al., 2020c) following a previous protocol for spinal cord (Amo-Aparicio et al., 2018).

In short, both OBs and half cerebellums were mechanically homogenized using an MM-400 mixer mill (Retsch GmbH, Haan, Germany), followed by ultrasonic homogenization using Sartorius-LABSONIC P (Sartorius AG, Göttingen, Germany). Samples were homogenized in 100 µl (OB) and 200 µl (cerebellum) of ice-cold protein extraction buffer. Every 10 milliliters of homogenization buffer contained: 2,5 mL of 25 mM HEPES, 20 µl of 10% IGEPAL, 0,5 ml of 0.1 M $MgCl_2$, 130 µl of 1.3 mM EDTA (pH 8.0), and 100 µl of 0.1 M EGTA (pH 8.0). Homogenization buffer was supplemented with a 1% protease inhibitor cocktail and 0.1 M phenylmethylsulphonyl fluoride (Sigma-Aldrich P8340 and P7626, respectively). After sonication, the homogenate was centrifuged at 12000 g for 5 min. The supernatant was collected to determine the protein concentration using the PierceTM BCA Protein Assay (Thermofisher ref. 23.227). A protein concentration of 5–12 µg/µl of the tissue lysate was used to measure the abundance of IL-6, TNF-α, IL-10, and IL-1β using the Mouse High Sensitivity T Cell Magnetic Bead Panel (Millipore, ref. MHSTCMAG-70K) according to the manufacturer's instructions. Data were obtained using a Luminex MAGPIX instrument system (Luminex Corporation, Austin, TX, USA) and analyzed using the xPONENT software v4.2 (Luminex Corporation, Austin, TX, USA). All results were normalized to the protein concentration in the lysate. Results between the blank and the first standard of the standard curve were considered as 0. IL-1β levels were unquantifiable as the levels seemed to be below the detection threshold of the technique.

3.15 Representation and statistics

All graphics were generated using GraphPad Prism 8 software (GraphPad Software, Inc, San Diego, CA, USA) except for those of the RNAseq that were generated using the R software (version 4.2.1). The great majority of the graphics are shown as mean ± SEM, except for tidal volume and respiratory frequency (box and whisker plot), and survival (Kaplan-Meier curve). In addition, the "N" of the groups is consistently shown within the bars or next to the graph. Statistical analyses were performed using the Statistical Package for Social Sciences (SPSS) 19 (IBM, Armonk, NY, USA). Survival was analyzed using log-rank test. For comparisons between two groups (i.e., clasping), the homogeneity of the variances was assessed using Levene's test; unpaired Student's t-test (equal variances) or Mann-Whitney test (different variances) were selected accordingly. The analysis for the dosage pilot study, which involved more than two groups and just one variable, a one-way ANOVA test, followed by Tukey's multiple comparison test, was used. The chi-square test was used for frequency analysis (rotation

behavior). When there were two variables to compare, statistical analysis was performed using the generalized general model (GzLM) (McCulloch and Searle, 2010). The GzLM is more flexible than two-way ANOVA since it tolerates different distributions, heterogeneity of variances, and missing values. Similar to the two-way ANOVA, the GzLM tests for the two main effects and the interaction between them. Only when the interaction was significant we performed a sequential Bonferroni *post hoc* test for pairwise comparisons; relevant p-values are shown in brackets throughout the text. Similarly, for repeated measures (body weight gain), a generalized estimating equation (GEE) analysis was used. Statistical significance was defined as p-value ≤0.05. Both male and female mice were used in this study, and sex differences were reported when applicable. Regarding RNAseq, differential expression analysis of normalized gene counts was done in R (version 4.2.1) using the DESeq2 package (Love et al., 2014) which computes p-values using the two-sided Wald test method and corrects for multiple testing with the Benjamini–Hochberg method. Only genes with p-adjusted value ≤ 0.05 and log2Fold change ≥ 0.5 or ≤ -0.5 were used for data analysis, representation, and interpretation. Gene Ontology (GO) enrichment was performed with Metascape (Zhou et al., 2019), heatmaps and volcano plots were done using the Complexheatmap (Gu et al., 2016) and Enhancedvolcano R packages, respectively.

4

Results

Part 1. Microglial cells contribute to the Leigh-like disease of *Ndufs4 KO* mice

Microglia depletion increases lifespan and improves the motor performance of *Ndufs4 KO* mice

Resembling Leigh syndrome pathology (Lake et al., 2016; Lee et al., 2020), *Ndufs4 KO* mice develop a fatal early-onset progressive encephalopathy characterized by respiratory deficiencies, a strong decline in motor function, and neurodegeneration and neuroinflammation in several brain areas (Kruse et al., 2008; Quintana et al., 2010; Johnson et al., 2013). However, the role of neuroinflammation is poorly understood. To study the implications of neuroinflammation in the progression of the pathology in *Ndufs4 KO* mice, we induced a neuroimmune disruption by pharmacologically depleting microglial cells using the well-known inhibitor of CSF1R, PLX3397 (Elmore et al., 2014). Briefly, CSF1R signaling is necessary for microglial survival, and the receptor's blocking induces microglial death (Elmore et al., 2014).

In order to establish the effective working dose, different doses were tested in WT mice (**Figure 11**). As expected, a daily injection of PLX3397 caused a dose-dependent reduction in the number of microglial cells. 40 mg/kg 6 days a week reduced approximately 70% of the IBA-1^{+} cells across the whole brain after 14 days of treatment (**Figure 11 A**). This reduction seemed homogenous across different brain regions (**Figure 11 B**). Importantly, the different doses of PLX3397 did not produce significant body weight changes when compared to the vehicle-treated mice (**Figure 11 C**). Thus, we used the 40 mg/kg dose for further experiments aiming to understand the role of neuroinflammation in *Ndufs4 KO* mice. The breeding and experimental design are shown in **Figures 8 A** and **9**, respectively.

As expected, *Ndufs4 KO* mice exhibited early mortality (**Figure 12 A**), reduced body weight (**Figure 12 B**), progressive motor decline (**Figure 13 A-D**), and altered respiration (**Figure 13 E**). Since PLX3397 is documented to be well tolerated at low doses as the one used in this study, only a few control mice were included to monitor possible side effects. As expected, at P60, PLX3397-treated control mice showed no signs of illness. Regarding the effects the treatment in *Ndufs4 KO* mice, microglial depletion prominently increased the survival rate of *Ndufs4 KO* mice ($p = 0.001$) (**Figure 12 A**), but did not rescue the body weight loss (**Figure 12 B**). A small non-significant reduction of body weight was observed in control mice treated with PLX3397. Microglial depletion significantly rescued other abnormalities. Thus, it reduced the progressive deterioration of balance and motor coordination in

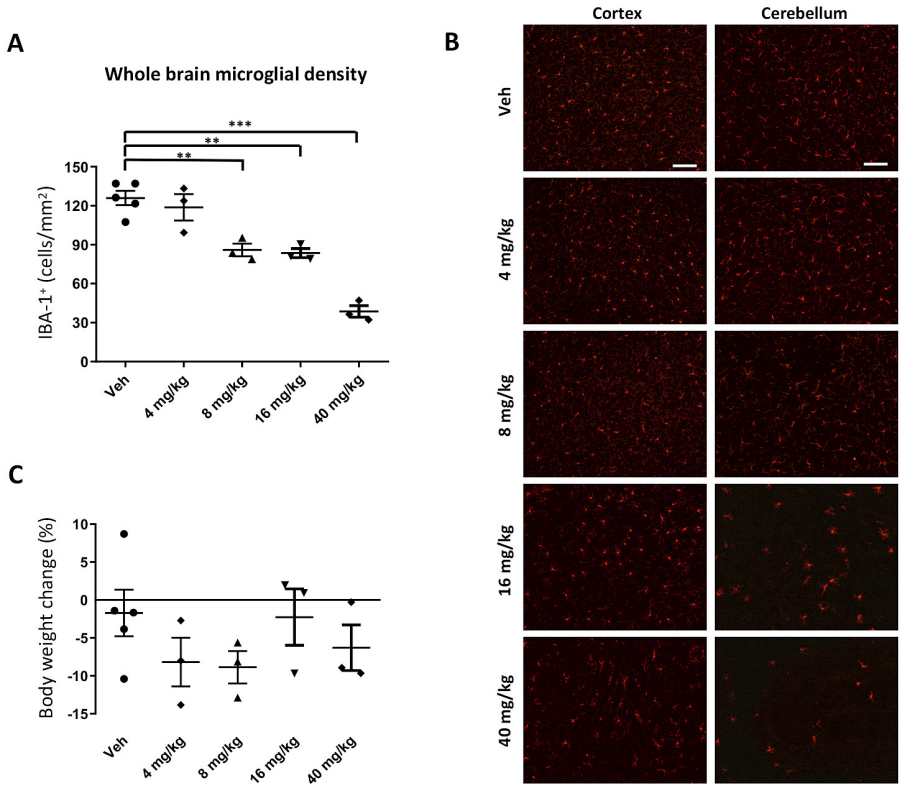

Figure 11. Intraperitoneal administration of PLX3397 at 40 mg/kg reduces approximately 70% of IBA-1⁺ cells in the mouse brain.

(A) Number of IBA-1⁺ cells in the mouse brain after injection of different doses of PLX3397 after 14 days of treatment. **(B)** A similar decrease in IBA-1⁺ cells was observed in different brain regions, as exemplified by the representative images of the cortex and cerebellums at the different doses. Scale bar 100 µm. ** $p \leq 0.01$, *** $p \leq 0.001$. **(C)** Body weight change in the different treated groups.

the rotarod (**Figure 13 A**), while vehicle-treated *Ndufs4 KO* mice were mostly incapable of performing the rotarod test by approximately two months of age (late stage), PLX3397-treated mice showed improved motor performance at the mid (P38–P39) and late stages (P47–P48) of the disease as revealed by the significant interaction followed by *post hoc* pairwise comparisons (*Ndufs4 KO*-Veh vs. *Ndufs4 KO*-PLX3397, $p = 0.042$ and $p = 0.009$, for mid and late stage, respectively). This presumably reflects the effects on motor coordination rather than general activity since microglia depletion did not rescue the decreased ambulation of *Ndufs4 KO* mice in the OF (**Figure 13 B**). Microglia depletion also reduced the frequency of spontaneous rotation behavior (mice circling on themselves, possibly due to vestibular lesions) in *Ndufs4 KO* mice at the P47–48 ($p = 0.014$) (**Figure 13 C**). PLX3397 also delayed the onset of clasping/twisting behavior in NDUFS4-deficient mice ($p \leq 0.001$). (**Figure 13 D**).

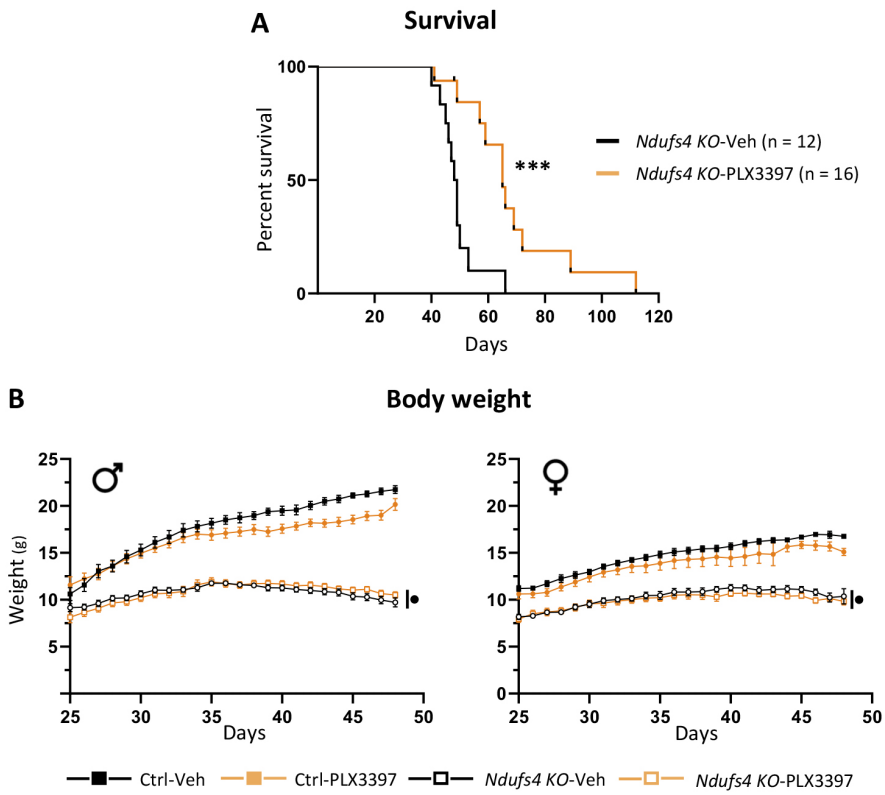

Figure 12. Inhibition of CSF1R signaling extends the lifespan of *Ndufs4 KO* mice.

(A) Kaplan–Meier survival curve for *Ndufs4 KO* mice treated with vehicle or PLX3397. **(B)** Total body weight for Ctrl-Veh, Ctrl-PLX3397, *Ndufs4 KO*-Veh, and *Ndufs4 KO*-PLX3397 of male and female mice (n = 7-15). *** $p \leq 0.001$, ● Ndufs4 effect $p \leq 0.05$.

Patients with LS normally present with respiratory abnormalities that are strongly associated with mortality (Arii and Tanabe, 2000). Constitutive *Ndufs4 KO* mice also show abnormal breathing patterns, which increase in severity as pathology progresses (Quintana et al., 2012b). Respiratory rhythm generation and control include numerous CNS regions, such as the VN, cerebellum, and different brainstem nuclei. Respiratory abnormalities in *Ndufs4 KO* mice are partially associated with mitochondrial dysfunction due to NDUFS4 loss in the VN and abnormal responses in the pre-Bötzinger complex of the brainstem (Quintana et al., 2012b). In line with these findings, using whole-body plethysmography (Prada-Dacasa et al., 2020), we observed an increased tidal volume (volume of air inspired by the animal in one breath) in *Ndufs4 KO* mice at P47–P48 (**Figure 13 E**), but no significant changes in respiratory frequency (**Figure 13 F**). Microglial depletion significantly increased the tidal volume, while a similar trend was observed for respiratory frequency (PLX3397 effect, p= 0.09).

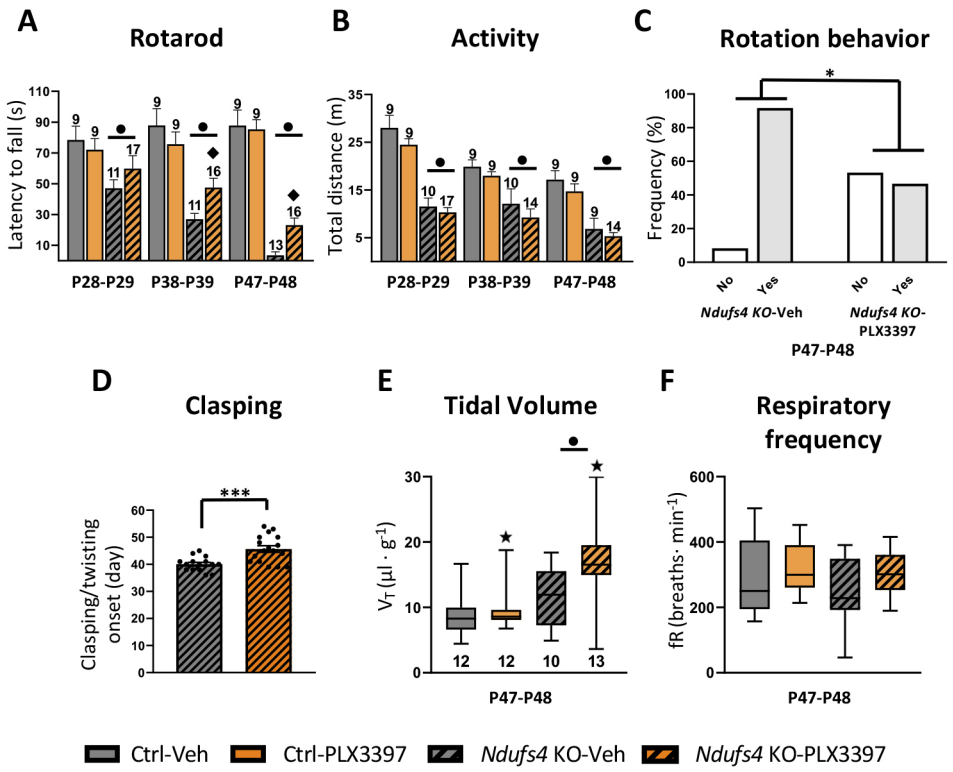

Figure 13. Inhibition of CSF1R signaling delays motor symptoms in *Ndufs4 KO* mice.

(A-D) Effects of PLX3397 on the motor phenotype of *Ndufs4 KO* mice: latency to fall in the accelerating rotarod **(A)**, total distance traveled in the open-field test **(B)**, rotation behavior in the open field at the late stage **(C)**, and clasping onset in vehicle and PLX3397-treated *Ndufs4 KO* mice **(D)**. **(E)** Tidal volume and **(F)** respiratory frequency of control and *Ndufs4 KO* mice treated with vehicle or PLX3397 at P47–P48. ● Ndufs4 effect p≤ 0.05, ★ treatment effect p ≤0.05, ♦ p ≤0.05 interaction between both factors, * p = 0.05–0.01, *** p ≤0.001.

PLX3397 treatment prevents IBA-1+ cell accumulation and proliferation in brain regions associated with neurodegeneration in *Ndufs4 KO* mice

The characteristic fatal encephalopathy of the *Ndufs4 KO* mice occurs in specific brain regions (Quintana et al., 2010; Johnson et al., 2013; Miller et al., 2020; Shil et al., 2021). We examined whether PLX3397 treatment could also reduce microglial cell numbers in *Ndufs4 KO* mice and prevent IBA-1^{+} cell accumulation in the known neurodegenerative areas in late stage mice. As expected, prominent glial reactivity (as revealed by IBA-1 and GFAP immunostaining) was observed in the VN, OB, and cerebellum, where abundant neurodegeneration is described to occur in *Ndufs4 KO* mice (**Figure 14**). At the late stage, in these three regions, most microglia and astrocytes present a reactive morphology as shown in magnified images (areas 1-4) of

cells showing microglia and astrocyte morphology in the VN of control or *Ndufs4 KO* mice. In addition, GFAP (but not IBA-1) immunostaining clearly increased in the cortex and hippocampus (**Figure 14**). Treatment with PLX3397 caused a robust decrease in IBA-1 fluorescence intensity in all the studied brain areas. Control animals showed microglial depletion similar to the observed in the pilot dosage study (**Figure 11 A**), which confirmed the reproducibility of the experiment. *Ndufs4 KO* mice also showed dramatic microglial depletion both in areas where microgliosis is prominent (VN, OB, and cerebellum) and in those lacking it (cortex and hippocampus). Massive microglial cell accumulation hindered adequate cellular segmentation in the first three areas and, thereby, a precise cell count. This was possible in the cortex and hippocampus, where PLX3397 administration reduced IBA-1^{+} cells by approximately 70 and 60%, respectively. Different results depending on the brain area were observed regarding GFAP immunoreactivity due to PLX3397 administration (**Figure 14**). Thus, in the VN, PLX3397 did not affect GFAP immunofluorescence in either control or *Ndufs4 KO* mice, whereas in the cerebellum, a reduction was observed in both genotypes. In contrast, within the OB, cortex, and hippocampus, PLX3397 treatment increased GFAP immunofluorescence. Taken together, the GFAP immunofluorescence results suggest that astrocytes respond to the microglial depletion in a region-dependent manner.

Reactive microglia promote neuronal loss in *Ndufs4 KO* mice

After showing that PLX3397 treatment could prevent microglial accumulation in major neurodegenerative areas of *Ndufs4 KO*, we investigated whether a reduction in the microglial response could prevent neuronal loss in *Ndufs4 KO* mice in two areas with prominent neuroinflammation, the OB (not shown) and the VN (**Figure 15 B**). By quantifying the area occupied by NeuN immunostaining, we observed that microglial depletion partially protected against neuronal loss in the granular cell layer of the olfactory bulb (GrOB), as revealed by a significant interaction between genotype and treatment (**Figure 15 A**). In the whole VN, in contrast, microglial depletion did not significantly prevent neuronal loss (**Figure 15 C, left**). However, a more thorough inspection indicated that although extensive microgliosis occurred in the whole VN of *Ndufs4 KO* mice, it was especially dramatic between the magnocellular part of the medial vestibular nucleus (MVeMC) and the lateral vestibular nucleus (LVe), where extensive bilateral symmetrical lesions appeared, usually surrounded by a glial scar (**Figure 15 B**)(Quintana et al., 2010). Analysis of neuronal loss in this area indicated that microglial depletion tended to rescue neuronal loss although no significance was obtained (**Figure 15 C, right**).

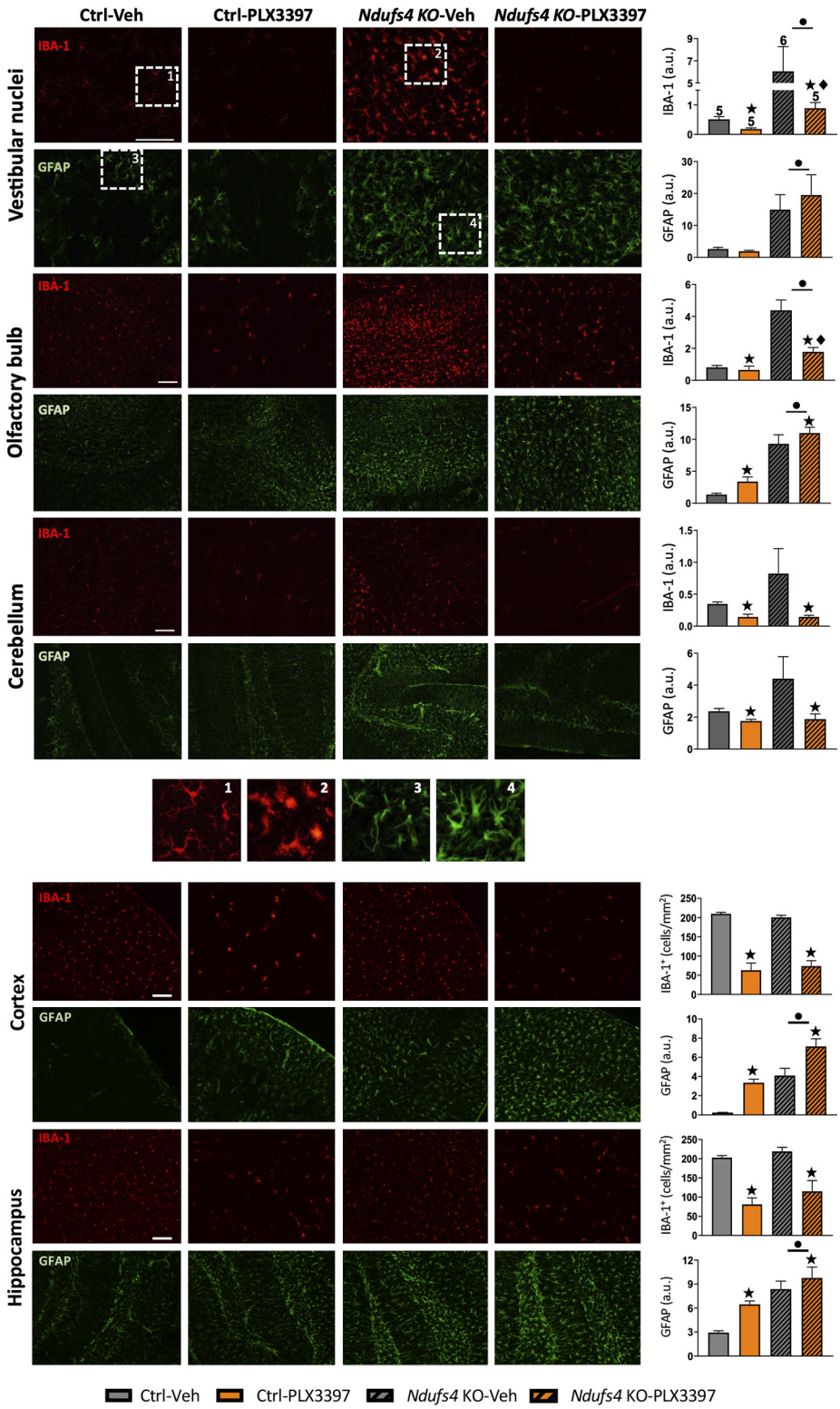
Ctrl-Veh
Ctrl-PLX3397
Ndufs4 KO-Veh
Ndufs4 KO-PLX3397
Vestibular nuclei
Olfactory bulb
Cerebellum
Cortex
Hippocampus
IBA-1
GFAP
IBA-1 (a.u.)
GFAP (a.u.)
IBA-1+ (cells/mm2)
1
2
3
4
Ctrl-Veh
Ctrl-PLX3397
Ndufs4 KO-Veh
Ndufs4 KO-PLX3397

Figure 14. Inhibition of the CSF1R prevents IBA-1+ cell accumulation in neurodegeneration-related areas of *Ndufs4 KO* mice.

Representative images of IBA-1 and GFAP immunofluorescence in VN, OB, cerebellum, cortex, and the hippocampus together with the quantification of IBA-1 fluorescence intensity or total IBA-1$^+$ positive cell and GFAP fluorescence intensity in control and *Ndufs4 KO* mice treated with vehicle or PLX3397 at P47–48 days of age. Amplified areas 1 and 3 show homeostatic microglial (1) and astrocytic (3) morphologies, whereas 2 and 4 show the typical reactive morphologies of microglia (2) and astrocytes (4) ● Ndufs4 effect p≤ 0.05, ★ treatment effect p ≤0.05, ♦ p ≤0.05 interaction between both factors. Scale bar 100 µm.

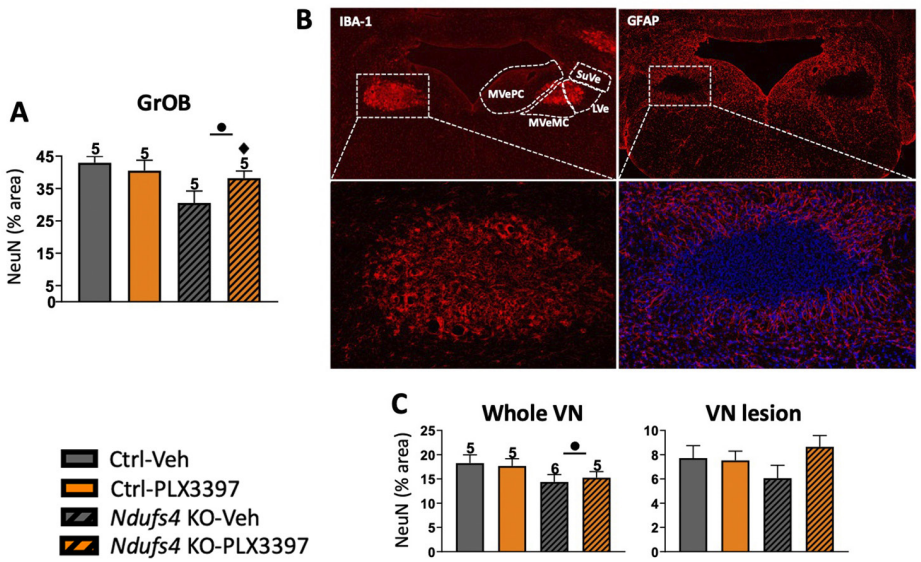

Figure 15.

(A) Percentage of the area occupied by NeuN staining in the GrOB. **(B)** Image of IBA-1 and GFAP stainings of the VN of a *Ndufs4 KO* mouse showing where *Ndufs4 KO* mice use to develop lesions. Lesions are typically formed by reactive IBA-1$^+$ cells surrounded by a glial scar **(C)** Percentage of the area occupied by NeuN staining in the whole VN and the area associated with the main lesion. Ndufs4 effect ● p ≤0.05, ♦ p ≤0.05 interaction between both factors. GrOB: granular cell layer of the olfactory bulb; VN: vestibular nucleus; MvePC: medial vestibular nucleus, parvicellular part; MveMC: medial vestibular nucleus, magnocellular part; SuVe: superior vestibular nucleus; LVe: lateral vestibular nucleus.

Microglia promote both glutamatergic and GABAergic neuronal loss in *Ndufs4 KO* mice

Since NeuN is a general neuronal marker, we sought to investigate if specific neuronal populations were affected by microglial depletion in the VN. To this end, we used ISH assays to assess specific transcripts as markers of glutamatergic (*Slc17a6*$^+$) and GABAergic (*Gad2*$^+$) neurons (**Figure 16**).

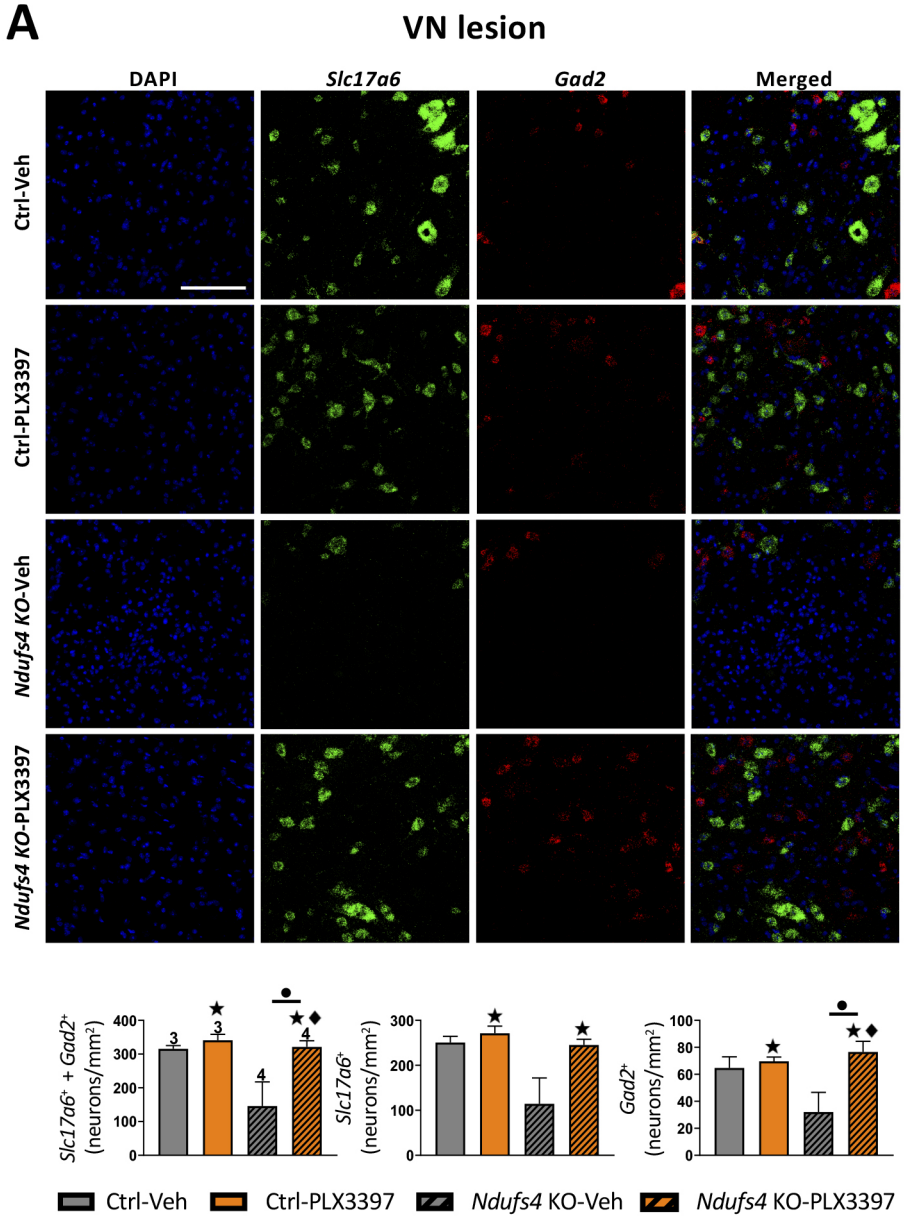

Figure 16. Microglia promotes neuronal loss in *Ndufs4 KO* mice.

(A) Representative ISH images and quantification of the number of glutamatergic and GABAergic neuronal subtypes in the lesion-associated areas of the VN in control and *Ndufs4 KO* mice treated with vehicle or PLX3397 at P47–48 days of age. **(B)** Representative ISH images and quantification of the number of glutamatergic and GABAergic neuronal subtypes in the non-lesioned areas in control and *Ndufs4 KO* mice treated with vehicle or PLX3397 at P47–48 days of age. Scale bar 100 µm. Ndufs4 effect ● $p \leq 0.05$, ★ treatment effect $p \leq 0.05$, ♦ $p \leq 0.05$ interaction between both factors.

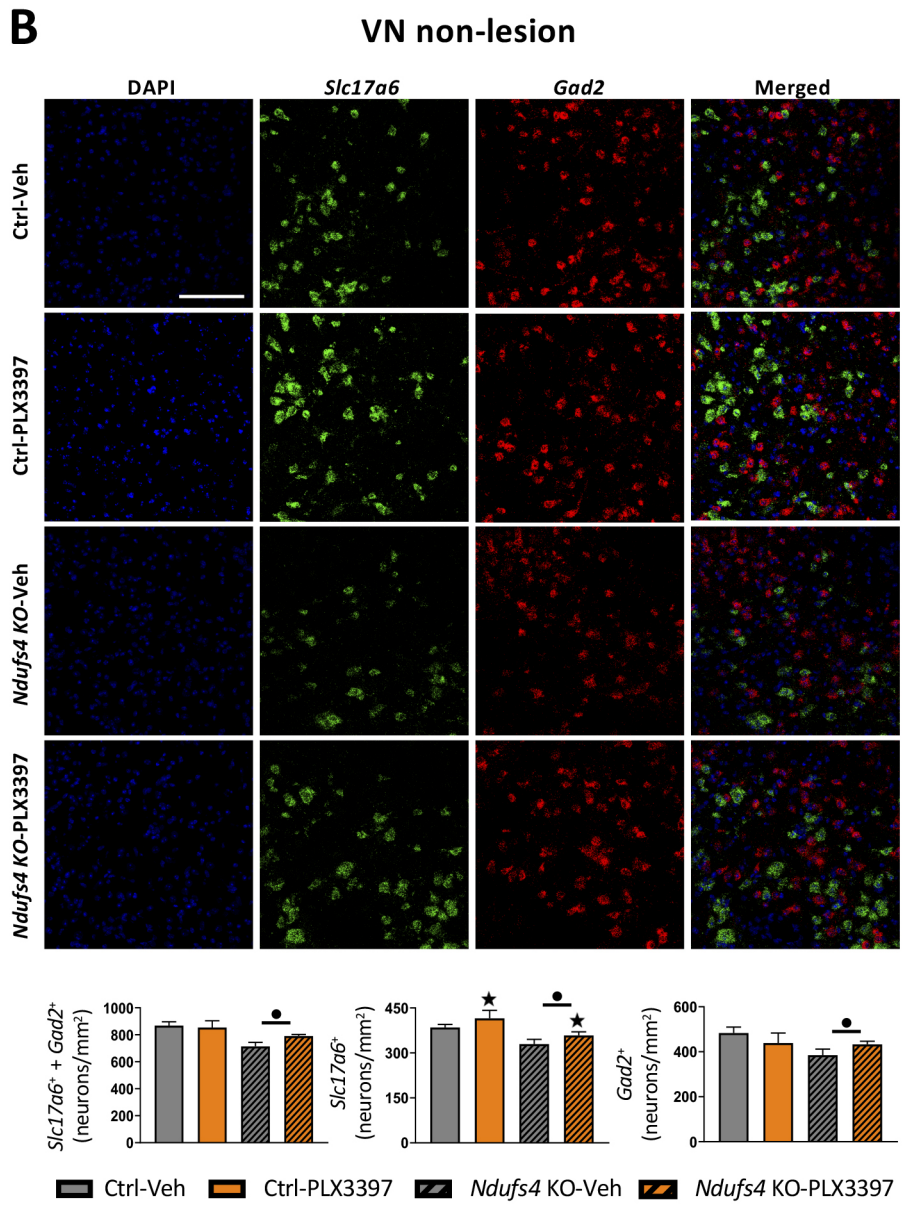

Figure 16 (*cont.*).

In the analysis, we divided the VN into lesion-associated (MVeMC and LVe) and non-lesioned (MVePC and SuVe) areas. As expected, glutamatergic and GABAergic neuronal loss of untreated *Ndufs4 KO* mice was much more prominent in the lesioned area (**Figure 16 A**) than in the non-lesioned (**Figure 16 B**). Importantly, microglial depletion rescued both glutamatergic and GABAergic neuronal loss in the lesion-associated area (**Figure 16 A**).

In the non-lesion area, PLX3397 partially prevented neuronal loss in glutamatergic neurons, but not in GABAergic neurons (**Figure 16 B**). Collectively, these results indicate that microglial cells promote neuronal loss in the VN of *Ndufs4 KO* mice regardless of the neuronal subtype.

Lack of evidence of infiltrating CD3+ cells in motor-related neurodegenerative regions of *Ndufs4 KO* mice

We observed that *Ndufs4 KO* mice develop aberrant blood vessel morphology with aneurism-like structures in the VN, but not in non-neurodegenerative regions such as the cortex (**Figure 17 A**). Some reports using PLX3397 at concentrations like those used in this study have described that besides depleting microglia, it may also alter the populations of other immune cells (Han et al., 2020; Lei et al., 2020). We reasoned that both the development of massive lesions in the VN and blood vessel abnormalities may promote some peripheral cell infiltration into the brain parenchyma. Thus, we investigated whether *Ndufs4 KO* mice presented T lymphocyte infiltrates in the most prominent neurodegenerative areas and whether PLX3397 treatment modified them to some extent. Interestingly, we did not find $CD3^+$ cell infiltrates in either the cerebellum or the VN of *Ndufs4 KO* mice at the late stage (**Figure 17 B**), but substantial $CD3^+$ cells infiltrates were present in the OB at this stage, which were not affected by microglial depletion (**Figure 17 C**). A GFAP-IL6 mouse cerebellum (a chronic model of neuroinflammation with $CD3^+$ cell infiltrates) was used as a positive control (**Figure 17 B**) (Giralt et al., 2013).

Effects of PLX3397 treatment in the transcriptome of the vestibular nuclei and the hippocampus of control and *Ndufs4 KO* mice

Next, we performed a whole-tissue transcriptomic analysis by bulk RNA-seq of the VN and the hippocampus of late stage control and *Ndufs4 KO* mice treated with vehicle or PLX3397. We selected the VN based on our results showing that PLX3397 is protective against neurodegeneration in this area in *Ndufs4 KO* mice, and the hippocampus as a "control" region that presents mild neuroinflammatory hallmarks, but not neurodegeneration.

Clustered heatmap based on the relative expression of 84 microglial-related genes selected from the literature (Bennett et al., 2016; Sousa et al., 2018; Hammond et al., 2019; Li et al., 2019; Masuda et al., 2019; Guttenplan et al., 2021; Hasel et al., 2021) revealed that untreated *Ndufs4 KO* mice samples cluster together and have the highest relative expression of most microglial genes (**Figure 18 A**). In addition, both control and *Ndufs4 KO* PLX3397-treated mice also tend to cluster together (except for 2 KO samples) indicating,

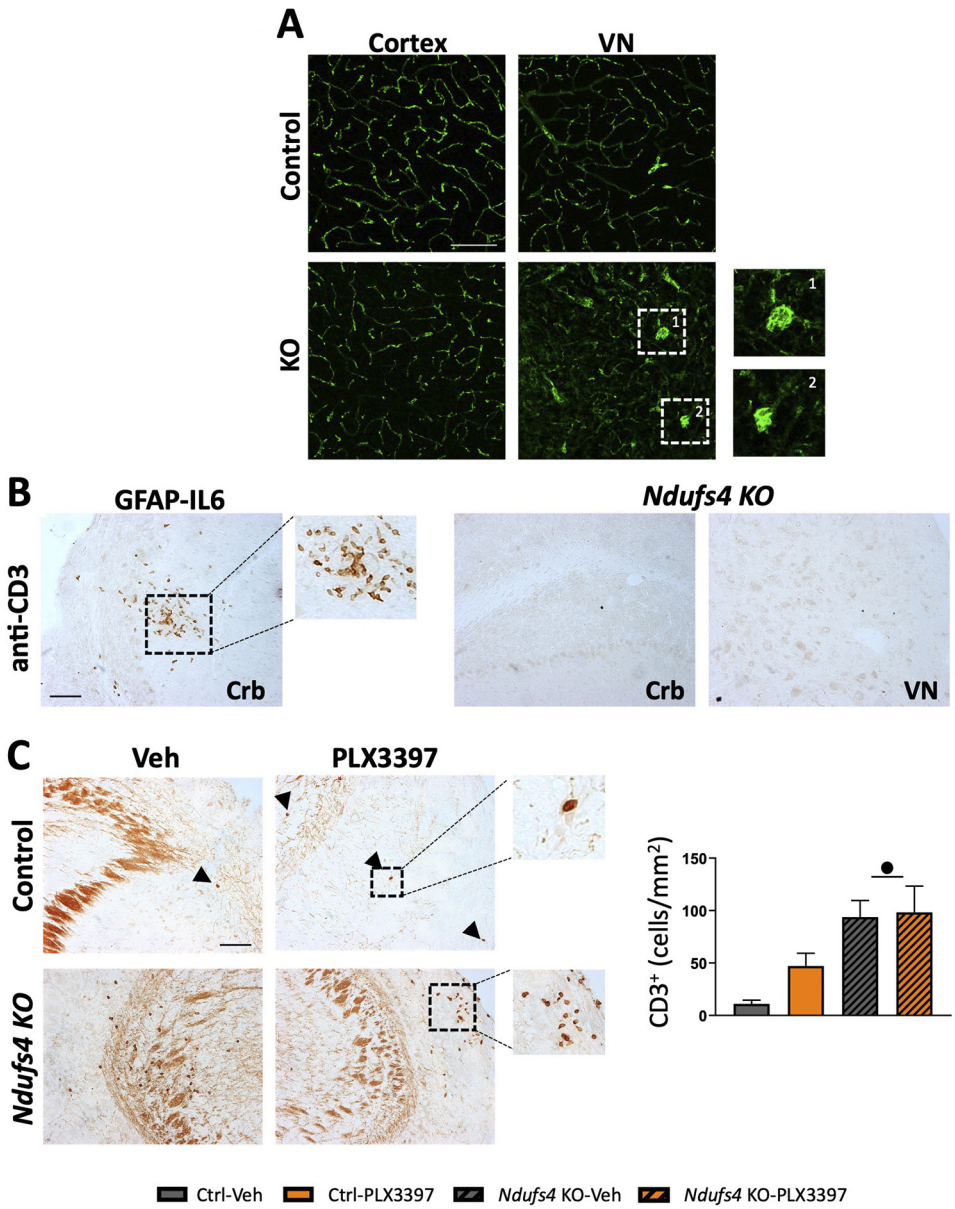

Figure 17. T-cells do not infiltrate into the VN and the cerebellum of *Ndufs4 KO* mice, but they do infiltrate in the OB at the late stage of the disease.

(A) *Ndufs4 KO* mice develop morphological blood vessel abnormalities in the VN, but not in the cortex. Magnified areas 1 and 2 indicate aneurism-like structures. **(B)** Image showing the positive control used in the CD3 immunohistochemistry (GFAP-IL6 mice cerebellum) together with representative images of the cerebellum and VN. **(C)** Representative images and quantification of the number of $CD3^+$ cells infiltrating the OB. Black arrows and amplified images indicate $CD3^+$ cells. Scale bars 100 µm. ● Ndufs4 effect $p \leq 0.05$.

as seen in immunofluorescence results, that the treatment is strongly acting on microglial cells in both genotypes (**Figure 18 A**). In contrast to microglial genes, clustered heatmap based on 85 astrocyte-related genes (Guttenplan et al., 2021; Hasel et al., 2021; Sadick et al., 2022) revealed that samples cluster depending on genotype rather than treatment (**Figure 18 B**). Hence, these results are in line with the observed reduced number of microglial cells with PLX3397 treatment compared to untreated mice and with the increase of reactive astrocyte morphology by GFAP staining in *Ndufs4 KO* mice (**Figure 14**).

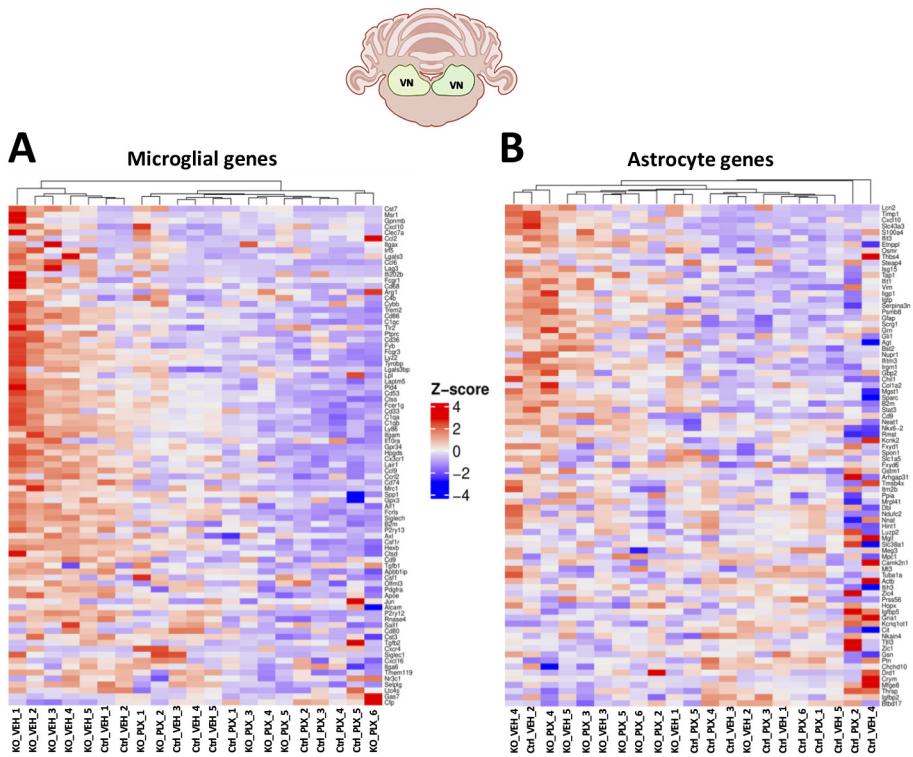

Figure 18. Clustered heatmap of microglial and astrocyte-associated genes in the VN of the different groups analyzed.

Hierarchical clustering showing Z score of most relevant **(A)** microglial and **(B)** astrocyte genes. Z-score indicates how far from the mean a particular data point is by representing the variation of each sample transformed in a logarithmic scale. Negative values indicate values below the average, whereas positive values indicate values above the average.

Similarly, in the hippocampus, when the different samples were clustered by the relative expression of the selected microglial genes, treated and untreated mice clustered together regardless of the genotype (**Figure 19 A**), whereas when clustered by the relative expression of astrocytic genes they mainly cluster by genotype (**Figure 19 B**).

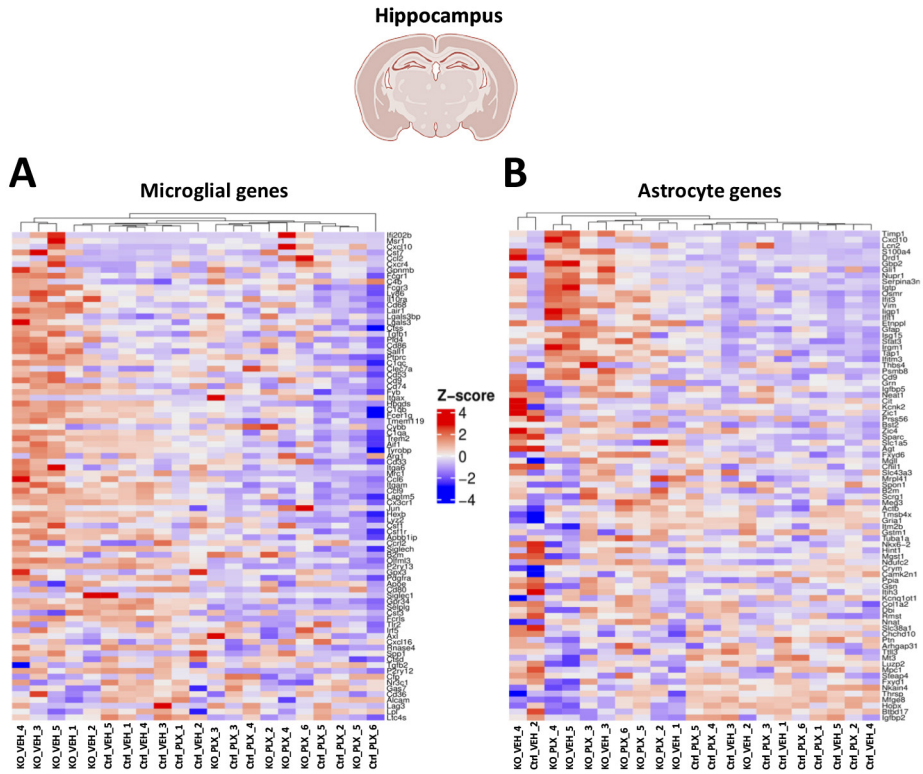

Figure 19. Clustered heatmap of microglial and astrocyte-associated genes in the hippocampus of the different groups analyzed.

Hierarchical clustering showing Z score of most relevant **(A)** microglial and **(B)** astrocyte genes.

In the VN, pairwise differential expression analysis between *Ndufs4 KO*-Veh and Ctrl-Veh revealed 205 differentially expressed genes (DEG); 142 upregulated and 63 downregulated (**Figure 20 A**). Gene ontology (GO) enrichment analysis (**see Note 1**) of upregulated genes (**Figure 20 B**) showed that a high number of enriched genes in *Ndufs4 KO* mice are associated with immune-related processes (**Figure 20 B, C**). For instance, phagocytosis-related genes were highly enriched in *Ndufs4 KO* mice (**Figure 20 B, D**), which is in accordance with the morphological features displayed by microglia in this region (**Figure 14**). Whereas no differences were found in the expression of homeostatic microglial genes (i.e., *Tmem119, P2ry12*), we found nine upregulated DEG (*Cst7, Cxcl10, Clec7a, Ccl6, Cd68, Lgals3bp, Lgals3, Trem2, and Tyrobp*) (**Figures 20 C**) that have been linked to a particular state of reactive microglial cells,

Note 1.

For the different pairwise comparisons, DEG for every GO term can be found at the supplementary information section at the end of this thesis manuscript.

found in several neurodegenerative diseases, known as disease-associated microglia (DAM)(Habib et al., 2020; Masuda et al., 2020). Furthermore, we found an increased expression of genes commonly upregulated in reactive astrocytes such as *Vim, Timp1,* or *Lcn2* (Liddelow et al., 2017; Escartin et al., 2021). GO enrichment analysis of downregulated genes showed that protein folding was the most significantly decreased GO term (**Figure 20 B, D**).

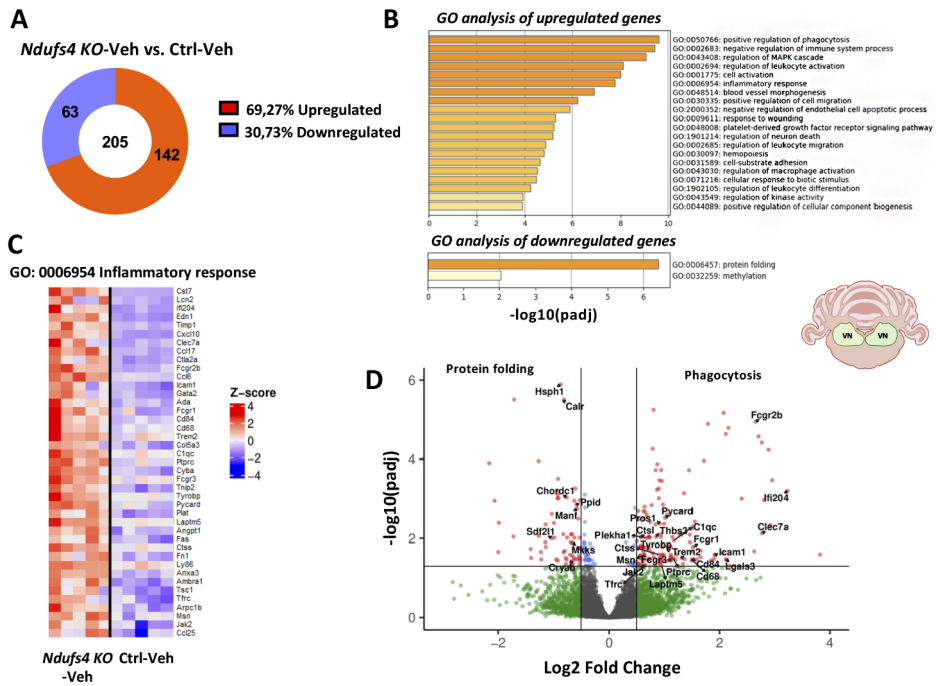

Figure 20. Upregulated DEG in the VN of *Ndufs4 KO* mice are mainly associated with immune-related processes.

(A) Number of upregulated and downregulated DEG between *Ndufs4 KO* and control mice treated with vehicle. **(B)** GO enrichment of upregulated and downregulated genes in *Ndufs4 KO*-Veh vs. Ctrl-Veh. **(C)** Heatmap showing Z score of genes of the inflammatory response GO term. **(D)** Volcano plot showing the comparison between *Ndufs4 KO*-Veh and Ctrl-Veh highlighting some of the significant upregulated phagocytosis-related genes and downregulated protein folding genes. padj: adjusted p-value.

Regarding PLX3397 effects on gene expression, Ctrl-PLX3397 mice had only downregulation of a few microglial-related genes when compared to untreated controls (**Figure 21 A**). Similarly, most DEG in PLX3397-treated vs. untreated *Ndufs4 KO* (**Figure 21 B**) were downregulated microglial genes (**Figures 21 C**). Within these genes, there are homeostatic microglial genes (e.g., *Tmem119, P2ry12, or Hexb*) as well as genes whose upregulation is usually associated with the reactive state of microglia (e.g., *Trem2, Aif1, or Tyrobp*). Consistently, most enriched GO terms were associated with the

inflammatory response and microglial reactivity (**Figure 21 D**). In order to test if the effect of treatment is different across genotypes, the interaction between the factors was tested and no DEG were found, meaning that both control and *Ndufs4 KO* mice responded similarly to treatment. Furthermore, no astrocytic genes were found to be differentially expressed in *Ndufs4 KO* due to treatment.

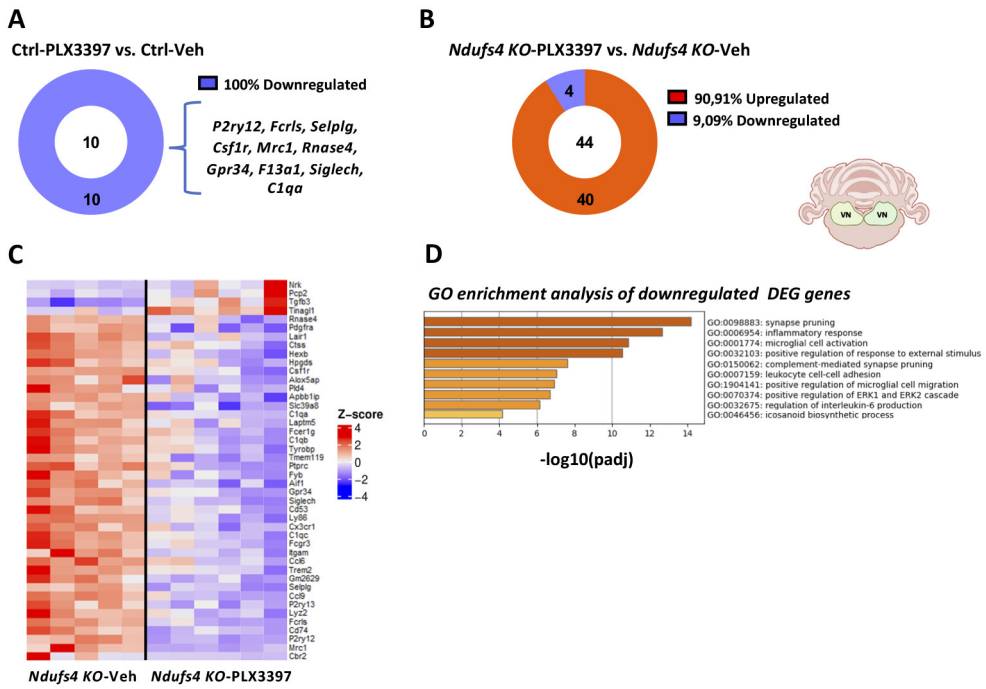

Figure 21. Downregulated DEG in the VN of PLX3397-treated *Ndufs4 KO* mice were mainly microglial-associated genes.

(A) All DEG in Ctrl-PLX3397 vs. Ctrl-Veh were downregulated. **(B)** Number of upregulated and downregulated DEG between *Ndufs4 KO*-PLX3397 and *Ndufs4 KO*-Veh mice. **(C)** Heatmap showing Z scores of all DEG genes between *Ndufs4 KO*-PLX3397 and *Ndufs4 KO*-Veh mice. **(D)** GO enrichment of downregulated genes in *Ndufs4 KO*-PLX3397 vs. *Ndufs4 KO*-Veh.

In the hippocampus, pairwise differential expression analysis between *Ndufs4 KO*-Veh and Ctrl-Veh revealed 298 DEG, of which 163 were upregulated and 135 downregulated (**Figure 22 A**). Gene ontology (GO) enrichment analysis of upregulated genes (**Figure 22 B**) showed that enriched genes in *Ndufs4 KO*-Veh mice are again associated with immune-related processes (**Figure 22 B, C**) as well as with the regulation of epithelial cell proliferation or astrocyte differentiation (**Figure 22 B**). Few microglial genes were upregulated in *Ndufs4 KO*-Veh mice, whereas important

reactive astrocyte-associated genes were upregulated in *Ndufs4 KO*-Veh mice compared to untreated controls such as *Gfap, Vim, Serpina3n, Osmr,* or *Stat3* (**Figures 22 C, D**). These observations are in line with both IBA-1 and GFAP stainings (**Figure 14**). Again, GO enrichment analysis of downregulated genes showed that protein folding was the most significantly decreased GO term (**Figure 22 B, D**).

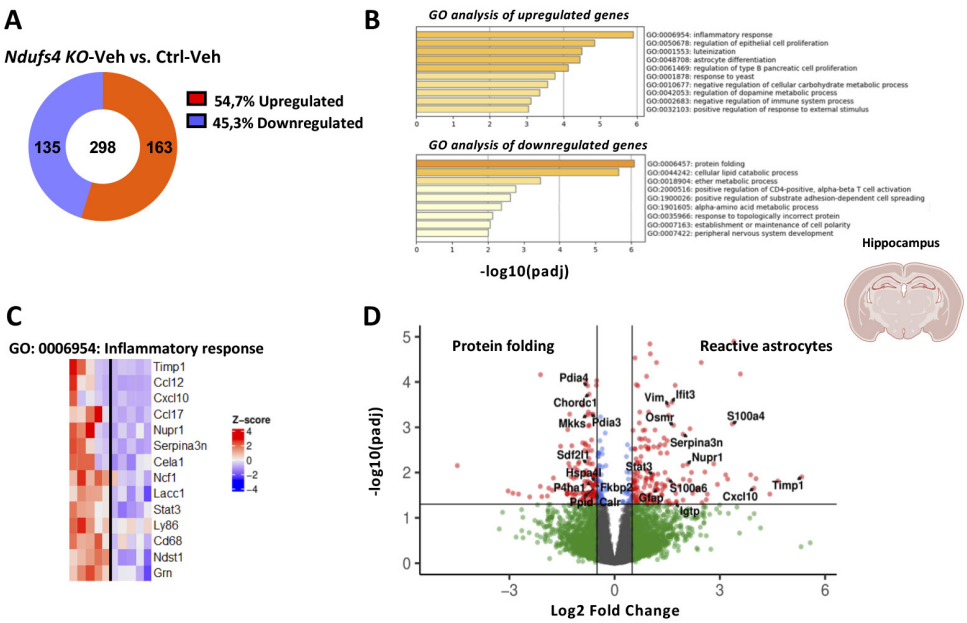

Figure 22. Hippocampal upregulated DEG associated with the inflammatory response were less abundant than in the VN of *Ndufs4 KO*-Veh mice when compared to Ctrl-Veh.

(A) Number of upregulated and downregulated DEG in the hippocampus of *Ndufs4 KO* mice treated with vehicle vs. Ctrl treated with vehicle. **(B)** GO enrichment of upregulated and downregulated genes in *Ndufs4 KO*-Veh vs. Ctrl-Veh. **(C)** Heatmap showing Z score of genes of the inflammatory response GO term. **(D)** Volcano plot showing the pairwise comparison between *Ndufs4 KO*-Veh and Ctrl-Veh highlighting DEG genes associated with protein folding (downregulated) and reactive astrocyte genes (upregulated).

Pairwise comparisons of *Ndufs4 KO*-PLX3397 versus *Ndufs4 KO*-Veh and Ctrl-PLX3397 versus Ctrl-Veh showed that treatment had little effect over the transcriptome of the different genotypes; only 19 and 13 DEG in *Ndufs4 KO*-PLX3397 versus *Ndufs4 KO*-Veh and Ctrl-PLX3397 versus Ctrl-Veh, respectively were affected (**Figure 23**). In both genotypes, similar to the VN, the few DEG observed were mainly microglial-related genes such as *P2ry12, P2ry13*, or *Selplg* (**Figure 23**). Consistently, the interaction did not reveal any DEG.

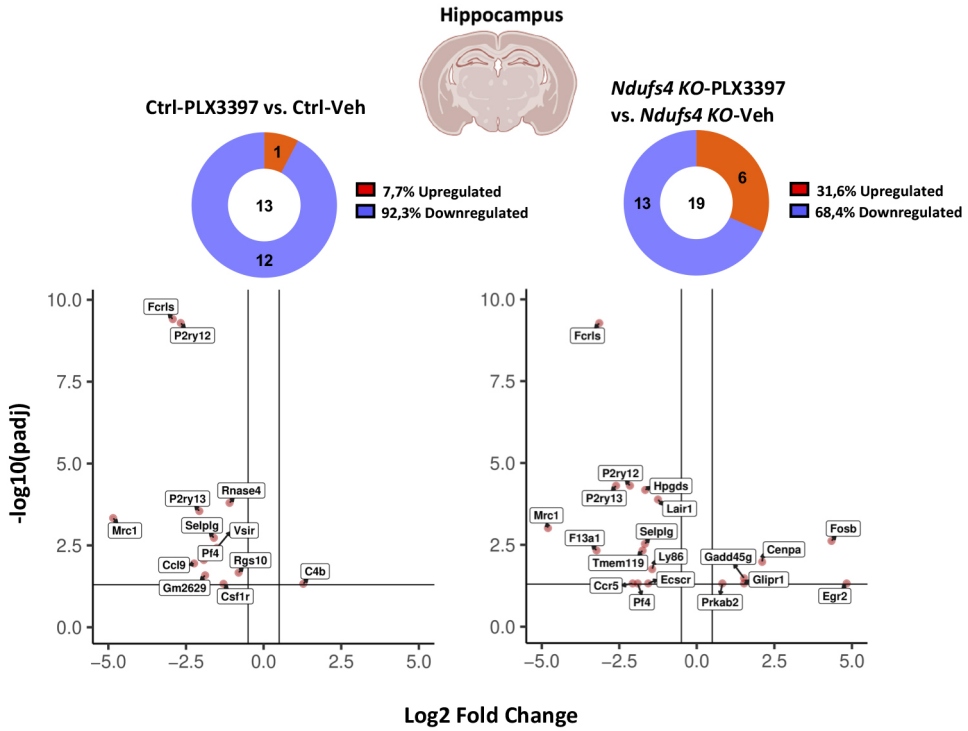

Figure 23. PLX3397 treatment mainly downregulates microglial-related genes in the hippocampus of Control and *Ndufs4 KO* mice.

Percentage and volcano plot of upregulated and downregulated DEG in Ctrl-PLX3397 compared to Ctrl-Veh and *Ndufs4 KO*-PLX3397 compared to *Ndufs4 KO*-Veh. padj: adjusted p-value.

Part 2. Effects of IL-6 deficiency on the *Ndufs4 KO* brain pathology

Since the microglial response is noxious in *Ndufs4 KO* mice, we next investigated one of the potential candidates implicated in this process: the cytokine IL-6, which is an important neuroinflammatory mediator that modulates microglial actions during disease (Spooren et al., 2011; Erta et al., 2012). Importantly, increased expression of *Il6* mRNA (Balsa et al., 2020) or IL-6 signaling pathways (McElroy et al., 2020) have been described in brains of NDUFS4- deficient mice. Thus, to dissect the possible contributions of IL-6 to the development of *Ndufs4 KO* pathology we generated a mouse line with combined IL-6 and NDUFS4 deficiency together with its respective littermate controls (**Figure 8 B and 10**). In addition, in Part 3 we will be presenting the results of another mouse line with CNS overexpression of IL-6.

IL-6 levels are increased in the olfactory bulb and cerebellum of *Ndufs4 KO* mice

The olfactory bulb and cerebellum are two of the main regions where neurodegeneration and neuroinflammation occur in *Ndufs4 KO* mice (Quintana et al., 2010). We investigated IL-6 protein synthesis by multiplex analysis in both regions and we found increased IL-6 levels in *Ndufs4 KO* mice at the late stage of the disease compared to control mice (Control vs. *Ndufs4 KO,* $p = 0.005$ and $p = 0.001$ for OB and cerebellum, respectively) (**Figure 24 A, left**), which is consistent with previous studies (Balsa et al., 2020; McElroy et al., 2020). In addition, in our RNAseq data set we also found that downregulated genes in the VN of PLX3397-treated *Ndufs4 KO* mice compared to untreated KOs might be linked, as revealed by GO enrichment analysis (GO:0032675), with IL-6 production (**Figure 21 D**). Although our *Il6 KO* mouse model was previously validated (Sanchis et al., 2020a), we wanted to confirm the absence of IL-6 protein expression in Double KO mice. As expected, we could not find detectable levels of IL-6 either in the olfactory bulb or in the cerebellum of Double KO mice. Moreover, we investigated whether other pro-inflammatory cytokines could also be involved and if IL-6 deficiency could be modifying their levels. In line with the described neuroinflammation in *Ndufs4 KO* mice (Kruse et al., 2008; Quintana et al., 2010; Johnson et al., 2013), we also observed a significant increase of tumor necrosis factor α (TNF-α) in the olfactory bulb of *Ndufs4 KO* and Double KO mice at the late stage compared to littermates (Ndufs4 effect, $p \leq 0.001$), and the same trend in the cerebellum (Ndufs4 effect, $p = 0.13$) (**Figure 24 A, right**). Surprisingly, interleukin-1β (IL-1β) levels were undetectable in any genotype or region (not shown).

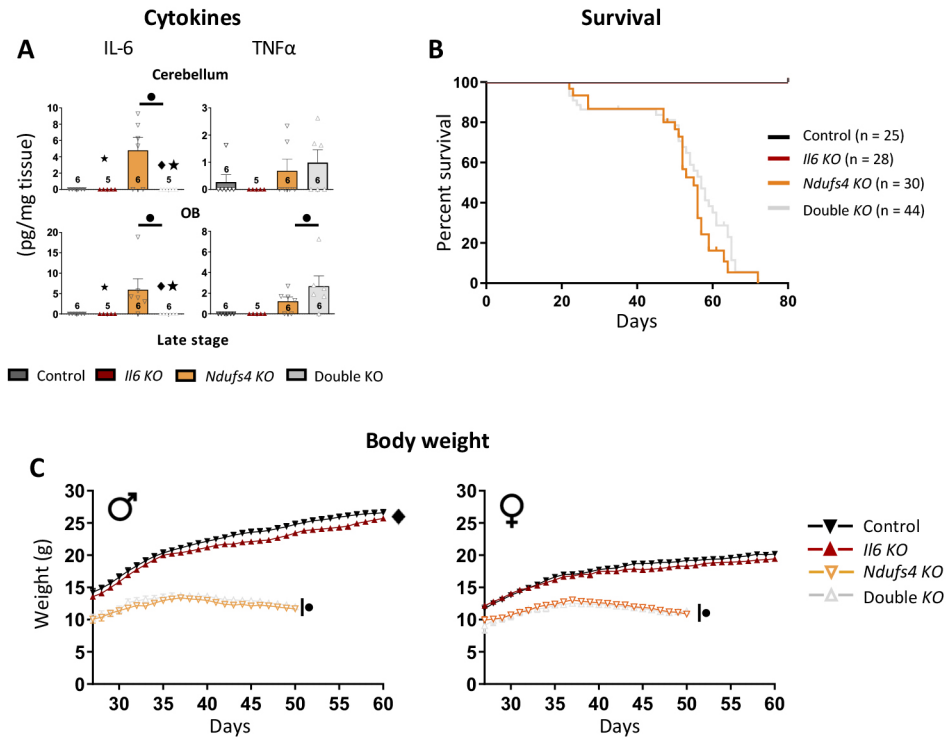

Figure 24. Survival and body weight remained unmodified by IL-6 deficiency in *Ndufs4 KO* mice.

(A) IL-6 and TNF-α levels in the olfactory bulb and cerebellum at the late stage. **(B)** Kaplan-Meier survival curve for control, *Il6 KO*, *Ndufs4 KO*, and Double KO mice. **(C)** Body weight curves of male and female mice of all genotypes (n = 11-17). ● Ndufs4 effect p≤ 0.05, ★IL-6 effect p≤ 0.05 , ♦ p≤ 0.05 interaction between both factors.

IL-6 deficiency does not modify lifespan or body weight in *Ndufs4 KO* mice

As expected, NDUFS4-deficient mice showed reduced lifespan (≈P55) and body weight compared to their littermate controls, but IL-6 deficiency did not have an impact on survival or body weight (**Figure 24 B, C**) in *Ndufs4 KO* mice. In contrast, *Il6 KO* male mice had reduced body weight compared to controls (Control vs. *Il6 KO*, p = 0.033), and the same trend was observed in females (**Figure 24 C**).

IL-6 is not involved in the motor decline of *Ndufs4 KO* mice

To determine whether IL-6 deficiency in *Ndufs4 KO* mice could have an impact on coordination, balance, and ambulation at any of the different disease stages we performed rotarod and open-field behavioral tests. As expected, *Ndufs4 KO* mice showed a progressive decline in balance and motor coordination as the pathology progresses compared to their littermate controls, and by ≈2 months of age (late stage of the disease) they were mostly

incapable of performing the rotarod test (**Figure 25 A**). This motor phenotype could not be rescued by IL-6 deficiency. Similarly, in the OF test mice with loss of NDUFS4 revealed decreased ambulation in all disease stages (Ndufs4 effect, $p \leq 0.001$), with no obvious effects of IL-6 deficiency (**Figure 25 B**). In this case, during the open-field test, we also monitored mice vertical activity measured by the number of rearings (**Figure 25 B, right**). Commonly, the number of rearings is used as an exploration trait, but it also can be used as a measure of rear limb strength (Reynaud-Dulaurier et al., 2020). Identically to the rotarod task results (**Figure 25 A**), the number of rearings decreased progressively over time in NDUFS4-deficient mice compared to controls (**Figure 25 B, right**) but, again, IL-6 deficiency did not revert this phenotype in *Ndufs4 KO* mice. In line with motor activity and coordination results, no statistical differences were found in the onset of the clasping behavior between *Ndufs4 KO* and Double KO mice (**Figure 25 C**). In addition, *Ndufs4 KO* mice again showed increased tidal volume in all disease stages compared to their littermate controls (**Figure 25 D**). Regarding IL-6 deficiency, we observed a statistically significant interaction between both factors at the mid stage of the disease suggesting that IL-6 deficiency partially rescued the altered breathing pattern in *Ndufs4 KO* mice at this stage (*Ndufs4 KO* vs. Double KO, $p \leq 0.001$) (**Figure 25 D**). Moreover, a non-significant trend was also observed in the other stages of the disease that becomes significant when *Ndufs4 KO* and Double KO groups are analyzed separately with genotype and age as factors (genotype effect, $p = 0.004$). We did not observe changes in respiratory frequency due to NDUFS4 deficiency in any stage (**Figure 25 E**). However, we observed a global increased respiratory frequency due to IL-6 deficiency at early stages. The same trend can be observed between control and *Il6 KO* at the mid and late stage (**Figure 25 E**), statistically significant (genotype effect, $p = 0.001$) when analyzed separately with genotype and age as statistic factors.

IL-6 deficiency in *Ndufs4 KO* mice has moderate effects on microgliosis and astrogliosis

Next, we wanted to examine whether IL-6 is involved in the neuro-inflammatory response present in *Ndufs4 KO* mice despite not affecting their survival or motor phenotype. For that purpose, we used the microglial markers IBA-1 and TMEM119 and the astrocytic marker GFAP to extensively study neuroinflammation at the mid and late stages of the disease.

At the late stage, NDUFS4-deficient mice presented a more prominent and generalized microgliosis, with dramatic increases of IBA-1 mean fluorescence intensity in the VN, OB, and cerebellum, together with a

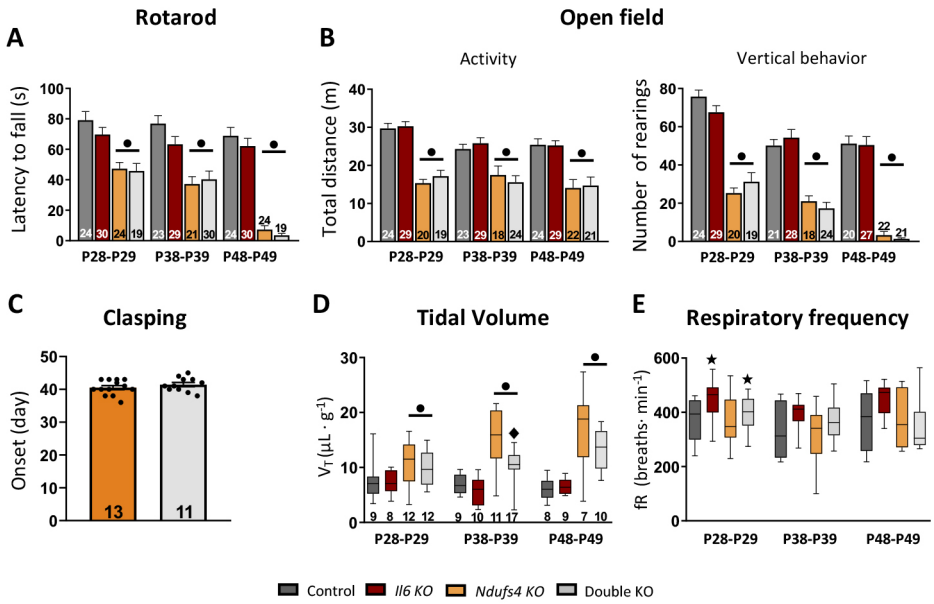

Figure 25. Total IL-6 deficiency does not rescue progressive motor deficits but modifies the altered breathing pattern in a mouse model of Leigh syndrome.

(A) Latency to fall in the accelerating rotarod. **(B)** Total distance travelled and vertical behaviour (rearings) in the open-field test. **(C)** Day of onset of clasping behavior in *Ndufs4 KO* and Double KO mice. **(D)** Tidal volume and **(E)** respiratory frequency of at the different stages.
● Ndufs4 effect p≤ 0.05, ★IL-6 effect p≤ 0.05 , ♦ p≤ 0.05 interaction between both factors.

slight increase in CA1 (**Figure 26 A, B**). We also stained for TMEM119, a microglial-specific homeostatic marker (Bennett et al., 2016) whose expression decreases once microglia activate and can be used as an indirect measure of microglial reactivity (Vankriekelsvenne et al., 2022). Consistent with IBA-1 results, TMEM119 fluorescence intensity was decreased in all regions studied (**Figure 27**), especially in areas where the most prominent microglial activation is observed such as the OB, and even it was totally absent in the VN of NDUFS4-deficient mice (**Figure 27 A, B**). Interestingly, IL-6 deficiency exacerbated microglial reactivity in CA1 of *Ndufs4 KO* mice (**Figure 26 B**). As shown in **Figure 26 B**, Double KO mice had a greater number of IBA-1^{+} cells (*Ndufs4 KO* vs. Double KO, $p \leq 0.001$) and a higher percentage of reactive microglia (sum of hypertrophic and ameboid microglial phenotypes) (*Ndufs4 KO* vs. Double KO, $p \leq 0.001$) compared to *Ndufs4 KO* mice.

Consistently, we also found decreased TMEM119 staining in CA1 of Double KO mice compared to *Ndufs4 KO* mice (**Figure 27 A**). In addition, we found a prominent decrease of TMEM119 in the cortex of NDUFS4-deficient mice

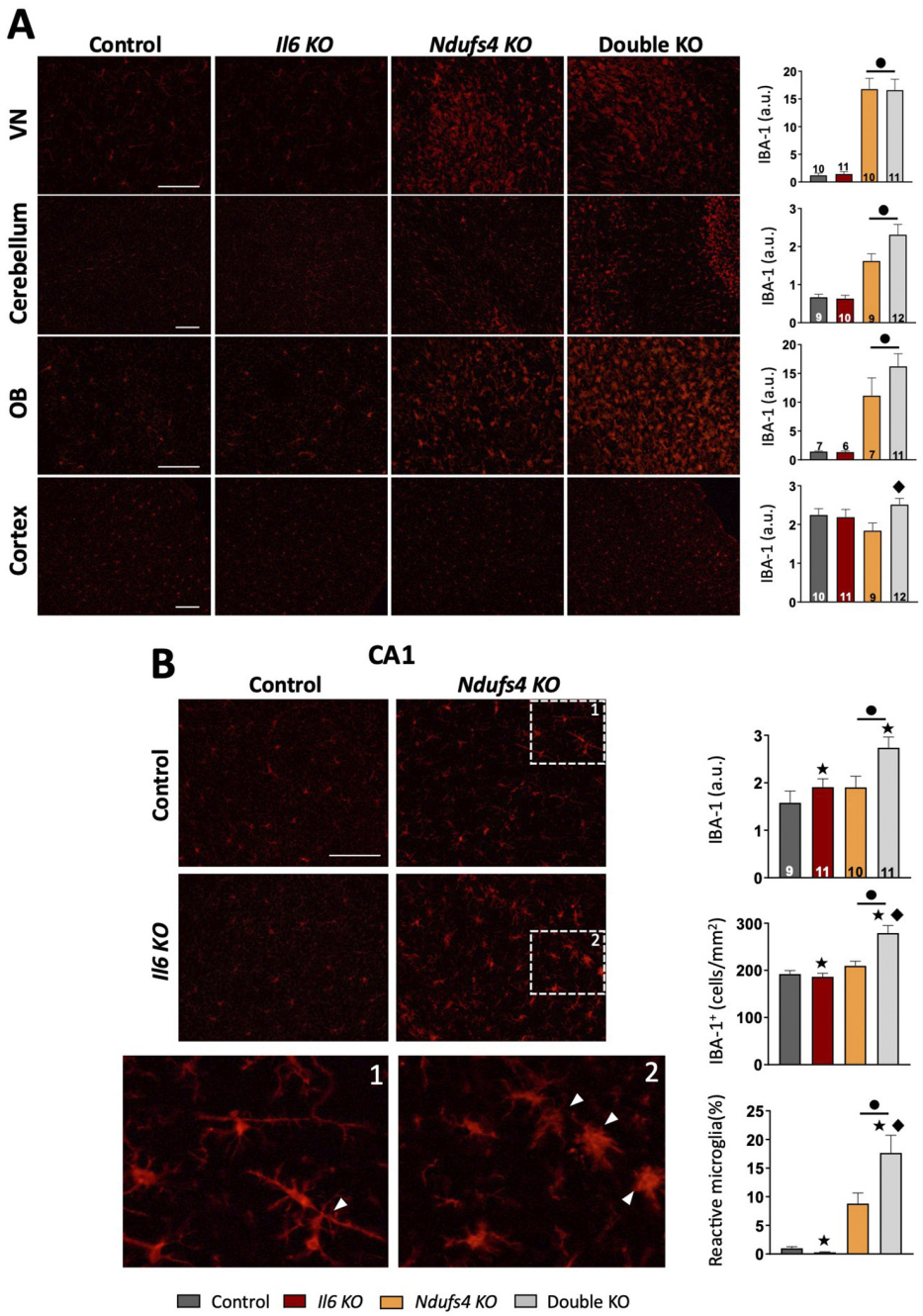

Figure 26. Analysis of microgliosis at the late stage mice in different brain regions revealed increased microglial reactivity in CA1 of *Ndufs4 KO* mice with IL-6 deficiency.

(A) Representative images of IBA-1 staining and quantification of IBA-1 fluorescence intensity at the late stage in VN, cerebellum, OB, and cortex of the different genotypes. **(B)** Representative images of IBA-1 staining and quantification of IBA-1 fluorescence intensity at the late stage in CA1. White arrows in the magnifications indicate reactive microglial morphology.

● Ndufs4 effect p≤ 0.05, ★IL-6 effect p≤ 0.05 , ♦ p≤ 0.05 interaction between both factors.

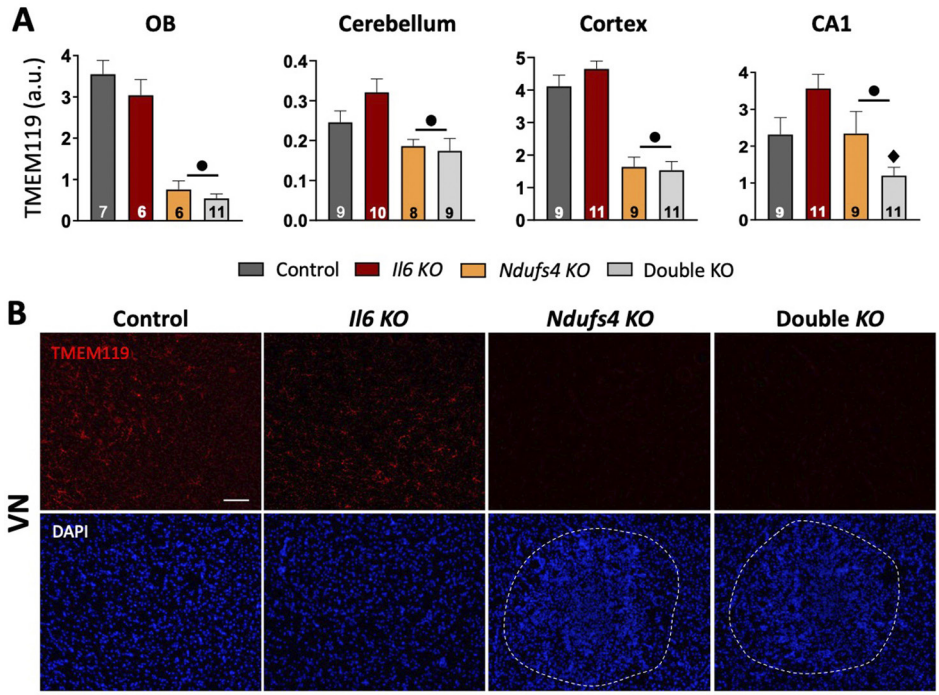

Figure 27. TMEM119 immunoreactivity is decreased in NDUFS4-deficient mice.

(A) Quantification of relative TMEM119 fluorescence intensity at the late stage in the cerebellum, OB, cortex, and CA1. **(B)** Representative images of TMEM119 signal and DAPI in the VN of the different genotypes. The dashed lines in *Ndufs4 KO* and Double KO images indicate an accumulation of cells where massive lesions are classically found, note that no TMEM119 signal is detected compared to the strong IBA-1 staining in the VN. Scale bar 100 µm. ● Ndufs4 effect p≤ 0.05, ♦ p≤ 0.05 interaction between both factors.

(**Figure 27 A**) indicating that despite no changes were found in IBA-1 (**Figure 26 A**), cortical microglia were indeed affected by NDUFS4 deficiency.

In line with IBA-1 and TMEM119 results, we found a global increase of GFAP in NDUFS4-deficient mice at the late stage in the VN, cerebellum, OB, cortex, and CA1 (**Figure 28**). In contrast, IL-6 deficiency did not have any effect in the VN, cerebellum, OB, and cortex. Surprisingly, we observed the opposite effect in the CA1 where GFAP intensity was lower in Double KO than in *Ndufs4 KO* mice (**Figure 28 B**) in comparison to IBA-1 staining where IBA-1$^+$ cells were increased in Double KO mice (**Figure 26 B**).

We also checked for IBA-1 (**Figure 29**) and GFAP (**Figure 30**) at the mid stage of the disease. We found an increase in both IBA-1 intensity and IBA-1$^+$ cells as well as the presence of reactive microglia in the VN of NDUFS4-deficient mice that was not affected by IL-6 deficiency (**Figure 29 A**). IBA-1 mean fluorescence intensity was also significantly increased in the OB of

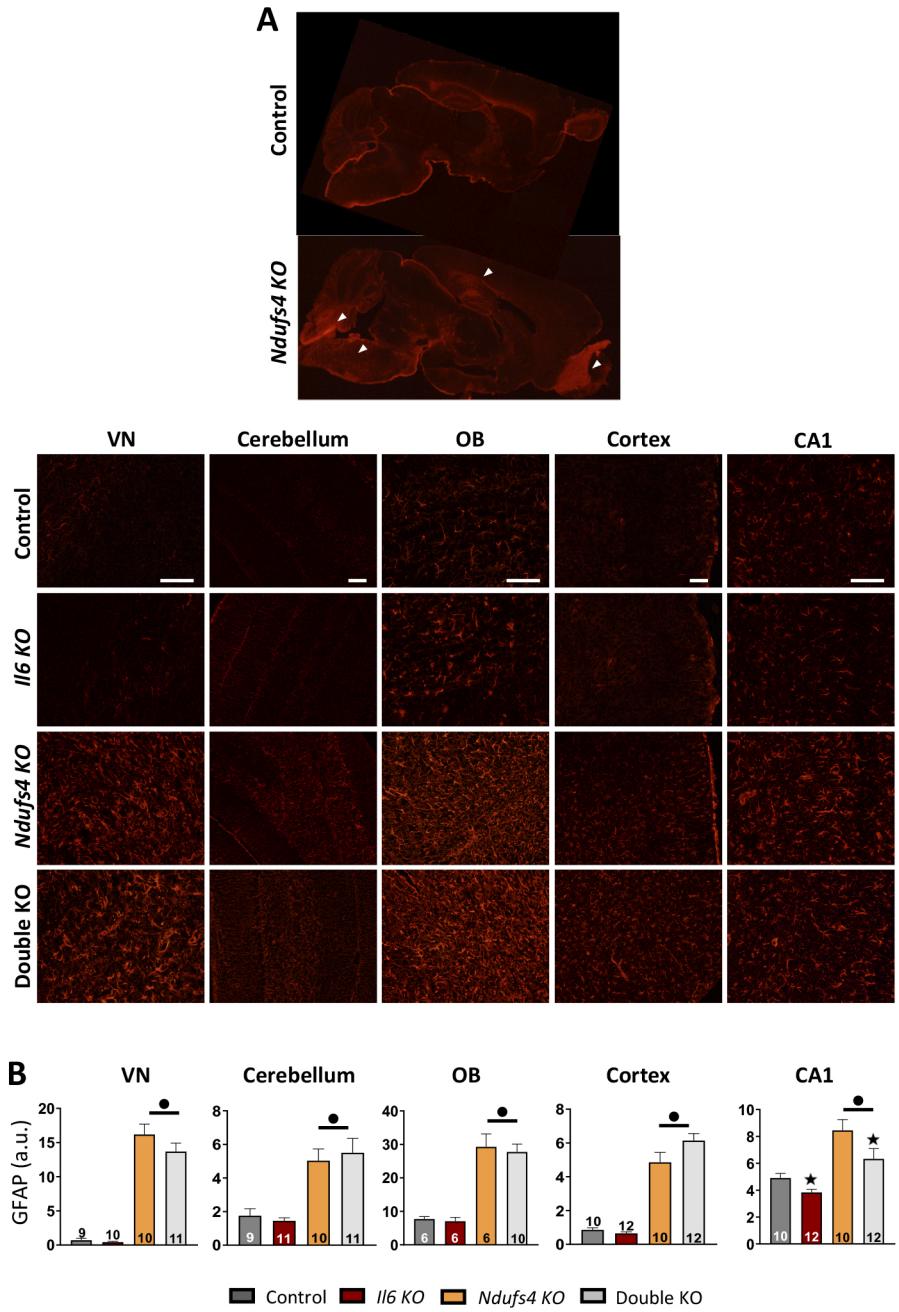

Figure 28. Analysis of astrocyte reactivity at the late stage in different brain regions.

(A) Representative images of GFAP immunofluorescence of the different brain regions at the late stage of the disease. At the top, whole-brain sagittal GFAP staining shows the regions of astrocyte reactivity in *Ndufs4 KO* mice (white arrows). At the bottom, representative images of GFAP staining in VN, Cerebellum, OB, cortex, and CA1 of the different genotypes. **(B)** Quantification of relative GFAP fluorescence intensity at the late stage in VN, cerebellum, OB, cortex, and CA1. Scale bar 100 µm. ● Ndufs4 effect p≤ 0.05, ★IL-6 effect p≤ 0.05 , ♦ p≤ 0.05 interaction between both factors.

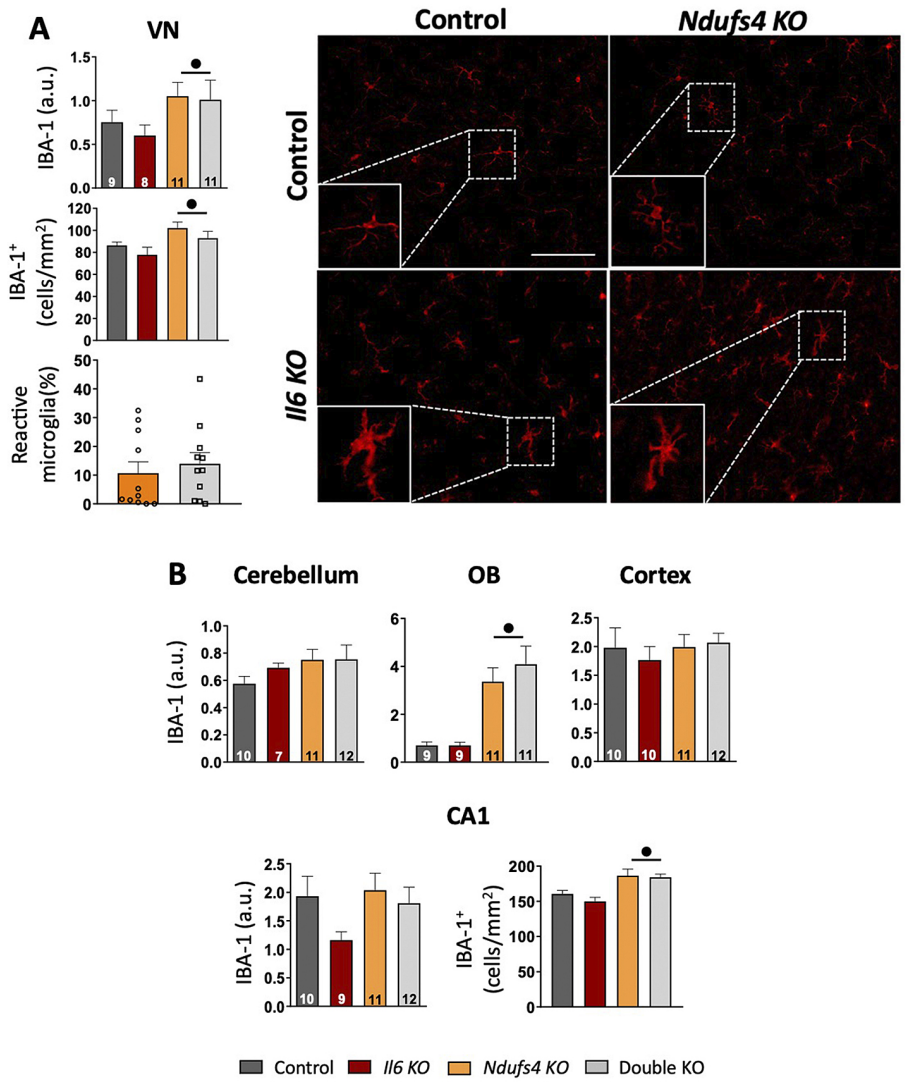

Figure 29. Analysis of microgliosis at the mid stage in the different brain regions.

(A) IBA-1 mean fluorescence intensity quantification in VN. Image show reactive-like phenotypes of microglial cells in the VN of *Ndufs4 KO* and Double KO mice **(B)** IBA-1 mean fluorescence intensity quantification in the cerebellum, cortex, and CA1. ● Ndufs4 effect p≤ 0.05.

NDUFS4-deficient mice, but not in the cerebellum or the cortex (**Figure 29 B**). In addition, we did not find differences in IBA-1 fluorescence intensity in the hippocampal CA1 area between controls and NDUFS4-deficient mice, but we did observe an increased number of IBA-1^{+} cells (**Figure 29 B, right**). No differences in IBA-1 were found between *Ndufs4 KO* and Doble KO mice in this region, which suggests that the increased number of microglial cells in the CA1 of Doble KO mice compared to *Ndufs4 KOs* at the late stage

(**Figure 28 B**) occurs during the progression of the pathology. Altogether, our results indicate an emerging microglial response in NDUFS4-deficient mice at the mid stage that is not affected by the IL-6 deficiency.

In contrast to what occurs with microgliosis, we observed a generalized increase in GFAP average fluorescence intensity at the mid stage in all regions studied (**Figure 30 B**) with the presence of hypertrophied astrocytes (**Figure 30 A**) similar to those found at the late stage (**Figure 28 B**). Therefore, it seems that reactive astrogliosis precedes microgliosis in *Ndufs4 KO* mice in most of the brain regions. Similar to IBA-1, IL-6 deficiency did not have any effect in either control or *Ndufs4 KO* mice.

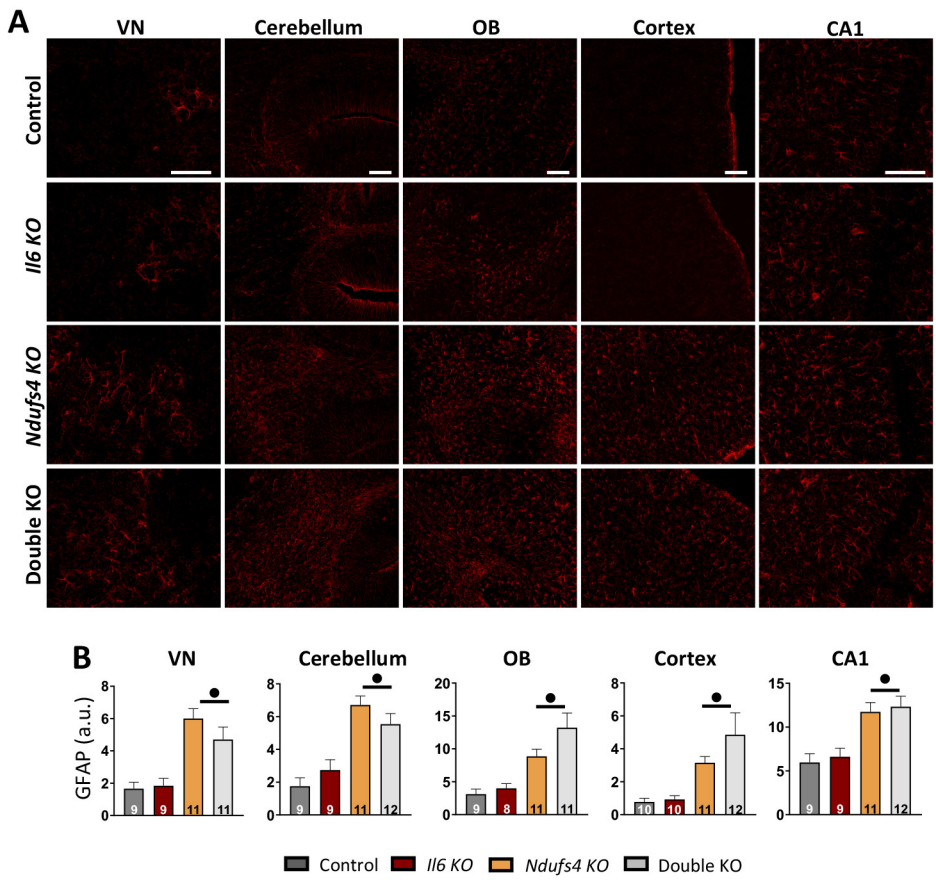

Figure 30. Astrocyte reactivity is already generalized at the mid stage of NDUFS4-deficient mice.

(A) GFAP representative images and **(B)** mean fluorescence intensity quantification in VN, cerebellum, OB, cortex, and CA1 of all genotypes. ● Ndufs4 effect p≤ 0.05.

Part 3. Effects of IL-6-induced chronic neuroinflammation in *Ndufs4 KO* mice

Once we proved that decreasing the neuroimmune response by partially depleting microglial cells has beneficial effects in *Ndufs4 KO* mice, we wanted to assess the opposite paradigm and test whether a chronic induction of a neuroinflammatory state in the CNS of *Ndufs4 KO* mice would exacerbate the pathology in these mice. For that purpose, we took advantage of the GFAP-IL6 mouse (Campbell et al., 1993). As briefly mentioned in Section 1.8.1, GFAP-IL6 mice overexpress IL-6 guided by the *Gfap* promoter which confines the overexpression to astrocytes. GFAP-IL6 mice present early postnatal astrocyte and microglial reactivity across the brain (Campbell et al., 1993, 2014; West et al., 2022a). By generating a mouse line with combined CNS IL-6 overexpression and NDUFS4 deficiency, together with its respective littermate controls (**Figures 8 C and 10**), we will be able to induce a chronic neuroinflammatory state in *Ndufs4 KO* mice before the neuropathology onset (Quintana et al., 2010) and assess its impact on pathology progression (**Figure 10**). In addition, this model could also give us information about how glial cells with NDUFS4 deficiency respond to a chronic CNS inflammation promoted by IL-6 overexpression.

NDUFS4 deficiency compromises cerebellar IL-6 production in GFAP-IL6 mice

We investigated the levels of specific cytokines at both mid and late stages in the cerebellum and the OB of the different genotypes as we did in the IL-6 deficiency experiment (**Figure 31**). Noteworthy, the cerebellum has been described to have, by far, the most prominent IL-6 production in GFAP-IL6 mice (Campbell et al., 1993); this has also been the case in our experiments. We found increased levels of IL-6 at mid and late stages in the cerebellums of NDUFS4-deficient mice, whereas in the OB was only significant at the mid stage since the high variability in the *Ndufs4 KO* mice at the late stage precluded statistical significance. Similar results were obtained regarding the IL-6 overexpression effect; IL-6 overexpression further increased IL-6 levels in the cerebellum at both stages, and at the mid stage in the OB (**Figure 31, left**). Strikingly, cerebellar IL-6 levels were around five and seven times lower at mid and late stages, respectively, in GFAP-IL6/*Ndufs4 KO* mice compared to GFAP-IL6 (mid, $p = 0.003$; late, $p < 0.001$) (**Figure 31, left**). Regarding TNF-α levels in the OB, there were no differences at the mid stage between genotypes, while NDUFS4-deficiency increased them at the late stage. IL-6 overexpression did not have any effect at any stage (**Figure 31, middle**). In

the cerebellum, both NDUFS4 deficiency and IL-6 overexpression induced an increase in TNF-α levels. After decomposing the interactions, we found increased TNF-α levels in *Ndufs4 KO* mice compared to control mice at both stages (mid, p = 0.017; late, p =0.018), but no difference between GFAP-IL6 mice and GFAP-IL6/*Ndufs4 KO* mice (**Figure 31, middle**). IL-10, a cytokine with anti-inflammatory functions, was increased by IL-6 overexpression but not by NDUFS4 deficiency in the cerebellum at both stages. On the contrary, in the OB, IL-10 levels were increased by NDUFS4 deficiency only at the late stage, but not by IL-6 overexpression (**Figure 31, right**). Furthermore, we again did not detect IL-1β (not shown). Altogether, these results show different patterns in cytokine levels depending on the brain region.

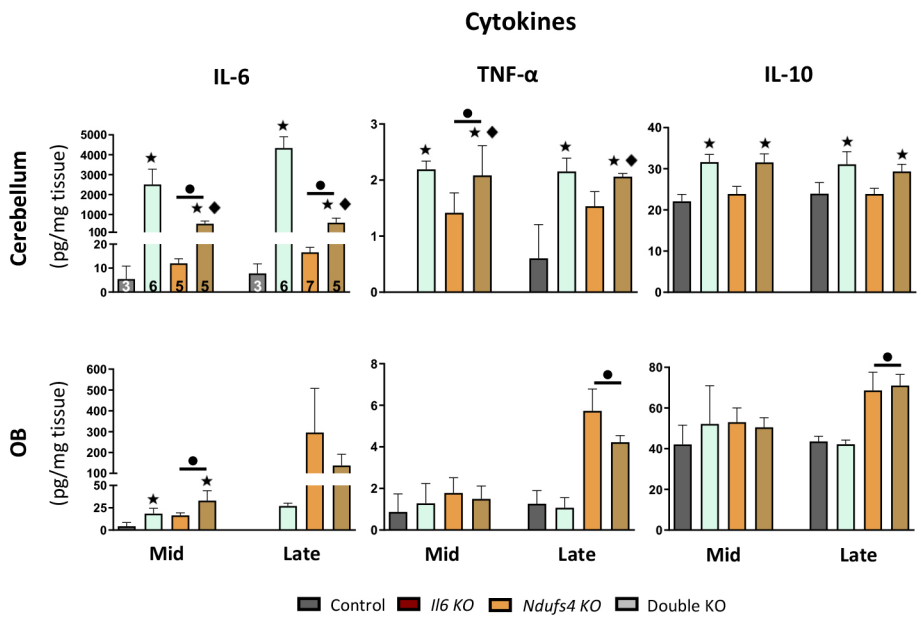

Figure 31. Region-dependent cytokine levels.

IL-6, TNF-α, and IL-10 levels in the cerebellum and olfactory bulb of the different genotypes at the mid and late stages. ● Ndufs4 effect p≤ 0.05, ★IL-6 effect p≤ 0.05 , ♦ p≤ 0.05 interaction between both factors.

Astrocytic-targeted IL-6 overexpression reduces female but not male *Ndufs4 KO* mice survival

Contrary to IL-6 deficiency, IL-6 overexpression negatively impacted the survival of *Ndufs4 KO* in a sex-dependent manner: female GFAP-IL6/*Ndufs4 KO* mice had decreased mean survival by around 20% (*Ndufs4 KO* vs. GFAP-IL6/*Ndufs4 KO,* p = 0.0019), whereas no significant differences

were found in GFAP-IL6/*Ndufs4 KO* male mice compared to *Ndufs4 KO* mice (**Figure 32 A**). Moreover, male and female NDUFS4-deficient mice again presented the typical severe decrease in body weight, but no differences were found between *Ndufs4 KO* and GFAP-IL6/*Ndufs4 KO* mice in any sex (**Figure 32 B**).

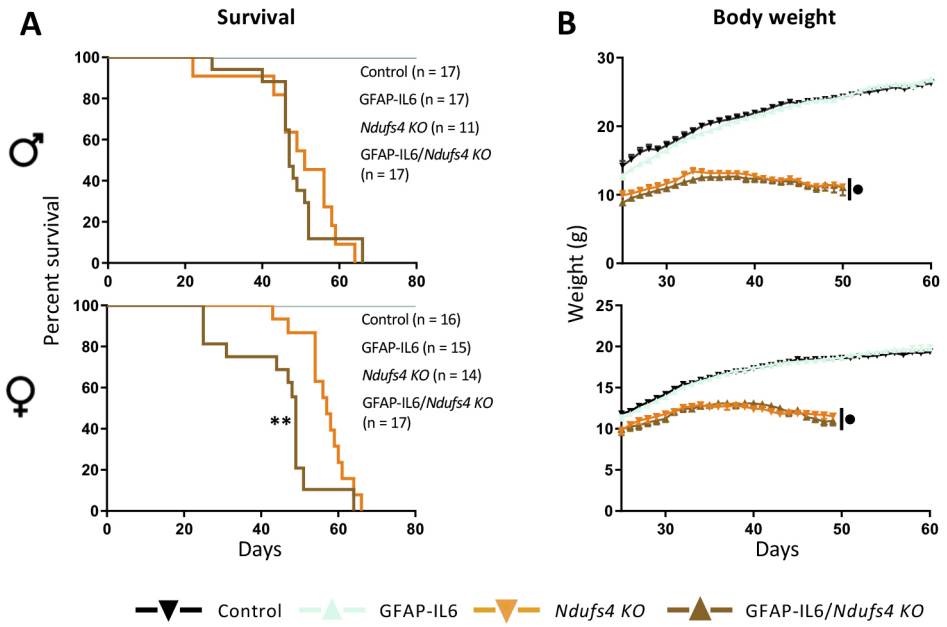

Figure 32. Reduced survival of female *Ndufs4 KO* mice with astrocytic IL-6 overexpression.

(A) Kaplan-Meier survival curve for control, GFAP-IL6, *Ndufs4 KO*, and GFAP-IL6/*Ndufs4 KO* mice. **(B)** Body weight curves for control, GFAP-IL6, *Ndufs4 KO,* and GFAP-IL6/*Ndufs4 KO* male and female mice (n = 11-25). ** p ≤0.01, ● Ndufs4 effect p≤ 0.05.

Astrocyte-targeted IL-6 overexpression barely modifies other phenotypic aspects of *Ndufs4 KO* mice

Astrocytic IL-6 overexpression had a negative impact on female *Ndufs4 KO* mice survival, but not in males. Thus, for a better comparison of disease progression between sexes, we present the results of the motor evaluation of disease progression divided by sex. Generally, NDUFS4-deficient mice had reduced motor coordination (**Figure 33 A**) and total motor activity (**Figure 33 B**) as well as increased tidal volume (**Figure 33 D**), and an unchanged respiratory frequency (**Figure 33 E**) when compared to control mice. Regarding IL-6 overexpression effects, GFAP-IL6 mice were comparable to their controls in motor coordination (**Figure 33 A**), motor activity (**Figure 33 B**), tidal volume (**Figure 33 D**), and respiratory frequency (**Figure 33**

E). In addition, IL-6 overexpression itself barely impacted the *Ndufs4 KO* phenotype regardless of sex; GFAP-IL6/*Ndufs4 KO* mice of both sexes had similar motor coordination, total motor activity, and ventilatory function as *Ndufs4 KO* mice at all disease stages (**Figure 33 A, B, D, E**). Only female GFAP-IL6/*Ndufs4 KO* showed a slightly advanced clasping onset ($p = 0.023$) (**Figure 33 C**), which is consistent with their decreased lifespan. On the contrary, we found a significant interaction between both factors in the respiratory frequency at the early stage; *post hoc* pairwise comparison revealed that NDUFS4 deficiency increased respiratory frequency in GFAP-IL6 mice (GFAP-IL6 vs. GFAP-IL6/*Ndufs4 KO*, $p = 0.037$) (**Figure 33 E**). Overall, these results suggest that a chronic IL-6-mediated neuroinflammatory state in *Ndufs4 KO* brains does not strongly affect disease progression.

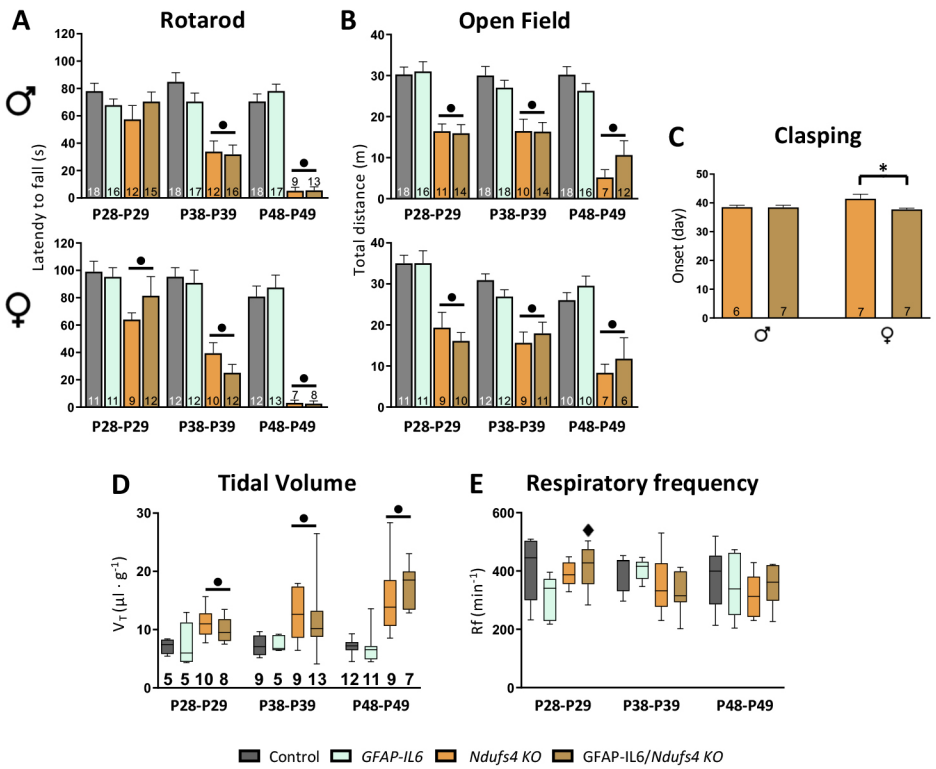

Figure 33. CNS IL-6 overexpression barely affects the motor or respiratory phenotype of *Ndufs4 KO* mice.

(A) Latency to fall in the accelerating rotarod. **(B)** Total distance travelled in the OF test. **(C)** Day of onset of clasping behavior in *Ndufs4 KO* and GFAP-IL6/*Ndufs4 KO* mice **(D)** Tidal volume and **(E)** respiratory frequency at the different stages. ● Ndufs4 effect $p \leq 0.05$, ♦ $p \leq 0.05$ interaction between both factors, * $p = 0.05–0.01$.

NDUFS4 deficiency decreases microgliosis in response to chronic IL-6 overexpression at both mid and late stages of the disease

After characterizing the effects of IL-6 overexpression in *Ndufs4 KO* mice in survival and disease progression we next assessed the glial reactivity by IBA-1 and GFAP stainings in the different brain regions at both mid and late stages of the disease. Importantly, we did not detect any sex-specific differences in gliosis, so the results of both sexes are presented together.

As expected, NDUFS4 deficiency again induced an increased IBA-1 fluorescence intensity in the VN and the cerebellum of *Ndufs4 KO* mice with the abundant presence of reactive microglia, especially in the VN, while in the CA1 and the cortex both IBA-1 intensity and the number of IBA-1$^+$ cells were comparable to control mice (**Figure 34**). Regarding IL-6 overexpression effects, in the VN, we found a significant interaction between both factors. In this case, the interaction indicated that IL-6 overexpression had no major impact on the IBA-1 intensity of *Ndufs4 KO* mice (*Ndufs4 KO* vs. GFAP-IL6/*Ndufs4 KO*, $p = 0.172$), whereas it induced a clear increase in NDUFS4 non-deficient mice (Control vs. GFAP-IL6, $p = 0.027$), probably because the massive microglia reactivity of NDUFS4-deficient mice in this region is mainly due to the effect of the genotype without the influence of IL-6 (**Figure 34 A**). Accordingly, GFAP-IL6/*Ndufs4 KO* mice developed the characteristic bilateral symmetrical lesions with no apparent differences between genotypes (**Figure 34 B**). In the other regions, IL-6 overexpression clearly induced a substantial increase in IBA-1 fluorescence intensity in both genotypes. Interestingly, even though *Ndufs4 KO* mice responded to IL-6 overexpression by increasing IBA-1 and the number of IBA-1$^+$ cells, they did it to a lesser extent when compared with GFAP-IL6 mice in the cerebellum, cortex, and CA1 (GFAP-IL6 vs. GFAP-IL6/*Ndufs4 KO,* $p \leq 0.001$ in all regions) (**Figure 34**).

In line with the PLX3397 and the IL-6 deficiency experiments, we again found a global increase of GFAP in late stage *Ndufs4 KO* mice in the VN, cerebellum, cortex, and CA1 (**Figure 35**). IL-6 overexpression also induced a clear increase in GFAP in GFAP-IL6 mice compared to control mice. However, in *Ndufs4 KO* mice, the effects of IL-6 overexpression varied by region. In the VN and the cerebellum, IL-6 overexpression further increased GFAP fluorescence intensity in *Ndufs4 KO* mice (IL-6 effect, $p = 0.013$ and $p \leq 0.001$, respectively), while it had no effect in the cortex (*Ndufs4 KO* vs. GFAP-IL6/*Ndufs4 KO*, $p=0.233$), and reduced GFAP intensity in the CA1 (*Ndufs4 KO* vs. GFAP-IL6/*Ndufs4 KO*, $p=0.009$) (**Figure 35 B**).

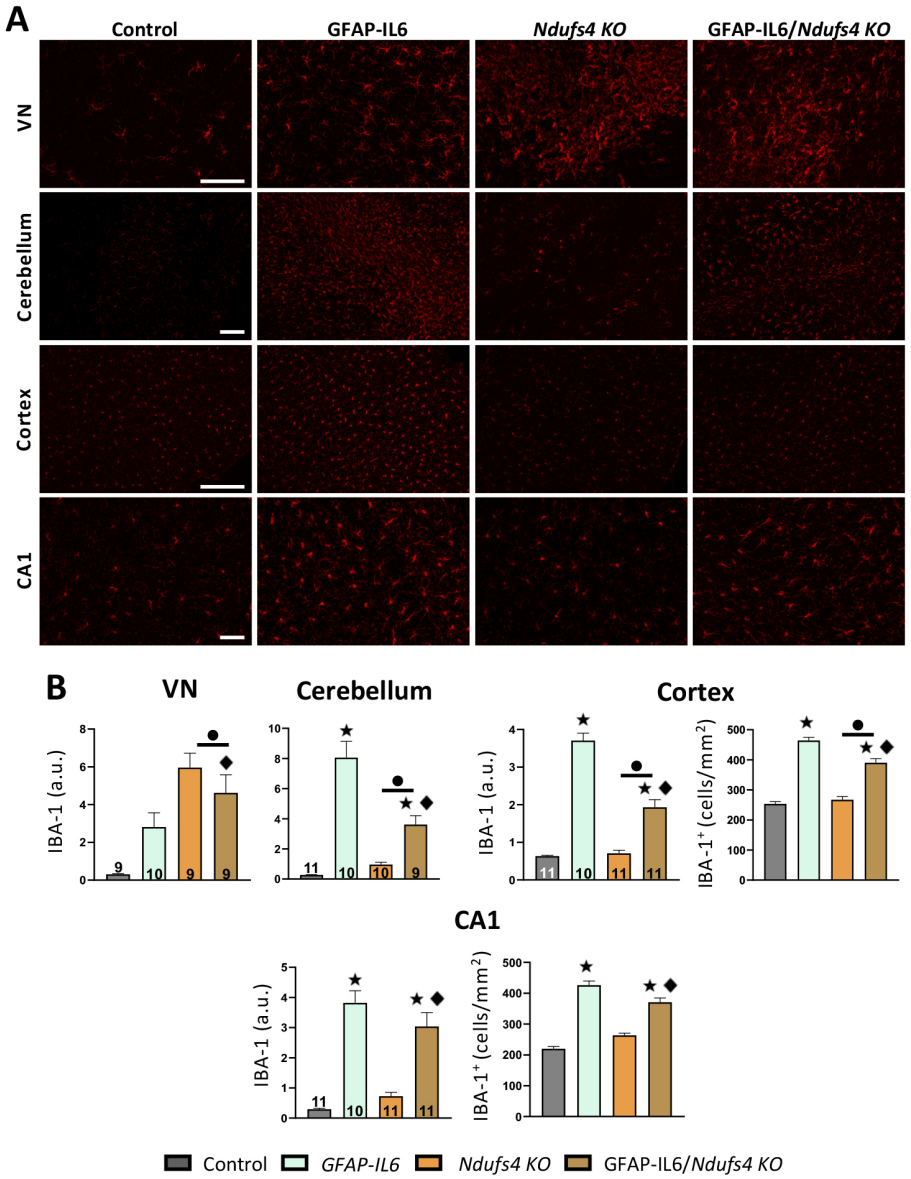

Figure 34. Analysis of microgliosis in the late stage mice in different brain regions revealed decreased microgliosis in *Ndufs4 KO* mice due to IL-6 overexpression.

(A) Representative images of IBA-1 staining **(B)** Quantification of IBA-1 fluorescence intensity in the VN, cerebellum, cortex, and CA1, as well as the number of IBA-1$^+$ cells in the cortex and CA1 of the different genotypes. ● Ndufs4 effect p≤ 0.05, ★IL-6 effect p≤ 0.05 , ♦ p≤ 0.05 interaction between both factors.

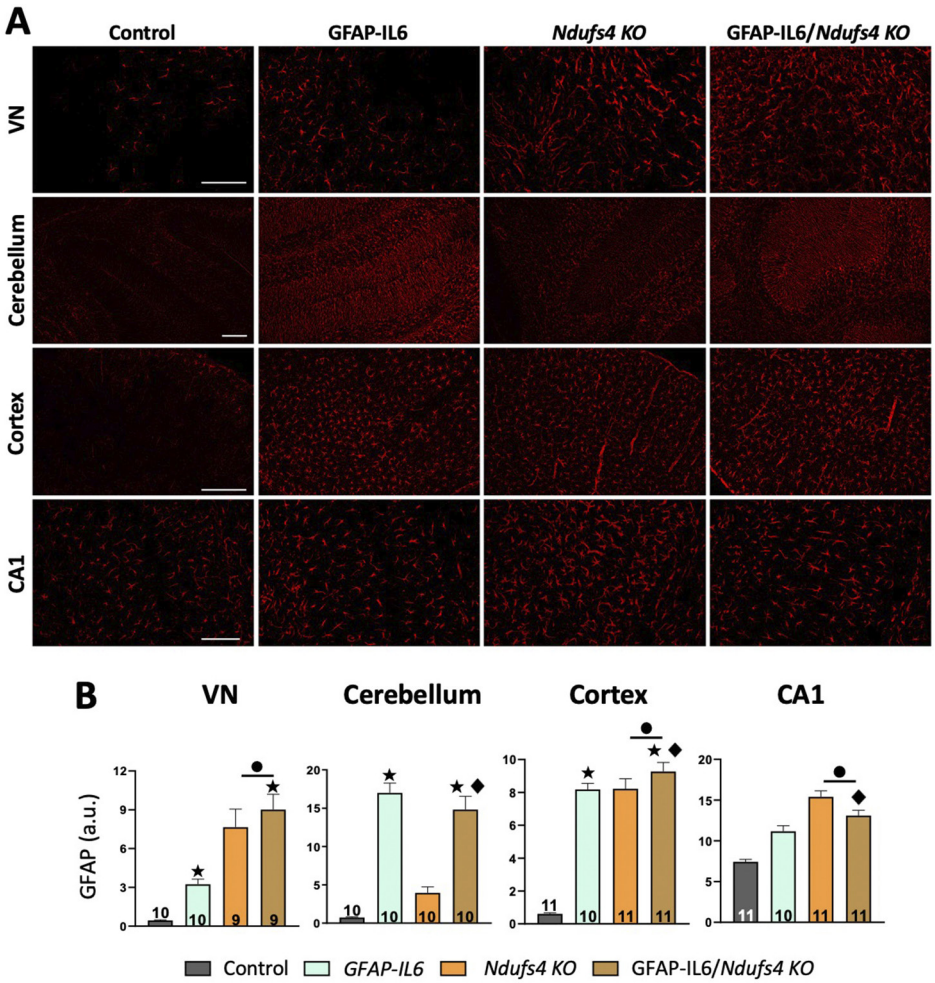

Figure 35. IL-6 overexpression effects over GFAP are region-dependent in *Ndufs4 KO* mice at the late stage.

(A) GFAP mean fluorescence intensity quantification in VN, cerebellum, OB, cortex, and CA1. **(B)** Representative images of GFAP staining. ● Ndufs4 effect p≤ 0.05, ★IL-6 effect p≤ 0.05 , ♦ p≤ 0.05 interaction between both factors.

At the mid stage, we did not find overt signs of microgliosis in *Ndufs4 KO* mice in any region (**Figure 36**). IL-6 overexpression again induced a clear increase in IBA-1 in all regions, notwithstanding the genotype. In line with the late stage observations, we again found a decrease in IBA-1 in GFAP-IL6/*Ndufs4 KO* mice compared to GFAP-IL6 in all regions studied, including the VN (GFAP-IL6 vs. GFAP-IL6/*Ndufs4 KO*, p = 0.015), probably because, contrary to the late stage, microglial reactivity in response to NDUFS4 deficiency in the VN is incipient and does not mask the effect of IL-6 overexpression (**Figure 36**). Remarkably, the magnitude of the decreasing effect appeared to

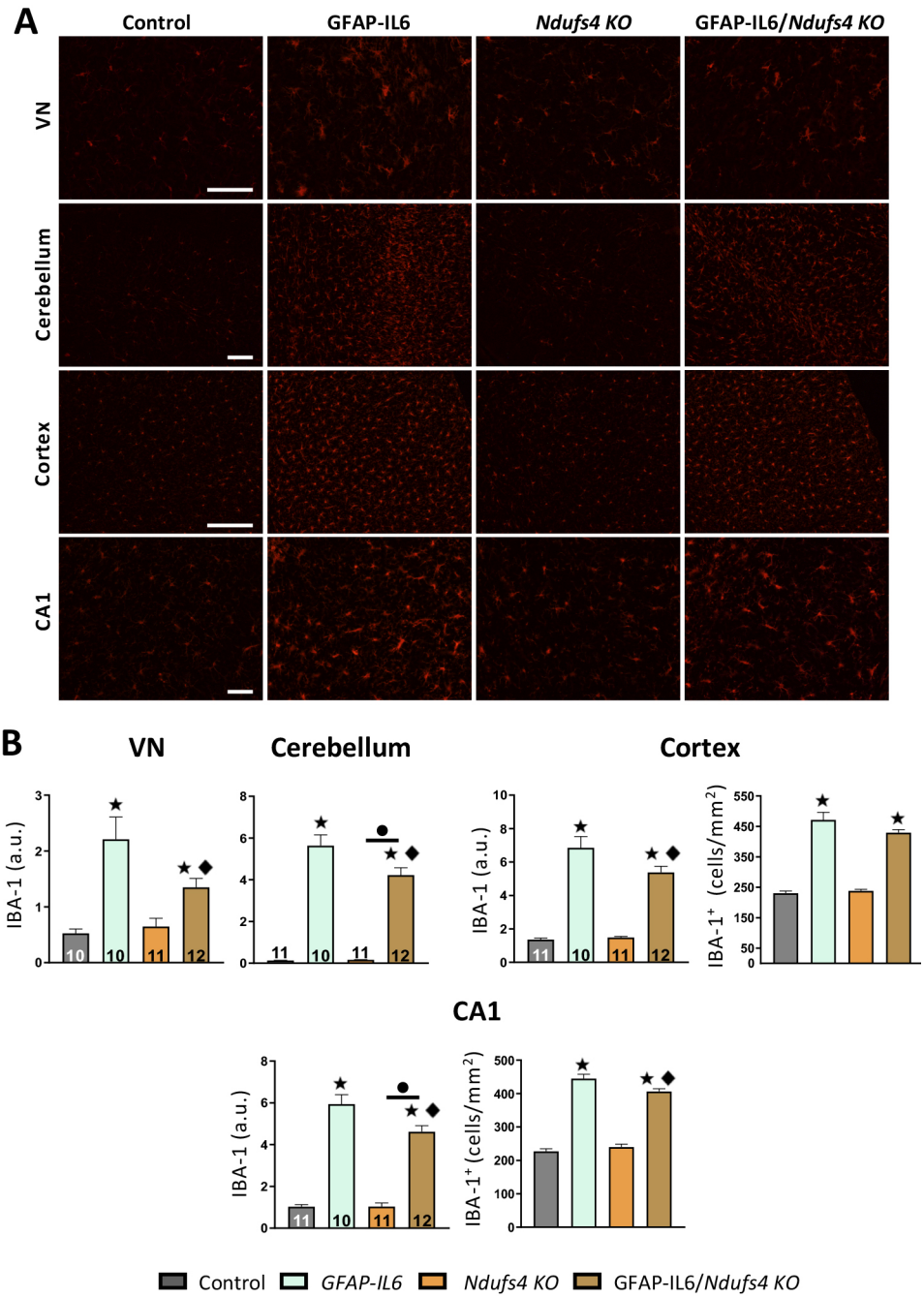

Figure 36. Analysis of microgliosis at the mid stage mice in different brain regions again revealed decreased microgliosis in *Ndufs4 KO* mice due to IL-6 overexpression.

(A) Quantification of IBA-1 fluorescence intensity in the VN, cerebellum, cortex, and CA1, as well as the number of IBA-1$^+$ cells in the cortex and CA1 of the different genotypes. **(B)** Representative images of IBA-1 staining. ● Ndufs4 effect p≤ 0.05, ★IL-6 effect p≤ 0.05 , ♦ p≤ 0.05 interaction between both factors.

be less pronounced at the mid stage, both in the fluorescence intensity and in the number of cells in the CA1 and cortex, than at the late stage (**Figure 35 B**).

Regarding astrocyte reactivity, we found increased GFAP intensity in the cortex and the CA1 but not in the VN or the cerebellum due to NDUFS4 deficiency. Moreover, we found increased GFAP in IL-6 overexpressing mice, regardless of the genotype, and contrary to IBA-1, GFAP intensity was similar between GFAP-IL6 and GFAP-IL6/*Ndufs4 KO* mice in the VN, cerebellum, and cortex, while it was slightly increased in the CA1 due to NDUFS4 deficiency (**Figure 37**).

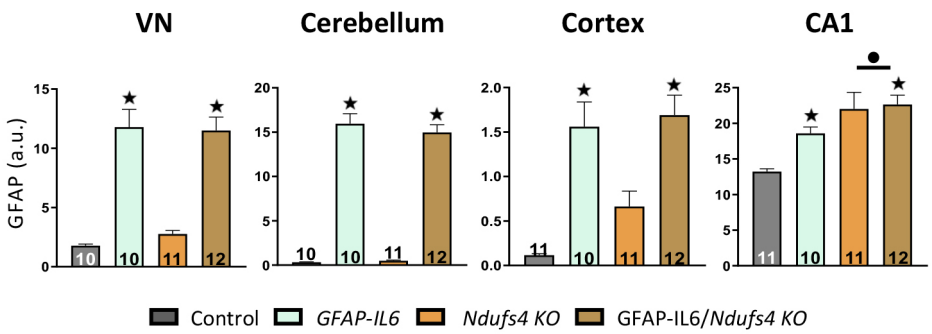

Figure 37. Analysis of astrogliosis at the mid stage mice in different brain regions.
(A) GFAP mean fluorescence intensity quantification in VN, cerebellum, OB, cortex, and CA1. **(B)** Representative images of GFAP staining. ● Ndufs4 effect p≤ 0.05, ★IL-6 effect p≤ 0.05 , ♦ p≤ 0.05 interaction between both factors.

5

Discussion

The aim of this thesis was to investigate the role of neuroinflammation on the *Ndufs4 KO* mouse model of Leigh syndrome using both pharmacological methods and transgenic mouse models. Through our studies, we were able to demonstrate that neuroinflammation plays a key role in the pathology of the LS mouse model, with microglia playing a central role. This paves the way for new treatments for the human disease.

5.1 Neuroinflammation as a contributor to *Ndufs4 KO* mice encephalopathy

Neuroinflammation, understood as the immune-like process that takes place in the CNS in response to an insult of any kind, is a key manifestation of the *Ndufs4 KO* mice encephalopathy. It has extensively been reported that *Ndufs4 KO* mice develop abundant neuroinflammation in brain areas where neurodegeneration takes place, which include the VN, the OB, the cerebellum, and specific brain areas in the brainstem. In addition, neuroinflammation, mainly astrocyte reactivity, has also been reported in the hippocampus, a region where neuronal death is not apparent. This neurodegenerative process leads to a severe phenotype in which *Ndufs4 KO* mice progressively present motor alterations, respiratory abnormalities, seizures, and ultimately, death around postnatal day 55 (Kruse et al., 2008; Quintana et al., 2010, 2012b; Johnson et al., 2013; Shil et al., 2021; van de Wal et al., 2022). Accordingly, the phenotype of all the *Ndufs4 KO* mice cohorts generated during the study consistently replicated the phenotype reported previously, even in the IL-6 experiments, where genetic background variations caused by crossing different mouse strains could have been introduced. The consistent phenotype confirms the validity of our experiments, strongly suggesting that the effects observed in *Ndufs4 KO* mice as a result of the interventions are due to their modulatory effects.

Remarkably, previous published interventions that either extend the lifespan or rescue motor decline in *Ndufs4 KO* mice, such as hypoxia (Jain et al., 2016, 2019), rapamycin treatment (Johnson et al., 2013), or doxycycline administration (Perry et al., 2021), have been shown to reduce microglia and astrocyte reactivity as well as immune-related pathways in *Ndufs4 KO* brains. Whether this neuroimmune process is a pathological mechanism contributing to the progression of the disease or simply is a consequence of neurodegeneration deserves adequate investigation in the context of brain-related mitochondrial disorders, and particularly, in the *Ndufs4 KO* mouse model of LS.

5.1.1 Characterizing microglia and astrocyte reactivity using IBA-1 and GFAP immunostaining: useful, but limited

5.1.1.1 IBA-1

Unlike other tissues, in healthy conditions, the CNS does not receive any additional myeloid cells from the periphery; thus, microglia are the only myeloid cells present in the brain parenchyma in basal conditions (Ginhoux et al., 2010; Hoeffel and Ginhoux, 2015; Li and Barres, 2018). Ionized calcium-binding adapter molecule1 (IBA-1), a protein that binds calcium and actin, is an extensively used marker of microglia. IBA-1 expression increases when microglia become reactive, but as other common microglial markers such as CD11b or CD68, is not microglia-specific (Li and Barres, 2018). The IBA-1 gene (*Aif1*) is expressed in all myeloid-derived cells, including CAMs and peripheral monocytes. In steady-state conditions, IBA-1 can be used as a reliable marker of the microglia present within the brain parenchyma, providing an accurate visualization of the microglial cell body and processes. However, during chronic neuroinflammation, peripheral monocytes can infiltrate and engraft the brain acquiring microglia-like phenotypes (e.g., morphology, clonal expansion capacity, markers)(Shemer et al., 2018; Grassivaro et al., 2020). Therefore, it is highly possible that some IBA-1^{+} cells of *Ndufs4 KO* mice are actually infiltrating myeloid cells and not microglia, especially at lesion sites, where we also observed aneurism-like vascular abnormalities that could compromise the BBB allowing peripheral cells to infiltrate (Knox et al., 2022). The same applies to GFAP-IL6 mice (Recasens et al., 2021). In fact, to clearly distinguish between microglia and other myeloid cells researchers have mainly relied on flow cytometry approaches (Martin et al., 2017). Moreover, only very recently, truly microglia-specific Cre-driven mouse lines have been developed (Dumas et al., 2021). In recent years, some additional microglial-specific markers have been described, which include TMEM119 or P2RY12. However, their expression decrease dramatically when microglia become reactive; thus, they are unsuitable for properly studying microglial cells under pathological conditions (Bennett et al., 2016; Paolicelli et al., 2022; Vankriekelsvenne et al., 2022). Indeed, we did not detect any TMEM119^{+} cells in the VN region of *Ndufs4 KO* mice and minimal staining in the OB, indicating, in accordance with their morphology and their strong IBA-1 immunoreactivity, that all or almost all microglial cells present in those regions are reactive. In summary, currently, there are no specific markers for reactive microglia that could not potentially overlap with other infiltrating myeloid cells and that would be useful to separate between both cell populations.

5.1.1.2 GFAP

Glial fibrillary acidic protein (GFAP), an essential protein of astrocyte intermediates filaments, is the most broadly used marker for reactive astrocytes since the upregulation of GFAP is a common early response to almost any type of injury or disease, often correlating with the severity of the trauma (Escartin et al., 2019, 2021). Similarly to IBA-1, despite its proven utility, some considerations must be taken into account when using GFAP as a marker for reactive astrocytes. Firstly, astrocytes have regional-dependent GFAP content (Haim and Rowitch, 2017); for instance, in basal conditions, cortical astrocytes are barely GFAP immunoreactive, while hippocampal astrocytes are strongly stained. Indeed, this can be appreciated in the multiple GFAP stainings of the cortex and the CA1 of control mice done in this project, in which very few astrocytes were detected per field in the cortex in comparison to the CA1. In disease conditions (NDUFS4 deficiency) or with IL-6 overexpression (GFAP-IL6), GFAP immunoreactivity in the cortex increased around eight times when compared to controls, whereas the GFAP mean fluorescence intensity was only doubled in the CA1. This would mean that both cortical and hippocampal astrocytes were responding to the particular condition, but in any case would be an evidence that cortical astrocytes are more reactive than CA1 astrocytes. Secondly, GFAP immunoreactivity does not enable to visualize the complete astrocyte morphology, since the thin distal ramifications are not marked. Moreover, GFAP overestimates astrocyte hypertrophy when they are reactive (Wilhelmsson et al., 2006). So, in order to entirely assess the particular state of astrocytes in a given condition, they should be accurately characterized through the use of a combination of several markers together with functional assessments (Escartin et al., 2021).

5.1.2 CSF1R inhibition to study microglia

Given that microglia are the innate immune cells of the brain and one of the most remarkable orchestrators of the neuroinflammatory response in the CNS (Borst et al., 2021), we focused on studying the contributions of microglia to the pathology of *Ndufs4 KO* mice. Over the past few years, several innovative methods have emerged for examining the effects of microglia in diverse contexts. One of the most notable of these approaches focuses on the colony-stimulating factor 1 receptor (CSF1R), which can be targeted either through genetic manipulation by mutating or removing the CSF1R gene, or through pharmacological means by using small-molecule inhibitors or anti-CSF1R antibodies (Hume et al., 2020). CSF1R signaling is indispensable for microglial survival and its antagonization has the capability of temporarily

depleting mouse microglia from the CNS parenchyma (Elmore et al., 2014). For our purposes, we decided to use a pharmacological approach, consisting of the chronic administration of a CSFR1 antagonist, PLX3397. CSF1R inhibitors such as PLX3397 or PLX5622 have been proven to be a good and safe method to assess global microglial functions in several mouse models of neurodegenerative diseases (Green et al., 2020; Dumas et al., 2021). Within their main advantages, we find that: they do not lead to cognitive and behavioral impairments, are orally bioactive, show BBB penetrance without damaging it, and allow for sustained microglial depletion without the need for costly and time-consuming transgenic strategies (Green et al., 2020). The latter is especially relevant in our study, since *Ndufs4 KO* mice are not able to mate, and the crossing must be established using only heterozygous mice for the deficiency (*Ndufs4*$^{+/-}$), making highly laborious to obtain *Ndufs4 KO* mice with other genetic modifications. Importantly, it is essential to administer these inhibitors chronically to maintain microglial depletion, since inhibitor withdrawal will allow microglia to repopulate the brain in around 3-7 days (Elmore et al., 2014; Najafi et al., 2018).

Typically, these inhibitors are delivered formulated in chow (Green et al., 2020), but given that *Ndufs4 KO* mice progressively develop severe motor problems and difficulties to thrive together with sudden body weight drops we were concerned about the possibility that PLX3397 administration in chow could be inconsistent for each animal along the experimental period. For these reasons, we deemed it appropriate to administer PLX3397 IP at a dosage that would result in significant microglia depletion, with the potential to significantly impact disease progression. By the time we set the experiment, we only found one study using PLX3397 administered IP (Kuse et al., 2018). Thus, we set a pilot study to select the dose. We found a dose-dependent microglial depletion in the brain; treating WT mice IP either with 8 or 16 mg/kg of PLX3397 reduced microglial numbers by 25% after 14 days of treatment compared to a 70% reduction when the dose was 40 mg/kg. This dose-dependent effect goes in line with oral formulations at different concentrations (Elmore et al., 2014; Najafi et al., 2018). So, we decided to use the 40 mg/kg PLX3397 dose for our experiment and found that partially depleting microglia using PLX3397 improved the motor phenotype and prevented microglia accumulation in the main neurodegenerative areas of *Ndufs4 KO* mice such as the VN, the OB, or the cerebellum. Furthermore, our results also strongly suggest that microglial response may be promoting neuronal loss in these regions. When we assessed neuronal loss by immunofluorescence using a general neuronal marker (NeuN), we

found that PLX3397 treatment partially prevented the neuronal loss in the GrOB, while a clear trend was observed in the VN. However, specific staining for glutamatergic and GABAergic neuronal subpopulations using ISH revealed that microglia promoted neuronal loss in both subtypes. Interestingly, although VN glutamatergic neurons are the ones that have been described to be susceptible to NDUFS4 deficiency, microglial depletion also prevented GABAergic neuron loss, suggesting that microglial-mediated neuronal loss is not limited to susceptible neurons. Of note, the VN also consists of a small glycinergic subpopulation that was not assessed in our study (Bagnall et al., 2007). Moreover, despite we did not evaluate the precise subpopulation preserved in the GrOB in microglial-depleted *Ndufs4 KO* mice, the preservation can most likely be attributed to the GABAergic neuronal subpopulation since it is eminently a region composed of GABAergic neurons (Nagayama et al., 2014). We did not investigate neuronal preservation in other neurodegenerative regions, but since we observed preservation in these two relatively unrelated brain areas, we belive that the neuronal preservation might be extensible to all involved areas.

In line with our neuropathological observations together with previous reports (McElroy et al., 2020; Perry et al., 2021), bulk RNAseq of the transcriptome of the VN and the hippocampus of Control and *Ndufs4 KO* mice revealed mainly an upregulation of genes related to the immune system, especially in the VN. Remarkably, PLX3397 treatment only induced changes in microglial-related genes and not in those associated with other cell types in both the VNs and hippocampus of Control and *Ndufs4 KO* mice, presumably meaning that the effects of the treatment are eminently related to its direct action on microglia. This goes in line with previous studies (Najafi et al., 2018). Of course, bulk RNA sequencing can give a good picture overview of transcriptomic changes but is relatively unable to detect subtle cell-type specific changes since the RNA produced by each cell type is diluted in the whole-tissue RNA pool. For instance, although abundant neuronal loss is present in the VN of *Ndufs4 KO* mice, we did not detect neuronal-related gene changes between *Ndufs4 KO*-Veh and *Ndufs4 KO*-PLX3397 mice. In addition, we found a robust increase in GFAP immunoreactivity in the hippocampus of PLX3397-treated groups, especially in control mice, but no upregulation of astrocyte-related genes including *Gfap*. This circumstance might be masking relevant pathways that primarily guide microglial actions in *Ndufs4 KO* mice.

Regarding the GFAP increase in PLX3397-treated mice, one study found that astrocytes are responsible for the phagocytosis of microglial cells that

die due to CSF1R inhibition. Moreover, they showed reactivity signatures, including the upregulation of the expression of the *Gfap* gene (Konishi et al., 2020). These findings align with other studies reporting similar results (Najafi et al., 2018), and may explain why we observed a GFAP increase in PLX3397-treated mice.

5.1.2.1 CSF1R inhibition: effects beyond microglia

Despite how useful CSF1R inhibitors are, the treatment using these drugs is not as microglial-specific as once believed. Increasing pieces of evidence indicate that CSF1R inhibition does not only affect microglia but also affects other peripheral immune cell populations, as well as CAMs (Han et al., 2020; Kerkhofs et al., 2020; Lei et al., 2020; Spiteri et al., 2022). This phenomenon can be mainly explained because *CSF1R*/*Csf1r* expression is not restricted to microglia and it is expressed by all the mononuclear phagocyte system that, as microglia, partially rely on CSF1R signaling for survival, leading to a partial depletion of mature peripheral immune cell populations and CAMs when CSF1R is chronically inhibited (Tushinski et al., 1982; Tushinski and Stanley, 1983; Grabert et al., 2020; Hume et al., 2020). Nevertheless, microglia seem to be way more dependent on CSF1R signaling since homozygous loss-of-function mutations of the *CSF1R/Csf1r* gene in both humans and mice provoke a total microglial loss, whereas they only lead to a partial loss of peripheral macrophages (Hume et al., 2020). In addition, the two main CSF1R inhibitors used, PLX3397 and PLX5622, which bind the CSF1R with comparable affinities, can also bind to important hematopoietic stem cell kinases such as c-Kit. Importantly, PLX5622 is expected to produce fewer hematopoietic off-target effects since its 20-fold more active against CSF1R than against c-Kit, whereas PLX3397 binds more or less with the same affinity to both (Chen and Abkowitz, 2009; DeNardo et al., 2011; Spangenberg et al., 2019). Despite this increased affinity for CSF1R, PLX5622 has been reported to affect both myelopoiesis and lymphopoiesis (Spangenberg et al., 2019; Spiteri et al., 2022). However, as far as we know there are no studies directly comparing the effects of both PLX3397 and PLX5622 on the peripheral immune population which makes it difficult to infer whether PLX5622 has lesser off-target effects than PLX3397. In any case, what seems clear is that the higher the dosage, the higher the effects both centrally and peripherally. For instance, PLX3397 administrated in chow at 290 parts per million (ppm) is able to deplete 99% of brain microglia within 21 days, whereas when administrated at 600 ppm 99% depletion is achieved only after 7 days of treatment (Elmore et al., 2014; Najafi et al., 2018). Something similar seems to happen in peripheral immune populations (Han et al., 2020).

In line with this idea, a recently published study using PLX3397 in *Ndufs4 KO* mice at higher concentrations, which may target and eliminate a wider range of immune cell types other than microglia, showed a dose-dependent increased lifespan and amelioration of clinical signs in *Ndufs4 KO* mice (Stokes et al., 2022). In short, they used three different PLX3397 concentrations in chow to treat *Ndufs4 KO* mice: 667, 1334, and 2001 ppm which corresponded to an approximate oral dose of 100, 200, and 300 mg/kg, respectively. At the lower dose of 100 mg/kg, Stokes and colleagues found a similar survival extension and clinical signs amelioration in *Ndufs4 KO* mice as the ones we have obtained. Importantly, at 100 mg/kg, microglia should be 99% depleted after 7 days of treatment (Najafi et al., 2018), meaning that, under certain circumstances, partial depletion (this thesis; Aguilar et al., 2022) and full depletion (Stokes et al, 2022) seem to have comparable effects in terms of delaying disease progression. One possible explanation is that, in our study, the remaining microglial cells of PLX3397-treated mice are not fully functional. Indeed, they have a very distinct morphology (e.g., less number of ramifications, increased cell body) when compared with those from untreated mice. Unfortunately, the authors did not report the exact numbers of IBA-1$^+$ cells in the group of *Ndufs4 KO* mice treated with PLX3397 at 100 mg/kg, only at 300 mg/kg, where the depletion was certainly complete. In addition, despite Stokes et al. claimed to obtain a general leukocyte depletion, they did not interrogate the numbers of other specific subpopulations of immune cells, neither centrally nor peripherally, with other approaches beyond a brain IBA-1 staining, which, indeed, is a shared limitation with our study. Despite this limitation, it seems reasonable to speculate that the dose-dependent effect of PLX3397 on the *Ndufs4 KO* mouse phenotype might be associated with the type(s) of the immune cell population being eliminated as the dose increases. The effects on peripheral myeloid cell populations could be partially addressed, for instance, by treating *Ndufs4 KO* mice with CSF1R inhibitors that are almost unable to cross the BBB such as PLX73086 (Bellver-Landete et al., 2019) or Ki20227 (Ohno et al., 2006).

To look at other leukocyte subpopulations, apart from those of myeloid origin (IBA-1$^+$ cells), we immunohistochemically stained for CD3, a well-described pan-T-cell marker, in the neurodegenerative areas of *Ndufs4 KO* mice. The absence of CD3$^+$ cell accumulation in the main areas responsible for the major symptoms of *Ndufs4 KO* (VN and cerebellum) suggests that myeloid-derived immune cells are the main ones responsible for the pathogenesis, reinforcing the idea that the pathogenic neuroimmune response present in

these mice is mainly guided by innate immunity mechanisms, as observed in bulk RNAseq data (McElroy et al., 2020; Perry et al., 2021).

With all the current pieces of evidence, we propose that neuroinflammation is a keystone in the development of *Ndufs4 KO* brain pathology that directly promotes and increases neuronal loss producing a severe negative impact (**Figure 38**). Henceforth, disentangling the specific contributions of different immune cell subpopulations with more refined approaches will be key for the complete understanding of the immune interplay that guides *Ndufs4 KO* mice encephalopathy and will allow the development of immunomodulatory therapies.

5.2 IL-6 deficiency in *Ndufs4 KO* mice

Once we proved that microglial response is pathogenic in *Ndufs4 KO* mice, we attempted to uncover possible mechanisms of action by which this cell type promotes neuronal loss. Based on existing literature (Balsa et al., 2020; McElroy et al., 2020) and our VN RNAseq data, we decided to study the role of the cytokine IL-6. This cytokine is an important mediator of neuroinflammation and is known to have strong detrimental effects during chronic neuroinflammation (Erta et al., 2012). Therefore, we hypothesized that IL-6 could potentially guide microglial activity in *Ndufs4 KO* mice. Collectively, our results indicate that although IL-6 protein levels were increased in the tested neurodegenerative regions of *Ndufs4 KO* mice compared to control mice, this cytokine would not appear to be responsible for the major consequences of neuroinflammation in *Ndufs4 KO* mice neuropathology, since IL-6 deficiency did not affect survival, disease progression, or gliosis. This is somewhat surprising, and perhaps the systemic IL-6 KO approach might be masking potential IL-6 effects.

Figure 38. Proposed hypothesis: how neuroinflammation promotes *Ndufs4 KO* mice encephalopathy.

Susceptible neurons to NDUFS4 deficiency (red) release danger signaling molecules, such as PAMPs and DAMPs, sensed by microglia and astrocytes that may serve as reactivity-trigger signals. Consequently, these cells engage a response, but the persistence of the NDUFS4 deficiency finally leads to the establishment of a positive feedback loop that promotes the over-reactivity of microglia, which, in turn, promotes a massive neuronal loss of both susceptible and non-susceptible neurons. Currently, the specific role of astrocytes and infiltrating cells in the pathology is unknown; we suggest that they may have important implications in the development of the pathology that require further investigation. Our data, along with other recent publications, highlight that the usefulness of some beneficial interventions may come from lowering neuroinflammation.

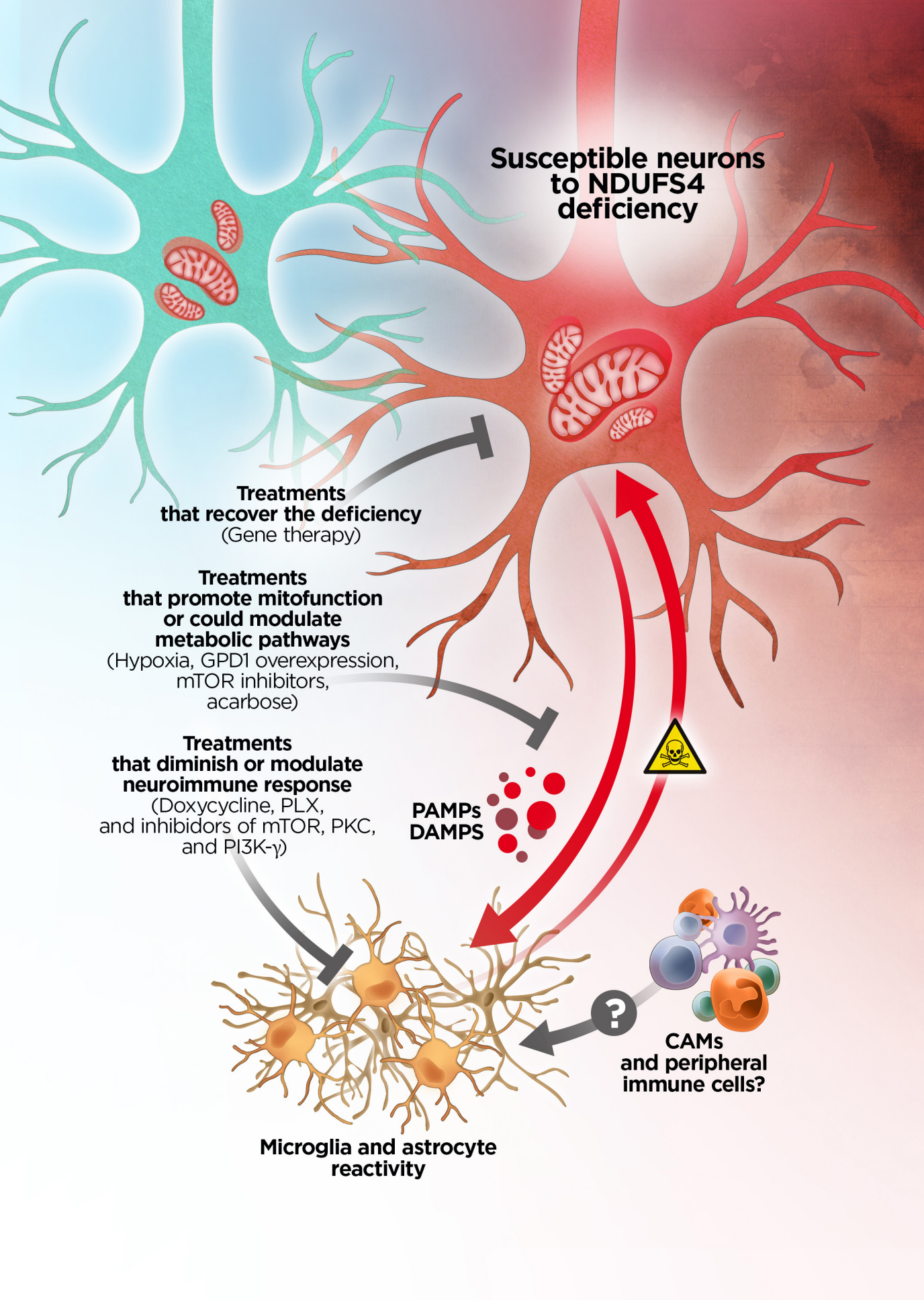
Susceptible neurons to NDUFS4 deficiency
Treatments that recover the deficiency (Gene therapy)
Treatments that promote mitofunction or could modulate metabolic pathways (Hypoxia, GPD1 overexpression, mTOR inhibitors, acarbose)
Treatments that diminish or modulate neuroimmune response (Doxycycline, PLX, and inhibidors of mTOR, PKC, and PI3K-γ)
PAMPs DAMPS
?
CAMs and peripheral immune cells?
Microglia and astrocyte reactivity

Two mechanisms could be at play: (i) opposite effects of IL-6 signaling and (ii) potential compensatory mechanisms due to constitutive IL-6 deficiency. The *Il6* KO mice used in this study were completely deficient in IL-6 (Sanchis et al., 2020a); therefore, they also had abolished all types of IL-6 signaling. As briefly mentioned in Section 1.8.1, IL-6 signaling is extremely complex. It has been proposed that classic signaling guides IL-6 protective effects, while trans-signaling mediates harmful effects, which emphasizes the importance of distinguishing between these two signaling pathways (Rothaug et al., 2016). Remarkably, microglia are the only cells in the CNS in which IL-6 can signal through classic signaling since the mIL-6R is not expressed in any other cell types (Hsu et al., 2015). Thus, we cannot rule out the possibility that both types of signaling are exerting opposite cell type-specific effects, and when IL-6 is eliminated, protective and harmful effects compensate each other, and the pathology remains unchanged. In the second mechanism, unknown developmental compensatory mechanisms in response to constitutive IL-6 deficiency could be occurring, again masking IL-6 contributions to the pathology of *Ndufs4 KO* mice. It could also be possible that other signaling pathways or cytokines compensate for the IL-6 deficiency. However, we did not find different levels of TNF-α between *Ndufs4 KO* and Double KO mice, in addition, IL-1β remained undetectable in both genotypes. Although the appearance of compensatory mechanisms in knockout models is well-documented, the identity of these remains mostly obscure(El-Brolosy and Stainier, 2017). To overcome these limitations, we have preliminary data (not shown) indicating that the specific blockade of IL-6 trans-signaling by administrating sgp130Fc, which binds to the IL-6/sIL-6R complex (Jostock et al., 2001), to *Ndufs4 KO* mice does not modify survival or disease progression. If this additional evidence is confirmed, it will certainly certify that IL-6 plays a minor role in the encephalopathy of *Ndufs4 KO* mice.

However, IL-6 deficiency partially reversed the respiratory abnormalities observed in *Ndufs4 KO* mice. Respiration rhythm generation and coordination require a complex circuitry in which the VN and brainstem are key components. Respiration is strongly influenced by inflammation (Peña-Ortega, 2019). Furthermore, microglia and different inflammatory mediators can modulate respiratory rhythm (Lorea-Hernández et al., 2016; Peña-Ortega, 2019). For instance, IL-1β (Lorea-Hernández et al., 2020) and IL-10 (Giannakopoulou et al., 2019) can modulate tidal volume and respiratory frequency in non-pathological conditions. To our knowledge, this is the first direct report showing that IL-6 can also modulate breathing.

The fact that IL-6 influences respiration in both non-pathological and pathological conditions, together with that we did not find differences in gliosis between *Ndufs4 KO* and Double KO mice, leads us to hypothesize that IL-6 has an intrinsic capacity to affect breathing, as observed in the case of other cytokines (Giannakopoulou et al., 2019; Lorea-Hernández et al., 2020). This could be achieved by changing neuronal firing or playing a relevant role in glia-neuron communication (Peña-Ortega, 2019). Consistently, we also found that PLX3397 administration was also capable of modulate breathing.

5.3 Possible mechanisms of microglia pathogenesis in the context of the *Ndufs4 KO* brain disease

5.3.1 Other potential inflammatory pathways involved

Regarding the strong neuroimmune response present in *Ndufs4 KO* mice, IL-6 signaling is only one of the multiple neuroinflammatory mediators that could be hypothesized to be contributing. Mitochondrial defects have been shown to elicit different inflammatory responses, including TLR9, inflammasome pathway, or IFN type I responses (Zhong et al., 2019; Luna-sánchez et al., 2021). We did not find evidence of inflammasome activation because one of the main mechanisms of action of this complex is the final conversion of pro-IL-1β into its active form (Yang et al., 2019) and we could not detect IL-1β in *Ndufs4 KO* mice. Interestingly, some studies have reported interferon-related response activation in NDUFS4-deficient mice (McElroy et al., 2020; Perry et al., 2021) and other mitochondrial disease mouse models (Lei et al., 2021). However, we did not find any GO pathway related to IFN signaling in our bulk RNAseq data.

5.3.2 Microglial phagocytosis

Microglia phagocyte both dead and stressed/dysfunctional neurons (Brown and Neher, 2014; Butler et al., 2021). There are three main evidence indicating that microglia could be actively phagocyting in *Ndufs4 KO* mice brain lesion sites.

First of all, IBA-1^{+} cells within *Ndufs4 KO* mice brain lesions (e.g., VN, OB, or cerebellum) are fully rounded, a morphological phenotype associated with the phagocytic activity of microglia. Secondly, as discussed above, microglial removal preserved neurons in the VN and the OB of *Ndufs4 KO* mice at the corresponding late stage of the disease, indicating that microglial response may be promoting direct neuronal loss in primary neurodegenerative regions

of *Ndufs4 KO* mice. Finally, the most upregulated GO pathway in *Ndufs4 KO* mice treated with vehicle compared to vehicle-treated control mice in the VN was the positive regulation of phagocytosis. Within the upregulated genes in *Ndufs4 KO mice* in our VN RNAseq dataset, we find *Trem2* and *Tyrobp,* which codify for the triggering receptor expressed on myeloid cells 2 (TREM2) and DNAX-activation protein 12 (DAP12), respectively. TREM2 is a membrane-bound receptor that can bind different ligands including phosphatidylserine, which is exposed in dying neurons, or DNA molecules that can be released under certain dysfunctional circumstances (Bouchon et al., 2000; Takahashi et al., 2005; Wang et al., 2015; Moya et al., 2021), whereas DAP12 is an adaptor protein for correct TREM2 surface expression and intracellular signaling (Humphrey et al., 2015). TREM2 signaling cascades promote microglia chemotaxis, motility, proliferation, survival, and phagocytosis, and it is necessary for microglia to acquire a DAM profile (Keren-Shaul et al., 2017; Ulland and Colonna, 2018; Butler et al., 2021). Indeed, we found several DAM-associated genes upregulated in the VN of *Ndufs4 KO*-Veh compared to Ctrl-Veh mice. TREM2-guided effects have context and time-dependent effects in neurodegenerative diseases. For example, the deletion of *Trem2* in mouse models of Alzheimer's disease is detrimental or beneficial depending on when it is eliminated (Ulland and Colonna, 2018). Even though the precise pathways by which microglia contribute to the progression of the diseases and promote neuronal death in *Ndufs4 KO* mice remain unclear, we suggest that both IFN-related pathways and phagocytosis may be in part responsible for the detrimental contributions of microglia to the pathology.

5.3.3 Microglia and astrocyte partnering

The main goal of our project has been focused on microglia, but astrocytes also exert crucial roles in pathological contexts. Even though it was beyond the scope of this project to directly interrogate the role of astrocytes, we consistently stained for GFAP, which gives clues about the state of astrocytes as discussed above, and we interrogated astrocyte-specific signatures in our RNAseq dataset. As mentioned in sections 1.5.1.2 and 1.7, astrocytes have been proven to negatively affect brain pathology under certain scenarios, as well as exacerbate pathology in some mitochondrial dysfunction contexts and respond abnormally when they present with a mitochondrial malfunction (Sofroniew and Vinters, 2010; Ignatenko et al., 2018, 2020; Murru et al., 2019). In fact, we observed a strong induction of GFAP together with reactive-like astrocyte morphology that, in most cases, precedes, in time and intensity, microglial reactivity in *Ndufs4 KO* mice. For instance, in

the IL-6 deficient mice experiment, we found a significant increase in GFAP immunoreactivity in all regions studied in *Ndufs4* KO mice compared to controls at the mid stage of the disease, while microglial reactivity was either absent or very low, except in the OB. This was also observed in the IL-6 overexpressing experiment in the cortex and CA1. Unfortunately, we do not know if astrocyte reactivity is already present at the early stage. Still, these findings definitively open the question of whether astrocytes are the first responders to the effects of NDUFS4 deficiency or whether they are intrinsically affected by it. These observations are especially interesting since microglia are commonly the first responders that guide astrocyte detrimental actions in a variety of scenarios, such as in TBI (Penkowa et al., 1999), epilepsy (Sano et al., 2021), or axotomized models (Liddelow et al., 2017). Importantly, in mice with specific *Ndufs4* deletion guided by the *Gfap* promoter, mice looked healthy without signs of illness (Ramadasan-Nair et al., 2019), indicating that in basal conditions NDUFS4 deficiency in astrocytes does not have major consequences. Unfortunately, the authors did not interrogate whether the deficiency could affect how astrocytes respond to a particular threatening stimulus. In addition, it is now clear that microglia and astrocyte "work" as partners (Liddelow et al., 2020), especially in disease conditions, so it is highly possible that their crosstalk may elicit coordinated responses in the context of NDUFS4 deficiency that impact the pathology of *Ndufs4 KO* mice that must be considered in future studies.

5.3.4 Context-dependent microglial responses

In our opinion, one final aspect should not be overlooked when investigating the mechanisms of microglial pathogenesis in complex diseases like the one developed in *Ndufs4 KO mice*: context-dependent microglial actions (Paolicelli et al., 2022). Given that neurodegeneration occurs in multiple brain areas that differ significantly in terms of neuronal composition and function, it is likely that region-specific microglial responses are taking place. For instance, susceptible GABAergic neurons in the OB and susceptible glutamatergic neurons in the VN may respond differently to the NDUFS4 deficiency (Bolea et al., 2019), hence, generating a different danger pattern that will make microglia react in a different fashion despite the final outcome being the same: microglial reactivity and neuronal loss. Another example could be that we detect T-cell infiltration in the OB of *Ndufs4 KO* mice, but not in the VN or the cerebellum. Could these infiltrating T-cells interact with microglia and somehow mutually modulate their responses as described in other brain scenarios? Are microglia attracting T-cells in the OB but not in other regions? (Schetters et al., 2018).

5.4 Effects of chronic neuroinflammation in *Ndufs4 KO* mice

The last goal of the thesis was to assess whether an increased inflammatory environment could affect *Ndufs4 KO* mice disease in an opposite fashion to that observed depleting microglia and reducing neuroinflammation. To do so, we used GFAP-IL6 and *Ndufs4 KO* mice to generate GFAP-IL6/*Ndufs4 KO* mice. GFAP-IL6 mice have been widely used as a model for chronic neuroinflammation. As mentioned above, these mice overexpress the cytokine IL-6 under the control of the *Gfap* promoter, which restricts the overexpression to astrocytes, since they are the unique cells expressing *Gfap* in the adult brain. As a result, GFAP-IL6 mice develop abundant microgliosis and astrogliosis in which both cell types show morphological signs of reactivity. They also promote tissue vacuolization, angiogenesis, peripheral cell infiltration, and ultimately neurodegeneration (Campbell et al., 1993; Erta et al., 2012; Giralt et al., 2013); as a result, these mice start to develop serious motor problems around six months of age (Gyengesi et al., 2019). Consistent with this, in young mice, we found prominent microgliosis and astrogliosis but no differences in total ambulation and motor coordination between control and GFAP-IL6 mice at any time point. We hypothesized that IL-6 overexpression would potentiate and advance *Ndufs4 KO* mice disease based on abundant literature indicating that a neuroinflammatory state can be neurotoxic by aggravating neurodegenerative mechanisms (Chitnis and Weiner, 2017). For example, IL-6 overexpression could allow microglial cells to become primed and potentiate their detrimental actions. Microglial priming refers to the heightened sensitivity of microglial cells to a secondary inflammatory stimulus, resulting in an enhanced inflammatory response compared to the response to an initial or ongoing stimulus. These processes have been described in multiple situations, but whether different combinations of stimuli guide different primed microglial phenotypes with different functionalities remains to be fully studied (Perry and Holmes, 2014; Neher and Cunningham, 2019). Importantly, IL-6 has been related to microglial priming, for instance, increased IL-6 production and signaling in the brain of aged mice compared to adult mice potentiates microglial response after a systemic inflammation (Garner et al., 2018). In this particular case, the primary stimulus would be IL-6, and the secondary, the NDUFS4 deficiency-mediated inflammatory response. Additionally, the presence of inflammatory by-products could further harm neurons that are already vulnerable to NDUFS4 deficiency.

Strikingly, IL-6 overexpression only reduced the survival of *Ndufs4 KO* female mice, which may indicate that *Ndufs4 KO* female mice have a higher sensitivity to brain inflammation than male mice, highlighting the importance of considering each sex in these types of studies. It is long known the existence of an interplay between IL-6 and estrogens that could partially explain the sex-dependent differences (Stein and Yang, 1995; Young et al., 1997). Moreover, some studies have reported IL-6 sex-dependent effects in a variety of neurodegenerative diseases, for instance, in a mouse model of EAE demyelination, T-cell infiltrates and gliosis in the spinal cord were regulated in a sex and cellular IL-6 source-dependent manner (Sanchis et al., 2020b). In addition, the inhibition of IL-6 trans-signaling modulated the phenotype of two different mouse models of Alzheimer's disease also in a sex-dependent manner (Escrig et al., 2019). To add another layer of complexity, it is now clear that not only can inflammatory mediators exert different effects depending on the sex, but also cellular components of the neuroimmune system can be highly influenced by sex, with particular relevance to those found in astrocytes and microglia (Osborne et al., 2018; Han et al., 2021a). For instance, pieces of evidence suggest a clear sexually dimorphic microglial response as a result of a CNS insult like a traumatic brain injury in mice (Villapol et al., 2017).

Apart from survival and a slight difference in clasping onset (3 days), female GFAP-IL6/*Ndufs4 KO* mice were phenotypically similar to males in terms of disease progression and gliosis. We did not further interrogate the specific cause of this sex-specific decreased survival, but since both GFAP-IL6/*Ndufs4 KO* female and male mice had similar disease progression compared to their *Ndufs4 KO* mice counterparts, it is unlikely that this observation is related to increased neuronal loss in females. We suggest that it may be due to the alteration of other aspects of the *Ndufs4 KO* phenotype, that we did observe but that were not addressed in this thesis, such as the appearance of seizures (Kruse et al., 2008; Quintana et al., 2010; Bolea et al., 2019). There is a significant correlation between inflammation and epilepsy, as seizures can trigger inflammation or inflammation exacerbate the severity of seizures (Vezzani et al., 2011). In addition, some studies have observed different sex susceptibilities to the development of specific epilepsy subtypes (Christensen et al., 2005; Reddy et al., 2021). Therefore, it cannot be ruled out that the sex-dependent effect on survival is due to a greater susceptibility to developing epilepsy, or a greater severity of seizures in GFAP-IL6/*Ndufs4 KO* female mice compared to GFAP-IL6/*Ndufs4 KO* male mice and *Ndufs4 KO* mice.

5.4.1 Decreased microgliosis in *Ndufs4 KO* mice in response to IL-6 overexpression

NDUFS4 deficiency compromised cerebellar IL-6 production in GFAP-IL6 mice. This may explain the decreased IBA-1 levels in this region in GFAP-IL6/*Ndufs4 KO* mice compared to GFAP-IL6 mice, as less IL-6 production may result in less microglial reactivity. Importantly, this seemed specific for IL-6 since NDUFS4 deficiency did not affect TNF-α or IL-10 production in GFAP-IL6 mice. Interestingly, the absence of NDUFS4 did not hinder IL-6 production in the olfactory bulb of GFAP-IL6/*Ndufs4 KO* mice but instead increased it due to the combined effects of IL-6 overexpression and NDUFS4 deficiency. These results indicate that NDUFS4 deficiency does have different effects on IL-6 levels depending on the brain region in GFAP-IL6 mice. Unfortunately, time constraints prevented us from including data on cytokine levels from other regions. To further explore the correlation between IL-6 expression and IBA-1 staining, we plan to measure IL-6 levels in the cortex of all genotypes. This will allow us to determine if the decrease of both IBA-1 staining and the number of IBA-1$^+$ cells found in the cortex of GFAP-IL6/*Ndufs4 KO* mice is also reflected in lower IL-6 levels, as was observed in the cerebellum.

Strikingly, GFAP levels measured by immunostaining were comparable between both IL-6 overexpressing mice in the cerebellum and other regions at both disease stages. Since *Il6* expression is guided by the *Gfap* promoter in GFAP-IL6 mice, one would expect a correlation between GFAP and IL-6 protein levels given their mRNA-coupled expression, but this may not be necessarily true. It is well known that mRNA and protein levels do not always correlate (Greenbaum et al., 2003; Liu et al., 2016). Additionally, the levels of GFAP immunoreactivity were already strongly elevated in GFAP-IL6 mice, suggesting that GFAP protein levels may be approaching saturation, even though *Gfap* transcription may still be active, and thus *Il6*. No studies have described the dynamics between *Gfap* and *Il6* expression and their protein expression levels in the context of GFAP-IL6 mice. Indeed, only a few studies have quantified IL-6 protein levels in GFAP-IL6 mice so far (Quintana et al., 2009; Recasens et al., 2021). On this matter, our results evidence that GFAP immunoreactivity and IL-6 levels do not necessarily correlate in GFAP-IL6 mice.

We have two hypotheses that could explain why microgliosis is consistently decreased at both mid and late stages in the cortex, CA1, and cerebellum of GFAP-IL6/*Ndufs4 KO* mice when compared to GFAP-IL6 mice. The first explanation is that NDUFS4 deficiency directly affects astrocytic IL-6

production depending on the brain regions. It is possible that OXPHOS defective astrocytes could not entirely sustain such an abundant IL-6 production in the cerebellum (McAvoy and Kawamata, 2019). For instance, an experiment to directly investigate this could involve establishing primary astrocyte cultures from the cerebellum and other regions, such as the cortex of GFAP-IL6 and GFAP-IL6/*Ndufs4 KO* mice, and see the effects of the absence of the *Ndufs4* gene on IL-6 secretion. Another possibility is that NDUFS4-deficient microglia are not able to respond to an inflammatory stimulus such as IL-6 appropriately. In the normal scenario (GFAP-IL6 mice), and given that microglia are important target and effector cells of this cytokine, it was believed that the primary IL-6 released by astrocytes would engage a paracrine immune response in microglia, which then would release other inflammatory mediators. These microglia-released factors could further exacerbate inflammation, leading to more astrocyte reactivity and increased expression of *Gfap* and, thus, the production of IL-6, establishing a positive feedback loop. Despite logic, a very recent work contradicts this previous conception. The authors of this study found that microglia-depleted GFAP-IL6 mice had similar *Il6* expression levels and comparable levels of astrocyte reactivity measured by GFAP (West et al., 2022b), indicating that astrocytes could produce identical amounts of IL-6 and become similarly reactive without any microglial input.

5.5 Future perspectives

With our current results, we cannot establish the cause of the decreased microgliosis in *Ndufs4 KO* mice with IL-6 overexpression when compared to GFAP-IL6 mice. Therefore, our immediate goal is to assess the potential explanations. As discussed above, the likely possibility is that astrocytes harboring the IL-6 transgene together with an NDUFS4 deficiency are unable to produce IL-6 at levels comparable to those without the deficiency, which may have a direct effect on microgliosis. As previously mentioned, to study this, we will measure cytokine levels in other brain regions, such as the cortex, as well as directly assess the IL-6 production in IL-6-overexpressing astrocytes with NDUFS4 deficiency in primary cultures. Furthermore, based on the existing literature, we could not rule out the possibility that microglia were responding abnormally due to NDUFS4 deficiency; thus, we also decided to set up a battery of experiments to study the effects of NDUFS4 deficiency in microglia. The great majority of the studies that interrogated which factors influence or modulate microglial response to inflammatory stimuli are based on challenging microglia with LPS (Hoogland et al., 2015). LPS is a component of the cell wall of gram-negative bacteria that

can stimulate microglia via TLR4 to produce pro-inflammatory cytokines, leading to the activation of the innate immune response (Carpentier et al., 2008). Recent studies have shown that LPS stimulation switches the microglial metabolic profile from OXPHOS to glycolysis (a process known as the "glycolytic switch") in rodents. This switch to glycolysis was necessary for producing pro-inflammatory cytokines, suggesting that the metabolic reprogramming of microglia is a crucial aspect of the immune response to LPS (Bernier et al., 2020; Hu et al., 2020; Cheng et al., 2021; Vizuete et al., 2022). During this conversion, LPS stimulation has also been reported to induce a transient increase in microglial OXPHOS O_2 consumption (Nair et al., 2019). Significantly, mitochondrial dynamics has been described to influence microglial response to LPS (Park et al., 2013; Nair et al., 2019; Harland et al., 2020; Stavropoulos et al., 2021). Taken together, this evidence indicate that fine-tuned mitochondrial function is indispensable for normal microglial response upon LPS stimulation. Since previous works have primarily used LPS to study aspects of mitochondrial functioning in microglial cells, we decided to study the effects of NDUFS4 deficiency in microglia upon an LPS challenge. To do so, we are investigating this response both *in vitro* and *in vivo*.

Firstly, we established primary microglia and astrocyte cultures from WT and *Ndufs4 KO* mice to compare their transcriptomic changes and measure the levels of cytokines released into the culture media in response to LPS stimulation. In parallel, we administered LPS to *Ndufs4 KO* mice prior to the onset of neurological symptoms at P30 to investigate the total tissue cytokine levels and microglial morphological changes in various brain regions. We are confident that we will see changes in the response of NDUFS4-deficient microglia at different levels, especially considering a recent study from December 2022 that described that NDUFS4-deficient macrophages produced more cytokines in response to LPS and had a negative impact on tissue repair after a myocardial infarction (Cai et al., 2022).

To summarize, immune-related alterations are commonly observed in patients suffering from a mitochondrial disease (Hanaford and Johnson, 2022). We demonstrated that microglial response is *per se* a pathogenic driving mechanism of the *Ndufs4 KO* mice encephalopathy. Our data support the notion that unraveling the specific roles of immune cells and their responses could have significant implications for understanding mitochondrial diseases. This is not only because immune cells could play a direct role in the pathology, as microglia do in *Ndufs4 KO* mice, but also because their dysfunction resulting from intrinsic mitochondrial impairment could lead to a detrimental secondary response that aggravates the disease.

6

Conclusions

Overall, our results indicate that neuroinflammation has a detrimental effect in *Ndufs4 KO* mice, revealing the pathogenicity of the neuroimmune response in *Ndufs4 KO* mice as more than just a consequence of neurodegeneration. This study serves as a proof-of-concept to investigate and consider neuroimmune-related processes in other mitochondrial diseases that affect the brain. Specifically, our work has led to the following conclusions:

1. Intraperitoneal injection of PLX3397 depletes microglia in a dose-dependent manner, similar to the effects previously reported using chow formulations of the drug.
2. Partial microglial depletion extends survival and delays the motor decline of *Ndufs4 KO* mice. Importantly, it does not affect the phenotype of control mice, which appear healthy at P60.
3. PLX3397 treatment is able to prevent IBA-1^{+} cell accumulation in both non-neurodegenerative and neurodegenerative areas of *Ndufs4 KO* mice. In contrast, it produced an increase in GFAP levels, which suggest astrogliosis, in several regions, including the OB, the hippocampal area CA1, and the cortex.
4. The depletion of microglia partially prevents neuronal loss in the GrOB, as evidenced by NeuN immunostaining. Analysis using ISH for specific neuronal subpopulations revealed that microglial depletion prevents the loss of glutamatergic and GABAergic neurons in the VN of *Ndufs4 KO* mice. These findings suggest that microglia play a direct role in mediating general neuronal cell death in *Ndufs4 KO* mice.
5. *Ndufs4 KO* mice show vascular abnormalities in the VN at a late stage, however, T-cells do not infiltrate the region. There is also no infiltration of T-cells in the cerebellum, but substantial infiltration is observed in the OB, which is unaffected by microglial depletion.
6. At the transcriptomic level, the main GO terms enriched in *Ndufs4 KO* mice are related to the immune system in the VN and the hippocampus. The administration of PLX3397 predominantly affects microglial-related genes in both control and *Ndufs4 KO* mice, indicating that PLX3397 has its major effects on microglia. However, subtle changes might have not been accurately detected through bulk RNAseq.

7. IL-6 levels are elevated in the OB and the cerebellum of *Ndufs4 KO* mice. Besides, downregulated genes in the VN of PLX3397-treated *Ndufs4 KO* mice compared to vehicle-treated mice are associated with IL-6 production. Despite this increased production of IL-6, systemic IL-6 deficiency in *Ndufs4 KO* mice does not modify their survival nor ameliorates disease progression and barely impacts gliosis. These findings indicate that IL-6 has a modest role in the development and progression of the *Ndufs4 KO* mice encephalopathy.

8. In contrast, IL-6 deficiency modulates breathing in both control and *Ndufs4 KO* mice, strongly suggesting, for the first time, a role of IL-6 in breathing modulation.

9. Chronic neuroinflammation induced by transgenic overexpression of IL-6 in astrocytes reduces the survival of female *Ndufs4 KO* mice, but not males, indicating that female *Ndufs4 KO* mice may have an increased susceptibility to chronic neuroinflammation. Contrarily, GFAP-IL6/*Ndufs4 KO* mice of both sexes show a similar motor decline as *Ndufs4 KO* mice. However, female GFAP-IL6/*Ndufs4 KO* mice have a slight advance in clasping onset.

10. Despite we found few sex-specific differences along this thesis, the differences in the responses to IL-6 overexpression between male and female GFAP-IL6/*Ndufs4 KO* mice compared to *Ndufs4 KO* mice of the same sex highlight the importance of considering possible sex-specific effects in this type of studies.

11. NDUFS4 deficiency compromises cerebellar IL-6 production in GFAP-IL6 mice, but not TNF-α and IL-10. This effect is not observed in the OB.

12. Microgliosis, measured by the number of IBA-1^{+} cells and/or the IBA-1 mean fluorescence intensity, is consistently decreased in GFAP-IL6/*Ndufs4 KO* mice compared to GFAP-IL6 mice at both mid and late stages and does not correlate with GFAP levels in the majority of brain areas. This effect could be explained either by the defective production of IL-6 by NDUFS4-deficient astrocytes or by abnormal responses of NDUFS4-deficient microglia to IL-6 stimulation.

7

References

A

Acín-Pérez R, Fernández-Silva P, Peleato ML, Pérez-Martos A, Enriquez JA (2008) Respiratory active mitochondrial supercomplexes. Mol Cell 32:529-539.

Agip A-NA, Blaza JN, Fedor JG, Hirst J (2019) Mammalian Respiratory Complex I Through the Lens of Cryo-EM. Annu Rev Biophys 48:165-184.

Agnew T, Goldsworthy M, Aguilar C, Morgan A, Simon M, Hilton H, Esapa C, Wu Y, Cater H, Bentley L, Scudamore C, Poulton J, Morten KJ, Thompson K, He L, Brown SDM, Taylor RW, Bowl MR, Cox RD (2018) A Wars2 Mutant Mouse Model Displays OXPHOS Deficiencies and Activation of Tissue-Specific Stress Response Pathways. Cell Rep 25:3315-3328.

Aguilar K, Comes G, Canal C, Quintana A, Sanz E, Hidalgo J (2022) Microglial response promotes neurodegeneration in the Ndufs4 KO mouse model of Leigh syndrome. Glia 70:2032-2044.

Ajami B, Bennett JL, Krieger C, Tetzlaff W, Rossi FM v (2007) Local self-renewal can sustain CNS microglia maintenance and function throughout adult life. Nat Neurosci 10:1538-1543.

Allen NJ, Eroglu C (2017) Cell Biology of Astrocyte-Synapse Interactions. Neuron 96:697-708.

Amo-Aparicio J, Martínez-Muriana A, Sánchez-Fernández A, López-Vales R (2018) Neuroinflammation Quantification for Spinal Cord Injury. Curr Protoc Immunol 123:e57.

Andjelkovic AV, Nikolic B, Pachter JS, Zecevic N (1998) Macrophages/microglial cells in human central nervous system during development: an immunohistochemical study. Brain Res 814:13-25.

Andriezen WL (1893) The Neuroglia Elements in the Human Brain. Br Med J 2:227-230.

Argaw AT, Asp L, Zhang J, Navrazhina K, Pham T, Mariani JN, Mahase S, Dutta DJ, Seto J, Kramer EG, Ferrara N, Sofroniew M v, John GR (2012) Astrocyte-derived VEGF-A drives blood-brain barrier disruption in CNS inflammatory disease. J Clin Invest 122:2454-2468.

Arii J, Tanabe Y (2000) Leigh Syndrome: Serial MR Imaging and Clinical Follow-up. American Journal of Neuroradiology 21:1502–1509

Askew K, Li K, Olmos-Alonso A, Garcia-Moreno F, Liang Y, Richardson P, Tipton T, Chapman MA, Riecken K, Beccari S, Sierra A, Molnár Z, Cragg MS, Garaschuk O, Perry VH, Gomez-Nicola D (2017) Coupled Proliferation and Apoptosis Maintain the Rapid Turnover of Microglia in the Adult Brain. Cell Rep 18:391-405.

Assouline Z, Jambou M, Rio M, Bole-Feysot C, de Lonlay P, Barnerias C, Desguerre I, Bonnemains C, Guillermet C, Steffann J, Munnich A, Bonnefont JP, Rötig A, Lebre AS (2012) A constant and similar assembly defect of mitochondrial respiratory chain complex I allows rapid identification of NDUFS4 mutations in patients with Leigh syndrome. Biochim Biophys Acta 1822:1062-1069.

B

Baertling F, Rodenburg RJ, Schaper J, Smeitink JA, Koopman WJH, Mayatepek E, Morava E, Distelmaier F (2014) A guide to diagnosis and treatment of Leigh syndrome. J Neurol Neurosurg Psychiatry 85:257-265.

Bagnall MW, Stevens RJ, du Lac S (2007) Transgenic Mouse Lines Subdivide Medial Vestibular Nucleus Neurons into Discrete, Neurochemically Distinct Populations. J Neurosci 27:2318-2330.

Balsa E, Perry EA, Bennett CF, Jedrychowski M, Gygi SP, Doench JG, Puigserver P (2020) Defective NADPH production in mitochondrial disease complex I causes inflammation and cell death. Nat Commun 11:1-12

Batiuk MY, Martirosyan A, Wahis J, de Vin F, Marneffe C, Kusserow C, Koeppen J, Viana JF, Oliveira JF, Voet T, Ponting CP, Belgard TG, Holt MG (2020) Identification of region-specific astrocyte subtypes at single cell resolution. Nat Commun 11:1220.

Baxter PS, Dando O, Emelianova K, He X, McKay S, Hardingham GE, Qiu J (2021) Microglial identity and inflammatory responses are controlled by the combined effects of neurons and astrocytes. Cell Rep 34:108882.

Bayraktar OA et al. (2020) Astrocyte layers in the mammalian cerebral cortex revealed by a single-cell in situ transcriptomic map. Nat Neurosci 23:500-509.

Bellver-Landete V, Bretheau F, Mailhot B, Vallières N, Lessard M, Janelle M-E, Vernoux N, Tremblay M-È, Fuehrmann T, Shoichet MS, Lacroix S (2019) Microglia are an essential component of the neuroprotective scar that forms after spinal cord injury. Nat Commun 10:518.

Bennett FC, Bennett ML, Yaqoob F, Mulinyawe SB, Grant GA, Hayden Gephart M, Plowey ED, Barres BA (2018) A Combination of Ontogeny and CNS Environment Establishes Microglial Identity. Neuron 98:1170-1183.

Bennett ML, Bennett FC, Liddelow SA, Ajami B, Zamanian JL, Fernhoff NB, Mulinyawe SB, Bohlen CJ, Adil A, Tucker A, Weissman IL, Chang EF, Li G, Grant GA, Hayden Gephart MG, Barres BA (2016) New tools for studying microglia in the mouse and human CNS. Proc Natl Acad Sci USA 113:1738-1746.

Bernier L-P, York EM, MacVicar BA (2020) Immunometabolism in the Brain: How Metabolism Shapes Microglial Function. Trends Neurosci 43:854-869.

Bock FJ, Tait SWG (2020) Mitochondria as multifaceted regulators of cell death. Nat Rev Mol Cell Biol 21:85-100.

Bohlen CJ, Bennett FC, Tucker AF, Collins HY, Mulinyawe SB, Barres BA (2017) Diverse Requirements for Microglial Survival, Specification, and Function Revealed by Defined-Medium Cultures. Neuron 94:759-773.

Boisvert MM, Erikson GA, Shokhirev MN, Allen NJ (2018) The Aging Astrocyte Transcriptome from Multiple Regions of the Mouse Brain. Cell Rep 22:269-285.

Bolea I, Gella A, Sanz E, Prada-Dacasa P, Menardy F, Bard AM, Machuca-Msárquez P, Eraso-Pichot A, Mòdol-Caballero G, Navarro X, Kalume F, Quintana A (2019) Defined neuronal populations drive fatal phenotype in a mouse model of Leigh syndrome. Elife 8.

Bolger AM, Lohse M, Usadel B (2014) Trimmomatic: a flexible trimmer for Illumina sequence data. Bioinformatics 30:2114-2120.

Bornstein R, James K, Stokes J, Park KY, Kayser E-B, Snell J, Bard A, Chen Y, Kalume F, Johnson SC (2022) Differential effects of mTOR inhibition and dietary ketosis in a mouse model of subacute necrotizing encephalomyelopathy. Neurobiol Dis 163:105594.

Borst K, Dumas AA, Prinz M (2021) Microglia: Immune and non-immune functions. Immunity 54:2194-2208.

Bouchon A, Dietrich J, Colonna M (2000) Cutting edge: inflammatory responses can be triggered by TREM-1, a novel receptor expressed on neutrophils and monocytes. J Immunol 164:4991-4995.

Brambilla R, Persaud T, Hu X, Karmally S, Shestopalov VI, Dvoriantchikova G, Ivanov D, Nathanson L, Barnum SR, Bethea JR (2009) Transgenic inhibition of astroglial NF-kappa B improves functional outcome in experimental autoimmune encephalomyelitis by suppressing chronic central nervous system inflammation. J Immunol 182:2628-2640.

Bravo-Sagua R, Parra V, López-Crisosto C, Díaz P, Quest AFG, Lavandero S (2017) Calcium transport and signaling in mitochondria. Compr Physiol 7:623-634.

Brown GC, Neher JJ (2014) Microglial phagocytosis of live neurons. Nat Rev Neurosci 15:209-216.

Butler CA, Popescu AS, Kitchener EJA, Allendorf DH, Puigdellívol M, Brown GC (2021) Microglial phagocytosis of neurons in neurodegeneration, and its regulation. J Neurochem 158:621–639.

C

Cai S, Zhao M, Zhou B, Yoshii A, Bugg D, Villet O, Sahu A, Olson GS, Davis J, Tian R (2022) Mitochondrial dysfunction in macrophages promotes inflammation and suppresses repair after myocardial infarction. J Clin Invest e159498.

Calvaruso MA, Willems P, van den Brand M, Valsecchi F, Kruse S, Palmiter R, Smeitink J, Nijtmans L (2012) Mitochondrial complex III stabilizes complex I in the absence of NDUFS4 to provide partial activity. Hum Mol Genet 21:115-120.

Campbell IL, Abraham CR, Masliah E, Kemper P, Inglis1 JD, Oldstone MBA, Mucke L (1993) Neurologic disease induced in transgenic mice by cerebral overexpression of interleukin 6. Proc Natl Acad Sci USA 90:10061-5.

Campbell IL, Erta M, Lim SL, Frausto R, May U, Rose-John S, Scheller J, Hidalgo J (2014) Trans-Signaling Is a Dominant Mechanism for the Pathogenic Actions of Interleukin-6 in the Brain. J Neurosci 34:2503-2513

Ceyzériat K et al. (2018) Modulation of astrocyte reactivity improves functional deficits in mouse models of Alzheimer's disease. Acta Neuropathol Commun 6:104.

Chance B, Estabrook RW, Lee CP (1963) Electron Transport in the Oxysome. Science 140:379-380

Chance B, Williams GR (1956) The respiratory chain and oxidative phosphorylation. Advances in Enzymology and Related Areas of Molecular Biology 17:65-134.

Chen B, Hui J, Montgomery KS, Gella A, Bolea I, Sanz E, Palmiter RD, Quintana A (2017) Loss of Mitochondrial Ndufs4 in Striatal Medium Spiny Neurons Mediates Progressive Motor Impairment in a Mouse Model of Leigh Syndrome. Front Mol Neurosci 10:265.

Cheng J, Zhang R, Xu Z, Ke Y, Sun R, Yang H, Zhang X, Zhen X, Zheng L-T (2021) Early glycolytic reprogramming controls microglial inflammatory activation. J Neuroinflammation 18:129.

Chen J, Abkowitz JL (2009) Hematopoietic Stem Cell Defect in c-Kit Deficient Mice. Blood 114:2542-2542.

Chen P-C, Vargas MR, Pani AK, Smeyne RJ, Johnson DA, Kan YW, Johnson JA (2009) Nrf2-mediated neuroprotection in the MPTP mouse model of Parkinson's disease: Critical role for the astrocyte. Proc Natl Acad Sci USA 106:2933-2938.

Chhatbar C, Detje CN, Grabski E, Borst K, Spanier J, Ghita L, Elliott DA, Jordão MJC, Mueller N, Sutton J, Prajeeth CK, Gudi V, Klein MA, Prinz M, Bradke F, Stangel M, Kalinke U (2018) Type I Interferon Receptor Signaling of Neurons and Astrocytes Regulates Microglia Activation during Viral Encephalitis. Cell Rep 25:118-129.

Choi W-S, Kim H-W, Tronche F, Palmiter RD, Storm DR, Xia Z (2017) Conditional deletion of Ndufs4 in dopaminergic neurons promotes Parkinson's disease-like non-motor symptoms without loss of dopamine neurons. Sci Rep 7:44989.

Christensen J, Kjeldsen MJ, Andersen H, Friis ML, Sidenius P (2005) Gender Differences in Epilepsy. Epilepsia 46:956-960.

Chucair-Elliott AJ, Conrady C, Zheng M, Kroll CM, Lane TE, Carr DJJ (2014) Microglia-induced IL-6 protects against neuronal loss following HSV-1 infection of neural progenitor cells. Glia 62:1418–1434.

Chung HK et al. (2017) Growth differentiation factor 15 is a myomitokine governing systemic energy homeostasis. J Cell Bio 216:149-165.

Civiletto G, Varanita T, Cerutti R, Gorletta T, Barbaro S, Marchet S, Lamperti C, Viscomi C, Scorrano L, Zeviani M (2015) Opa1 overexpression ameliorates the phenotype of two mitochondrial disease mouse models. Cell Metab 21:845-854.

Clark IC et al. (2021) Barcoded viral tracing of single-cell interactions in central nervous system inflammation. Science 372:abf1230

Cogliati S, Enriquez JA, Scorrano L (2016) Mitochondrial Cristae: Where Beauty Meets Functionality. Trends Biochem Sci 41:261-273.

Colonna M, Butovsky O (2017) Microglia Function in the Central Nervous System During Health and Neurodegeneration. Annu Rev Immunol 35:441-468.

Corrà S, Cerutti R, Balmaceda V, Viscomi C, Zeviani M (2022) Double administration of self-complementary AAV9NDUFS4 prevents Leigh disease in Ndufs4$^{-/-}$ mice. Brain 145:3405-3414.

Cunningham JT, Rodgers JT, Arlow DH, Vazquez F, Mootha VK, Puigserver P (2007) mTOR controls mitochondrial oxidative function through a YY1-PGC-1alpha transcriptional complex. Nature 450:736-740.

Cusick MF, Libbey JE, Patel DC, Doty DJ, Fujinami RS (2013) Infiltrating macrophages are key to the development of seizures following virus infection. J Virol 87:1849-1860.

D

Damisah EC, Hill RA, Rai A, Chen F, Rothlin C v., Ghosh S, Grutzendler J (2020) Astrocytes and microglia play orchestrated roles and respect phagocytic territories during neuronal corpse removal in vivo. Sci Adv 6:3239.

D'Autréaux B, Toledano MB (2007) ROS as signalling molecules: mechanisms that generate specificity in ROS homeostasis. Nat Rev Mol Cell Biol 8:813-824.

de Benedetti F, Rucci N, del Fattore A, Peruzzi B, Paro R, Longo M, Vivarelli M, Muratori F, Berni S, Ballanti P, Ferrari S, Teti A (2006) Impaired skeletal development in interleukin-6-transgenic mice: a model for the impact of chronic inflammation on the growing skeletal system. Arthritis Rheum 54:3551-3563.

de Jager PL et al. (2009) Meta-analysis of genome scans and replication identify CD6, IRF8 and TNFRSF1A as new multiple sclerosis susceptibility loci. Nat Genet 41:776-782.

DeNardo DG, Brennan DJ, Rexhepaj E, Ruffell B, Shiao SL, Madden SF, Gallagher WM, Wadhwani N, Keil SD, Junaid SA, Rugo HS, Hwang ES, Jirström K, West BL, Coussens LM (2011) Leukocyte complexity predicts breast cancer survival and functionally regulates response to chemotherapy. Cancer Discov 1:54-67.

Dhir A, Dhir S, Borowski LS, Jimenez L, Teitell M, Rötig A, Crow YJ, Rice GI, Duffy D, Tamby C, Nojima T, Munnich A, Schiff M, de Almeida CR, Rehwinkel J, Dziembowski A, Szczesny RJ, Proudfoot NJ (2018) Mitochondrial double-stranded RNA triggers antiviral signalling in humans. Nature 560:238-242.

Diaz-Castro B, Gangwani MR, Yu X, Coppola G, Khakh BS (2019) Astrocyte molecular signatures in Huntington's disease. Sci Transl Med 11:aaw8546.

Diaz F, Garcia S, Padgett KR, Moraes CT (2012) A defect in the mitochondrial complex III, but not complex IV, triggers early ROS-dependent damage in defined brain regions. Hum Mol Genet 21:5066–5077.

Dibble CC, Cantley LC (2015) Regulation of mTORC1 by PI3K signaling. Trends Cell Biol 25:545-555.

di Filippo M, Chiasserini D, Tozzi A, Picconi B, Calabresi P (2010) Mitochondria and the Link Between Neuroinflammation and Neurodegeneration. J Alzheimers Dis 20:369-379.

di Santo E, Alonzi T, Fattori E, Poli V, Ciliberto G, Sironi M, Gnocchi P, Ricciardi-Castagnoli P, Ghezzi P (1996) Overexpression of interleukin-6 in the central nervous system of transgenic mice increases central but not systemic proinflammatory cytokine production. Brain Res 740:239-244.

di Virgilio F (2013) The therapeutic potential of modifying inflammasomes and NOD-like receptors. Pharmacol Rev 65:872-905.

D'Mello C, Le T, Swain MG (2009) Cerebral Microglia Recruit Monocytes into the Brain in Response to Tumor Necrosis Factor Signaling during Peripheral Organ Inflammation. J Neurosci 29:2089-2102.

Dobin A, Davis CA, Schlesinger F, Drenkow J, Zaleski C, Jha S, Batut P, Chaisson M, Gingeras TR (2013) STAR: ultrafast universal RNA-seq aligner. Bioinformatics 29:15-21.

Drögemüller K, Helmuth U, Brunn A, Sakowicz-Burkiewicz M, Gutmann DH, Mueller W, Deckert M, Schlüter D (2008) Astrocyte gp130 expression is critical for the control of Toxoplasma encephalitis. J Immunol 181:2683-2693.

Dumas AA, Borst K, Prinz M (2021) Current tools to interrogate microglial biology. Neuron 109:2805-2819.

E

El-Brolosy MA, Stainier DYR (2017) Genetic compensation: A phenomenon in search of mechanisms. PLoS Genet 13:e1006780.

Elmore MRP, Najafi AR, Koike MA, Dagher NN, Spangenberg EE, Rice RA, Kitazawa M, Matusow B, Nguyen H, West BL, Green KN (2014) Colony-stimulating factor 1 receptor signaling is necessary for microglia viability, unmasking a microglia progenitor cell in the adult brain. Neuron 82:380-397.

Emmerzaal TL, Preston G, Geenen B, Verweij V, Wiesmann M, Vasileiou E, Grüter F, de Groot C, Schoorl J, de Veer R, Roelofs M, Arts M, Hendriksen Y, Klimars E, Donti TR, Graham BH, Morava E, Rodenburg RJ, Kozicz T (2020) Impaired mitochondrial complex I function as a candidate driver in the biological stress response and a concomitant stress-induced brain metabolic reprogramming in male mice. Transl Psychiatry 10:176.

Enríquez JA (2016) Supramolecular Organization of Respiratory Complexes. Annu Rev Physiol 78:533-561.

Ernster L, Schatz G (1981) Mitochondria: A Historical Review. J Cell Biol 91:227-255

Erta M, Quintana A, Hidalgo J (2012) Interleukin-6, a major cytokine in the central nervous system. Int J Biol Sci 8:1254-1266.

Escartin C et al. (2021) Reactive astrocyte nomenclature, definitions, and future directions. Nat Neurosci 24:312-325.

Escartin C, Guillemaud O, Carrillo-de Sauvage M-A (2019) Questions and (some) answers on reactive astrocytes. Glia 67:2221-2247.

Escrig A, Canal C, Sanchis P, Fernández-Gayol O, Montilla A, Comes G, Molinero A, Giralt M, Giménez-Llort L, Becker-Pauly C, Rose-John S, Hidalgo J (2019) IL-6 trans-signaling in the brain influences the behavioral and physio-pathological phenotype of the Tg2576 and 3xTgAD mouse models of Alzheimer's disease. Brain Behav Immun 82:145-159.

F

Fassone E, Rahman S (2012) Complex I deficiency: clinical features, biochemistry and molecular genetics. J Med Genet 49:578-590.

Faulkner JR, Herrmann JE, Woo MJ, Tansey KE, Doan NB, Sofroniew M v (2004) Reactive astrocytes protect tissue and preserve function after spinal cord injury. J Neurosci 24:2143–2155.

Fernández-de la Torre M, Fiuza-Luces C, Valenzuela PL, Laine-Menéndez S, Arenas J, Martín MA, Turnbull DM, Lucia A, Morán M (2020) Exercise Training and Neurodegeneration in Mitochondrial Disorders: Insights From the Harlequin Mouse. Front Physiol 11:594223.

Ferrari M, Jain IH, Goldberger O, Rezoagli E, Thoonen R, Cheng K-H, Sosnovik DE, Scherrer-Crosbie M, Mootha VK, Zapol WM (2017) Hypoxia treatment reverses neurodegenerative disease in a mouse model of Leigh syndrome. Proc Natl Acad Sci USA 114:4241-4250.

Fiebig C, Keiner S, Ebert B, Schäffner I, Jagasia R, Lie DC, Beckervordersandforth R (2019) Mitochondrial Dysfunction in Astrocytes Impairs the Generation of Reactive Astrocytes and Enhances Neuronal Cell Death in the Cortex Upon Photothrombotic Lesion. Front Mol Neurosci 12:40.

G

Garner KM, Amin R, Johnson RW, Scarlett EJ, Burton MD (2018) Microglia priming by interleukin-6 signaling is enhanced in aged mice. J Neuroimmunol 324:90-99.

Gerards M, Sallevelt SCEH, Smeets HJM (2016) Leigh syndrome: Resolving the clinical and genetic heterogeneity paves the way for treatment options. Mol Genet Metab 117:300-312.

Giannakopoulou CE, Sotiriou A, Dettoraki M, Yang M, Perlikos XF, Toumpanakis D, Prezerakos G, Koutsourelakis I, Kastis GA, Vassilakopoulou V, Mizi E, Papalois A, Greer JJ, Theodoros Vassilakopoulos X (2019) Regulation of breathing pattern by IL-10. Am J Physiol Regul Integr Comp Physiol 317:190-202.

Ginhoux F, Greter M, Leboeuf M, Nandi S, See P, Gokhan S, Mehler MF, Conway SJ, Ng LG, Stanley ER, Samokhvalov IM, Merad M (2010) Fate mapping analysis reveals that adult microglia derive from primitive macrophages. Science 330:841-845.

Giralt M, Ramos R, Quintana A, Ferrer B, Erta M, Castro-Freire M, Comes G, Sanz E, Unzeta M, Pifarré P, García A, Campbell IL, Hidalgo J (2013) Induction of atypical EAE mediated by transgenic production of IL-6 in astrocytes in the absence of systemic IL-6. Glia 61:587-600.

Goldmann T et al. (2015) USP18 lack in microglia causes destructive interferonopathy of the mouse brain. EMBO J 34:1612-1629.

Goldmann T et al. (2016) Origin, fate and dynamics of macrophages at central nervous system interfaces. Nat Immunol 17:797-805.

Gong T, Liu L, Jiang W, Zhou R (2020) DAMP-sensing receptors in sterile inflammation and inflammatory diseases. Nat Rev Immunol 20:95-112.

Gopinathan G, Milagre C, Pearce OMT, Reynolds LE, Hodivala-Dilke K, Leinster DA, Zhong H, Hollingsworth RE, Thompson R, Whiteford JR, Balkwill F (2015) Interleukin-6 Stimulates Defective Angiogenesis. Cancer Res 75:3098-3107.

Gorman GS, Chinnery PF, DiMauro S, Hirano M, Koga Y, McFarland R, Suomalainen A, Thorburn DR, Zeviani M, Turnbull DM (2016) Mitochondrial diseases. Nat Rev Dis Primers 2:16080.

Gorman GS, Schaefer AM, Ng Y, Gomez N, Blakely EL, Alston CL, Feeney C, Horvath R, Yu-Wai-Man P, Chinnery PF, Taylor RW, Turnbull DM, McFarland R (2015) Prevalence of nuclear and mitochondrial DNA mutations related to adult mitochondrial disease. Ann Neurol 77:753-759.

Grabert K, Sehgal A, Irvine KM, Wollscheid-Lengeling E, Ozdemir DD, Stables J, Luke GA, Ryan MD, Adamson A, Humphreys NE, Sandrock CJ, Rojo R, Verkasalo VA, Mueller W, Hohenstein P, Pettit AR, Pridans C, Hume DA (2020) A Transgenic Line That Reports CSF1R Protein Expression Provides a Definitive Marker for the Mouse Mononuclear Phagocyte System. J Immunol 205:3154-3166.

Grassivaro F, Menon R, Acquaviva M, Ottoboni L, Ruffini F, Bergamaschi A, Muzio L, Farina C, Martino G (2020) Convergence between Microglia and Peripheral Macrophages Phenotype during Development and Neuroinflammation. J Neurosci 40:784795.

Greenbaum D, Colangelo C, Williams K, Gerstein M (2003) Comparing protein abundance and mRNA expression levels on a genomic scale. Genome Biol 4:117.

Green KN, Crapser JD, Hohsfield LA (2020) To Kill a Microglia: A Case for CSF1R Inhibitors. Trends Immunol 41:771-84.

Guttenplan KA, Weigel MK, Prakash P, Wijewardhane PR, Hasel P, Rufen-Blanchette U, Münch AE, Blum JA, Fine J, Neal MC, Bruce KD, Gitler AD, Chopra G, Liddelow SA, Barres BA (2021) Neurotoxic reactive astrocytes induce cell death via saturated lipids. Nature 599:102-107.

Gu Z, Eils R, Schlesner M (2016) Complex heatmaps reveal patterns and correlations in multidimensional genomic data. Bioinformatics 32:2847-2849.

Gyengesi E, Rangel A, Ullah F, Liang H, Niedermayer G, Asgarov R, Venigalla M, Gunawardena D, Karl T, Münch G (2019) Chronic Microglial Activation in the GFAP-IL6 Mouse Contributes to Age-Dependent Cerebellar Volume Loss and Impairment in Motor Function. Front Neurosci 13:303.

H

Habib N, McCabe C, Medina S, Varshavsky M, Kitsberg D, Dvir-Szternfeld R, Green G, Dionne D, Nguyen L, Marshall JL, Chen F, Zhang F, Kaplan T, Regev A, Schwartz M (2020) Disease-associated astrocytes in Alzheimer's disease and aging. Nat Neurosci 23:701-706.

Hackenbrock C (1977) Molecular organization and the fluid nature of the mitochondrial energy transducing membrane. Struct Biol Membr 34:199-234.

Haim L ben, Rowitch DH (2017) Functional diversity of astrocytes in neural circuit regulation. Nat Rev Neurosci 18:31–41.

Hammans SR, Sweeney MG, Brockington M, Morgan-Hughes JA, Harding AE (1991) Mitochondrial encephalopathies: molecular genetic diagnosis from blood samples. Lancet 337:1311-1313.

Hammond TR, Dufort C, Dissing-Olesen L, Giera S, Young A, Wysoker A, Walker AJ, Gergits F, Segel M, Nemesh J, Marsh SE, Saunders A, Macosko E, Ginhoux F, Chen J, Franklin RJM, Piao X, McCarroll SA, Stevens B (2019) Single-Cell RNA Sequencing of Microglia throughout the Mouse Lifespan and in the Injured Brain Reveals Complex Cell-State Changes. Immunity 50:253-271.

Han J, Fan Y, Zhou K, Blomgren K, Harris RA (2021a) Uncovering sex differences of rodent microglia. J Neuroinflammation 18:1-11

Han J, Fan Y, Zhou K, Zhu K, Blomgren K, Lund H, Zhang XM, Harris RA (2020) Underestimated Peripheral Effects Following Pharmacological and Conditional Genetic Microglial Depletion. Int J Biol Sci 21:8603**.**

Han RT, Kim RD, Molofsky A v, Liddelow SA (2021) Astrocyte-immune cell interactions in physiology and pathology. Immunity 54:211-224.

Hanaford A, Johnson SC (2022) The immune system as a driver of mitochondrial disease pathogenesis: a review of evidence. Orphanet J Rare Dis 17:335.

Hara M, Kobayakawa K, Ohkawa Y, Kumamaru H, Yokota K, Saito T, Kijima K, Yoshizaki S, Harimaya K, Nakashima Y, Okada S (2017) Interaction of reactive astrocytes with type I collagen induces astrocytic scar formation through the integrin-N-cadherin pathway after spinal cord injury. Nat Med 23:818-828.

Harland M, Torres S, Liu J, Wang X (2020) Neuronal Mitochondria Modulation of LPS-Induced Neuroinflammation. J Neurosci 40:1756-1765.

Hasel P, Rose IVL, Sadick JS, Kim RD, Liddelow SA (2021) Neuroinflammatory astrocyte subtypes in the mouse brain. Nat Neurosci 24:1475-1487.

Heink S et al. (2017) Trans-presentation of IL-6 by dendritic cells is required for the priming of pathogenic TH17 cells. Nat Immunol 18:74-85.

Heinrich PC, Behrmann I, Haan S, Hermanns HM, Müller-Newen G, Schaper F (2003) Principles of interleukin (IL)-6-type cytokine signalling and its regulation. Biochem J 374:1-20.

Heinrich PC, Castell J v, Andus T (1990) Interleukin-6 and the acute phase response. Biochem J 265:621-636.

Hirano T, Taga T, Nakano N, Yasukawa K, Kashiwamura S, Shimizu K, Nakajima K, Pyun KH, Kishimoto T (1985) Purification to homogeneity and characterization of human B-cell differentiation factor (BCDF or BSFp-2). Proc Natl Acad Sci USA 82:5490-5494.

Hoeffel G, Ginhoux F (2015) Ontogeny of Tissue-Resident Macrophages. Front Immunol 6:486.

Holt IJ, Harding AE, Morgan-Hughes JA (1988) Deletions of muscle mitochondrial DNA in patients with mitochondrial myopathies. Nature 331:717-719.

Hoogland ICM, Houbolt C, van Westerloo DJ, van Gool WA, van de Beek D (2015) Systemic inflammation and microglial activation: systematic review of animal experiments. J Neuroinflammation 12:114.

Hsu M-P, Frausto R, Rose-John S, Campbell IL (2015) Analysis of IL-6/gp130 family receptor expression reveals that in contrast to astroglia, microglia lack the oncostatin M receptor and functional responses to oncostatin M. Glia 63:132-141.

Huang Y, Xu Z, Xiong S, Sun F, Qin G, Hu G, Wang J, Zhao L, Liang Y-X, Wu T, Lu Z, Humayun MS, So K-F, Pan Y, Li N, Yuan T-F, Rao Y, Peng B (2018) Repopulated microglia are solely derived from the proliferation of residual microglia after acute depletion. Nat Neurosci 21:530-540.

Hume DA, Caruso M, Ferrari-Cestari M, Summers KM, Pridans C, Irvine KM (2020) Phenotypic impacts of CSF1R deficiencies in humans and model organisms. J Leukoc Biol 107:205-219.

Humphrey MB, Xing J, Titus A (2015) The TREM2-DAP12 signaling pathway in Nasu-Hakola disease: a molecular genetics perspective. Res Rep Biochem 5:89-100.

Hurst SM, Wilkinson TS, McLoughlin RM, Jones S, Horiuchi S, Yamamoto N, Rose-John S, Fuller GM, Topley N, Jones SA (2001) Il-6 and its soluble receptor orchestrate a temporal switch in the pattern of leukocyte recruitment seen during acute inflammation. Immunity 14:705-714.

Hu Y, Mai W, Chen L, Cao K, Zhang B, Zhang Z, Liu Y, Lou H, Duan S, Gao Z (2020) mTOR-mediated metabolic reprogramming shapes distinct microglia functions in response to lipopolysaccharide and ATP. Glia 68:1031-1045.

I

Ignatenko O, Chilov D, Paetau I, de Miguel E, Jackson CB, Capin G, Paetau A, Terzioglu M, Euro L, Suomalainen A (2018) Loss of mtDNA activates astrocytes and leads to spongiotic encephalopathy. Nat Commun 9:70.

Ignatenko O, Nikkanen J, Kononov A, Zamboni N, Ince-Dunn G, Suomalainen A (2020) Mitochondrial spongiotic brain disease: Astrocytic stress and harmful rapamycin and ketosis effect. Life Sci Alliance 3: e202000797.

Ingraham CA, Burwell LS, Skalska J, Brookes PS, Howell RL, Sheu S-S, Pinkert CA (2009) NDUFS4: creation of a mouse model mimicking a Complex I disorder. Mitochondrion 9:204-10.

Iommarini L, Peralta S, Torraco A, Diaz F (2015) Mitochondrial Diseases Part II: Mouse models of OXPHOS deficiencies caused by defects in regulatory factors and other components required for mitochondrial function. Mitochondrion 22:96-118.

Irazoki A, Gordaliza-Alaguero I, Frank E, Giakoumakis NN, Seco J, Palacín M, Gumà A, Sylow L, Sebastián D, Zorzano A (2023) Disruption of mitochondrial dynamics triggers muscle inflammation through interorganellar contacts and mitochondrial DNA mislocation. Nat Commun 14:108.

Ising C et al. (2015) Inhibition of insulin/IGF-1 receptor signaling protects from mitochondria-mediated kidney failure. EMBO Mol Med 7:275-287.

Itoh N, Itoh Y, Tassoni A, Ren E, Kaito M, Ohno A, Ao Y, Farkhondeh V, Johnsonbaugh H, Burda J, Sofroniew M v, Voskuhl RR (2018) Cell-specific and region-specific transcriptomics in the multiple sclerosis model: Focus on astrocytes. Proc Natl Acad Sci USA 115:302-309.

J

Jain IH, Zazzeron L, Goldberger O, Marutani E, Wojtkiewicz GR, Ast T, Wang H, Schleifer G, Stepanova A, Brepoels K, Schoonjans L, Carmeliet P, Galkin A, Ichinose F, Zapol WM, Mootha VK (2019) Leigh Syndrome Mouse Model Can Be Rescued by Interventions that Normalize Brain Hyperoxia, but Not HIF Activation. Cell Metab 30:824-832

Jain IH, Zazzeron L, Goli R, Alexa K, Schatzman-Bone S, Dhillon H, Goldberger O, Peng J, Shalem O, Sanjana NE, Zhang F, Goessling W, Zapol WM, Mootha VK (2016) Hypoxia as a therapy for mitochondrial disease. Science 352:54-61.

Javadov S, Jang S, Chapa-Dubocq XR, Khuchua Z, Camara AK (2004) Mitochondrial respiratory supercomplexes in mammalian cells: structural versus functional role. J Mol Med 99:57-73.

Jin Z, Wei W, Yang M, Du Y, Wan Y (2014) Mitochondrial complex I activity suppresses inflammation and enhances bone resorption by shifting macrophage-osteoclast polarization. Cell Metab 20:483-498.

Johnson SC, Yanos ME, Kayser EB, Quintana A, Sangesland M, Castanza A, Uhde L, Hui J, Wall VZ, Gagnidze A, Oh K, Wasko BM, Ramos FJ, Palmiter RD, Rabinovitch PS, Morgan PG, Sedensky MM, Kaeberlein M (2013) MTOR inhibition alleviates mitochondrial disease in a mouse model of Leigh syndrome. Science 342:1524-1528.

Jones S, Jenkins B (2018) Recent insights into targeting the IL-6 family of in inflammatory diseases and cancer. Nat Rev Immunol 12:773-789.

Jostock T, Müllberg J, Ozbek S, Atreya R, Blinn G, Voltz N, Fischer M, Neurath MF, Rose-John S (2001) Soluble gp130 is the natural inhibitor of soluble interleukin-6 receptor transsignaling responses. Eur J Biochem 268:160-167.

K

Kahlhöfer F, Gansen M, Zickermann V (2021) Accessory Subunits of the Matrix Arm of Mitochondrial Complex I with a Focus on Subunit NDUFS4 and Its Role in Complex I Function and Assembly. Life 11:455

Kahlhöfer F, Kmita K, Wittig I, Zwicker K, Zickermann V (2017) Accessory subunit NUYM (NDUFS4) is required for stability of the electron input module and activity of mitochondrial complex I. Biochim Biophys Acta 1858:175-181.

Kano S, Choi EY, Dohi E, Agarwal S, Chang DJ, Wilson AM, Lo BD, Rose IVL, Gonzalez S, Imai T, Sawa A (2019) Glutathione S -transferases promote proinflammatory astrocyte-microglia communication during brain inflammation. Sci Signal 12:aar2124.

Karamanlidis G, Lee CF, Garcia-Menendez L, Kolwicz SC, Suthammarak W, Gong G, Sedensky MM, Morgan PG, Wang W, Tian R (2013) Mitochondrial Complex I Deficiency Increases Protein Acetylation and Accelerates Heart Failure. Cell Metab 18:239-250.

Katsouri L, Birch AM, Renziehausen AWJ, Zach C, Aman Y, Steeds H, Bonsu A, Palmer EOC, Mirzaei N, Ries M, Sastre M (2020) Ablation of reactive astrocytes exacerbates disease pathology in a model of Alzheimer's disease. Glia 68:1017-1030.

Keren-Shaul H, Spinrad A, Weiner A, Matcovitch-Natan O, Dvir-Szternfeld R, Ulland TK, David E, Baruch K, Lara-Astaiso D, Toth B, Itzkovitz S, Colonna M, Schwartz M, Amit I (2017) A Unique Microglia Type Associated with Restricting Development of Alzheimer's Disease. Cell 169:1276-1290.

Kerkhofs D, van Hagen BT, Milanova I v., Schell KJ, van Essen H, Wijnands E, Goossens P, Blankesteijn WM, Unger T, Prickaerts J, Biessen EA, van Oostenbrugge RJ, Foulquier S (2020) Pharmacological depletion of microglia and perivascular macrophages prevents vascular Cognitive Impairment in Ang II-induced Hypertension. Theranostics 10:9512-9527.

Kettenmann H, Verkhratsky A (2008) Neuroglia: the 150 years after. Trends Neurosci 31:653-659.

Khan NA, Nikkanen J, Yatsuga S, Jackson C, Wang L, Pradhan S, Kivelä R, Pessia A, Velagapudi V, Suomalainen A (2017) mTORC1 Regulates Mitochondrial Integrated Stress Response and Mitochondrial Myopathy Progression. Cell Metab 26:419-428.

Kierdorf K et al. (2013a) Microglia emerge from erythromyeloid precursors via Pu.1- and Irf8-dependent pathways. Nat Neurosci 16:273-280.

Kierdorf K, Katzmarski N, Haas CA, Prinz M (2013b) Bone Marrow Cell Recruitment to the Brain in the Absence of Irradiation or Parabiosis Bias. PLoS One 8:e58544.

Kigerl KA, de Rivero Vaccari JP, Dietrich WD, Popovich PG, Keane RW (2014) Pattern recognition receptors and central nervous system repair. Exp Neurol 258:5-16.

Kim RY, Hoffman AS, Itoh N, Ao Y, Spence R, Sofroniew M v, Voskuhl RR (2014) Astrocyte CCL2 sustains immune cell infiltration in chronic experimental autoimmune encephalomyelitis. J Neuroimmunol 274:53-61.

Knox EG, Aburto MR, Clarke G, Cryan JF, O'Driscoll CM (2022) The blood-brain barrier in aging and neurodegeneration. Mol Psychiatry 27:2659–2673.

Konishi H et al. (2020) Astrocytic phagocytosis is a compensatory mechanism for microglial dysfunction. EMBO J 39:e104464.

Kraft AW, Hu X, Yoon H, Yan P, Xiao Q, Wang Y, Gil SC, Brown J, Wilhelmsson U, Restivo JL, Cirrito JR, Holtzman DM, Kim J, Pekny M, Lee J-M (2013) Attenuating astrocyte activation accelerates plaque pathogenesis in APP/PS1 mice. FASEB J 27:187-198.

Kruse SE, Watt WC, Marcinek DJ, Kapur RP, Schenkman KA, Palmiter RD (2008) Mice with Mitochondrial Complex I Deficiency Develop a Fatal Encephalomyopathy. Cell Metab 7:312-320.

Kölliker A (1889) Handbuch der gewebelehre des menschen. 6 umgearb. aufl.

Kuse Y, Ohuchi K, Nakamura S, Hara H, Shimazawa M (2018) Microglia increases the proliferation of retinal precursor cells during postnatal development. Mol Vis 24:536–545.

L

Lake NJ, Compton AG, Rahman S, Thorburn DR (2016) Leigh syndrome: One disorder, more than 75 monogenic causes. Ann Neurol 79:190-203.

Lane N, Martin W (2010) The energetics of genome complexity. Nature 467:929-934.

Laplante M, Sabatini DM (2009) mTOR signaling at a glance. J Cell Sci 122:3589-3594.

Lawson LJ, Perry VH, Dri P, Gordon S (1990) Heterogeneity in the distribution and morphology of microglia in the normal adult mouse brain. Neuroscience 39:151-170.

Lee JS, Yoo T, Lee M, Lee Y, Jeon E, Kim SY, Lim BC, Kim KJ, Choi M, Chae J-H (2020) Genetic heterogeneity in Leigh syndrome: Highlighting treatable and novel genetic causes. Clin Genet 97:586-594.

Lei F, Cui N, Zhou C, Chodosh J, Vavvas DG, Paschalis EI (2020) CSF1R inhibition by a small-molecule inhibitor is not microglia specific; affecting hematopoiesis and the function of macrophages. Proc Natl Acad Sci USA 117:23336-23338.

Leigh D (1951) Subacute necrotizing encephalomyelopathy in an infant. J Neurol Neurosurg Psychiat 14:216-211.

Lei Y, Martinez CG, Torres-Odio S, Bell SL, Birdwell CE, Bryant JD, Tong CW, Watson RO, West LC, Phillip West A (2021) Elevated type I interferon responses potentiate metabolic dysfunction, inflammation, and accelerated aging in mtDNA mutator mice. Sci Adv 7:1-16.

Lenz KM, Nelson LH (2018) Microglia and Beyond: Innate Immune Cells As Regulators of Brain Development and Behavioral Function. Front Immunol 9:698.

Leong DW et al. (2012) Proteomic and metabolomic analyses of mitochondrial complex I-deficient mouse model generated by spontaneous B2 short interspersed nuclear element (SINE) insertion into NADH dehydrogenase (ubiquinone) Fe-S protein 4 (Ndufs4) gene. J Biol Chem 287:20652-20663.

Leyh J, Paeschke S, Mages B, Michalski D, Nowicki M, Bechmann I, Winter K (2021) Classification of Microglial Morphological Phenotypes Using Machine Learning. Front Cell Neurosci 15:701673.

Liddelow SA et al. (2017) Neurotoxic reactive astrocytes are induced by activated microglia. Nature 541:481-487.

Liddelow SA, Barres BA (2017) Reactive Astrocytes: Production, Function, and Therapeutic Potential. Immunity 46:957-967.

Liddelow SA, Marsh SE, Stevens B (2020) Microglia and Astrocytes in Disease: Dynamic Duo or Partners in Crime? Trends Immunol 41:820-835.

Linnerbauer M, Wheeler MA, Quintana FJ (2020) Astrocyte Crosstalk in CNS Inflammation. Neuron 108:608-622.

Li Q, Barres BA (2018) Microglia and macrophages in brain homeostasis and disease. Nat Rev Immunol 18:225-242.

Li Q, Cheng Z, Zhou L, Darmanis S, Neff NF, Okamoto J, Gulati G, Bennett ML, Sun LO, Clarke LE, Marschallinger J, Yu G, Quake SR, Wyss-Coray T, Barres BA (2019) Developmental Heterogeneity of Microglia and Brain Myeloid Cells Revealed by Deep Single-Cell RNA Sequencing. Neuron 101:207-223.

Liu L, Zhang K, Sandoval H, Yamamoto S, Jaiswal M, Sanz E, Li Z, Hui J, Graham BH, Quintana A, Bellen HJ (2015) Glial lipid droplets and ROS induced by mitochondrial defects promote neurodegeneration. Cell 160:177-190.

Liu S, Fu S, Wang G, Cao Y, Li L, Li X, Yang J, Li N, Shan Y, Cao Y, Ma Y, Dong M, Liu Q, Jiang H (2021) Glycerol-3-phosphate biosynthesis regenerates cytosolic NAD+ to alleviate mitochondrial disease. Cell Metab 33:1974-1987.

Liu Y, Beyer A, Aebersold R (2016) On the Dependency of Cellular Protein Levels on mRNA Abundance. Cell 165:535-550.

Liu Z, Li Y, Cui Y, Roberts C, Lu M, Wilhelmsson U, Pekny M, Chopp M (2014) Beneficial effects of gfap/vimentin reactive astrocytes for axonal remodeling and motor behavioral recovery in mice after stroke. Glia 62:2022-2033.

Li Z, Peng Y, Hufnagel RB, Hu Y-C, Zhao C, Queme LF, Khuchua Z, Driver AM, Dong F, Lu QR, Lindquist DM, Jankowski MP, Stottmann RW, Kao WWY, Huang T (2017) Loss of SLC25A46 causes neurodegeneration by affecting mitochondrial dynamics and energy production in mice. Hum Mol Genet 26:3776-3791.

Lorea-Hernández JJ, Camacho-Hernández NP, Peña-Ortega F (2020) Interleukin 1-beta but not the interleukin-1 receptor antagonist modulates inspiratory rhythm generation in vitro. Neurosci Lett 734:134934.

Lorea-Hernández JJ, Morales T, Rivera-Angulo AJ, Alcantara-Gonzalez D, Peña-Ortega F (2016) Microglia modulate respiratory rhythm generation and autoresuscitation. Glia 64:603-619.

Love MI, Huber W, Anders S (2014) Moderated estimation of fold change and dispersion for RNA-seq data with DESeq2. Genome Biol 15:550.

Luna-sánchez M, Bianchi P, Quintana A (2021) Mitochondria-induced immune response as a trigger for neurodegeneration: A pathogen from within. Int J Mol Sci 22:8523.

Lütticken C, Wegenka UM, Yuan J, Buschmann J, Schindler C, Ziemiecki A, Harpur AG, Wilks AF, Yasukawa K, Taga T (1994) Association of transcription factor APRF and protein kinase Jak1 with the interleukin-6 signal transducer gp130. Science 263:89-92.

Lyu J, Zhao Y, Zhang N, Xu X, Zheng R, Yu W, Xin W, Yan C, Ji K (2022) Bezafibrate Rescues Mitochondrial Encephalopathy in Mice via Induction of Daily Torpor and Hypometabolic State. Neurotherapeutics 19:994-1006.

M

Martin E, El-Behi M, Fontaine B, Delarasse C (2017) Analysis of Microglia and Monocyte-derived Macrophages from the Central Nervous System by Flow Cytometry. J Vis Exp 124:55781.

Martin-Perez M, Grillo AS, Ito TK, Valente AS, Han J, Entwisle SW, Huang HZ, Kim D, Yajima M, Kaeberlein M, Villén J (2020) PKC downregulation upon rapamycin treatment attenuates mitochondrial disease. Nat Metab 2:1472-1481.

Martins LM, Morrison A, Klupsch K, Fedele V, Moisoi N, Teismann P, Abuin A, Grau E, Geppert M, Livi GP, Creasy CL, Martin A, Hargreaves I, Heales SJ, Okada H, Brandner S, Schulz JB, Mak T, Downward J (2004) Neuroprotective role of the Reaper-related serine protease HtrA2/Omi revealed by targeted deletion in mice. Mol Cell Biol 24:9848-9862.

Masuda T et al. (2022) Specification of CNS macrophage subsets occurs postnatally in defined niches. Nature 604:740-748.

Masuda T, Sankowski R, Staszewski O, Böttcher C, Amann L, Sagar, Scheiwe C, Nessler S, Kunz P, van Loo G, Coenen VA, Reinacher PC, Michel A, Sure U, Gold R, Grün D, Priller J, Stadelmann C, Prinz M (2019) Spatial and temporal heterogeneity of mouse and human microglia at single-cell resolution. Nature 566:388-392.

Masuda T, Sankowski R, Staszewski O, Prinz M (2020) Microglia Heterogeneity in the Single-Cell Era. Cell Rep 30:1271-1281.

Matyash V, Kettenmann H (2010) Heterogeneity in astrocyte morphology and physiology. Brain Res Rev 63:2-10.

McAlpine CS et al. (2021) Astrocytic interleukin-3 programs microglia and limits Alzheimer's disease. Nature 595:701-706.

McAvoy K, Kawamata H (2019) Glial mitochondrial function and dysfunction in health and neurodegeneration. Mol Cell Neurosci 101:103417.

McCulloch C, Searle S (2010) Generalized, linear and mixed models. John Wiley & Sons, New York.

McElroy GS, Reczek CR, Reyfman PA, Mithal DS, Horbinski CM, Chandel NS (2020) NAD+ Regeneration Rescues Lifespan, but Not Ataxia, in a Mouse Model of Brain Mitochondrial Complex I Dysfunction. Cell Metab 32:301-308.

McKelvie P, Infeld B, Marotta R, Chin J, Thorburn D, Collins S (2012) Late-adult onset Leigh syndrome. J Clin Neurosci 19:195-202.

Medzhitov R, Preston-Hurlburt P, Janeway CA (1997) A human homologue of the Drosophila Toll protein signals activation of adaptive immunity. Nature 388:394-397.

Mildner A, Mack M, Schmidt H, Brück W, Djukic M, Zabel MD, Hille A, Priller J, Prinz M (2009) CCR2+Ly-6Chi monocytes are crucial for the effector phase of autoimmunity in the central nervous system. Brain 132:2487-2500.

Mildner A, Schmidt H, Nitsche M, Merkler D, Hanisch U-K, Mack M, Heikenwalder M, Brück W, Priller J, Prinz M (2007) Microglia in the adult brain arise from Ly-6ChiCCR2+ monocytes only under defined host conditions. Nat Neurosci 10:1544-1553.

Miller HC, Louw R, Mereis M, Venter G, Boshoff J-D, Mienie L, van Reenen M, Venter M, Lindeque JZ, Domínguez-Martínez A, Quintana A, van der Westhuizen FH (2020) Metallothionein 1 Overexpression Does Not Protect Against Mitochondrial Disease Pathology in Ndufs4 Knockout Mice. Mol Neurobiol 2020 58:1 58:243-262.

Miller V, Lawrence D, Coccaro G, Mondal T, Andrews K, Dreiem A, Seegal R (2010) Sex effects of Interleukin-6 deficiency on neuroinflammation in aged C57Bl/6 mice. Brain Res 1318:11.

Mimaki M, Wang X, McKenzie M, Thorburn DR, Ryan MT (2012) Understanding mitochondrial complex I assembly in health and disease. Biochim Biophys Acta 1817:851-862.

Mitchell P (1961) Coupling of Phosphorylation to Electron and Hydrogen Transfer by a Chemi-Osmotic type of Mechanism. Nature 191:144-148.

Mittal M, Siddiqui MR, Tran K, Reddy SP, Malik AB (2014) Reactive Oxygen Species in Inflammation and Tissue Injury. Antioxid Redox Signal 20:1126-1167.

Morin C, Mitchell G, Larochelle J, Lambert M, Ogier H, Robinson BH, de Braekeleer M (1993) Clinical, metabolic, and genetic aspects of cytochrome C oxidase deficiency in Saguenay-Lac-Saint-Jean. Am J Hum Genet 53:488-496.

Mottis A, Herzig S, Auwerx J (2019) Mitocellular communication: Shaping health and disease. Science (1979) 366:827-832.

Moya GE, Rivera PD, Dittenhafer-Reed KE (2021) Evidence for the Role of Mitochondrial DNA Release in the Inflammatory Response in Neurological Disorders. Int J Mol Sci 22:7030.

Mühleip A, Flygaard RK, Haapanen O, Baradaran R, Gruhl T, Tobiasson V, Maréchal A, Sharma V, Amunts A (2022) Structural basis of mitochondrial membrane bending by I-II-III2-IV2 supercomplex. bioRxiv 2022.06.26.497646.

Mukherjee S, Ghosh A (2020) Molecular mechanism of mitochondrial respiratory chain assembly and its relation to mitochondrial diseases. Mitochondrion 53:1-20.

Müllberg J, Dittrich E, Graeve L, Gerhartz C, Yasukawa K, Taga T, Kishimoto T, Heinrich PC, Rose-John S (1993) Differential shedding of the two subunits of the interleukin-6 receptor. FEBS Lett 332:174-178.

Murakami M, Kamimura D, Hirano T (2019) Pleiotropy and Specificity: Insights from the Interleukin 6 Family of Cytokines. Immunity 50:812-831.

Murphy MP (2009) How mitochondria produce reactive oxygen species. Biochem J 417:1-13.

Murru S, Hess S, Barth E, Almajan ER, Schatton D, Hermans S, Brodesser S, Langer T, Kloppenburg P, Rugarli EI (2019) Astrocyte-specific deletion of the mitochondrial m-AAA protease reveals glial contribution to neurodegeneration. Glia 67:1526-1541.

N

Nagayama S, Homma R, Imamura F (2014) Neuronal organization of olfactory bulb circuits. Front Neural Circuits 8:98.

Najafi AR, Crapser J, Jiang S, Ng W, Mortazavi A, West BL, Green KN (2018) A limited capacity for microglial repopulation in the adult brain. Glia 66:2385-2396.

Neher JJ, Cunningham C (2019) Priming Microglia for Innate Immune Memory in the Brain. Trends Immunol 40:358-374.

Nemeth CL, Tomlinson SN, Rosen M, O'Brien BM, Larraza O, Jain M, Murray CF, Marx JS, Delannoy M, Fine AS, Wu D, Trifunovic A, Fatemi A (2020) Neuronal ablation of mt-AspRS in mice induces immune pathway activation prior to severe and progressive cortical and behavioral disruption. Exp Neurol 326:113164.

Ng YS, Bindoff LA, Gorman GS, Klopstock T, Kornblum C, Mancuso M, Mcfarland R, Sue CM, Suomalainen A, Taylor RW, Thorburn DR, Turnbull DM (2021) Mitochondrial disease in adults: recent advances and future promise. Lancet Neurol 20:573-584.

Nikkanen J et al. (2016) Mitochondrial DNA Replication Defects Disturb Cellular dNTP Pools and Remodel One-Carbon Metabolism. Cell Metab 23:635-648.

Niyazov DM, Kahler SG, Frye RE (2016) Primary Mitochondrial Disease and Secondary Mitochondrial Dysfunction: Importance of Distinction for Diagnosis and Treatment. Mol Syndromol 7:122-137.

O

Oberheim NA, Goldman SA, Nedergaard M (2012) Heterogeneity of Astrocytic Form and Function. Methods Mol Biol 814:23-45.

Ohno H, Kubo K, Murooka H, Kobayashi Y, Nishitoba T, Shibuya M, Yoneda T, Isoe T (2006) A c-fms tyrosine kinase inhibitor, Ki20227, suppresses osteoclast differentiation and osteolytic bone destruction in a bone metastasis model. Mol Cancer Ther 5:2634-2643.

Okamoto K, Kondo-Okamoto N (2012) Mitochondria and autophagy: Critical interplay between the two homeostats. Biochim Biophys Acta 1820:595-600.

Oosterhof N, Chang IJ, Karimiani EG, Kuil LE, Jensen DM, Daza R, Young E, Astle L, van der Linde HC, Shivaram GM, Demmers J, Latimer CS, Keene CD, Loter E, Maroofian R, van Ham TJ, Hevner RF, Bennett JT (2019) Homozygous Mutations in CSF1R Cause a Pediatric-Onset Leukoencephalopathy and Can Result in Congenital Absence of Microglia. Am J Hum Genet 104:936-947.

Ortigoza-Escobar JD, Oyarzabal A, Montero R, Artuch R, Jou C, Jiménez C, Gort L, Briones P, Muchart J, López-Gallardo E, Emperador S, Pesini ER, Montoya J, Pérez B, Rodríguez-Pombo P, Pérez-Dueñas B (2016) Ndufs4 related Leigh syndrome: A case report and review of the literature. Mitochondrion 28:73-78.

Osborne BF, Turano A, Schwarz JM (2018) Sex Differences in the Neuroimmune System. Curr Opin Behav Sci 23:118.

Ostergaard E, Hansen FJ, Sorensen N, Duno M, Vissing J, Larsen PL, Faeroe O, Thorgrimsson S, Wibrand F, Christensen E, Schwartz M (2007) Mitochondrial encephalomyopathy with elevated methylmalonic acid is caused by SUCLA2 mutations. Brain 130:853-861.

Ozaki K, Leonard WJ (2002) Cytokine and cytokine receptor pleiotropy and redundancy. J Biol Chem 277:29355-29358.

P

Paolicelli RC et al. (2022) Microglia states and nomenclature: A field at its crossroads. Neuron 110:3458-3483.

Paxinos G, Franklin KBJ (2013) Paxinos and Franklin's The mouse brain in stereotaxic coordinates. Academic Press.

Penkowa M, Carrasco J, Giralt M, Moos T, Hidalgo J (1999) CNS Wound Healing Is Severely Depressed in Metallothionein I- and II-Deficient Mice. J Neurosci 19:2535-2545.

Peña-Ortega F (2019) Clinical and experimental aspects of breathing modulation by inflammation. Autonomic Neuroscience 216:72-86.

Peralta S, Pinto M, Arguello T, Garcia S, Diaz F, Moraes CT (2020) Metformin delays neurological symptom onset in a mouse model of neuronal complex I deficiency. JCI Insight 5:e141183.

Peralta S, Torraco A, Wenz T, Garcia S, Diaz F, Moraes CT (2014) Partial complex I deficiency due to the CNS conditional ablation of Ndufa5 results in a mild chronic encephalopathy but no increase in oxidative damage. Hum Mol Genet 23:1399-1412.

Perry EA, Bennett CF, Luo C, Balsa E, Jedrychowski M, O'Malley KE, Latorre-Muro P, Ladley RP, Reda K, Wright PM, Gygi SP, Myers AG, Puigserver P (2021) Tetracyclines promote survival and fitness in mitochondrial disease models. Nat Metab 3:33-42.

Perry VH, Holmes C (2014) Microglial priming in neurodegenerative disease. Nat Rev Neurol 10:217-224.

Plemel JR et al. (2020) Microglia response following acute demyelination is heterogeneous and limits infiltrating macrophage dispersion. Sci Adv 6:eaay6324.

Pocock JM, Kettenmann H (2007) Neurotransmitter receptors on microglia. Trends Neurosci 30:527-535.

Powell JD, Pollizzi KN, Heikamp EB, Horton MR (2012) Regulation of Immune Responses by mTOR. Annu Rev Immunol 30:39-68.

Prada-Dacasa P, Urpi A, Sánchez-Benito L, Bianchi P, Quintana A (2020) Measuring Breathing Patterns in Mice Using Whole-body Plethysmography. Bio Protoc 10:3741.

Prinz M, Masuda T, Wheeler MA, Quintana FJ (2021) Microglia and Central Nervous System-Associated Macrophages-From Origin to Disease Modulation. Annu Rev Immunol 39:251-277.

Prinz M, Priller J (2017) The role of peripheral immune cells in the CNS in steady state and disease. Nat Neurosci 20:136-144.

Q

Quintana A, Kruse SE, Kapur RP, Sanz E, Palmiter RD (2010) Complex I deficiency due to loss of Ndufs4 in the brain results in progressive encephalopathy resembling Leigh syndrome. Proceedings of the National Academy of Sciences 107:10996-11001.

Quintana A, Morgan PG, Kruse SE, Palmiter RD, Sedensky MM (2012a) Altered Anesthetic Sensitivity of Mice Lacking Ndufs4, a Subunit of Mitochondrial Complex I. PLoS One 7:e42904.

Quintana A, Müller M, Frausto RF, Ramos R, Getts DR, Sanz E, Hofer MJ, Krauthausen M, King NJC, Hidalgo J, Campbell IL (2009) Site-specific production of IL-6 in the central nervous system retargets and enhances the inflammatory response in experimental autoimmune encephalomyelitis. J Immunol 183:2079-2088.

Quintana A, Zanella S, Koch H, Kruse SE, Lee D, Ramirez JM, Palmiter RD (2012b) Fatal breathing dysfunction in a mouse model of Leigh syndrome. J Clin Invest 122:2359-2368.

Quirós PM, Mottis A, Auwerx J (2016) Mitonuclear communication in homeostasis and stress. Nat Rev Mol Cell Biol 17:213-226.

R

Rademakers R et al. (2011) Mutations in the colony stimulating factor 1 receptor (CSF1R) gene cause hereditary diffuse leukoencephalopathy with spheroids. Nat Genet 44:200-205.

Rahman S, Blok RB, Dahl HH, Danks DM, Kirby DM, Chow CW, Christodoulou J, Thorburn DR (1996) Leigh syndrome: clinical features and biochemical and DNA abnormalities. Ann Neurol 39:343-351.

Ramadasan-Nair R, Hui J, Itsara LS, Morgan PG, Sedensky MM (2019) Mitochondrial Function in Astrocytes Is Essential for Normal Emergence from Anesthesia in Mice. Anesthesiology 130:423-434.

Ransohoff RM (2016) A polarizing question: do M1 and M2 microglia exist? Nat Neurosci 19:987-991.

Ransohoff RM, Perry VH (2009) Microglial physiology: unique stimuli, specialized responses. Annu Rev Immunol 27:119-145.

Rathinam VAK, Jiang Z, Waggoner SN, Sharma S, Cole LE, Waggoner L, Vanaja SK, Monks BG, Ganesan S, Latz E, Hornung V, Vogel SN, Szomolanyi-Tsuda E, Fitzgerald KA (2010) The AIM2 inflammasome is essential for host defense against cytosolic bacteria and DNA viruses. Nat Immunol 11:395-402.

Recasens M, Almolda B, Pérez-Clausell J, Campbell IL, González B, Castellano B (2021) Chronic exposure to IL-6 induces a desensitized phenotype of the microglia. J Neuroinflammation 18:31.

Restelli LM, Oettinghaus B, Halliday M, Agca C, Licci M, Sironi L, Savoia C, Hench J, Tolnay M, Neutzner A, Schmidt A, Eckert A, Mallucci G, Scorrano L, Frank S (2018) Neuronal Mitochondrial Dysfunction Activates the Integrated Stress Response to Induce Fibroblast Growth Factor 21. Cell Rep 24:1407-1414.

Reddy DS, Thompson W, Calderara G (2021) Molecular mechanisms of sex differences in epilepsy and seizure susceptibility in chemical, genetic and acquired epileptogenesis. Neurosci Lett 750:135753.

Reynaud-Dulaurier R, Benegiamo G, Marrocco E, Al-Tannir R, Surace EM, Auwerx J, Decressac M (2020) Gene replacement therapy provides benefit in an adult mouse model of Leigh syndrome. Brain 143:1686-1696.

Rich P (2003) Chemiosmotic coupling: The cost of living. Nature 421:583-583.

Rio-Hortega P (1919a) El "tercer elemento" de los centros nerviosos. I. La microglía en estado normal. Bol Soc Esp Biol VIII:67-82.

Rio-Hortega P (1919b) El "tercer elemento" de los centros nerviosos. II. Intervención de la microglía en los procesos patológicos (células en bastoncito y cuerpos granuloadiposos). Bol Soc Esp Biol VIII:91-103.

Rio-Hortega P (1919c) El "tercer elemento" de los centros nerviosos. III. Naturaleza probable de la microglía. Bol Soc Esp Biol VIII:108-115.

Rio-Hortega P (1919d) El "tercer elemento" de los centros nerviosos. IV. Poder fagocitario y movilidad de la microglía. Bol Soc Esp Biol VIII:154-166.

Ritzel RM, Patel AR, Grenier JM, Crapser J, Verma R, Jellison ER, McCullough LD (2015) Functional differences between microglia and monocytes after ischemic stroke. J Neuroinflammation 12:106.

Rodríguez-Nuevo A et al. (2018) Mitochondrial DNA and TLR9 drive muscle inflammation upon Opa1 deficiency. EMBO J 37:e96553.

Roger AJ, Muñoz-Gómez SA, Kamikawa R (2017) The Origin and Diversification of Mitochondria. Curr Biol 27:1177-1192.

Rojo AI, McBean G, Cindric M, Egea J, López MG, Rada P, Zarkovic N, Cuadrado A (2014) Redox Control of Microglial Function: Molecular Mechanisms and Functional Significance. Antioxid Redox Signal 21:1766-1801.

Rose J, Brian C, Woods J, Pappa A, Panayiotidis MI, Powers R, Franco R (2017) Mitochondrial dysfunction in glial cells: Implications for neuronal homeostasis and survival. Toxicology 391:109-115.

Rose-John S (2012) IL-6 Trans-Signaling via the Soluble IL-6 Receptor: Importance for the Pro-Inflammatory Activities of IL-6. Int J Biol Sci 8:1237–1247.

Rothhammer V et al. (2018) Microglial control of astrocytes in response to microbial metabolites. Nature 557:724-728.

Rothaug M, Becker-Pauly C, Rose-John S (2016) The role of interleukin-6 signaling in nervous tissue. Biochim et Biophys Acta 1863:1218-1227.

Rowitch DH, Kriegstein AR (2010) Developmental genetics of vertebrate glial-cell specification. Nature 468:214-222.

Rumyantseva A, Popovic M, Trifunovic A (2022) CLPP deficiency ameliorates neurodegeneration caused by impaired mitochondrial protein synthesis. Brain 145:92-104.

Russell OM, Gorman GS, Lightowlers RN, Turnbull DM (2020) Mitochondrial Diseases: Hope for the Future. Cell 181:168-188.

S

Sadick JS, O'Dea MR, Hasel P, Dykstra T, Faustin A, Liddelow SA (2022) Astrocytes and oligodendrocytes undergo subtype-specific transcriptional changes in Alzheimer's disease. Neuron 110:1788-1805.

Safaiyan S, Besson-Girard S, Kaya T, Cantuti-Castelvetri L, Liu L, Ji H, Schifferer M, Gouna G, Usifo F, Kannaiyan N, Fitzner D, Xiang X, Rossner MJ, Brendel M, Gokce O, Simons M (2021) White matter aging drives microglial diversity. Neuron 109:1100-1117.

Sagan L (1967) On the Origin of Mitosing Cells. J Theor Biol 14:255-274.

Samoilova EB, Horton JL, Hilliard B, Liu TS, Chen Y (1998) IL-6-deficient mice are resistant to experimental autoimmune encephalomyelitis: roles of IL-6 in the activation and differentiation of autoreactive T cells. J Immunol 161:6480-6486.

Sanchis P, Fernández-Gayol O, Comes G, Aguilar K, Escrig A, Giralt M, Palmiter RD, Hidalgo J (2020a) A new mouse model to study restoration of interleukin-6 (IL-6) expression in a Cre-dependent manner: microglial IL-6 regulation of experimental autoimmune encephalomyelitis. J Neuroinflammation 17:1-17.

Sanchis P, Fernández-Gayol O, Comes G, Escrig A, Giralt M, Palmiter RD, Hidalgo J (2020b) Interleukin-6 Derived from the Central Nervous System May Influence the Pathogenesis of Experimental Autoimmune Encephalomyelitis in a Cell-Dependent Manner. Cells 9:330.

Sanchis P, Fernández-Gayol O, Vizueta J, Comes G, Canal C, Escrig A, Molinero A, Giralt M, Hidalgo J (2020c) Microglial cell-derived interleukin-6 influences behavior and inflammatory response in the brain following traumatic brain injury. Glia 68:999-1016.

Sano F, Shigetomi E, Shinozaki Y, Tsuzukiyama H, Saito K, Mikoshiba K, Horiuchi H, Cheung DL, Nabekura J, Sugita K, Aihara M, Koizumi S (2021) Reactive astrocyte-driven epileptogenesis is induced by microglia initially activated following status epilepticus. JCI Insight 6:e135391.

Schägger H, Pfeiffer K (2000) Supercomplexes in the respiratory chains of yeast and mammalian mitochondria. EMBO J 19:1777-1783.

Schetters STT, Gomez-Nicola D, Garcia-Vallejo JJ, van Kooyk Y (2018) Neuroinflammation: Microglia and T Cells Get Ready to Tango. Front Immunol 8:1905.

Schieber M, Chandel NS (2014) ROS Function in Redox Signaling and Oxidative Stress. Curr Biol 24:453-462.

Schieke SM, Phillips D, McCoy JP, Aponte AM, Shen R-F, Balaban RS, Finkel T (2006) The mammalian target of rapamycin (mTOR) pathway regulates mitochondrial oxygen consumption and oxidative capacity. J Biol Chem 281:27643-27652.

Schirris TJJ, Rossell S, de Haas R, Frambach SJCM, Hoogstraten CA, Renkema GH, Beyrath JD, Willems PHGM, Huynen MA, Smeitink JAM, Russel FGM, Notebaart RA (2021) Stimulation of cholesterol biosynthesis in mitochondrial complex I-deficiency lowers reductive stress and improves motor function and survival in mice. Biochim Biophys Acta 1867:166062.

Schubert MB, Vilarinho L (2020) Molecular basis of Leigh syndrome: A current look. Orphanet J Rare Dis 15:31.

Schumacher N, Meyer D, Mauermann A, von der Heyde J, Wolf J, Schwarz J, Knittler K, Murphy G, Michalek M, Garbers C, Bartsch JW, Guo S, Schacher B, Eickholz P, Chalaris A, Rose-John S, Rabe B (2015) Shedding of Endogenous Interleukin-6 Receptor (IL-6R) Is Governed by A Disintegrin and Metalloproteinase (ADAM) Proteases while a Full-length IL-6R Isoform Localizes to Circulating Microvesicles. J Biol Chem 290:26059-26071.

Schwabenland M, Mossad O, Peres AG, Kessler F, Maron FJM, Harsan L-A, Bienert T, von Elverfeldt D, Knobeloch K-P, Staszewski O, Heppner FL, Meuwissen MEC, Mancini GMS, Prinz M, Blank T (2019) Loss of USP18 in microglia induces white matter pathology. Acta Neuropathol Commun 7:106.

Shemer A, Grozovski J, Tay TL, Tao J, Volaski A, Süß P, Ardura-Fabregat A, Gross-Vered M, Kim J-S, David E, Chappell-Maor L, Thielecke L, Glass CK, Cornils K, Prinz M, Jung S (2018) Engrafted parenchymal brain macrophages differ from microglia in transcriptome, chromatin landscape and response to challenge. Nat Commun 9:5206.

Shil SK, Kagawa Y, Umaru BA, Nanto-Hara F, Miyazaki H, Yamamoto Y, Kobayashi S, Suzuki C, Abe T, Owada Y (2021) Ndufs4 ablation decreases synaptophysin expression in hippocampus. Sci Rep 11:1-10.

Sierra A, Paolicelli RC, Kettenmann H (2019) Cien Años de Microglía: Milestones in a Century of Microglial Research. Trends Neurosci 42:778-792.

Sims R et al. (2017) Rare coding variants in PLCG2, ABI3, and TREM2 implicate microglial-mediated innate immunity in Alzheimer's disease. Nat Genet 49:1373-1384.

Smoly JM, Kuylenstierna B, Ernster L (1970) Topological and Functional Organization of the Mitochondrion. Proc Natl Acad Sci USA 66:125-131.

Sofou K, de Coo IFM, Isohanni P, Ostergaard E, Naess K, de Meirleir L, Tzoulis C, Uusimaa J, de Angst IB, Lönnqvist T, Pihko H, Mankinen K, Bindoff LA, Tulinius M, Darin N (2014) A multicenter study on Leigh syndrome: Disease course and predictors of survival. Orphanet J Rare Dis 9:52.

Sofroniew M v (2020) Astrocyte Reactivity: Subtypes, States, and Functions in CNS Innate Immunity. Trends Immunol 41:758-770.

Sofroniew M v, Vinters H v (2010) Astrocytes: biology and pathology. Acta Neuropathol 119:7-35.

Sörensen L, Ekstrand M, Silva JoséP, Lindqvist E, Xu B, Rustin P, Olson L, Larsson N-G (2001) Late-Onset Corticohippocampal Neurodepletion Attributable to Catastrophic Failure of Oxidative Phosphorylation in MILON Mice. J Neurosci 21:8082-8090.

Sousa C, Golebiewska A, Poovathingal SK, Kaoma T, Pires-Afonso Y, Martina S, Coowar D, Azuaje F, Skupin A, Balling R, Biber K, Niclou SP, Michelucci A (2018) Single-cell transcriptomics reveals distinct inflammation-induced microglia signatures. EMBO Rep 19:e46171.

Spangenberg E et al. (2019) Sustained microglial depletion with CSF1R inhibitor impairs parenchymal plaque development in an Alzheimer's disease model. Nat Commun 10:3758.

Spinazzi M, Radaelli E, Horré K, Arranz AM, Gounko N v, Agostinis P, Maia TM, Impens F, Morais VA, Lopez-Lluch G, Serneels L, Navas P, de Strooper B (2019) PARL deficiency in mouse causes Complex III defects, coenzyme Q depletion, and Leigh-like syndrome. Proc Natl Acad Sci USA 116:277-286.

Spiteri AG, Ni D, Ling ZL, Macia L, Campbell IL, Hofer MJ, King NJC (2022) PLX5622 Reduces Disease Severity in Lethal CNS Infection by Off-Target Inhibition of Peripheral Inflammatory Monocyte Production. Front Immunol 13:851556.

Spooren A, Kolmus K, Laureys G, Clinckers R, de Keyser J, Haegeman G, Gerlo S (2011) Interleukin-6, a mental cytokine. Brain Res Rev 67:157-183.

Stahl N, Boulton TG, Farruggella T, Ip NY, Davis S, Witthuhn BA, Quelle FW, Silvennoinen O, Barbieri G, Pellegrini S (1994) Association and activation of Jak-Tyk kinases by CNTF-LIF-OSM-IL-6 beta receptor components. Science 263:92-95.

Stahl N, Farruggella TJ, Boulton TG, Zhong Z, Darnell JE, Yancopoulos GD (1995) Choice of STATs and other substrates specified by modular tyrosine-based motifs in cytokine receptors. Science 267:1349-1353.

Stavropoulos F, Sargiannidou I, Potamiti L, Kagiava A, Panayiotidis MI, Bae JH, Yeom SC, Lee JY, Kleopa KA (2021) Aberrant Mitochondrial Dynamics and Exacerbated Response to Neuroinflammation in a Novel Mouse Model of CMT2A. Int J Mol Sci 22:11569.

Stein B, Yang MX (1995) Repression of the interleukin-6 promoter by estrogen receptor is mediated by NF-kappa B and C/EBP beta. Mol Cell Biol 15:4971-4979.

Stepanova A, Konrad C, Manfredi G, Springett R, Ten V, Galkin A (2019) The dependence of brain mitochondria reactive oxygen species production on oxygen level is linear, except when inhibited by antimycin A. J Neurochem 148:731-745.

Stogsdill JA, Ramirez J, Liu D, Kim YH, Baldwin KT, Enustun E, Ejikeme T, Ji R-R, Eroglu C (2017) Astrocytic neuroligins control astrocyte morphogenesis and synaptogenesis. Nature 551:192-197.

Stokes JC, Bornstein RL, James K, Park KY, Spencer KA, Vo K, Snell JC, Johnson BM, Morgan PG, Sedensky MM, Baertsch NA, Johnson SC (2022) Leukocytes mediate disease pathogenesis in the Ndufs4(KO) mouse model of Leigh syndrome. JCI Insight 7:e156522.

Sun N, Youle RJ, Finkel T (2016) The Mitochondrial Basis of Aging. Mol Cell 61:654-666.

Suomalainen A, Battersby BJ (2018) Mitochondrial diseases: The contribution of organelle stress responses to pathology. Nat Rev Mol Cell Biol 19:77-92.

Supplie LM, Düking T, Campbell G, Diaz F, Moraes CT, Götz M, Hamprecht B, Boretius S, Mahad D, Nave K-A (2017) Respiration-Deficient Astrocytes Survive As Glycolytic Cells In Vivo. J Neurosci 37:4231-4242.

Szabo A, Bene K, Gogolák P, Réthi B, Lányi Á, Jankovich I, Dezső B, Rajnavölgyi É (2012) RLR-mediated production of interferon-β by a human dendritic cell subset and its role in virus-specific immunity. J Leukoc Biol 92:159-169.

T

Taanman J-W (1999) The mitochondrial genome: structure, transcription, translation and replication. Biochim Biophys Acta 1410:103-123.

Takahashi K, Rochford CDP, Neumann H (2005) Clearance of apoptotic neurons without inflammation by microglial triggering receptor expressed on myeloid cells-2. J Exp Med 201:647-657.

Takeuchi O, Akira S (2010) Pattern Recognition Receptors and Inflammation. Cell 140:805-820.

Tamura K, Fujimura T, Iwasaki K, Sakuma S, Fujitsu T, Nakamura K, Shimomura K, Kuno T, Tanaka C, Kobayashi M (1994) Interaction of tacrolimus(FK506) and its metabolites with FKBP and calcineurin. Biochem Biophys Res Commun 202:437-443.

Terburgh K, Coetzer J, Lindeque JZ, van der Westhuizen FH, Louw R (2021a) Aberrant BCAA and glutamate metabolism linked to regional neurodegeneration in a mouse model of Leigh syndrome. Biochim Biophys Acta 1867:166082.

Terburgh K, Lindeque JZ, van der Westhuizen FH, Louw R (2021b) Cross-comparison of systemic and tissue-specific metabolomes in a mouse model of Leigh syndrome. Metabolomics 17:101.

Torraco A, Peralta S, Iommarini L, Diaz F (2015) Mitochondrial Diseases Part I: mouse models of OXPHOS deficiencies caused by defects in respiratory complex subunits or assembly factors. Mitochondrion 21:76-91.

Trifunovic A, Wredenberg A, Falkenberg M, Spelbrink JN, Rovio AT, Bruder CE, Bohlooly-Y M, Gidlöf S, Oldfors A, Wibom R, Törnell J, Jacobs HT, Larsson N-G (2004) Premature ageing in mice expressing defective mitochondrial DNA polymerase. Nature 429:417-423.

Tushinski RJ, Oliver IT, Guilbert LJ, Tynan PW, Warner JR, Stanley ER (1982) Survival of mononuclear phagocytes depends on a lineage-specific growth factor that the differentiated cells selectively destroy. Cell 28:71-81.

Tushinski RJ, Stanley ER (1983) The regulation of macrophage protein turnover by a colony stimulating factor (CSF-1). J Cell Physiol 116:67-75.

U

Ulland TK, Colonna M (2018) TREM2 - a key player in microglial biology and Alzheimer disease. Nat Rev Neurol 14:667-675.

V

Vainchtein ID, Chin G, Cho FS, Kelley KW, Miller JG, Chien EC, Liddelow SA, Nguyen PT, Nakao-Inoue H, Dorman LC, Akil O, Joshita S, Barres BA, Paz JT, Molofsky AB, Molofsky A v. (2018) Astrocyte-derived interleukin-33 promotes microglial synapse engulfment and neural circuit development. Science 359:1269-1273.

Vainchtein ID, Molofsky A v. (2020) Astrocytes and Microglia: In Sickness and in Health. Trends Neurosci 43:144-154.

van de Wal MAE, Adjobo-Hermans MJW, Keijer J, Schirris TJJ, Homberg JR, Wieckowski MR, Grefte S, van Schothorst EM, van Karnebeek C, Quintana A, Koopman WJH (2022) Ndufs4 knockout mouse models of Leigh syndrome: pathophysiology and intervention. Brain 145:45-63.

Vankriekelsvenne E, Chrzanowski U, Manzhula K, Greiner T, Wree A, Hawlitschka A, Llovera G, Zhan J, Joost S, Schmitz C, Ponsaerts P, Amor S, Nutma E, Kipp M, Kaddatz H (2022) Transmembrane protein 119 is neither a specific nor a reliable marker for microglia. Glia 70:1170-1190.

Varvel NH, Neher JJ, Bosch A, Wang W, Ransohoff RM, Miller RJ, Dingledine R (2016) Infiltrating monocytes promote brain inflammation and exacerbate neuronal damage after status epilepticus. Proc Natl Acad Sci USA 113:5665-5674.

Vercellino I, Sazanov LA (2021) The assembly, regulation and function of the mitochondrial respiratory chain. Nat Rev Mol Cell Biol 23:141-161.

Vezzani A, French J, Bartfai T, Baram TZ (2011) The role of inflammation in epilepsy. Nat Rev Neurol 7:31-40.

Villapol S, Loane DJ, Burns MP (2017) Sexual dimorphism in the inflammatory response to traumatic brain injury. Glia 65:1423-1438.

Vizuete AFK, Fróes F, Seady M, Zanotto C, Bobermin LD, Roginski AC, Wajner M, Quincozes-Santos A, Gonçalves CA (2022) Early effects of LPS-induced neuroinflammation on the rat hippocampal glycolytic pathway. J Neuroinflammation 19:255.

W

Wallace DC, Singh G, Lott MT, Hodge JA, Schurr TG, Lezza AM, Elsas LJ, Nikoskelainen EK (1988) Mitochondrial DNA mutation associated with Leber's hereditary optic neuropathy. Science 242:1427-1430.

Wang M, Huang Y-P, Wu H, Song K, Wan C, Chi A-N, Xiao Y-M, Zhao X-Y (2017) Mitochondrial complex I deficiency leads to the retardation of early embryonic development in Ndufs4 knockout mice. PeerJ 5:e3339.

Wang X, Haroon F, Karray S, Martina Deckert, Schlüter D (2013) Astrocytic Fas ligand expression is required to induce T-cell apoptosis and recovery from experimental autoimmune encephalomyelitis. Eur J Immunol 43:115-124.

Wang Y, Cella M, Mallinson K, Ulrich JD, Young KL, Robinette ML, Gilfillan S, Krishnan GM, Sudhakar S, Zinselmeyer BH, Holtzman DM, Cirrito JR, Colonna M (2015) TREM2 lipid sensing sustains the microglial response in an Alzheimer's disease model. Cell 160:1061-1071.

West AP, Khoury-Hanold W, Staron M, Tal MC, Pineda CM, Lang SM, Bestwick M, Duguay BA, Raimundo N, MacDuff DA, Kaech SM, Smiley JR, Means RE, Iwasaki A, Shadel GS (2015) Mitochondrial DNA stress primes the antiviral innate immune response. Nature 520:553-557.

West AP, Shadel GS (2017) Mitochondrial DNA in innate immune responses and inflammatory pathology. Nat Rev Immunol 17:363-375.

West PK, McCorkindale AN, Guennewig B, Ashhurst TM, Viengkhou B, Hayashida E, Jung SR, Butovsky O, Campbell IL, Hofer MJ (2022a) The cytokines interleukin-6 and interferon-α induce distinct microglia phenotypes. J Neuroinflammation 19:96.

West PK, Viengkhou B, Campbell IL, Hofer MJ (2022b) Microglia shield the murine brain from damage mediated by the cytokines IL-6 and IFN-α. Front Immunol 13:1036799.

Wheeler MA et al. (2020) MAFG-driven astrocytes promote CNS inflammation. Nature 578:593-599.

White SL, Collins VR, Wolfe R, Cleary MA, Shanske S, DiMauro S, Dahl HH, Thorburn DR (1999) Genetic counseling and prenatal diagnosis for the mitochondrial DNA mutations at nucleotide 8993. Am J Hum Genet 65:474-482.

Wilhelmsson U, Bushong EA, Price DL, Smarr BL, Phung V, Terada M, Ellisman MH, Pekny M (2006) Redefining the concept of reactive astrocytes as cells that remain within their unique domains upon reaction to injury. Proc Natl Acad Sci USA 103:17513–17518.

Y

Yagi M, Uchiumi T, Sagata N, Setoyama D, Amamoto R, Matsushima Y, Kang D (2017) Neural-specific deletion of mitochondrial p32/C1qbp leads to leukoencephalopathy due to undifferentiated oligodendrocyte and axon degeneration. Sci Rep 7:15131.

Yamasaki K, Taga T, Hirata Y, Yawata H, Kawanishi Y, Seed B, Taniguchi T, Hirano T, Kishimoto T (1988) Cloning and expression of the human interleukin-6 (BSF-2/IFN beta 2) receptor. Science 241:825-828.

Yamasaki S, Ishikawa E, Sakuma M, Hara H, Ogata K, Saito T (2008) Mincle is an ITAM-coupled activating receptor that senses damaged cells. Nat Immunol 9:1179-1188.

Yang Y, Wang H, Kouadir M, Song H, Shi F (2019) Recent advances in the mechanisms of NLRP3 inflammasome activation and its inhibitors. Cell Death Dis 10:1-11.

Ylikallio E, Suomalainen A (2012) Mechanisms of mitochondrial diseases. Ann Med 44:41-59.

Young LJ, Muns S, Wang Z, Insel TR (1997) Changes in Oxytocin Receptor mRNA in Rat Brain During Pregnancy and the Effects of Estrogen and Interleukin-6. J Neuroendocrinol 9:859–865

Yu AK, Song L, Murray KD, van der List D, Sun C, Shen Y, Xia Z, Cortopassi GA (2015) Mitochondrial complex I deficiency leads to inflammation and retinal ganglion cell death in the Ndufs4 mouse. Hum Mol Genet 24:2848.

Z

Zhang H, Gong G, Wang P, Zhang Z, Kolwicz SC, Rabinovitch PS, Tian R, Wang W (2018) Heart specific knockout of Ndufs4 ameliorates ischemia reperfusion injury. J Mol Cell Cardiol 123:38-45.

Zhong F, Liang S, Zhong Z (2019) Emerging Role of Mitochondrial DNA as a Major Driver of Inflammation and Disease Progression. Trends Immunol 40:1120-1133.

Zhou Y, Zhou B, Pache L, Chang M, Khodabakhshi AH, Tanaseichuk O, Benner C, Chanda SK (2019) Metascape provides a biologist-oriented resource for the analysis of systems-level datasets. Nat Commun 10:1523.

Zimin PI, Woods CB, Quintana A, Ramirez J-M, Morgan PG, Sedensky MM (2016) Glutamatergic Neurotransmission Links Sensitivity to Volatile Anesthetics with Mitochondrial Function. Curr Biol 26:2194-2201.

8

Supplementary information

Supplementary table 1.

Genes associated with the first ten significantly enriched terms of the GO analysis for both upregulated and downregulated genes in the VN and the hippocampus for the different pairwise comparisons. In orange for upregulated genes and blue for downregulated genes.

Vestibular nuclei	
***Ndufs4 KO*-Veh vs. Ctrl-Veh**	
GO term	**Genes**
Positive regulation of phagocytosis	*Ada, Angpt1, Ankrd13a, Anxa3, Arpc1b, C1qc, Cd68, Cd84, Clec7a, Ctsl, Ctss,Cyba, Fas, Fcgr1, Fcgr2b, Fcgr3, Fn1, Gata2, H2-D1, Icam1, Ifi204, Jak2, Laptm5, Lgals3, Msn, Plekha1, Pros1, Ptprc, Pycard, Ramp2, Rhoj, Tfrc, Thbs3, Trem2, Tsc1, Tyrobp.*
Negative regulation of immune system process	*Ace2, Ada, Adgrf5, Ambra1, Angpt1, C1qc, Ccl25, Cd68, Cd84, Cdkn1a, Cst7, Ctsl, Eng, Fas, Fcgr2b, Gata2, Ifi204, Ifit3, Itga1, Jak2, Laptm5, Lgals3, Nf1, Ptprc, Trem2, Tsc1, Tyrobp, Zfas1.*
Regulation of MAPK cascade	*Ace2, Adipor2, Angpt1, Ccl17, Ccl25, Ccl6, Ccn2, Cd84, Cdk5rap3, Cxcl10, Edn1, Eng, Fas, Fcgr1, Fcgr2b, Fcgr3, Fn1, Gipr, Icam1, Id1, Ifi204, Itga1, Jak2, Laptm5, Lgals3, Msn, Nf1, Plce1, Ptprc, Pycard, Ramp2, Sema3c, Tnip2, Trem2, Tsc1, Vim.*
Regulation of leukocyte activation	*Ada, Adgrf5, Ambra1, Angpt1, Ccl25, Ccn2, Cd84, Cdkn1a, Clec7a, Cst7, Ctla2a, Fas, Fcgr2b, Fn1, Gata2, Icam1, Jak2, Laptm5, Lgals3, Ptprc, Pycard, Tfrc, Tnip2, Trem2, Tsc1, Tyrobp.*
Cell activation	*Ada, Anxa3, Cd84, Ctsl, Fas, Fcgr3, Fn1, Icam1, Cxcl10, Jak2, Msn, Plat, Ptprc, Timp1, Tyrobp, Vwf, Tsc1, Pycard, Trem2, Itgad.*
Inflammatory response	*Ada, Ambra1, Angpt1, Anxa3, Arpc1b, C1qc, Ccl17, Ccl25, Ccl6,Cd68, Cd84, Clec7a, Col5a3, Cst7, Ctla2a, Ctss, Cxcl10, Cyba, Edn1, Fas, Fcgr1, Fcgr2b, Fcgr3, Fn1, Gata2, Icam1, Ifi204, Jak2, Laptm5, Lcn2, Ly86, Msn, Plat, Ptprc, Pycard, Tfrc, Timp1, Tnip2, Trem2, Tsc1, Tyrobp.*
Blood vessel morphogenesis	*Adgrf5, Adipor2,Angpt1, Ccn2, Cdkn1a, Edn1, Eng, Epas1, Fn1, Gata2, Gjc1, Id1, Nf1, Ramp2, Rhoj, Sema3c, Sgpl1, Sin3b, Sox18, Tsc1.*
Positive regulation of cell migration	*Ace2, Adipor2,Angpt1, Anxa3, Cd84, Clec7a, Ctss, Cxcl10, Cyba, Edn1, Fn1, Gata2, Icam1, Jak2, Lcn2, Lgals3, Ptprc, Pycard, Rhoj, Sema3c, Sgk1, Trem2.*
Negative regulation of endothelial cell apoptotic process	*Angpt1, Anxa3, Gata2, Icam1, Jak2, Lcn2, Nf1, Ramp2, Rhoj, Tnip2.*
Response to wounding	*Ada, Adipor2, Angpt1, C1qc, Cd84,Cdkn1a, Cyba, Edn1, Eng, Fn1, Gata2, Itpk1, Jak2, Kif1c, Lgals3bp, Nf1, Plat, Pros1, Timp1, Trem2, Tyrobp, Vwf.*
Protein folding	*Calr, Chordc1, Cryab, Hsph1, Manf, Mkks, Ppid, Sdf2l1.*
Methylation	*As3mt, Eef1akmt1, Gamt, Mettl16.*

Ndufs4 KO-PLX3397 vs. *Ndufs4 KO*-Veh	
GO term	**Genes**
Synapse pruning	*Apbb1ip,C1qa, C1qb, C1qc, Cd74, Csf1r, Ctss, Cx3cr1, Fcer1g, Fcgr3, Fyb, Itgam, Ptprc, Selplg, Trem2, Tyrobp.*
Inflammatory response	*Aif1, Alox5ap, C1qa, Ccl6, Ccl9, Cd74, Csf1r, Cx3cr1, Fcer1g, Fcgr3, Itgam, Ly86, Mrc1, P2ry12, P2ry13, Pdgfra, Pld4, Selplg, Trem2, Tyrobp.*
Microglial cell activation	*Aif1, Apbb1ip, C1qa, C1qc, Cd53, Cd74, Csf1r, Cx3cr1, Fcer1g, Fcgr3, Fyb, Hpgds, Itgam, Laptm5, Mrc1, P2ry12, Pdgfra, Pld4, Ptprc, Selplg, Siglech, Trem2, Tyrobp.*
Positive regulation of response to external stimulus	*Aif1, Alox5ap, Cd74, Csf1r, Ctss, Cx3cr1, Fcer1g, Fcgr3, Itgam, Ly86, Mrc1, P2ry12, Trem2, Tyrobp.*
Complement-mediated synapse pruning	*Apbb1ib,C1qa, Csf1r, Fyb, Hexb, Itgam, P2ry12, Pdgfra, Trem2.*
Leukocyte cell-cell adhesion	*Cx3cr1, Itgam, P2ry12, Pdgfra, Ptprc, Selplg, Slc39a8.*
Positive regulation of microglial cell migration	*Csf1r,Cx3cr1, Gpr34, Itgam, P2ry12, P2ry13, Pdgfra , Ptprc, Trem2, Tyrobp.*
Positive regulation of ERK1 and ERK2 cascade	*Aif1, Ccl6, Ccl9, Cd74,Csf1r, Cx3cr1, Laptm5, P2ry12, Pdgfra, Pld4, Ptprc, Tmem119, Trem2.*
Regulation of interleukin-6 production	*Aif1, Apbb1ip, Cd74, Csf1r, Cx3cr1, Fcer1g, Itgam, Laptm5, Ly86, P2ry12, Pdgfra, Ptprc, Trem2, Tyrobp.*
Icosanoid biosynthetic process	*Alox5ap, Cd74, Hpgds.*
Hippocampus	
***Ndufs4 KO*-Veh vs. Ctrl-Veh**	
GO term	**Genes**
Inflammatory response	*C3ar1, Ccl12, Ccl17, Cd68, Cela1, Cxcl10, Grn, Lacc1, Ly86, Ncf1, Ndst1, Nupr1, Serpina3n, Stat3, Timp1.*
Regulation of epithelial cell proliferation	*C3ar1, Ccl12,Cdh13, Cpeb1, Cxcl10, Deaf1, Drd1, Fgfbp1, Grn, Hrh3, Nr1d1, Nupr1, Ptprn, Stat3, Stx3, Wnt10b, Zfas1.*
Luteinization	*Cry1, Id3, Nr1d1, Plekha1 ,Ptprn,Ptx3, Sgpl1.*

Astrocyte differentiation	*Ccl12,Drd1, Fam53a, Gfap, Grn, Hrh3, Ipo9, Npy, Nr1d1, Nup93, Stat3, Ube2i, Vim.*
Regulation of type B pancreatic cell proliferation	*Ctla2a, Fcgr2b, Grn, Igtp, Lacc1, Mtmr3, Ncf1, Npy, Nr1d1, Nupr1,Ptprn, Rab34.*
Response to yeast	*Ccl12,Ncf1, Npy, Prkn, Ptx3.*
Negative regulation of cellular carbohydrate metabolic process	*Cry1, Stat3, Prkn, Nupr1, Lacc1, Fcgr2b, Grn, Mt1, Ccl12, Npy, Wdr5.*
Regulation of dopamine metabolic process	*Deaf1, Drd1, Farp1, Gfap, Hrh3, Npy, Pias3, Prkn, Sgk1, Stat3, Stx3, Stxbp2.*
Negative regulation of immune system process	*C4b, Ccl12,Cd68, Fbxo38, Fcgr2b, Grn, Hmgb3, Lacc1, Ncf1, Npy, Nr1d1, Olfm4, Parp3, Pias3, Shb, Stxbp2.*
Positive regulation of response to external stimulus	*C3ar1, Cdh13, Cxcl10, Fbxo38, Grn, Igtp, Ipo9, Ly86, Npy, Nupr1, Prkn, Rab34, Stx3, Trak2, Wnt10b.*
Protein folding	*Calr, Chordc1, Fkbp2, Hspa4l, Mkks, P4ha1, Pdia3, Pdia4, Ppid, Sdf2l1.*
Cellular lipid catabolic process	*Abhd3, Acaa2, Acsbg1, Adhfe1, Aldh9a1, Alkbh7, Cyp26b1, Echdc1,Eci1, Ephx1, Ephx2, Gamt, Hadhb, Phyh, Pla2g7, Plcxd2, Scly, Smpdl3a.*
Ether metabolic process	*Ephx1, Ephx2, Pla2g7.*
Positive regulation of CD4-positive, alpha-beta T cell activation	*Cd55, Cd83, Prkcq.*
Positive regulation of substrate adhesion-dependent cell spreading	*Calr, Jam2, Mdk, Myoc, Pla2g7.*
Alpha-amino acid metabolic process	*Adhfe1, Apip, Dalrd3, Gamt, Spr, Scly.*
Response to topologically incorrect protein	*Hspa4l, Manf, Pacrg, Sdf2l1.*
Establishment or maintenance of cell polarity	*Cep290, Cyp26b1,Fgf10, Frmd4b, Rhobtb3.*
Peripheral nervous system development	*Cntnap1, Etv1, Myoc.*

9

Acknowledgments

Esta, debería ser la última sección tanto en ser escrita como en ser leída; lo primero es cierto, lo segundo no. Contrariamente a lo que indica la lógica, todos acudimos a esta última sección cada vez que nos llega una tesis recién salida del horno, ni resumen, ni conclusiones, ni siquiera el "*Ay, a ver si las figuras al menos son bonitas, aunque no me vaya a enterar de nada*"; nada, directos a agradecimientos. Bien pensado, no es tan ilógico, porque sin las múltiples personas que directa o indirectamente han vivido este proceso, sin su apoyo y su cariño, os aseguro, que todo este papel, no serían más que un puñado de hojas en blanco.

Han estat més de 5 anys a Fisio animal, si contem TFM i tesi, i no son poques les persones responsable de que hagin estat uns anys meravellosos. En primer lloc, les meves dues incansable companyes, la Carla i la Gemma. **Carla**, encara record aquells temps on érem certament incapaços d'entendre'ns, entre el meu accent mesopotàmic i el teu de la Catalunya central, no hi havia manera. Per sort, aquells moments han quedat enrere, i ara, quan xerram entre noltros, qui no ens entén és la resta. Infinites gràcies per aquests anys espatlla contra espatlla. Gràcies pel teu suport i la teva ajuda, el camí ha estat infinitament més fàcil tenint algú al costat que comprenia les meves inquietuds i problemes, i que estava allà per celebrar les alegries. A tu encara et queden uns mesos, però ja saps que en la mesura del possible, aquí o allà, estaré pel que necessitis. **Gemma**, sense dubte, la més jove del grup, gràcies per estar allà quan el temps i la feina ofegaven, per ser el nostre salvavides. Malauradament, se que t'has hagut d'anar acostumant a que tots anem passant i marxant, però vull que sàpigues que tots ens emportem alguna cosa de tu. Crec que puc xerrar en nom de molts i dir-te que la teva fermesa, caràcter i experiència ens ha mostrat que algunes coses que acostumem a prendre'ns tan seriosament no son tan importants, i que, *there is life, after all*. També vull donar les gràcies a **l'Olaya, l'Anna i la Paula** per haver estat part d'aquesta història i per haver-me ajudat a donar les meves primeres passetes dins el laboratori. A més a més, a la Paula, m'agradaria demanar-li que comparteixi amb tots noltros la fórmula de la benzina que la fa funcionar, i donar-li les gràcies pel seu hooliganisme científic que tantes coses m'ha aportat. **Mercè**, a tu m'agradaria agrair-te el teu constat bon rotllo i alegria, al igual que la teva ajuda en mil petites coses que he pogut necessitar. Per altra banda, a la **Amalia**, fer-li saber que he gaudit moltíssim les nostres converses sobre infinitud de temes, però si m'hagués de quedar amb una cosa, em quedaria amb el seu esperit de defensa d'aquest ens públic que és la Universitat. Gaudeix del teu sabàtic, de viatges, pel·lícules i llibres, que és ben merescut. Gracias también a las dos estudiantes de máster que he tenido

el honor de supervisar en el curso de esta tesis, Sandra y Nins, cuyo trabajo sin duda está integrado en esta breve historia que he podido contar. **Sandra**, al ser la primera fuiste la que seguramente se comió mis errores de "profe" novato. Espero que tu experiencia fuera tan buena como la mía, dale duro en Londres, ¡demuestra a los british que tú lo vales! **Nins**, no he podido guiarte tanto como me gustaría, la coyuntura final ciertamente no ha ayudado. ¡Te deseo mucha suerte en esta nueva etapa, estoy seguro de que JM tendrá un buen cierre contigo! Y, por último, pero no por ello menos importante, me gustaría dedicarle unas palabras a mi jefe. **Juanma**, muchas gracias por todo: por aguantar mi impetuosidad y darle sosiego, por confiar en mí y dejarme emprender aquello en lo que creía, por tus innumerables palabras en tiempos de dudas, por alumbrarme con tus conocimientos y experiencia, por tu apoyo y cariño a lo largo y ancho de esta tesis; en definitiva, por haber sido un mentor maravilloso.

Dentro de Fisio animal, mis compañeros de grupo no han sido los únicos que han contribuido a que todo esto llegara a buen término. Gran parte también se lo debo al grupo de *ratas*: a Sara, Antonio, Xavi, Patricia y Humberto. **Sara**, ahora la más benjamina de todos nosotros, no hemos tenido la oportunidad de compartir mucho tiempo, pero ha sido el suficiente para saber que las cosas te irán bien. Habrá momentos de desesperación, pero cuando lleguen, refuérzate en las personas bonitas que trabajan a tu lado, todo será inmensamente más fácil. Agradecerte a ti **Antonio**, esa rigurosidad científica de la que todos nos embebemos, pero también tus infinitas opiniones sobre cualquier tema, desde la solución perfecta a todos los problemas de este mundo hasta, cómo olvidarlo, tu fascinante teoría sobre en qué parte del estropajo hay que dejar caer el jabón para que dure más y limpie mejor. Moltes gràcies a tu també **Xavi**, pels teus infinits acudits dolents que tant m'han fet riure, alguns realment son molt dolents eh! Gràcies també per la teva ajuda repetida amb coses del lab i de la maleïda estadística, i sobretot, gràcies per la teva visió serena quan les coses venen girades. Et desitjo el millor en aquesta etapa incerta, estic segur que tot anirà bé. **Patri**, es fa trist saber que d'aquí poc ja no continuarem fent feina junts, però tot sigui per continuar avançant. Molts sort a la nova etapa que comença, estic convençut de que tot anirà bé perquè si hi ha algú que pot de tots nosaltres, ets tu. Ha sigut tot un luxe compartir aquesta etapa amb tu. El teu interès i suport han estat una constant, y las risas, esas también, així que només em queda dir-te que visca Manel i visca el reggeton! **Humbertito**, qué decirte a ti, tantas cosas… pero seré breve. Eres el diamante en bruto que me llevo de todos estos años que se ha ido puliendo día tras día. Echaré tantísimo de menos

nuestros momentos, todos esos libros, películas y músicas, te echaré tanto de menos a ti. Gracias por todo, has sido un punto de fuga indispensable, tu constante apoyo y cariño no los olvidaré nunca. Me quedo con el consuelo de saber que no estarás tan lejos, amigo.

Fisio animal aún alberga más gente, así que gracias también a **Vicente** por enseñarme que ingerir calorías no es requisito indispensable para sobrevivir y por no ser tan serio como aparenta. Gracias al grupo de peces: **Lluís, Irene, Mariana**… con mención especial a **Ali** y **Sheida** por haber sido mis compañeros de despacho en esta última etapa, y que son, realmente, las dos personas más buenas que uno pueda imaginar. Així mateix, també infinites gràcies al **Joan Carles** per fer que aquesta tesi sigui mil vegades més bonica del que jo hagués pogut arribar a aconseguir mai. Finalment, gràcies a totes les que formen part dels tres grups: a la **Pilar**, per sempre estar allà per fer un cop de mà i recollir els nostres petits desastres, i a les quatre secretaries que han passat per la unitat durant aquests anys: **la Paqui, la Toñi, la Rosario i la Cristina**, sense elles, la ciència certament no avançaria.

Agraïment especial a un altre grup de persones, que malgrat trobar-se escales amunt, m'han permès ampliar els meus coneixements sempre des del bon rotllo i les ganes d'ajudar per avançar. En primer lloc, a la meva codirectora. **Eli**, moltes gràcies per acceptar ser part d'aquesta tesi quan ni tan sols mos coneixíem, és ben possible que sense la teva disposició no hagués pogut obtenir la FPU que m'ha permès realitzar aquest treball en bones condicions, així que infinites gràcies per això. A més a més, me'n enduc el teu esperit crític que tant m'ha enriquit, i més, quan sempre ha estat sense perdre les bones paraules. Un gràcies enorme també a **l'Albert** per haver-me donat l'oportunitat de treballar amb aquest model tan fascinant i per ser el principal responsable d'haver pogut anar Helsinki; espero que la col·laboració amb l'Anu dugui a llocs interessant. Suposo que no és massa agosarat dir-vos que ambdós sou una dupla magnífica i un clar reflex del que molts juniors voldríem aconseguir, però més enllà de què, és més la forma de ser-ho, gràcies. I com no, agrair a tota la resta del Quintana Lab, passats i presents, per tota l'ajuda durant aquests anys: **Andrea, Pati, Pablo, Patrizia, Laura Sánchez, Emma, Mel, Isabella, Mónica, Laura Cutando,** entre molts d'altres.

Me gustaría también agradecer inmensamente a los técnicos del INc que tanto me han ayudado durante todos estos años: a **Mar** con la histología, a **Cristina** por esos maravillosos cultivos, que aun que no estén en esta tesis bien lo merecerían, a **Meri** por su enorme ayuda con la microscopía,

su desparpajo e increíble buen rollo, y finalmente a **Javier**, parece serio pero realmente ser un cachondo, por habernos ayudarnos a detectar estas citoquinas nuestras que pensaba que eran un sueño antes de que él entrara en escena. Agradecer también la gestión de nuestras colonias de ratones al **personal del estabulario** de la UAB, con especial énfasis a **Juan Ramón**, por haberlos cuidado con tanta dedicación y cariño; sin su labor, esta tesis no habría sido posible.

Además, y ahora en inglés, I would also like to thank **Dr. Anu Suomalainen** for kindly accepting me in her lab during those 3 months. Anu, the time in your lab was certainly a blast, it allowed me to realize that my interests go far beyond our brains. Your love and dedication to science were truly inspiring. Thank you also for your honest support that helped me to get a new position once this little story ends. I would also like to thank all ASW lab for their great acceptance, and especially to **Sofiia, Swagat, and Nahid**, who guided me through my stay in Helsinki and made things easy. A big hug to all of you!

Y luego, hay todo un conjunto de personas que a pesar de haber estado alejadas del fluir diario de esta tesis han influido en ella hasta extremos que ni se imaginan. Empezando por lo múltiples compañeros de piso de esta etapa, algunos de ellos, más que compañeros de piso son grandes amigos: **Vasilena, Arianna, Luis, Pau, Morey, Jordan, Adi y Viviana.** También personas como **Sergio, Toni, Miguel, Julián, Teo y Joan**; conocidos aquí, como mis amigos de allí, de allí de Mallorca, claro. Pronto se cumplirán diez años que me fui para vivir esta vida en Barcelona y que prometen ser muchos más. En el camino me he perdido muchas cosas, pero por suerte, no a vosotros. Está de más enumerar todo aquello que podría deciros, lo dejaré en que os quiero con una profundidad inabarcable. O personas como **Gerard, Tomás, Víctor y Marc,** conocidos allí, como mis amigos de aquí, de aquí de Barcelona, claro. Heu estat una de les parts vertebradores més importants de la meva vida aquí. Durant aquests anys hem passat de ser un *pipiolillos* que donaven tombs de festa en festa i de biblioteca en biblioteca a ser persones adultes. Tenim mil i un moments junts, la gran majoria d'ells bons, però també experiències crues, i jo, almenys, també una certesa: malgrat les coses no m'haguessin anat tant bé com han anat, no dubtaria un segon en repetir tots aquests anys només per vosaltres. Vos estim.

De manera muy especial también quería dar la gracias a toda mi familia: a mi **padre**, a mis primos, **Aida y Marc**, y a mis tíos **Isabel, Pep y Ramón**, pilar indispensable todos estos años desde la distancia. Papá, el momento

de irse puede ser fácil, pero tomar consciencia de que te has ido no siempre lo es tanto. Imagino que algo parecido debe suceder con los que se quedan, y no habrá sido fácil hacerse a la idea de que mi futuro no está allí, así que gracias Papá por tu apoyo incondicional y por transmitirme el coraje para emprender todo aquello en lo que se cree. Un recuerdo especial para los dos **Sebastianes** de mi vida, mi padrino y mi abuelo, que tanto creyeron en mí; que injusto que hoy no estéis aquí. Seréis un recuerdo imperecedero haga lo que haga y vaya donde vaya, esto solo acaba de empezar. Os quiero a todos.

I per últim, al meu far de llum, la **Gemma**. Els dos sabem que no ha estat fàcil arribar fins aquí, però aquí estem. No m'esplaiaré molt i utilitzaré les paraules d'algú altre que tan fidedignament expressen tot allò que jo no se fer, perquè Gemma "*tota la meva vida es lliga a tu, com en la nit les flames a la fosca*".

Gràcies a tots, y que viva Radio 3.